Modelling Soil Erosion Risk in the Black Volta Transboundary River Basin of West Africa

A cumulative dissertation for the degree of Doctor rerum naturalium (Dr. rer. nat)

Submitted to the Department of Earth Sciences

By

Mawuli Asempah

Berlin, 2024

Date of disputation: 25th April 2024

First Reviewer
Prof. Dr. Brigitta Schütt
Freie Universität Berlin
Department of Earth Sciences
Institute of Earth Sciences
Malteserstraße 74-100
12249 Berlin
Germany

Second Reviewer
Prof. Dr. Tilman Rost
Freie Universität Berlin
Department of Earth Sciences
Institute of Earth Sciences
Malteserstraße 74-100
12249 Berlin
Germany

Dedication

To the memory of my late parents, Mr. Cephas Komla Asempah and Mrs. Victoria Ami Fianu Asempah.

Acknowledgements

I would like to express my deepest gratitude to the German Academic Exchange Service (DAAD) for providing the scholarship that made my doctoral studies possible. My sincere appreciation goes to my supervisor, Prof. Brigitta Schütt, for her invaluable guidance, and to Prof. Christopher Shisanya for his unwavering support throughout my academic journey. I am also grateful to my colleagues, especially Dr. Fabian Becker, Dr. Subham Mukherjee, Dr. Xun Yang, Dr. Jacob Hardt, Dr. Nadav Nir, Dr. Andrew Marondedze, and Mr. Robert Busch from the Department of Geography at Freie Universität Berlin. Additionally, I extend my heartfelt thanks to Dr. Moses Muriuki of Kenyatta University, Nairobi, Kenya; Ms. Phoebe Oduor of the Regional Centre for Mapping of Resources for Development (RCMRD), Nairobi, Kenya; and Dr. Paul Asare Tetteh of Gnubiotics Sciences, Swaziland, for their invaluable support throughout my doctoral journey. I appreciate my fellow German alumni, particularly Dr. Michael Kyei-Agyekum, Dr. Evelyn Asante-Yeboah, Dr. Jubilant Abledu, Dr. Benedict Boateng Antuamwine, Dr. Albert Kobina Mensah, Mr. Oliver Dayou, Ms. Jackie Makumator-Jones and Mr. Nathan Tetteh, for their enriching peer engagement during my studies—I am truly grateful to you all!

A special posthumous appreciation goes to Prof. Joy Obando, Dr. Daniel Adom and Dr. Kodwo Andah for their mentorship and support. Though they did not witness the completion of my doctoral studies, their guidance was instrumental in my journey. May God grant them eternal peace. I also extend my appreciation to my colleagues at the Water Resource Commission of Ghana, particularly Dr. Joachim Ayiiwe Abungba, head of the Black Volta Basin Office in Wa Municipality, Ghana, for his tremendous logistical support during my fieldwork. My heartfelt thanks to Mr. Kabah Abakeh, whose assistance was crucial to the success of my field survey.

This achievement would not have been possible without the unwavering support of my family. My deepest gratitude goes to my uncles, Samuel and Sitsofe Agorkpa, for their dedication to my academic success. I am equally grateful to my mother, Elsie G. Attafuah; my grandmother, Matilda Asare-Addy; my siblings, Ernest, Emefa, and Kobena; and my dear Nana Adwoa Ackon for their constant encouragement and support. Above all, I give thanks to Almighty God for granting me the strength, resilience, and perseverance to reach this milestone!

Abstract

Environmental degradation within river basins arises from both natural factors, such as climatic variability and biophysical attributes like topography and soil characteristics, as well as anthropogenic influences. Human-induced degradation, driven by factors such as population growth, urban expansion, and shifts in land use patterns, exacerbates the natural degradation processes. The study sought to model soil erosion risk in the Black Volta River basin. Specifically, the study (1) evaluated and determined the land use and land cover dynamic and drivers of urban expansion in the Wa municipality of Ghana between 1990 and 2020, (2) estimated soil erosion risk in a typical savannah landscape of Wa municipality of Ghana between 1990 and 2020 and (3) estimated and evaluated soil erosion risk across various landscape units of the Black Volta River basin over the periods of 1992, 2006 and 2020. Landsat satellite data (30 x 30 m resolution) was processed using Geographical Information System and remote sensing techniques to establish the spatial and temporal dynamics of land cover in the Wa municipality for the years 1990, 2001, 2010 and 2020. The thematic maps were used to assess the drivers of urban expansion (objective 1) and the potential and soil erosion risk (objective 2) in the Wa municipality. In the basin scale and landscape units' erosion risk modelling for the years 1992, 2006 and 2020 (objective 3), a 300 x 300 m resolution land cover data from the Copernicus Global Land Cover Services was used. Based on the spatial and temporal analysis of land cover change, it was evident that settlement expansion led to the depletion of woody biomass over the three decades (1990 to 2020). Settlement expansion was influenced by accessibility and connectivity factors, such as distance to existing settlements, rivers, and primary, tertiary, and unclassified roads, which were established as predictors of settlement expansion in the Wa municipality. By employing the Revised Universal Soil Loss Equation model, potential erosion risk was higher in 1990 (mean annual rate = 8.5 t $ha^{-1}yr^{-1}$) due to higher rainfall erosivity compared to 2020 (6.5 t $ha^{-1}yr^{-1}$) when rainfall erosivity was lower. However, the estimated soil erosion risk was lower in 1990 (2.6 t $ha^{-1}yr^{-1}$) due to greater vegetation cover, compared to 2020 (3.1 t $ha^{-1}yr^{-1}$) when vegetation cover declined. Soil loss was notably high in settlement, urbanising and areas with long and steep slopes, emphasising the influence of human and topographic factors on high erosion risk. This was statistically validated with data from a field survey that measures the spatial extents of soil erosion damages in 2 km^2 each of settlement, open savannah and closed savannah areas in the Wa municipality. It was established that settlement areas were the most damaged followed by open savannah and closed savannah units. Statistical correlation analysis reveals a positive relationship between the spatial extent of damages and the predicted soil erosion risk rates from the RUSLE model. At the basin scale and across landscape units, erosion risk and soil loss are primarily driven by topographic attributes and rainfall erosivity factors. The Savannah Escarpment and Sahelian Highlands with steep slope characteristics were identified as extreme erosion risk landscape units, while the Low Sahelian Plains and Sahelian Uplands, characterised by flat and gentle slopes, were predicted to have low erosion risk. Also, localised concave areas in the Savannah Escarpment and Sahelian Highland coupled with low TWI characteristics further heightened erosion risk. Additionally, a positive increase in the rainfall erosivity factor resulted in a positive change in soil loss while a decrease in rainfall erosivity factor led to a negative change in soil loss across all the landscape units, thus, underscoring the influence of rainfall erosivity factor on high erosion risk. Overall, the findings enhance the understanding of the erosion risk dynamic in the Black Volta River basin and would serve as a guide in planning management practices in line with global goals that seek to ensure environmental sustainability.

Zusammenfassung

Landdegradierung wird sowohl auf natürliche Faktoren wie Klimaschwankungen und biophysikalische Eigenschaftebn wie Topografie und Bodenbeschaffenheit als auch durch anthropogene Einflüsse gesteuert. Die vom Menschen verursachte Degradation, die durch Faktoren wie Bevölkerungswachstum, städtische Expansion und veränderte Landnutzungsmuster bedingt ist, verschärft die natürlichen Degradationsprozesse. Ziel der Studie war die Modellierung des Bodenerosionsrisikos im Black Volta River basin. Konkret wurden in der Studie (1) die Dynamik der Landnutzung und Landbedeckung sowie die Faktoren der städtischen Expansion in der Gemeinde Wa in Ghana zwischen 1990 und 2020 bewertet und bestimmt, (2) das Bodenerosionsrisiko in einer typischen Savannenlandschaft der Gemeinde Wa in Ghana zwischen 1990 und 2020 abgeschätzt und (3) das Bodenerosionsrisiko in verschiedenen Landschaftseinheiten des Black Volta River basin für die Zeiträume 1992, 2006 und 2020 abgeschätzt und bewertet. Landsat-Satellitendaten (30 x 30 m Auflösung) wurden mit Hilfe von geografischen Informationssystemen und Fernerkundungstechniken verarbeitet, um die räumliche und zeitliche Dynamik der Bodenbedeckung in der Gemeinde Wa für die Jahre 1990, 2001, 2010 und 2020 zu ermitteln. Die thematischen Karten wurden verwendet, um die Triebkräfte der städtischen Expansion (Ziel 1) sowie das Potenzial und das Risiko der Bodenerosion (Ziel 2) in der Gemeinde Wa zu bewerten. Für die Modellierung des Erosionsrisikos auf der Ebene des Einzugsgebiets und der Landschaftseinheiten für die Jahre 1992, 2006 und 2020 (Ziel 3) wurden Landbedeckungsdaten mit einer Auflösung von 300 x 300 m aus den Copernicus Global Land Cover Services verwendet. Aus der räumlichen und zeitlichen Analyse der Landbedeckungsveränderung ging hervor, dass die Ausdehnung der Besiedlung in den drei Jahrzehnten (1990 bis 2020) zu einer Verarmung der holzigen Biomasse führte. Die Siedlungsexpansion wurde durch Faktoren der Zugänglichkeit und Vernetzung beeinflusst, da die Entfernung zu bestehenden Siedlungen, Flüssen, primären, tertiären und nicht klassifizierten Straßen als Prädiktoren für die Siedlungsexpansion in der Gemeinde Wa ermittelt wurden. Bei Anwendung des überarbeiteten Modells der universellen Bodenverlustgleichung war das potenzielle Erosionsrisiko im Jahr 1990 (mittlere jährliche Rate = 8,5 t $ha^{-1}yr^{-1}$) aufgrund der höheren Niederschlagserosivität höher als im Jahr 2020 (6,5 t $ha^{-1}yr^{-1}$), als die Niederschlagserosivität geringer war. Allerdings war das geschätzte Bodenerosionsrisiko 1990 (2,6 t $ha^{-1}yr^{-1}$) aufgrund der größeren Vegetationsdecke geringer als 2020 (3,1 t $ha^{-1}yr^{-1}$), als die Vegetationsdecke abnahm. Die Bodenverluste waren in Siedlungsgebieten, urbanen Gebieten und Gebieten mit langen und steilen Hängen besonders hoch, was den Einfluss menschlicher und topografischer Faktoren auf das hohe Erosionsrisiko unterstreicht. Im Gelände erhobene Daten validieren das räumliche Ausmaß der Bodenerosionsschäden in jeweils 2 km^2 großen Siedlungs-, offenen Savannen- und geschlossenen Savannengebieten in der Gemeinde Wa. Es wurde festgestellt, dass Siedlungsgebiete am stärksten geschädigt wurden, gefolgt von offenen Savannen- und geschlossenen Savanneneinheiten. Die statistische Korrelationsanalyse zeigt eine positive Beziehung zwischen der räumlichen Ausdehnung der Schäden und den mit dem RUSLE-Modell vorhergesagten Bodenerosionsrisiken. Auf der Ebene des Einzugsgebiets und der verschiedenen Landschaftseinheiten werden Erosionsrisiko und Bodenverlust in erster Linie durch topografische Merkmale und den Niederschlagsverhalten bestimmt. Das Savannah Escarpment und das Sahelian Highlands mit steilen Hängen wurden als Landschaftseinheiten mit extremem Erosionsrisiko identifiziert, während für die Low Sahelian Plains und die Sahelian Uplands, die durch flache und sanfte Hänge gekennzeichnet sind, ein geringes Erosionsrisiko vorhergesagt wurde. Auch lokal begrenzte konkave Bereiche im Savannah Escarpment und im Sahelian Highland in Verbindung mit niedrigen TWI-Merkmalen erhöhten das Erosionsrisiko weiter. Darüber hinaus führte ein Anstieg der Niederschläge zu einer Zunahme der Bodenverluste, was den Einfluss des Erosionsfaktors der Niederschläge auf ein hohes Erosionsrisiko unterstreicht. Insgesamt verbessern die Ergebnisse das Verständnis für die Dynamik des Erosionsrisikos im Einzugsgebiet des Schwarzen Volta und können als Leitfaden für die Planung der Bewirtschaftungspraxis im Einklang mit den globalen Zielen zur Gewährleistung der ökologischen Nachhaltigkeit dienen.

Table of Contents

Lists of Figures

List of Tables

List of Abbreviations

AnnAGNPS	Annual Agriculture Non-Point Source
AUC	Area Under the Curve
CCI	Climate Change Initiative
CGIAR-CSI	International Agricultural Research Centers' Consortium for Spatial Information
CRU	Climatic Research Unit
DEM	Digital Elevation Model
EPIC	Environmental Policy Integrated Climate
EPM	Erosion Potential Model
ESA	European Space Agency
EUROSEM	European Soil Erosion Model
GASEMT	Global Applications of Soil Erosion Modelling Tracker
GeoWEPP	Geo-spatial Interface for WEPP
HWSD	Harmonised World Soil Database
IPCC	Intergovernmental Panel on Climate Change
ISRIC	International Soil Reference Information Centre
ITCZ	Inter-Tropical Convergence Zone
LISEM	LImburg Soil Erosion Model
LULC	Land Use and Land Cover
MMF	Morgan-Morgan-Finney
MNDW	Modified Normalised Difference Water Index
MUSLE	Modified Universal Soil Loss Equation
NASA	National Aeronautics and Space Administration
NBR2	Normalised Burn Ratio 2
NDBI	Normal Difference Built-Up Index
NDVI	Normalised Difference Vegetation Index
OLI	Enhance Thematic Mapper
POWER	Prediction of World Energy Resources
ROC	Operating Characteristic Curve
RUSLE	Revised Universal Soil Loss Equation
RUSLE-SDR	Revised Universal Soil Loss Equation with a Sediment Delivery Ratio
SAVI	Soil Adjusted Vegetation Index
SDGs	Sustainable Development Goals
SRID	Statistics, Research and Information Directorate
SRTM	Shuttle Radar Topography Mission
SWAT	Soil and Water Assessment Tool
TM	Thematic Mapper
TWI	Topographic Wetness Index
UNDESA-POP	United Nations Department of Economic and Social Affairs- Population Division
USGS	United States Geological Survey
USLE	Universal Soil Loss Equation
USLE-SDR	Universal Soil Loss Equation combined with a Sediment Delivery Ratio
USPED	Unit Stream Power-based Erosion Deposition
WaTEM/SEDEM	Water and Tillage Erosion Model and Sediment Delivery Model
WEPP	Water Erosion Prediction Project

CHAPTER 1: INTRODUCTION

1.1 Background

River basins provide essential ecosystem services that sustain lives; however, most basins are faced with degradation due to both natural and anthropogenic causes (Akinsete et al., 2019). The natural exposure to degradation stems from their physical characteristics and climate change and climate variability (AbdelRahman, 2023; Akinsete et al., 2022). The anthropogenic causes of environmental degradation on the other hand emanate from population increase and its associated activities that put pressure on environmental resources (AbdelRahman, 2023). The Black Volta River basin is one of the major river basins in the West Africa Sub-region, and it plays a vital role in the economic development of riparian countries. The Black Volta River basin is a transboundary and is shared between Ghana, Mali, Burkina Faso and Ivory Coast who rely on the basin's resources, especially water, for domestic, livestock, crop production, and hydropower purposes (Mul et al., 2015; Rodgers et al., 2007).

Despite its tremendous contribution and potential, the basin is vulnerable to climate impact, particularly increased rainfall intensity coupled with rapid human population growth and its resultant degradation. The rapid population growth and settlement expansion of the basin are reflected in the census data of the highly urbanising Wa municipality within the Ghana part of the basin. There is potential competition over the already stressed basin's resources due to increased demand from the fast-growing population and economic growth exacerbated by environmental changes and degradation (Boretti & Rosa, 2019; Mul et al., 2015). The competition for environmental resources and its associated degradation is expected to worsen in the future with consequences for environmental sustainability, food security and economic growth in the four transboundary basin countries (McCartney et al., 2012; Mul et al., 2015).

The Black Volta basin is predominantly characterised by a semi-arid environment especially in its central and northern parts, making the area more vulnerable to excessive evapotranspiration, drought, and soil erosion (Gebrechorkos et al., 2022). Environmental degradation and soil erosion in the basin emanate from over-exploitation of the landscape coupled with erratic but high-intensity-rainfalls (Barry et al., 2005; Jin et al., 2018). The characteristic savannah and woodland vegetation of the basin faces an expected depletion of 25% deforestation because of the increasing population (Abungba et al., 2022). Since the 1960s, there existed a trend of settlement expansion and agricultural development that led to encroachment of forestland (Tengapoe et al., 2023, Barry et al., 2005). Also, timber extraction and tree cutting for fuel wood and charcoal production in low-income regions propagated (Tengapoe et al., 2023, Barry et al., 2005). The extensive exploitation of the basin creates bare and impervious soil surfaces that accelerate run-off, erosion and sedimentation (Peng & Dai, 2022). Soil erosion and sedimentation are major threats in the Volta Basin leading to low agricultural productivity, decreasing water storage capacity of river channels, siltation of reservoirs, degradation of water quality and a general destruction of the ecosystem (Nyamekye et al., 2018; UNEP-GEF, 2013).

Quantitative assessment of environmental degradation such as soil erosion risk is a fundamental step in developing and planning sustainable measures to reduce their impacts on landscapes and the populace (Alewell et al., 2019; Prasannakumar et al., 2012). This study seeks to assess soil erosion risk in the Black Volta River by applying a coupled approach of on-site geomorphological survey and the application of the Revised Universal Soil Loss Equation (RUSLE) model. By assessing and understanding the soil erosion risk dynamics in the different landscape units of the basin, conservation

and adaptation strategies would be informed in line with the Volta Basin Authority's mandate of integrated water resources management to achieving global goals such as the United Nations' Sustainable development goals to ensure environmental sustainability. The study therefore bases on three specific objectives to understand the changes in land cover, driver of settlement expansion and soil erosion risk over the past three decades. The study focuses on the transboundary Black Volta River basin, however, a case study in a highly urbanising Wa municipality of Ghana, a typical savannah landscape within the Black Volta River basin inspired the study.

1.2 Objectives

The overall objective of the study is to evaluate soil erosion risk under varied conditions in the Black Volta River basin. The specific objectives are as follows:

(a) To evaluate and determine the land use and land cover change (LULC change) dynamic and the drivers of urban expansion in the Wa municipality between 1990 and 2020.

(b) To estimate soil erosion risk in a typical savannah landscape of Wa municipality/Ghana between 1990 and 2020.

(c) To estimate and evaluate soil erosion risk across various landscape units of the Black Volta River basin over the periods of 1992, 2006 and 2020.

Based on the specific objectives, the study wants to find answers to the following questions:

- What is the extent of land use land cover change in the Wa municipality during the past three decades? What are the drivers of land use land cover change and urban expansion in the Wa municipality?
- What is the extent of soil erosion risk in the Wa municipality between 1990 and 2020?
- How do soil erosion risk estimates vary across different landscape units of the Black Volta River basin during the past three decades?

1.3 Outline of the Thesis

The thesis is a cumulative dissertation that comprises eight chapters including four introducing chapters, three core chapters and a final synthesis Chapter.

The introductory chapters entail Chapters 1 to 4. Chapter 1 is the introduction chapter that gives a general background to the study, introduces the research objective and question, and provides the outline of the thesis. Chapter 2 provides the state of the art and particularly reviews relevant literature related to the study objectives. In Chapter 3, a comprehensive description of the Black Volta basin is given by detailing the location and administrative settings, the natural and physical characteristics, population dynamic and urbanisation and the socioeconomics and livelihood diversification options in the basin. Chapter 4 of the thesis highlights the material and methods employed in achieving the set research objectives that form the core chapters of the thesis.

The core chapters: The thesis is composed of three peer-reviewed journal articles of which two have been published in international journals while the third article is under review. The three peer-reviewed

journal articles form the core chapters 5, 6 and 7 of the thesis and correspond to the three specific objectives 1, 2 and 3.

The synthesis chapter: This chapter synthesises the findings of the three main objectives and draws general conclusions. Based on the findings, the chapter highlights some potential implications with regard to biodiversity and ecological sustainability, agricultural productivity, hydrological impacts and economic cost of erosion damages. The chapter also entails a general conclusion based on the objectives and findings of the study.

The detailed outline of the three core chapters is as follows

Chapter 5: Asempah, M., Sahwan, W., & Schütt, B. (2021). Assessment of land cover dynamics and drivers of urban expansion using geospatial and logistic regression approach in Wa municipality, Ghana. Land, 10(11). https://doi.org/10.3390/land10111251. Own contribution: 70%. Published under CC BY.

Within the scope of the general aim of the thesis, this chapter focuses on assessing the changes in land cover and the geospatial drivers of urban expansion from the year 1990 to 2020 in Wa municipal of Ghana. This was imperative due to the growing population in the past decade that renders savannah, arid and semi-arid landscapes vulnerable to environmental degradations such as forest-cover depletion, soil erosion risk and overall destruction of the ecosystem (Dudley et al., 2020). The Wa municipal is a typical savannah landscape that is a true representation of the Black Volta River basin. The chapter expatiated the methodological approaches, analysis, and discussions of results of the first objective of the research. This was achieved through GIS and remote sensing techniques that were applied in classifying Landsat satellite images to assess the land use dynamic of the Wa municipal over time. Owing to the heterogeneity of the Wa municipality preprocesses such as image enhancement using spectral indices were performed before a supervised classification of Landsat images that was achieved by employing a non-parametric random forest classifier. Four thematic maps for the years 1990, 2001, 2010 and 2020 were produced to better understand the decadal trend in land cover over the three decades. Settlement expanded in each consecutive time slice at the expense of vegetation cover. In assessing the geophysical drivers of urban expansion, the chapter asses the influence of location factors (distance from existing settlement, distance to primary roads, distance to tertiary roads, distance to stream, and distance to rivers) and topographic factors (slope, aspect, and topographic wetness index (TWI) on urban expansion over the three decades using binomial logistic regression.

Chapter 6: Asempah, M.; Shisanya, C.A. & Schütt, B (2024). Modelling of soil erosion risk in a typical tropical savannah landscape. Scientific African, 23(July 2023), e02042. https://doi.org/10.1016/j.sciaf.2023.e02042. Own contribution: 70%. Published under CC BY.

This chapter elaborates on the spatial soil erosion risk dynamics in the Wa municipal. The study employed the RUSLE empirical model for the estimation of soil erosion risk following the land cover dynamic and settlement expansion modelled in Chapter 5. The RUSLE model's input parameters are from two broad sources: natural (rainfall, soil, and topography) and vegetation cover and cover management practices. The required data were obtained from various sources for the estimation of rainfall erosivity factor (R), soil erodibility factor (K), slope length and steepness factor (LS), cover factor (C) and support practice factor (P). The spatial soil erosion risk was modelled by incorporating all the five input parameters required by the RUSLE model after harmonising the parameters into the

same cell resolution and projection. The chapter details the various relationships between the input parameters and high soil erosion risk in the Wa municipality. It was evident that areas with long and steep slopes corresponding to bareland areas especially within settlement areas correlate positively with high soil erosion risk in the years 1990 and 2020. Data from field surveys that measured the spatial extent of erosion damages validate the results from the RUSLE model. Based on the *in-situ* measurement of erosion damages, it was revealed that settlement areas are of the highest erosion risk due to the continued human activities that lead to the removal of vegetation cover, creation of impervious surfaces and movement of earth.

Chapter 7: Asempah, M., Becker, F., C.A., Shisanya & B., Schütt (submitted). Major Landscape Units of the Black Volta basin and their Exposure to Soil Erosion Risk – Manuscript to be published as an open-access article distributed under the terms and conditions of the Creative Commons Attribution (CC BY) license.
(https://creativecommons.org/licenses/by/4.0/). Own contribution: 65%.

This chapter assesses the exposure of the landscapes of the Black Volta River basin to soil erosion risk for the years 1992, 2006 and 2020. Firstly, the study basin was characterised into landscape units mainly based on the geology and climatic characteristics. In all, six landscape units were characterised for the onward soil erosion risk estimation. They include Low Sahelian Plains, Sahelian Uplands, Sahelian Highlands, Savannah Transition, Mixed Terrain Plateau and Savannah Escarpment landscape units. The landscape units across the northern corridor (Low Sahelian Plains, Sahelian Uplands and Sahelian Highlands) are characterised by a higher proportion of grassland and cropland than the landscape units in the south (Savannah Transition, Mixed Terrain Plateau and Savannah Escarpment). Also, rainfall amounts are lower in the north than south. Similar to the step in Chapter 6, the RUSLE model's input parameters (rainfall erosivity factor (R), soil erodibility factor (k), slope length and steepness factor (LS), cover factor (C) and support management practice (P) factor) were estimated and evaluated for the onward soil erosion risk modelling and assessment. The RUSLE model was used in the soil erosion risk estimation at both basin and landscape unit levels. This was followed by a scenario analysis of soil loss across the basin and the six landscape units. Overall, it was established that the rainfall erosivity factor is the main influencing factor of soil erosion risk and soil loss across all the landscape units.

CHAPTER 2: STATE OF THE ART

Chapter 2 presents the discourse of environmental degradation with an emphasis on soil erosion risk. The Chapter gives an account of the historical and contemporary soil erosion risk and elaborates on the contributing factors such as climate change and variability, topographic factors and soil physical characteristics. Also, the impact of Population growth and urbanisation that drive land use and cover dynamics as contribution factors to environmental degradation, particularly soil erosion, is captured.

2.1 The Historical and Contemporary Account of Soil Erosion Risk

Soil erosion has been of major interest due to the tremendous effect it has on human survival which has necessitated scientific research over the past centuries (Pimentel, 2006). Historically, the impact of soil erosion has been severely felt especially in the semiarid to dry-subhumid regions of West Africa which are characterised by savannah vegetation cover (Sissoko et al., 2011). The savannah vegetation areas within the Sahel region of West Africa were reported as severely most vulnerable to erosion as estimates show that the area erodes above the tolerable level for soil formation to compensate for soil loss (Giertz et al., 2005; Sissoko et al., 2011). Soil erosion rate of 2.4 t $ha^{-1}yr^{-1}$, corresponding to 0.90–0.95 mm from the land surface removed soil each year most likely has a devastating impact on food production (Ostovari et al., 2021; Lanlan Zhang et al., 2021). The severity of soil erosion within the Sahel region of West Africa is exemplarily manifested in about 150-300 m^2 gullies formation during one short rainy season on small alluvial fans of 5000-10,000 m^2 area (Talbot & Williams, 1978). Similarly, Lal, (1984), reports a severe soil erosion risk on arable lands in river basins in Upper Volta, Niger, Mali and Chad within the West African sub-region. The menace is aggravated by bushfires, deforestation, and agricultural activities in savannah woodlands (Nyamekye et al., 2018; Olanipekun et al., 2019; Zhou, 2016). The magnitude of degradation affects soil organic carbon contents, effective soil water holding capacity and major soil nutrients such as nitrogen and phosphorus reserves. Depletion of soil directly affects essential functions, such as organic matter storage, nutrient recycling, and food production (Pimentel, 2006) thereby causing stunted growth of food crops, low productivity, and food insecurity (Dominati et al., 2010; Ferreira et al., 2022; Gerke, 2022).

In the early-mid-20^{th} century, there was a great revolution in tropical agriculture where vast tropical forests and savannah vegetated land converted stepwise into arable land (Tosh, 1980; Tripathi et al., 2021). The continuing tillage renders vast areas of arable land unproductive due to accelerated soil erosion and the resulting destruction of the terrestrial (AbdelRahman, 2023; Larson et al., 1983). Also, globally distributed data compiled by Montgomery, (2007) Indicate that conventional agriculture predisposes arable lands to about 10-100 times higher soil loss rates compared to conservation agriculture. Healthy soils drive sustainable food production, however, human-controlled activities such as unsustainable agricultural practices, deforestation, bushfires, and overgrazing, usually increase the rate of ecological destruction and natural ecological imbalances and intensify soil erosion (Abdalrahman et al., 2010; Keesstra et al., 2016; Stanchi et al., 2015). This is in line with the Millenium Ecosystem Assessment, (2005)that identified unregulated land-use decisions, unsustainable agricultural practices and poor soil management practices as the principal drivers of accelerating soil erosion risk.

Globally an estimated 75 billion metric tons of soil is eroded from arable lands annually while about 80% of the world's arable land is classified as moderately to severely eroded (Pimentel & Kounang, 1998). Previous studies affirm the significant impact of soil erosion-induced nutrient variability on

agricultural productivity and food security (Gu et al., 2018; Visser et al., 2019). The annual reduction in crop production over the year attributed to soil erosion risk and coinciding loss of soil nutrients heighten the threat of soil erosion to global food security (Liu et al., 2015; Pimentel & Burgess, 2013; Xie et al., 2019; Lanlan Zhang et al., 2021). Besides food insecurity, other repercussions associated with accelerated soil erosion risk include, increasing atmospheric carbon dioxide concentrations (Lal, 2019), water quality degradation characterised by increased turbidity, sedimentation of reservoirs leading to reduction of their water holding capacity and the overall disturbances in hydrological regimes (Ayele et al., 2021; Shah et al., 2022). The disturbance in hydrological regimes is heightened in many river basins as flood risks due to the siltation of river channels and the blockage of watercourses (Lal, 2003; Locatelli et al., 2011). Due to the rapid degradation of land cover due to anthropogenic impacts, tropical landscapes have high erosion potential given high rainfall intensity and distribution (Flores et al., 2019; Malhi et al., 2014).

2.2 Natural Drivers of Erosion

In the context of the RUSLE model's requirement for modelling soil erosion risk, three main natural influencing factors are eminent. These include the climatic conditions represented in rainfall intensity and distribution, soil characteristics and the topographic influence. These factors play pivotal roles in shaping the erosive potential of a given landscape and are integral to the accurate prediction of soil loss.

2.2.1 Topography Controlling Erosion

A major controlling factor of soil erosion is topography and the general configuration of land surfaces (Dalzell et al., 2022; Dialynas et al., 2016). Specifically, terrain characteristics in terms of steepness, slope length and curvature are critical topographic attributes that control erosion (Wang et al., 2020). Long slopes are characterised by expanded surface area for water collection and an increased volume of runoff (Deng et al., 2021; Hrachowitz et al., 2021). Generally, the steeper the slope, the higher the flow velocity of the runoff and associated sediment transport capacity (Fang et al., 2015). Land with slope characteristics of greater than 15% is in general considered to be vulnerable to erosion and to be unsuitable for arable farming (Siswanto & Sule, 2019). The erosive potential of runoff is contingent upon velocity and volume as increased velocity and volume increase soil particle detachment and transport capacity (Deng et al., 2021; Hecht & Oguchi, 2017).

The influence of topography on erosion damages such as rill, sheet and gully erosion is controlled by certain thresholds and triggered and intensified by various predisposing factors (Arabameri et al., 2018; Cen et al., 2022; Gayen et al., 2019). Topographic factors such as slope gradient, slope aspect, topographic wetness index, curvature, stream power index and drainage density are major determinants of soil erosion (Conoscenti et al., 2014; Roy et al., 2020). In many contexts, slope gradient is proven to be highly influential on soil erosion risk (Ahmad et al., 2023; Conoscenti et al., 2014).

2.2.2 Climate Change and Variability Influence on Soil Erosion Risk

The climatic factor affecting soil erosion risk primarily encompasses rainfall characteristics such as rainfall intensity and distribution. Intense rainfall can lead to increased surface runoff and erosion due to saturation overland flow and Horton flow (Ahnert, 1996), while the distribution of rainfall over time

influences soils' water saturation and erosion susceptibility (Renard et al., 1997). This underscores the importance of considering both the quantity and temporal distribution of rainfall events in erosion risk modelling including changes and variations of climatic conditions, particularly in rainfall and temperature, over time.

Climate change and variability are critical environmental issues that directly affect land degradation and soil erosion through desertification, drought, and flood (Lal, 2012; Stringer et al., 2009). Over 4 billion hectares of land across the globe are mainly affected by climate change and variability affecting over 1.5 billion people (Berberoglu et al., 2021). The impact of climate change and its associated soil and environmental degradation significantly sways environmental sustainability, economic efficiency and food security (Nguyen et al., 2023). The dynamics of climate changes and precipitation regimes are undoubtedly precursors of risk to surface runoff, soil erosion, and related environmental consequences (Berberoglu et al., 2021). According to the Intergovernmental Panel on Climate Change (IPCC, 2021), the trends of temperature and precipitation regimes across the globe generally show an increase in surface temperature and erratic precipitation variations in the past century. In the West African sub-region, the impact of climate variability is manifested in the 1970s drought with ripple impacts of desertification and low agricultural productivity which in turn affected development in the sub-region (Held et al., 2005; Sissoko et al., 2011). Employing the mesoscale meteorological model MM5 (Georg et al., 1994) for the Black Volta basin for the two-time steps 1991–2000 and 2030–2039 Jung & Kunstmann, (2007) show an annual mean temperature increase of about 1.3°C and a mean annual change in precipitation from -20 to +50 % significantly exceeding the interannual variability.

Besides the past and the current established trends of climatic change, projections have been made for the coming years. Based on spatial and temporal variability climate change simulations on a global scale project an increase in precipitation in warmer regions (Iles et al., 2020; Rehfeld et al., 2020). This has been affirmed by temporal observations of precipitation for both simulated climate regimes and current established climate records. Rainfall intensities are expected to increase, though the average annual precipitation is projected to decrease by the end of the 21st century, especially in the Mediterranean region (Stefanidis & Stathis, 2018; Zittis et al., 2022). In Sub-Saharan Africa, changes in hydrological regimes and early rainfall onset and cessation influence the average annual precipitation over time (Shongwe et al., 2009). The global circulation models (GCMs) projected erratic rainfall events until the end of the 21st century for countries including Ghana, Burkina Faso and Mali which are major contributors to the Black Volta transboundary river basin (Shongwe et al., 2009). As part of the IPCC's Climate Model Intercomparison Project 3 (CMIP3), the evaluation of CNRM and the IPSL show the uncertainty of the rainfall regime in West Africa with a contradictory rainfall projection for towards the end of the 21st century (Ibrahim e t al., 2014). In support of this assertion, half of the models included in the CMIP3 indicate an increase in precipitations especially in the Sahel region of West Africa while the other half gives the opposite scenario (Seto et al., 2012).

Several research alluded to the impacts of climate variability and climate change on soil erosion (Eekhout & de Vente, 2022; Klik & Eitzinger, 2010). The integration of regional climate models (RCMs) for Sub-Saharan Africa indicates an increase in consecutive dry days with intermittent high-intensity rainfall that exacerbates soil erosion risk, particularly during the onset of the wet season (Girmay et al., 2021; Ligonja & Shrestha, 2015) In assessing the drivers of erosion risk in the context of climate change and human impact within East Kagera Basin Li et al. (2021) point out a greater impact of climate change

on soil erosion risk than human influence. Owing to the hydrological alterations in many river basins stemming from climate change and variability, the rates of soil erosion are expected to change over time due to the change in erosivity potential associated with the changes in climate regimes (Girmay et al., 2021). The degree of rainfall impact on the detachment and transport of soil particles depends on the topographic characteristic of the area (Uber et al., 2022).

2.2.3 Soil Characteristics

Soil aggregates are formed through several physical, chemical, and biological processes and are sub-divided into micro aggregates of < 0.25 mm and macro-aggregates of > 0.25 mm size (Kpemoua et al., 2022; Mustafa et al., 2020; Zeraatpisheh et al., 2021). Following the aggregate hierarchy theory, soil aggregates serve as the foundational elements of soil structure that play a pivotal role in determining soil structural stability that influences a range of soil physical and chemical properties (Mustafa et al., 2020). Soil with good structural and aggregate stability favours the nutrient cycle, soil water balance, soil temperature and air exchange thereby promoting good soil health and vegetation growth (Tahat et al., 2020). Overall, aggregate stability is a good predictor of soil nutrient availability, distribution of soil porosity, crusting, detachment, and transport (Khanifar & Khademalrasoul, 2021; Le Bissonnais, 2016).

The response of soil exposed to rainfall energy includes the mechanical destruction of soil aggregates to smaller aggregates or particles, the dispersion of particles and the translocation (Chen et al., 2022). The destruction and breakdown of soil aggregates by raindrops depends on the strength of the soil aggregates and the kinetic energy inherent in the raindrops to effect detachment (Alivio et al., 2023; Mineo et al., 2019). Soil particles of <0.125 mm in size require low kinetic energy to effect detachment, thus soils with high content of loamy, silty loam, fine sandy, and sandy loam poorly respond to the impact of rainfall energy and are most susceptible soils to detachment (Wang et al., 2022).

Soil erodibility differs in different soils based on their inherent characteristics that determine the capacity to detach (Bernik et al., 2018; Fell et al., 2017) Major physical and chemical soil properties such as soil structure, texture, organic content, permeability or porosity, temperature, air content, pH, and surface-aggregation ratios directly influence erodibility (Bonilla & Johnson, 2012; Özdemir et al., 2022). These control processes such as infiltration, nutrient cycling, and biological activity determine the soil health, productivity, and suitability of use (Tahat et al., 2020; Vereecken et al., 2016). Because of the importance of soil characteristics on soil erosion, modelling of soil erosion risk considers textural properties, organic matter content, stone coverage and grain size composition, especially considering fines (Pontes et al., 2022; Schweizer et al., 2021). Generally, clay is a significant active part of soil texture which has a very small particle size and a large amount of surface area per unit mass that helps in storing water and ions (Stavi & Lal, 2011). Fine sand and silt-dominated soils are prone to erosion due to their high porosity rate, and poor water-holding ability and contribute very little to the soil's ability to restore nutrients and water (Stavi & Lal, 2011). In consequence, soils with high proportions of fine sands and silts are mainly susceptible to erosion (Scherer et al., 2012) while soil with significant clay and humus contents presents a better protection function against raindrop impacts and erosion (Pintaldi et al., 2018).

Due to earthy fabric and low cohesiveness, tropical soils exhibit low structure stability with a low propensity to resist the impact of raindrops and actions of external mechanical stresses with a high tendency to erosion (Wuddivira et al., 2013). Soils with good structural stability may have a low infiltration rate because of the inevitable decrease in the gradient of matrix potential (Vereecken et al.,

2016; Zhipeng et al., 2018). Similarly, deterioration of soil structure reduces infiltration rate in case of the formation of clay crusts and due to this sealing of the soil thereby hinders infiltration and promotes surface runoff and associated sediment transport (Badorreck et al., 2013).

2.3 Anthropogenic Causes of Erosion

Anthropogenic activities crucially determine land use and drive soil erosion as well as the general interference of both aquatic and terrestrial ecosystems (Li et al., 2022; Li & Fang, 2016; Tarboton, 1997). As the human population grows ecosystem destructive activities such as deforestation, tillage, overgrazing, bushfire and settlement expansion are prevalent in many landscapes (Ahmad et al., 2023). Anthropogenic activities accelerate soil erosion to about 60% (D. Yang et al., 2003) which accounted for about a 2.5% rise in soil erosion by water for the last two decades (Borrelli et al., 2017). According to Lal (2003), globally about 10^9 hectares of land is affected by soil erosion. Soil erosion and soil degradation have negative repercussions on agricultural production and profitability (Llena et al., 2019; van der Waal & Rowntree, 2018). The soil erosion menace is likely to continue as projections indicate a doubling of the global urban population by the end of the 21st century, which will be followed by escalating landscape urbanisation to satisfy population demands (Jiang & O'Neill, 2017).

2.3.1 The Impacts of Population and Urbanisation on Soil Erosion

It has been projected that the global urban population might increase up to 66% of the global population by 2050 (Bettencourt, 2013; Borrelli et al., 2020)including secondary cities urban population is envisaged to reach 80% (United Nations Department of Economic and Social Affairs- Population Division (UNDESA-POP), 2018). In Africa, the growth of population is reflected in urbanisation and settlement expansion, especially in big cities, districts, regional and state capitals (Osawe & Ojeifo, 2019). In 1950, it was observed that Africa was the least urbanised continent having only 14.5% of the population living in urban areas (Osawe & Ojeifo, 2019). In the year 1990, however, 34.5%of the African population out of 749 million people was living in urban areas. Based on a projection by the United Nations, Africa's urban population might reach 2.5 billion people by 2050 (International Monetary Fund (IMF), 2023). The West African sub-region has seen intensive population growth and associated urbanisation since independence, which has strongly affected urbanisation processes and in total an increased number of cities with evidence of reduced average distance from 111 km to 33 km between agglomerations (Ofoezie et al., 2022).

As the impact of population growth and land use changes is evident on soil erosion risk, depopulation and changes from intensive land use to more conservational practices lead to decreasing soil erosion risk (Borrelli et al., 2017; Zorn & Komac, 2009, Uddin et al, 2918). The continuously increasing population drives urbanisation and environmental degradation as the expansion of built-up areas is directly connected to the expansion of infrastructure, agricultural spread and the development of various livelihood activities (Fang et al., 2005). These result in the encroachment of sensitive ecosystems, forest depletion, degradation of water bodies, pollution, and finally soil erosion (Leh et al., 2013). The exposure of soils to erosion in urbanising landscapes is predominantly high and controlled by soil compaction and earthworks (Leh et al., 2013; Lei Zhang et al., 2022).

The modification of urban landscape includes the spread of impervious surfaces and decreasing soil infiltration capacity (Sinha et al., 2015). This, in turn, induces increased runoff with increased sediment

transport capacity (McVey et al., 2023), leading to sedimentation of river channels, reduced water holding capacity, blockage of water canals and culverts (Hajigholizadeh et al., 2018). Peri-urban and rural areas also experience increased soil erosion risk owing to the intensification of agricultural practices that are required to produce food for the increasing urban population (Ssewankambo et al., 2023). The agricultural impact on soil erosion is inextricably documented as sediment yield and transport are influenced by tillage (Pimentel & Burgess, 2013; H. Wang et al., 2021). Removal of natural vegetation cover increasingly exposes bare soil surfaces to direct raindrop impacts, especially at the onset of the wet season contributing to massive soil loss (Ligonja & Shrestha, 2015; Shikangalah et al., 2017). Ristić et al. (2012) report torrential floods and sediment deposition due to inappropriate land use.

Based on the complexity and magnitude of processes triggering land degradation spanning from population growth and urbanisation up to climate change, the management of environmental degradation such as soil erosion is of major sustainability concern (Borrelli et al., 2020). The lack of effective management exacerbates damages and leads to high costs of environmental restoration such as channel dredging and desilting, implementation of soil conservation measures and replanting of vegetation and buffer strips (Llena et al., 2019; Stenfert Kroese et al., 2020).

2.3.2 Types of Population Growth and Urban Expansion

Human population growth is a complex phenomenon, it shapes and is shaped by various factors, influencing social, economic, and environmental landscapes (UNDESA-POP, 2022). The three main types of human population growth are exponential growth, linear growth, and demographic transition (Bongaarts, 2009; Demetrius et al., 2004). The exponential population growth is characterised by a constant rate of increase over time and is often associated with rapid population expansion, leading to increased demands on resources and potential environmental degradation (Hunter, 2000; Yap et al., 2024). According to Yap et al. (2024) uncontrolled exponential growth might be detrimental to sustainable resource use and the environment. With rapid and unsustainable demands on natural resources, the exponential population growth can result in overexploitation of land, water, and other essential resources, contributing to deforestation, soil erosion, loss of biodiversity, and increased pollution – thus to environmental degradation (Ehrlich & Ehrlich, 1991). Historically, human population growth has exhibited exponential characteristics, especially during the last few centuries (Ehrlich, 1985). Typical of growth by a fixed number in each successive period, linear population growth is less common in human populations compared to exponential growth and is often associated with stable or slowly increasing populations (Smith, 1977). In the case where the death rate exceeds the birth rate, without an inflow of migrant population growth can be described as negative growth (Bongaarts, 2009).

Based on the concept of demographic transition, population growth is considered an evolving process linked to different stages of societal economic and social development. It involves a shift from high birth and mortality rates to low birth and mortality rates with typical occurrences in four stages (Bongaarts, 2009; Frejka, 2016). The first stage involves high birth and death rates while the second stage is when there are high birth rates and declining death rates (Frejka, 2016). Declining birth and death rates are considered as the third stage of the transition while the fourth stage is when there are low birth and mortality rates. The different stages of the demographic transition model, can impact the environment differently at each stage (Bongaarts, 2009; Frejka, 2016). Initially, there may be increased demand for

resources during population growth, but as societies move towards lower birth rates, the pressure on the environment may ease (Bongaarts, 2009; Frejka, 2016).

As contemporary urbanisation is marked by a fast increase in urban population and rapid expansion of urban areas (Altrock, 2022), growth can lead to severe adverse consequences for the environment and socioeconomic aspects if there is no effective management. These repercussions include the formation of urban heat islands, reduced green spaces leading to soil erosion, inadequate infrastructure and services, and inefficient resource utilisation (S. Li et al., 2018; Viana et al., 2019). A fundamental step in comprehending the impacts of urbanisation involves analyzing the spatiotemporal dynamics of the built-up area within a specific urban landscape (Kindu et al., 2020). Understanding the spatial pattern and intensity of urban land changes is crucial for addressing issues related to human-environmental interactions, providing urban environmental services, and formulating land-use policies for sustainable urbanisation (Estoque & Murayama, 2015). Recent emphasis on urban change detection has shifted towards quantifying change, measuring patterns, and analyzing the patterns, processes, and drivers of urban expansion (Li et al., 2014). Also, there has been concern about the types and nature of urban expansions for statistical inferences in environmental modelling (Anees et al., 2020).

2.3.3 Land-use Changes

The terrestrial land surface cover has undergone continuous changes (Pielke et al., 2011). The major inevitable land use land cover changes occur due to the expansion of agriculture and settlement to meet the needs of a growing population (Berihun et al., 2019). According to Goldewijk, (2001), intensification and expansion of agriculture are the major drivers of global land use land cover changes. The proliferation of croplands in originally vegetated landscapes such as forests is reported to be among the most prominent land use land cover transformations in Sub-Sahara Africa (Kuule et al., 2022). During the past three centuries, there has been an increase in the area of crop-cultivated land from 300 million ha to 1530 million ha (Pielke et al., 2011).

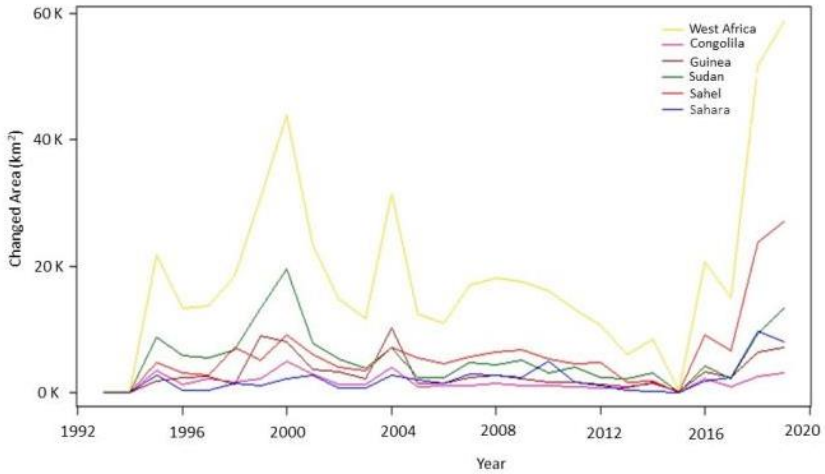

Figure 2.1. Land Use and Land Cover Dynamics of West Africa. Changed Area in Thousands (k) of km² (copy from Mortey et al., 2023).

Ramankutty & Foley (1999) estimated the expansion of cropland in Sub-Sahara Africa from 400 million ha in the year 1700 to 2000 million ha in the year 1990. The drastic land use land cover changes have a direct impact on the biophysical characteristics such as vegetative cover loss and associated albedo

modification (Ito & Hajima, 2020), which greatly affects the net radiative and hydrological budgets at land surfaces.

Within the West Africa sub-region, changes in the total land cover vary from year to year, notably spiking in 1995, 2000, 2004, 2016, and 2018 (Figure 2.1). These spikes consistently occur across all climatic zones, indicating that the phenomenon is not localised to any specific zone but rather appears to be associated with more regional factors (Mortey et al., 2023). Critical drivers of land use land cover changes especially the expansion of cropland at the expense of primary forest associated with the human population and economic growth (Foley et al., 2005). Land cover changes in a broad sense are driven by activities such as shifting cultivation, pasturing, grazing of livestock harvesting trees for fuelwood, population growth, settlement expansion and its associated infrastructure development, land tenure and poverty (Tola, 2023). Also. extensive deforestation of tropical rainforests such as in the Amazon basin and Southeast Asia has garnered attention owing to the detriment environmental consequences it poses (DeFries & Rosenzweig, 2010). The unsustainable land use land cover changes exacerbate soil erosion and sedimentation menace (Moisa et al., 2022; Uddin et al., 2018). It is evident that the global land use land cover changes from the years 2001 and 2012 contribute to about 2.5% of the global average soil erosion (Borrelli et al., 2017; Uddin et al., 2018). The vegetation cover's protective function against the erosive powers is lost in most river basins owing to unsustainable land uses (Nut et al., 2021).

Human-induced degradation of rangeland has been observed in Sub-Sahara Africa because of land use changes that vary in both space and time (Kuule et al., 2022). The historical LULC changes exert pressure on rangelands with an estimated 12.8 million km^2 changes in habitable drylands of arid, semiarid, and dry sub-humid zones in Sub-Sahara Africa (Kuule et al., 2022). Population growth is a major factor that promotes sedentary pastoralism effecting an increase in rangeland degradation (Holechek et al., 2017), leading to vegetation cover loss and increased surface runoff (Nyatuame et al., 2020), consequently, aggravating soil erosion risk due to lack of resistive and protective mechanisms (Aghsaei et al., 2020; Stocking & Elwell, 1976). This is in line with Borrelli et al. (2017) who affirmed the effects of vegetation cover loss on the resistance mechanism inherent in soil physicochemical properties affecting erosion rate. According to Maetens et al. (2012), the impact of human-induced soil erosion risk is greater than erosion from natural causes. By analyzing the impact of land use land cover changes on 1056 soil erosion plots it was evident that soil erosion risk under semi-natural vegetation conditions produced a lower soil erosion risk rate (<1 $Mgha^{-1}yr^{-1}$) compared to soil erosion risk under plots that are directly influenced by human activities (between 6–20 $Mgha^{-1}yr^{-1}$) (Maetens et al., 2012).

2.4 Remote Sensing and Environmental Modelling

Remote sensing and environmental modelling are integral components of modern environmental science, providing valuable tools for monitoring, assessing, and understanding Earth's ecosystems (Senf, 2022). By using satellite and aerial platforms equipped with various sensors for conducting remote measurement operations, remote sensing enhances the acquisition of the earth's surface information for environmental modelling and monitoring purposes (Jafarbiglu & Pourreza, 2022). Given the variety of options with distinct characteristics, the selection of appropriate satellite and aerial platforms depends on the specific nature of the problem at hand (Jafarbiglu & Pourreza, 2022; Zhu et al., 2022). Typically, satellite images can be useful based on their temporal and spatial characteristics with high-resolution data required for extensive surveys in certain precision agriculture purposes (Jafarbiglu & Pourreza,

2022) Over time, remote sensing techniques have evolved significantly, enabling the collection of diverse data types, including optical, thermal, radar, and lidar imagery (Kanga, 2023). These data are invaluable for monitoring changes in land cover such as vegetation health and urban spread (Hong et al., 2023). Satellite-based sensors, such as those on NASA's Landsat and European Space Agency's Sentinel missions, have been instrumental in global-scale environmental monitoring (Wulder et al., 2019).

In environmental modelling and monitoring, mathematical and computational techniques are required to simulate and predict environmental processes; thus, a combination of remote sensing and environmental models enhances the capacity to evaluate complex environmental dynamics (Maurya et al., 2023). These models range from simple to complex, encompassing atmospheric, hydrological, ecological, and climatic processes (P. Young et al., 1996). Notable environmental models include climate models (Flato et al., 2013), hydrological models like SWAT, ecosystem models such as LPJ (Sitch et al., 2003) as well as soil erosion models such as RUSLE (Renard et al., 1997) and USPED (Mitasova et al., 1996). These models are useful in predicting the impact of various driving factors on the environment, thereby helping to make informed decisions toward environmental sustainability. The synergy between remote sensing and environmental modelling enhances our ability to monitor and understand environmental changes (Cavender-Bares et al., 2020). Remote sensing data provide critical input for model calibration, validation, and scenario development (Dangol et al., 2023; Li et al., 2018). A typical case is the derivation of land cover information that is integrated into hydrological models to assess the impact of land use changes on water resources (Abbaspour et al., 2007). Similarly, land cover data are a critical component of most soil erosion models that predict soil erosion risk.

2.5 Different Soil Erosion Models and their Applicability in Various Contexts

Soil erosion models are valuable tools in predicting soil erosion risk, for assessing environmental degradation, thereby planning, designing and implementing conservation measures (Simensen et al., 2018). To understand soil loss patterns under diverse conditions spanning from natural occurrences to environmental and anthropogenic conditions, soil erosion models are designed for empirical to physically-based approaches, each with specific strengths and limitations (Alewell et al., 2019; Borrelli et al., 2021). Despite the design and availability of models for specific contexts, there are major challenges such as high data demands and parameter sensitivity that hinder the accuracy and applicability (Razavi et al., 2021). Other practical issues that impede the broader applicability and reliability of soil erosion models include calibration challenges, and scale limitations (Alewell et al., 2019). In many regions, the application of the Revised Universal Soil Loss Equation (RUSLE) and its defunct Universal Soil Loss Equation (USLE) is common (Renard et al., 1997; Wischmeier & Smith, 1978). Based on specific context and data requirements, other soil erosion models including the Modified Universal Soil Loss Equation (MUSLE), the Water Erosion Prediction Project (WEPP) (Laflen et al., 1991), the Soil and Water Assessment Tool (SWAT) (Arnold et al., 2012), the Sediment Delivery Distributed Model (SEDD) (Ferro & Porto, 2000), the Agricultural Non-Point Source Pollution Model (AGNPS) (R. A. Young et al., 1989), and the European Soil Erosion Model (EUROSEM) (Morgan et al., 1998), identifying inherent challenges and limitations.

Its simplicity and minimal data requirements make the USLE one of the most favourite and widely used empirical erosion models (Wischmeier & Smith, 1978). Though it is designed to achieve the estimation

of long-term average soil loss on cultivated lands, the USLE faces major challenges in complex terrain and diverse climates (Schürz et al., 2020). Primarily it is designed for long-term averages as opposed to specific events, thereby posing a challenge to its predictive capacity in short-term, high-intensity rainfall events (Merritt et al., 2003). RUSLE advanced an empirical relationship superior to the USLE that incorporates more refined factors to represent varying rainfall and vegetation cover, yet it suffers from similar limitations as identified for the USLE. The RUSLE cannot achieve a temporal or spatial resolution with high precision as well as it has stringent calibration requirements which make its use a major challenge in data-scarce regions (Panagoset al., 2015). Similar to the RUSLE model, the MUSLE model is a modified version of the USLE that integrates sediment yield estimation options for individual storm events, thereby addressing some event-specific limitations in USLE (Benavidez et al., 2018). Despite its advantage, its application in many geographic contexts where seasonal rainfall intensity varies significantly may not yield accurate results owing to its overreliance on storm characteristics (Verheijen et al., 2009). A simple conceptual erosion model such as SEDD prevents an advantage over MUSLE in sediment yield estimation from catchments by simulating sediment transport pathways (Borrelli et al., 2021). Though the SEDD model has a simplified design, it could not adequately account for spatial variability in erosion, thereby making its use in complex terrains challenging.

Hydrological models such as the SWAT and WEPP are also applicable for soil erosion risk predictions (Pandey et al., 2021; Wang et al., 2023). With a wide hydrological simulation advantage, the SWAT model is a comprehensive watershed model suitable for large-scale applications (Pandey et al., 2021). Despite its versatility and advantage, its usage is constrained by its extensive data demand and calibration as well as the high cost thereby limiting its accessibility in resource-constraint settings (Pohlert et al., 2007). Similarly, the WEPP model simulates soil erosion processes across different temporal and spatial scales with the complexity of high data requirements as a limiting factor, especially in areas where access to extensive hydrological and climate datasets is limited (Lew et al., 2022). The application of the WEPP model offers high variability in predictions owing to the model's sensitivity to input parameters, justifying its rigorous calibration requirement (Borrelli et al., 2021). Typical to other empirical and physical models, EUROSEM's data demands make its application in data-limited regions not feasible though it offers a dynamic option for event-based erosion risk predictions (Morgan et al., 1998). In the context of Mediterranean environments, the design of the SEMMED model focuses on seasonal precipitation patterns peculiar to Mediterranean climates. Though its usage is highly relevant in Mediterranean regions, SEMMED's application outside the Mediterranean produced poor results, emphasising a critical limitation of highly specialised SEMMED models (De Jong et al., 1999).

For a better understanding of the global application of soil erosion prediction models, Borrelli et al. (2021) comprehensively reviewed relevant peer-reviewed research literature on soil erosion modelling published between 1994 and 2017. By creating Global Applications of Soil Erosion Modelling Tracker (GASEMT) a comprehensive insight into the state-of-the-art soil erosion models and model applications worldwide was provided. (Borrelli et al., 2021). Out of the numerous erosion models used, 25 models were identified as the most prominent with RUSLE and its defunct version, the USLE model being the most used in different regions (Table 2.1).

Table 2.1. Lists of the Top 25 Most Applied Soil Erosion Prediction Models According to the Records Reported In the GASEMT Database.

Model	Records	%	References
RUSLE	507	17.1	(Renard et al., 1997)
USLE	412	13.9	(Wischmeier & Smith, 1978)
WEPP	191	6.4	(Laflen et al., 1991)
SWAT	185	6.2	(Arnold et al., 2012)
WaTEM/SEDEM	139	4.7	(Van Oost et al., 2000)
RUSLE-SDR	115	3.9	-
USLE-SDR	64	2.2	-
LISEM	57	1.9	(De Roo et al., 1996)
Customised approach	53	1.8	
MUSLE	52	1.7	-
MMF	48	1.6	(Morgan et al., 1984)
AnnAGNPS	47	1.6	(R. A. Young et al., 1989)
RHEM	44	1.5	(Nearing et al., 2011)
Unknown	36	-	-
Erosion 3D	29	1.0	(J. Schmidt et al., 1999)
EPIC	25	0.8	(Williams et al., 1983)
PESERA	23	0.8	(Govers et al., 2003)
USPED	22	0.7	(Mitasova et al., 1996)
GeoWEPP	20	0.7	(Renschler, 2003)
RUSLE2	20	0.7	(Foster et al., 2013)
EPM	19	0.6	-
STREAM	19	0.6	(Cerdan et al., 2002)
RUSLE/SEDD	16	0.5	(Ferro & Porto, 2000)
DSESYM	15	0.5	(Yuan et al., 2015)
EUROSEM	15	0.5	(Morgan et al., 1998)

(Source: Borrelli et al., 2021).

Besides the peculiar models used in the context of soil erosion risk modelling, holistic approaches have enormous benefits for deforestation monitoring, climate change impact assessment, precision agriculture and disaster management (Hansen et al., 2013; Sitch et al., 2015; Wulder et al., 2019). Such approaches employ diverse models to simulate complex interactions within ecosystems between various variables. The SWAT model combines hydrological, land use, and water quality models and is useful in a holistic watershed and river basin assessment beyond water availability, water quality, sedimentation, and irrigation requirements (Arnold et al., 2012). Despite the significant advancement in environmental monitoring through the application of empirical models (Jinyue Chen et al., 2022; J. Li et al., 2020), data requirement and integration issues, model validation complexities, and the need for high-performance computing are some of the major bottlenecks (Linder & Horne, 2018). Overall, the integration of remote sensing into environmental modelling has significantly advanced the understanding of Earth's complex systems (Senf, 2022) and the prospects to monitor environmental changes to assess their impacts and formulate effective strategies for sustainable resource management and conservation.

2.6 Landscape and Soil Erosion

Landscape is a spatially heterogeneous space with attributes such as topography, vegetation, geology, soil, water bodies, and human structures among others (Turner et al., 2001). Similarly, Antrop (2005) defines landscape as a spatially diverse area shaped by the interaction of natural processes and human

activities over time. Landscapes are shaped by geomorphological processes, climatic conditions, and human interventions such as agriculture and urbanisation (Tarolli & Sofia, 2016). Owing to the multidimensional characteristics of landscapes, they are useful frameworks for understanding environmental processes such as soil erosion; assessment of changes, spatial variability and impacts of human activities (Shi et al., 2022). Major landscape units can be classified into mountainous, plains, plateaus as well as urban, coastal, and agricultural units based on their prevailing conditions and attributes (Reddy et al., 2017).

The degree of soil erosion risk is controlled by the prevailing landscape attributes. The factors topography, intensive agriculture, deforestation and climatic conditions such as rainfall intensity and distribution are key drivers of soil erosion (Guerra et al., 2020). The interaction of these influencing factors with the physical attributes of landscapes exposes the landscape's exposure to erosion (Tarolli & Sofia, 2016). Distinctively, mountainous landscapes with steep slopes are particularly characterised by high erosion risk due to their high energy potential and resulting high-velocity pf runoff. In contrast, landscapes with dense vegetation cover act as natural buffers that stabilise soil and intercept raindrops (Lann et al., 2024). Wetlands and riparian landscapes trap sediments and slow down run-off thereby reducing soil erosion risk (Prosser et al., 2020). Conversely, urban and agricultural landscapes that are strongly modified by human activities are characterised by high exposure to soil erosion due to soil land surface compaction, depletion of vegetation cover, and resulting surface runoff (Bettoni et al., 2023; Ferreira et al., 2022).

Landscapes can be categorised into homogeneous units by mapping and classifying key attributes (Cullum et al., 2016). With a landscape framework, the common tools and techniques used to classify landscape units include GIS and remote sensing, hydrologic and erosion models and participatory approaches (Arnold et al., 1998; Newton et al., 2009). GIS and remote sensing applications allow overlaying multiple satellite images to identify areas with homogenous attributes to be classified as landscape units. The topographic attributes such as elevation, slope, and aspect are major considerations in landscape characteristics (Singh, 2018; Wang & Cheng, 2023). The elevation is a primary factor in landscape characterisation as it affects other physical attributes, including vegetation cover types and climatic conditions (Wang et al., 2024). The influence of slope on runoff and its associated erosion makes it a crucial parameter in landscape characterisation. Steep slopes often result in rapid runoff and thereby controlled strong erosion, and reduced soil stability, which directly affect vegetation establishment and persistence (Scotton & Andreatta, 2021). Also, slope length and angle are important determinants of land-use potential and suitability, particularly for agricultural zoning and environmental planning while the aspect of slope influences sunlight exposure that creates localised microclimates within the landscape and shapes vegetation growth patterns (Dornik et al., 2022; Måren et al., 2015). In hydrological studies, the Topographic Wetness Index (TWI) is a widely used metric that quantifies soil moisture distribution and potential water accumulation based on the landscape's topography (Raduła et al., 2018). It combines slope and upstream contributing areas to identify areas prone to wetness or dryness, with emphasis on high TWI values as water accumulation areas with associated risks such as flooding. As such, TWI plays a critical role in landscape characterisation, aiding in the identification of areas with distinct hydrological properties and supporting the management of flood-prone areas and high erosion risks (Al-Kindi & Alabri, 2024). The integration of these attributes in landscape characterisation is important for a better understanding of the landscape and potential environmental risks such as erosion risk.

Overall, the landscape approach in soil erosion risk assessment underscores the critical need for integrated conservation management practices that address erosion at landscape units. According to (Gray et al., 2016), effective erosion control requires monitoring across administrative boundaries and land uses to ensure that conservation measures, such as reforestation and terracing, are implemented at a scale that maximises their impact. Because soil erosion is not confined to specific plots of land but affects entire landscapes, assessment of erosion risk at the landscape unit would help identify high erosion risk hotspots to inspire targeted conservation interventions (Arega et al., 2024).

CHAPTER 3: STUDY SITE

This Chapter presents a comprehensive description of the study site in terms of the natural and physical characteristics compositing the soil, geology, and climatic conditions. The chapter also highlights the population dynamics in the basin and the general socio-economic and livelihood diversification in the area.

3.1 Location and Administrative Settings of the Black Volta Basin

The Black Volta basin is a transboundary river basin shared between four West African countries (Mali, Burkina Faso, Ghana and Cote d'Ivoire) (Akpoti et al., 2016). As a transboundary river system, the basin stretches from North to South through Mali, Burkina Faso, Ghana and Côte d'Ivoire, and from Burkina Faso, Côte d'Ivoire and Ghana from West to East (Figure 3.1 C).

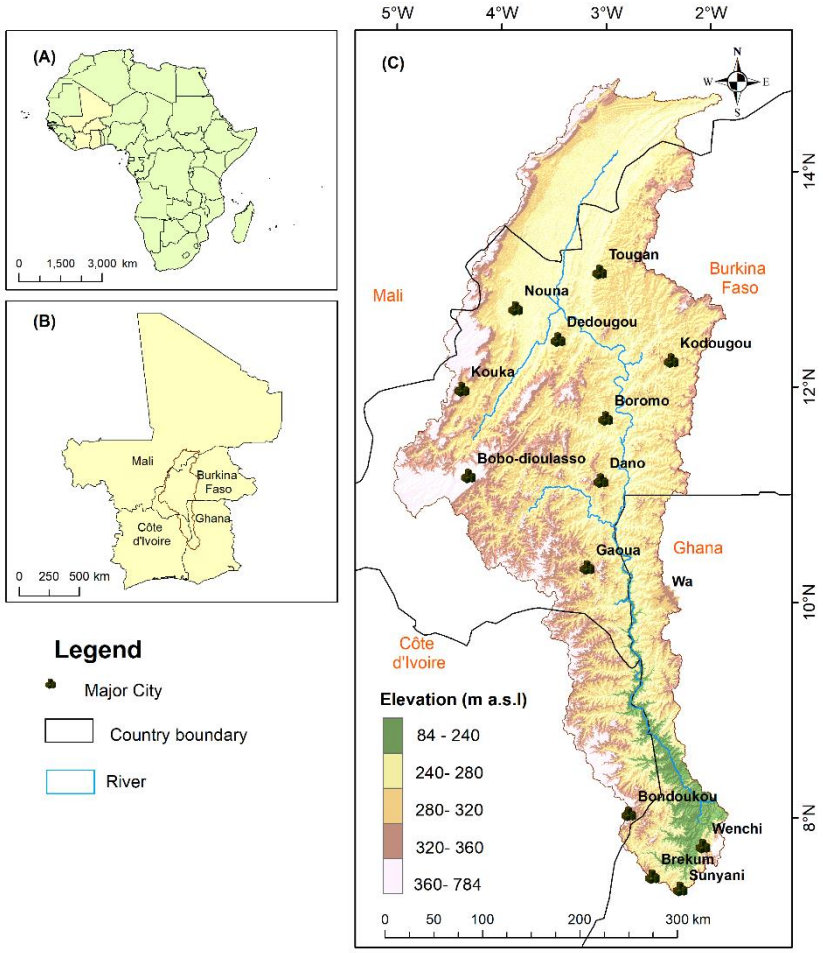

Figure 3.1. Land Elevation Map of the Black Volta River Basin Located in the West Africa Sub-Region Region. (A) A map of Africa displaying in shade, the four transboundary counties within the West Africa Sub-region. (B) Map of the Black Volta River basin located within the four transboundary countries (C) The map of the Black Volta River basin displayed in digital elevation model (DEM); emphasising cities and the Black Volta River (Source of data: Shuttle Radar Topography Mission (SRTM) DEM, obtained from United States Geological Survey's (USGS) Earth Explorer database. Retrieved from https://earthexplorer.usgs.gov/ on 18 April 2023).

The Black Volta basin is located between latitudes 7.0°N and 14.3°N, and from longitude 5.5°W to 1.5°W W with an estimated landmass of about 138,000 km^2 (Akpoti et al., 2016). It is a major sub-basin of the Volta river basin system which comprises the Black and White Volta and constitutes about 32.6% of the Volta basin. The topography of the Black Volta basin is generally slightly undulating with < 800 m a.s.l elevation. The elevation in the northern part of the basin is between 200 to 500 m a.s.l with very flat or moderately sloping terrain. A major urbanising municipality in the basin is the Wa municipality (Figure 3.1) located in the upper west region of Ghana (between 10◦ 14′ 46.32″ N and 09° 42′ 5.04″ N and 02° 33′ 14.04 W and 02° 0′ 57.96″ W). The municipality is characterised by slightly undulating terrain in the savannah high plains, with elevations between 160 and 300 m a.s.l. Further details of the Wa municipality are provided in Chapter 5 (Asempah et al., 2021) and Chapter 6 (Asempah et al., 2024).

3.2 Natural Characteristics of the Black Volta Basin

3.2.1 Climate

The Black Volta basin has a distinct climate which is primarily influenced by a southwesterly tropical maritime air mass and a northeasterly tropical continental air mass (Grams, 2008; Mul et al., 2015). By converging at the Inter-Tropical Convergence Zone (ITCZ), the two air masses create a region of low pressure with quasi-frontal characteristics that migrates across West Africa (Grams, 2008). The regional amount of rainfall is influenced by the ITCZ which exhibits vigorous frontal activity. The onset of the rainy season at any given location coincides with the northward passage of the ITCZ and concludes with its southward retreat, resulting in a general decrease in rainfall from south to north (Lélé and Lamb, 2010). The West African Monsoon occurs between May and August/September (Nicholson, 2009). During this time, the ITCZ shifts northward, and the countries within the Volta Basin are exposed to the influence of the tropical maritime air mass (McCartney et al., 2012). From November to March, the Harmattan with its hot, dry usually dusty wind originating from the northeast or east dominates the climate in the Black Volta basin (Kasei, 2010).

Annual rainfall patterns in the Black Volta basin are predominantly bimodal, especially in the southern part of the basin (Abungba et al., 2022; Akpoti et al., 2016). To the north of the Black Volta basin, the time interval between the two rainfall peaks diminishes until only a single peak is experienced. The amount of mean annual rainfall varies between 300 mm in the north of the Black Volta basin and 1,300 mm in its south (Figure 3.2). In general, the Basin is spread across four climatic zones based on the spatial distribution of rainfall, including from north to south the Sahelian Zone, the Sudano-Sahelian Zone, the Sudan Zone, and the Guinean Zone (Mul et al., 2015).

In the northern part of the Black Volta basin, the Sahelian (mean annual rainfall < 500 mm) and the Sudano-Sahelian zones (mean annual rainfall between 500 and 900 mm) have a unimodal rainfall season between May and September and distinctly lower annual rainfall than in its southern part (Mul et al., 2015). The Sudanian and Guinean zones are in the central and southern part of the Black Volta basin and experience a bimodal rainfall pattern, marked by two distinct rainfall seasons (Nkrumah et al., 2019). The Sudanian Zone is characterised by mean rainfall between 900 and 1,100 mm. The mean annual rainfall within the Guinean Zone ranges from 1,000 to 1,300 mm (Mul et al., 2015; Piacentini et al., 2018). The major rainy season within the Guinean Zone spans from April/May to June/July while the minor season occurs in September/October (Piacentini et al., 2018).

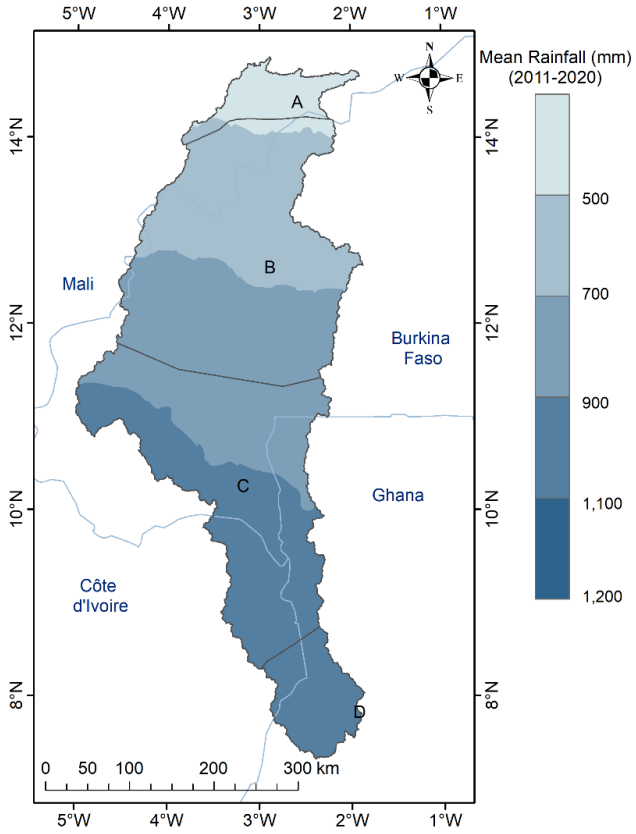

Figure 3.2. Mean Annual Rainfall Distribution Map Across the Agro-Climatic Zones A (the Sahelian Zone), B (the Sudano-Sahelian Zone), C (the Sudan Zone) and D (the Guinean Zone) of the Black Volta River basin. (source: Climatic Research Unit (CRU) of the University of East Anglia (https://crudata.uea.ac.uk/cru/data/hrg/).

The basin experiences relatively higher temperatures in its north compared to the south. Generally, the south is characterised by a mean annual temperature of about 27 °C in the south and increases to 36 °C in the north (Agyekum et al., 2022; Oguntunde & Abiodun, 2013). In some cases, the basin experiences a daily maximum temperature of up to 44 °C, whereas night temperatures could drop to 15 °C (Mul et al., 2015). The mean temperatures within the Sudanian and Guinean zones never fall below 24 °C. In contrast, the mean annual temperatures are higher than 29 °C in the Sahel and the Sudan-Sahelian zones (Barry et al., 2005).

The relative humidity is generally highest in the south of the Black Volta basin owing to the high rainfall with low temperatures experienced in this zone. Toward the Guinean zone, relative humidity increases temporally up to about 95–100% during the rainy season (Mul et al., 2015). The Sahelian and the Sudano-Sahelian zones in the north of the Black Volta basin are characterised by low relative humidity of about 20– 30%, especially during the Harmattan season, however, this rises to about 70– 80% during the rainy season (Barry et al., 2005). The mean annual potential evapotranspiration in the north of the Black Volta basin could exceed 2,500 mm. In the south of the Black Volta basin mean annual potential evapotranspiration is estimated to amount to 1,500 mm per annum with actual evapotranspiration

between 10 mm d^{-1} in the rainy season and about 2 mm d^{-1} in the dry season depending on the soil properties (Mul et al., 2015).

3.2.2 Geology

The parent materials of the Black Volta basin belong to two major geological provinces; the basement crystalline and the unconsolidated sedimentary provinces (Mul et al., 2015) (Figure 3.3). Bedrock of the crystalline formations and bedrock of the unconsolidated provinces is built by Tertiary sandstones and sedimentary formations (Carrier et al., 2008).

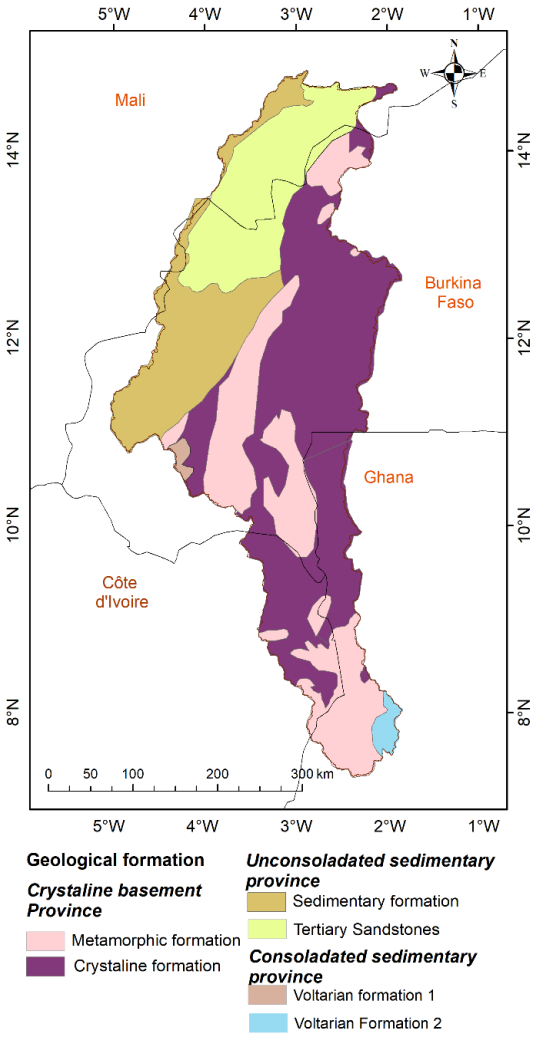

Figure 3.3. Geological Map of the Black Volta River Basin Showing Various Geological Formations (Source: Lemoalle and de Condappa 2009, Mul et al., 2015).

The Black Volta basin is primarily characterised by the dominance of basement crystalline rocks, which occur in the southeastern and southwestern part of the basin; these rocks underlie approximately 40% of the total land area in sub-Saharan Africa. The composition of the crystalline basement includes various types of strongly deformed metamorphic rocks, igneous rocks and granite-gneiss-greenstone rocks (Key, 1992). Generally, the crystalline basement constitutes a complex assemblage of igneous and metamorphic rocks that form stable and rigid foundations and are more resistant to weathering compared to sedimentary formations due to their dense and crystalline nature (Selby, 1982). The bedrock in the northern part of the Black Volta is characterised by the unconsolidated Tertiary sandstone and

sedimentary formations Mul et al. (2015) The crystalline basement and sedimentary formations are typically covered by regolith whose thickness varies locally controlled by topography, bedrock, structural characteristics, vegetation cover, and (paleo--) climate (Dewandel et al., 2006). Within the crystalline basement, the regolith may reach up to 140 meters, particularly central part of the basin; at least it reached c. 30 (Dapaah-Siakwan & Gyau-Boakye, 2000; Mul et al., 2015).

3.2.3 Relief and Hydrography

The terrain of the Black Volta River basin exhibits gently undulating characteristics with elevations ranging from 84-784 m a.s.l. The higher elevations are located around the western part of the basin. The northern part of the basin, which belongs to the Sahelian Zone, is almost flat with elevations of 240-780 m a.s.l. (Kwakye & Bárdossy, 2020). The southern portion of the basin is characterised by low-lying areas, with elevations between 84-300 m a.s.l. (Kwakye & Bárdossy, 2020).

Within the scope of the wider Volta River system, the Black Volta River serves as the primary headwater that originates from southern Mali. It traverses the major transboundary countries Burkina Faso, Côte d'Ivoire, and Ghana, encompassing a drainage area of about 138,000 km² (Akpoti et al., 2016). The main tributaries of the Black Volta River are Grand Bale, Bougouriba, Gbongbo, Voun Hou, Sourou, Wenare, Bondami, Bambassou, Tain and Poni rivers (Mul et al., 2015). The water resources in the basin are mainly used for hydropower generation, small-scale irrigation and domestic water supply (Kwakye & Bárdossy, 2020). The morphological attributes of the water courses are changing as major constructions such as dams cause a diversion of the Black Volta River. The Black Volta River used to join the White Volta River in the south-eastern part of Ghana, but after the construction of the Volta Dam the Black and White Voltas do not confluence anymore, but rather drain into the lake through a separate channel (Kwakye & Bárdossy, 2020).

3.2.4 Soils

The Black Volta River basin is characterized by a diverse range of soil types (Fischer et al., 2008). The most prominent soil types in the basin include Ferric Luvisols, Gleyic Luvisols, Eutric Cambisols and plinthic Luvisols (Figure 3.4). The Ferric Luvisols which are dominant in the southern part of the basin (Ghana part) and in its northern part (Burkina Faso) are classified as Ferric due to the presence of iron oxides, which impart a reddish-brown coloration to the soil profile (Fischer et al., 2008; Mul et al., 2015). The presence of Ferric Luvisols in the Black Volta River basin has implications for agricultural productivity, water and nutrient retention, and ecosystem dynamics within the region (Kombat et al., 2021; Mul et al., 2015). The distinctive properties of these soils, such as their clay content, organic matter, and iron oxide content, contribute to their ability to support various vegetation types and land use practices (de Andrade Bonetti et al., 2017).

Also, the Gleyic Luvisols which predominantly occur along the alluvial plains is characterised by poor drainage or periodic waterlogging (Fischer et al., 2008). The Gleyic Luvisols areas affect land use, agriculture, ecosystem dynamics, vegetation distribution and nutrient availability owing to their variable drainage patterns and waterlogged conditions (Kibblewhiteet al. 2015). While Ferric Luvisols show moderate resistance to erosion due to the presence of clay particles in the soil matrix, agricultural activities can increase vulnerability. On the other hand, Gleyic Luvisols, which develop under

periodically waterlogged or poorly drained conditions, tend to be more susceptible to erosion due to the in general flat relief in the alluvial plains where they predominantly occur (Bedard-Haughn 2011).

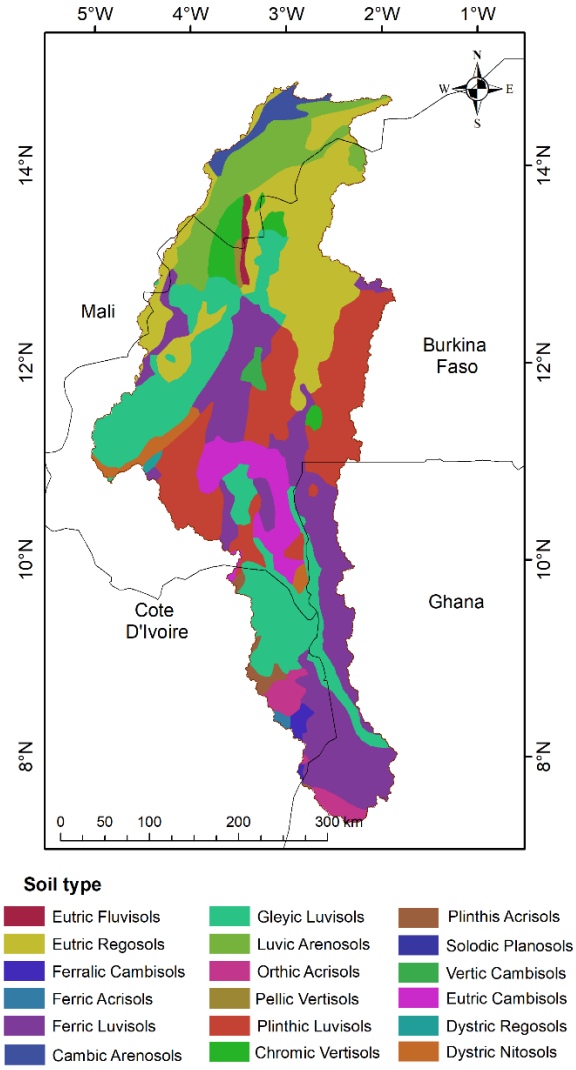

Figure 3.4. Soil Map of the Black Volta Basin (Data source: Food and Agriculture Organisation of the United Nations (FAO), 2008).

The Eutric Cambisols and Plinthic Luvisols are located predominantly in the central part of the basin (Fischer et al. 2008). The dominance of Eutric Cambisols stretches across Burkina Faso and Ghana. The Eutric Cambisols in the Black Volta basin are typical soils in slopy positions of the slightly rolling terrain and support crop production due to their high nutrient content and well drainage properties (Fischer et al. 2008). Patches of other major soil types such as Chromic Vertisols, Ferralic Cambisols and Plinthis Acrisols spread across the basin but are minor in distribution (Fischer et al. 2008).

3.2.5 Vegetation Cover

The northern part of the Black Volta basin is characterised by sparse vegetation in the savannah plain and dominated by drought-resistant grasses, shrubs, and tree species such as *Acacia spp*., *Balanites aegyptiaca*, and *Commiphora africana* (Akpoti et al., 2016). The Central toward the southern part of the

basin is characterised by a semi-deciduous forest with *Celtic-Triplochiton* and *Antiaris-Chlorophora* as the primary vegetation cover (Barry et al., 2005). These areas are extensively cultivated with cash crops such as cocoa and shea (Barry et al., 2005). The extensive agriculture coupled with logging activities makes vegetation outside of forest reserves largely reduced to forb regrowth, thickets, secondary forests, and swamp thickets (Mechiche-Alami & Abdi, 2020). The southmost part of the Black Volta basin is characterised by closed savannah vegetation with a mosaic of woody biomass, grasses of varying heights, interspersed with fire-resistant, deciduous, broad-leaved forests, and forest margins within the southern corridor of the basin (Barry et al., 2005). Some major tree species in this area include *Afzelia Africana*, *Prosopis Africana*, *Lophira lanceolata*, and *Butyrospermum parkii* among others (Gordon et al., 2013). The main land use and land cover classes of the basin based on Copernicus global landcover data (https://cds.climate.copernicus.eu/) include Closed Savannah, Open Savannah, Grassland, Cropland, Urban Area, and Bareland. Vegetated Wetlands and Water Bodies (Figure 3.5) (Buchhorn et al., 2020).

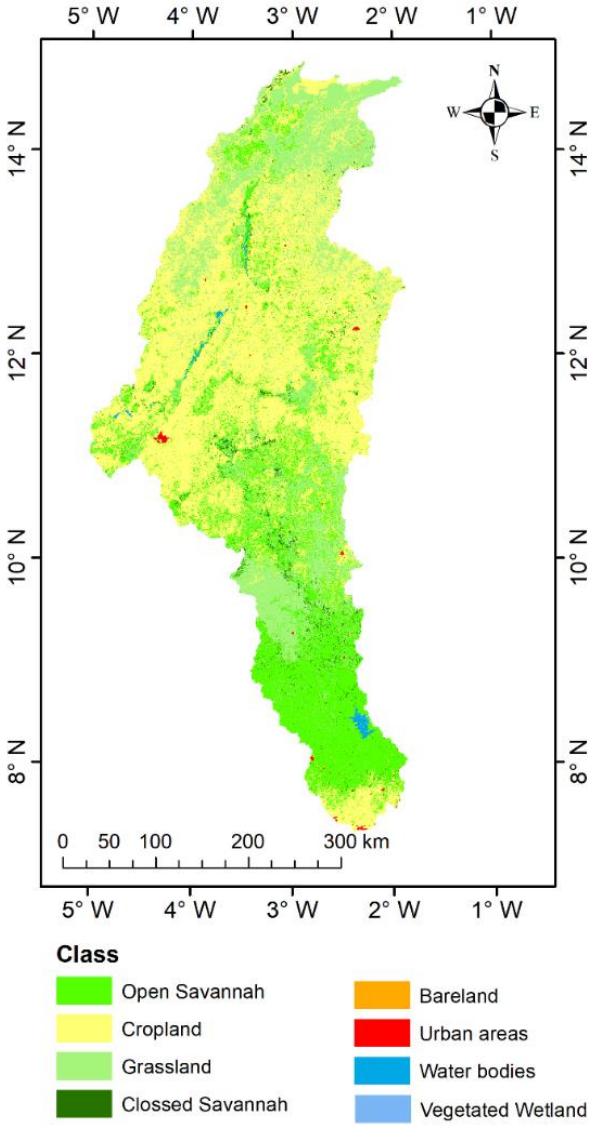

Figure 3.5. Land Use and Land Cover Map of the Black Volta Basin for the Year 2020.

3.3 Characterisation of the Major Landscape Units

A landscape, as defined by (Antrop, 2005) is a spatially diverse area shaped by the interaction of natural processes and human activities over time. It can be classified into homogeneous units by identifying, categorising, and mapping its features to describe key characteristics for planning (Zoderer et al., 2019). The Black Volta River basin exhibits significant diversity in its topographic, climatic, geological, and soil characteristics, which influence its geomorphology, hydrology, and land-use potential. The basin was classified into major landscape units by processing spatially differentiated data on topography (slope, aspect, elevation, curvature, TWI) (Table 3.1), climate, land cover, geology, and soil using GIS. Six major landscape units were identified: Low Sahelian Plains, Sahelian Uplands, Sahelian Highlands, Savannah Transition, Mixed Terrain Plateau, and Savannah Escarpment (Figure 3.6).

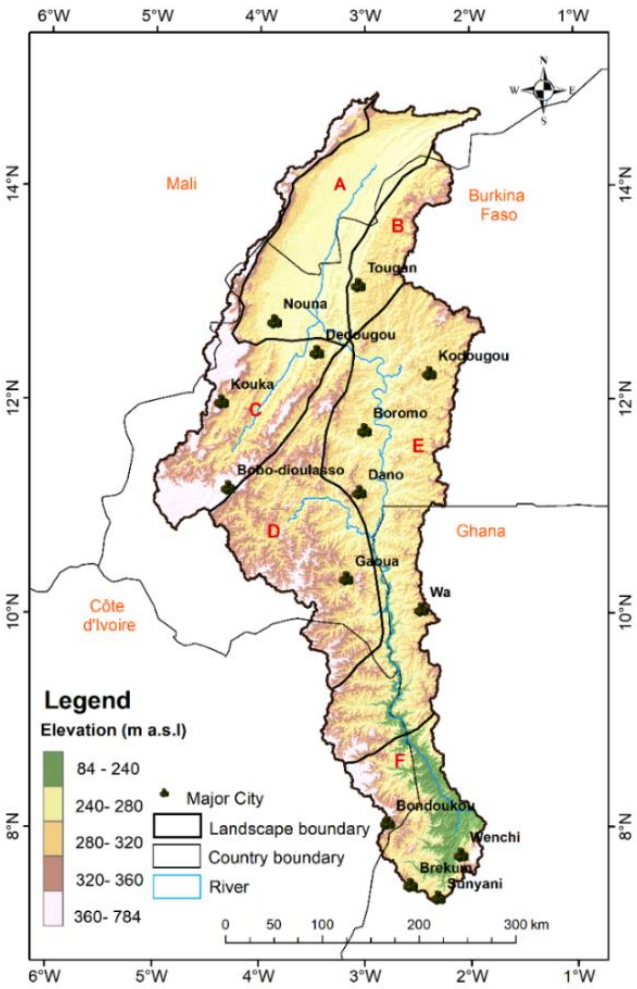

Figure 3.6. Topographic Map of the Black Volta River Basin Displaying Major Cities, Rivers and Landscape Units. Major landscape units correspond to: (A) Low Sahelian Plains, (B) Sahelian Uplands, (C) Sahelian Highlands, (D) Savannah Transition, (E) Mixed Terrain Plateau, (F) Savannah Escarpment. (Data source: Shuttle Radar Topography Mission (SRTM) DEM, obtained from the United States Geological Survey's (USGS) Earth Explorer database https://earthexplorer.usgs.gov/ on 18 April 2023).

The underlying geological formations of the basin include sedimentary, crystalline, and metamorphic bedrock. Sedimentary formations dominate the Low Sahelian Plains and Sahelian Highlands, while crystalline formations are prevalent in the Sahelian Uplands and Mixed Terrain Plateau. The Savannah

Transition and Savannah Escarpment landscape units are primarily characterised by metamorphic formations. Soils in the landscape units of the Black Volta basin are mainly characterised by Ferric Luvisols and Gleyic Luvisols. Beyond, Eutric Regosols dominate in the Sahelian Highlands, Low Sahelian Plains, Sahelian Uplands and the Mixed Terrain Plateau landscape units.

Rainfall in the northern landscape units (Sahelian Plains, the Sahelian Uplands, the Sahelian Highlands) is generally low with a mean annual rainfall of less than 700 mm with a single rainfall season. The mean annual temperature of these landscape units is about 36 °C (Agyekum et al., 2022; Oguntunde & Abiodun, 2013). The Savannah Transition and Savannah Escarpment landscape units are characterised by two distinct rainfall seasons with the primary rainy season beginning in April or May and peaking in June or July, while the secondary rainfall season starts in September or October, with its peak occurring around the same time (Piacentini et al., 2018). The mean annual rainfall within these landscape units amounts below 1,100 mm, and the mean annual temperature averages 27 °C (Agyekum et al., 2022).

Table 3.1. The Summary Statistics of Topographic Features.

Elevation	Mean (μ)	Std (σ)	Min.	Max.
Low Sahelian Plains	274	19.4	243	459
Sahelian Uplands	302	21.0	256	486
Sahelian highlands	356	70.3	251	772
Savannah Transition	312	33.6	231	568
Mixed Terrain Plateau	291	30.8	191	580
Savannah Escarpment	268	72.1	84	729
Slope				
Low Sahelian Plains	0.7	0.52	0.0	18.3
Sahelian Uplands	0.7	0.58	0.0	16.3
Sahelian highlands	1.3	1.89	0.0	51.4
Savannah Transition	1.4	1.38	0.0	29.1
Mixed Terrain Plateau	1.1	0.90	0.0	31.0
Savannah Escarpment	2.0	1.98	0.0	43.7
Planform Curvature				
Low Sahelian Plains	0.0	0.03	-0.4	0.5
Sahelian Uplands	0.0	0.02	-0.5	0.3
Sahelian highlands	0.0	0.03	-1.4	1.2
Savannah Transition	0.0	0.03	-0.6	0. 6
Mixed Terrain Plateau	0.0	0.03	-0.6	0.5
Savannah Escarpment	0.0	0.03	-1.4	0.7
Profile Curvature				
Low Sahelian Plains	0.0	0.03	-0.3	0.4
Sahelian Uplands	0.0	0.02	-0.9	1.1
Sahelian highlands	0.0	0.03	-0.5	0.5
Savannah Transition	0.0	0.03	-0.4	0.8
Mixed Terrain Plateau	0.0	0.03	-0.6	1.2
Savannah Escarpment	0.0	0.04	-0.3	0.4
TWI				
Low Sahelian Plains	-0.3	2.54	-6.0	14.7
Sahelian Uplands	-1.0	2.14	-5.8	11.7
Sahelian highlands	-1.5	2.22	-7.1	14.2
Savannah Transition	-1.7	2.10	-6.4	14.1
Mixed Terrain Plateau	-1.5	2.13	-6.3	15.2
Savannah Escarpment	-2.1	2.07	-6.9	14.1

The vegetation cover across the Black Volta drainage basin is characterised by open savanna vegetation. The northern landscape units (Low Sahelian Plains, Sahelian Uplands and Sahelian highlands) mainly serve as cropland. Grassland and the open savannah vegetation dominate the Savannah Transition and the Mixed Terrain Plateau landscape units. Topographic attributes such as elevation, slope, and aspect are fundamental parameters that strongly influence landscape characteristics (Singh, 2018; Wang & Cheng, 2023). The elevation gradient is especially critical in mountainous or hilly terrains, where strong inclinations create zones with distinct ecological characteristics (Gong et al., 2017). Also, strong inclinations affect high runoff velocities, erosion, and soil stability (Bettoni et al., 2023; Jourgholami et al., 2021). The most elevated (251–772 m a.s.l.) and steepest landscape unit is located in the northern part of the Black Volta basin and corresponds to the Sahelian Highlands. The Low Sahelian Plains, on the other hand, are characterised by a flat and low-lying terrain with elevation ranges of 243-459 m a.s.l. The southmost part of the basin is delineated as the Savannah Escapement landscape unit and shows a wide range of elevations (84–729 m a.s.l.) and is characterised by mean slopes of 2.04° /σ= 1.98 (Table 3.1). The Savannah Transition and the Mixed Terrain Plateau landscape units spread from the central to the southern part of the basin and are characterised by moderate elevation ranges of 191–568 m a.s.l., with average slopes in the Savannah Transition landscape unit of 1.39° (σ= 1.38) and moderately mean slopes of 1.13° (σ= 0.90) in the Mixed Terrain Plateau landscape unit.

The TWI estimates show a negative mean across all six landscape units, indicating limited water accumulation across the basin. The lowest mean TWI (-2.12) was estimated for the Savannah Escarpment landscape unit, causing the driest topographic conditions, likely due to steep slopes that inhibit water accumulation. The Low Sahelian Plains landscape unit on the other hand records the highest mean TWI (-0.30), indicating relatively wet terrain conditions. Altogether high standard deviations and ranges of TWI across all landscape units (Table 3.1) indicate strong heterogeneity in water accumulation patterns. The mean plan and profile curvature are 0 across all the landscape units underscores the altogether flat terrain. The variability of the curvature is low with a standard deviation in the range of 0.02 and 0.04.

3.4. Population Dynamics and Urbanisation in the Black Volta Basin

There is limited information about the current overall population of the Black Volta basin due to a lack of harmonisation of population census data for all the districts and provinces transcending Mali, Burkina Faso, Côte d'Ivoire, and Ghana. In the year 2000, the basin had a population density in the range of 8 to 133 people/km^2 with a total of about 4.5 million inhabitants (Akpoti et al., 2016; Allwaters Consult, 2012). It has been projected that the population within the Black Volta basin will grow to about 8 million by the year 2025 with an estimated annual population growth rate of 3% (Akpoti et al., 2016). A low population density of 8 people/km^2 in the year 2000 was estimated for the rural Bouna department in Côte d'Ivoire and Sissala district in Ghana (Allwaters Consult, 2012). In contrast, the 2021 population and housing census estimated a population density of 33.41/km^2 for the Bouna department and 34.43/km^2 for the Sissala districts. Other major districts within the Black Volta basin such as the Lawra district and the Wa municipality, both Ghana, are fast-growing with high population density and are considered as highly urbanising (Dambeebo & Jalloh, 2018).

3.5. Socioeconomics and Livelihood in the Black Volta Basin

Owing to the transboundary nature of the Black Volta basin, cross-border migration is a core aspect of the population dynamics. The major economic and livelihood activities in the basin are agriculture and fishing with a significant number of the inhabitants engaged in subsistence farming (Nkpeebo & Mavimbela, 2023). In the Burkina Faso part within the Sahelian and Sudano-Sahelian climatic zones of the basin rain-fed agriculture covers more than 90% of cultivated land (Sylla et al., 2021). The Ghana part of the Black Volta basin is located in the Guinean agro-climatic zone and is dominated by rainfed subsistent farming (Nkpeebo & Mavimbela, 2023). Due to the great agricultural production potential, there has been cross-border migration for crop farming and pastoral activities within the Guinean zone in Ghana (Tonah, 2002).

Despite the dominance of rain-fed agriculture, the riparian communities practice small-scale irrigation farming. The major crops produced in the basin especially in Ghana part of the Black Volta basin include yam, cassava, groundnuts, beans and cereals such as rice, millet, sorghum, and maize (Barry et al., 2005). Though the free-range grazing system of animal rearing is mainly practised in the basin, livestock owners and herdsmen seasonally migrate with their animals from the Sahehel region in search of water and greener pasture to the south during the dry season (Andah et al., 2003; Timpong-Jones et al., 2023). Also, small-scale mineral mining operations have become prevalent in the Black Volta basin. (Barry et al., 2005; Locatelli et al., 2011). As a significant economic activity in the Black Volta River basin, particularly in Burkina Faso and Ghana, gold is extracted using rudimentary methods and technologies (Barry et al., 2005). Due to the livelihood and revenue potential many inhabitants are redirecting their livelihood activities to the small-scale gold mining operations, in Burkina Faso dominated by women (Hentschel et al., 2003).

CHAPTER 4: MATERIALS AND METHODS

The research applied geospatial tools and techniques in processing remote sensed data to answer the pertinent research questions of the study. This chapter highlights the core methodological approaches used in accomplishing the objectives of the study.

Table 4.1. Overview of the Methodological Flow

Objective	**1** Evaluation and determination of the LULC dynamics and its drivers in the Wa municipality between 1990 and 2020.	**2** Estimation of soil erosion risk in the savannah landscape of Wa municipality, Ghana between 1990 and 2020.	**3** Estimation and evaluation of soil erosion risk across various landscape units of the Black Volta River basin considering the time slices 1992, 2006 and 2020.
Data	Landsat satellite data: Landsat 5, pathway: 195/053, date: 12.10.1990), Landsat 7, pathway: 195/053, date: 3.11. 2001 Landsat 5, pathway: 195/053, date: 12.11.2010 Landsat 5, pathway: 195/053, date: 15.11.2020, Shuttle radar topography mission (SRTM) Digital Elevation Model (DEM) (https://earthexplorer.usgs.gov/), Location data from the open street map (https://download.geofabrik.de/) and ground truth data.	Land cover maps (Asempah et al., 2021) soil maps (https://soil.grids.org), meteorological data (https://power.larc.nasa.gov/) and in-situ data of measured erosion damages.	Copernicus Global land cover map (https://cds.climate.copernicus.eu/), meteorological data (https://crudata.uea.ac.uk/cru/data/hrg/), soil grid data (https://soil.grids.org), SRTM DEM (https://bigdata.cgiar.org/srtm-90m-digital-elevation-database/), Geological data (Mul et al., 2015) and (https://www.fao.org/soils-portal/data-hub/soil-maps-and-databases/harmonised-world-soil-database-v12/en/).
Methods	Ground truthing of land uses and land cover, supervised LULC and accuracy assessment applying tools and metrics such as Error matrix (overall accuracy, producer accuracy, user accuracy), binomial logistic regression and model evaluation.	Field mapping of land cover and erosion damages, estimation of potential and actual soil erosion risks applying the RUSLE model, on-site spatial measurement of soil erosion damages, statistical correlation analysis	Quantitative Landscape Characterisation, estimation of soil erosion risk applying RUSLE model, Assessing the major influencing factor on soil loss.
Outputs	LULC maps and associated statistical outputs, predictor drivers of settlement expansion and model-evaluated outputs.	soil erosion risk estimation, maps of erosion damages	Landscape units, LULC maps, soil erosion risk estimation per landscape unit applying RUSLE model, estimates of soil loss.

4.1 Data Sources

The required data include topography, soil, climate, land use and land cover. This was acquired from an array of sources.

4.1.1 Topographic Data

The topographic features of the Black Volta River basin were extracted from the shuttle radar topography mission (SRTM) digital elevation model (DEM). The 30 m x 30 m ground resolution SRTM DEM acquired from the United States Geological Survey database (https://earthexplorer.usgs.gov/) served as data for extracting derivatives such as slope, aspect and topographic wetness index for characterising the Wa municipality. The derivatives were also used in modelling the drivers of urban expansion in the Wa municipality.

At a macro level a 90 m x 90 m SRTM DEM was used to extract derivatives for large-scale and basin-wide soil erosion risk modelling. The 90 x 90 m resolution SRTM DEM was obtained from the database of the Consortium of International Agricultural Research Centers' Consortium for spatial-information (CGIAR-CSI) (https://bigdata.cgiar.org/srtm-90m-digital-elevation-database/) in mosaiced 5° x 5° tiles for easy accessibility and download.

4.1.2 Soil Data

Global soil gridded data was obtained from the International Soil Reference Information Centre (ISRIC) database (https://soil.grids.org). SoilGrid is designed as a universally consistent, data-driven framework that forecasts soil characteristics and categories by leveraging worldwide covariates and globally calibrated models. The specific data relevant to the study include contents of clay, silt, sand, and organic carbon, which are available in the spatial resolution of 250 m x 250 m. At the ISRIC database, the data are available for soil depth below the surface of 0, 5 15, 30 and 60 cm. Weighted averages were estimated to derive a single raster of each of the soil characters required in the empirical model for the estimation of soil erosion risk.

Data obtained from the Harmonised World Soil Database (HWSD) (https://www.fao.org/soils-portal/data-hub/soil-maps-and-databases/harmonized-world-soil-database-v12/en/) corroborated the study to classify the Black Volta River basin's soil types. The HWSD is a 30 arc-second raster database encompassing more than 15,000 distinct soil mapping units. It integrates existing regional and national soil data updates from sources like SOTER, ESD, Soil Map of China, and WISE, while also incorporating the information found within the 1:5,000,000 scale FAO-UNESCO Soil Map of the World (Food and Agriculture Organisation of the United Nations (FAO), 2008).

4.1.3 Climate Data

The NASA Prediction of World Energy Resources (POWER) meteorological data and the Climatic Research Unit (CRU) of the University of East Anglia were the two main sources of rainfall data for the study. The POWER data is available in 2-days of real-time, monthly and annual temporal resolution. The monthly and annual data were explored for modelling soil erosion risk in the area of Wa municipality. For the macro-level basin-wide analysis of soil erosion risk, rainfall data was acquired from the database of the Climatic Research Unit (CRU) of the University of East Anglia

(https://crudata.uea.ac.uk/cru/data/hrg/). The CRU data is high resolution gridded time-series dataset that spans from the year 1901 to 2022 and is available in network Common Data Form (NetCDF) format in monthly temporal resolution and 0.5° x 0 .5° spatial resolution.

4.1.4 Landsat and Global Land Cover Data

Global classified land cover data are available in low temporal and spatial resolution but are crucial for macro-scale change analysis. At a micro level, Landsat data was accessed from the United States Geological Survey's (USGS) Earth Explorer website (https://earthexplorer.usgs.gov/) to classify land cover changes in the Wa municipality for the years 1990 to 2020. The satellite images for the Wa municipality with a spatial resolution of 30 m x 30 m are covered by Landsat Path 195 and Row 053 of the Landsat. For spatiotemporal analysis, satellite images from the Landsat thematic mapper (TM) were obtained for 12 October 1990, the enhanced thematic mapper (ETM) were obtained for 3 November 2001 and 12 November 2001 and the operational land imager (OLI) were obtained for 15 November 2001. All imageries were selected for the time period of October to November to ensure the minimal effect of seasonal variation in the vegetation pattern and distribution and cloud-free cover. Out of the satellite data land use land cover maps for Wa municipality of the years 1990, 2001, 2010 and 2020 were generated.

A historical global land cover classified gridded data for the years 1992, 2006 and 2020 was obtained from the Copernicus database (https://cds.climate.copernicus.eu/) (Buchhorn et al., 2020) as a basis for modelling the basin-wide potential erosion risk for the entire Black Volta River basin. The land cover data conforms with a series of global annual land cover maps from the 1990s to 2015 produced by the European Space Agency (ESA) Climate Change Initiative (CCI). The data is available in 300 m x300 m horizontal resolution and spans from the year 1992 to 2020.

4.1.5 Field Survey

For land use land cover mapping based on satellite images and soil erosion risk modelling, in-situ observations were conducted for the validation of the results (d'Andrimont et al., 2020). With technical assistance from the Black Volta basin office in Wa municipality, the study implemented two phases of field survey. The first field survey was conducted in January 2020 and focussed on mapping land use and land cover. On this basis six main land use land cover classes (closed savannah vegetation, open savannah vegetation, other land types, human settlements, vegetated wetlands, and water bodies) were identified by Ghana's LULC classification framework for visual interpretation of remotely sensed data (Basommi et al., 2015). For on-site geocoding of findings, a Garmin 60Cx GPS was used.x Further details and the onward validation are elaborated in Chapter 5 (Asempah et al., 2021).

A second field survey was conducted in January and February 2022 to map on-site soil erosion damages. On-site soil erosion damages, specifically, rills and inter-rills were measured on 2 km^2 plots of each of the three different land use land cover types closed savannah, open savannah, and settlement areas in the Wa municipality. The individual damage points were systematically compared with the model's results. For on-site geocoding of findings, a Garmin 60Cx GPS was used. Further description of the field survey and the onward validation are detailed in Chapter 6 (Asempah et al., 2021).

4.2 Processing and Classification of Satellite Images

A series of preprocesses were conducted before image classification and change detection analyses (Figure 4.1). To ensure temporal alignment of time series data for the change analyses considering the years 1990, 2001, 2010 and 2020 for the Wa municipality, Level 1 terrain corrected (L1T) Landsat images were preferentially utilised as primary input data in algorithms for classification of land use land cover. L1T Landsat images are renowned for their exceptional geometric precision, characterised by root mean square errors (RMSE) consistently below 30 meters in over 99% of the dataset, as documented by the United States Geological Survey (USGS) (http://landsat.usgs.gov/geometry.php). Consequently, the inclusion of solely L1T Landsat images within the context of land use land cover classification required geometric accuracy. Besides the generally acceptable quality of Level 1 terrain-corrected Landsat images, the Enhanced Thematic Mapper (ETM) imagery exhibited defects stemming from a malfunctioning scan line corrector (SLC) system. This defect was corrected using the Landsat Toolbox which is integrated within ArcGIS 10.5 software. Following these initial correction steps, further pre-processing steps were applied to the Landsat imagery from all time slices. This encompassed stacking spectral bands and applying clipping using a projected study area vector boundary. The stacked spectral bands included blue, green, red, near-infrared (NIR), and shortwave infrared (SWIR) (Sinha et al., 2015; Weng et al., 2004).

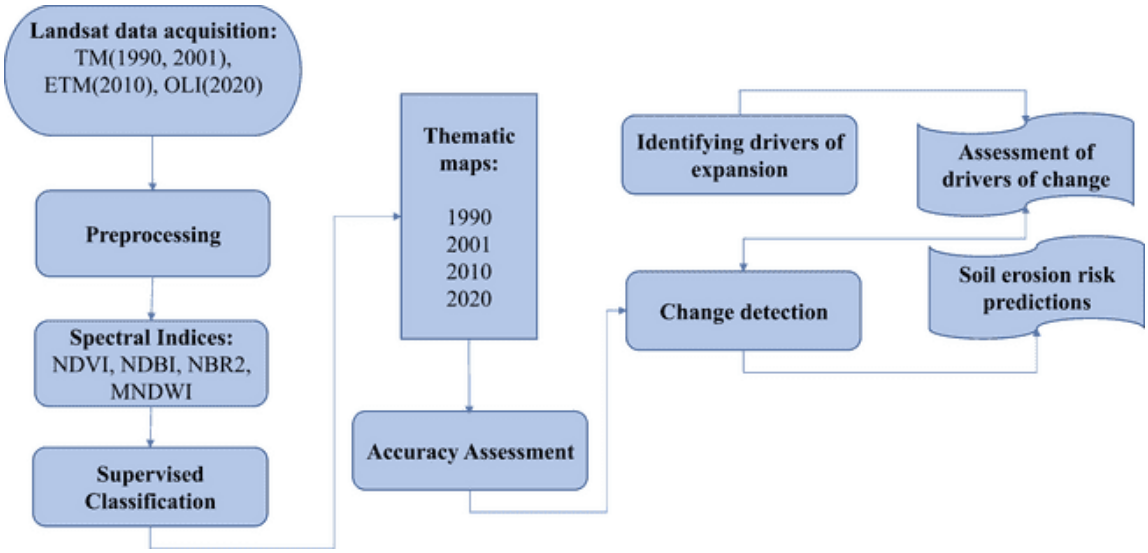

Figure 4.1. Flow Chart of Landsat Data Processing For Urban Expansion And Soil Erosion Risk Prediction in Wa Municipality of Ghana

To enhance the features of the images and to ensure precision in classification, several spectral indices were applied, including the Normalised Difference Vegetation Index (NDVI), Soil Adjusted Vegetation Index (SAVI) (Huete, 1988), Normal Difference Built-up Index (NDBI), Normalised Burn Ratio 2 (NBR2) and Modified Normalised Difference Water Index (MNDW) (Rouse et al., 1973; Singh et al., 2015) This was followed by a pixel-based supervised land use land cover classification for the years 1990, 2001, 2010, and 2020. The output maps were used to assess land use land cover change and the driver of urban expansion (objective 1) and the modelling of potential and soil erosion risk (objective 2).

4.3 Application of the RUSLE Model

Soil erosion models fall into three main categories; empirical, conceptual and physical models depending on the processes simulated by the model and the model's algorithms describing these processes (Merritt et al., 2003). Empirical models such as the RUSLE and MUSLE are the simplest of all models that can be implemented in data-scared landscapes as they make use of limited input data (Adams et al., 2013; Buhai et al., 2020). The RUSLE model was used in the spatio-temporal soil erosion risk modelling (objectives 1 and 2). The model is universally accepted for the estimation of soil erosion risk. The model for the estimation of average soil erosion rate per annum $A_{SE,}$ (t ha^{-1} yr^{-1}) is based on five input parameters, including the three natural parameters soil erodibility factor (*K*), rainfall erosivity factor (*R*), slope length and steepness factor (*LS*) and the two land use and land management controlled parameters the cover factor (*C*) and conservation and support practice factor (*P*) (equation 4.1).

$$A_{SE}\ [t\ ha^{-1}\ yr^{-1}] = R \times K \times L\ S \times C \times P \qquad (4.1)$$

The schematic diagram (Figure 4.2) presents the data requirement and the data flow of the model. The detailed description of the model's input data and their implications as well as the validation procedures are provided in chapter 6.

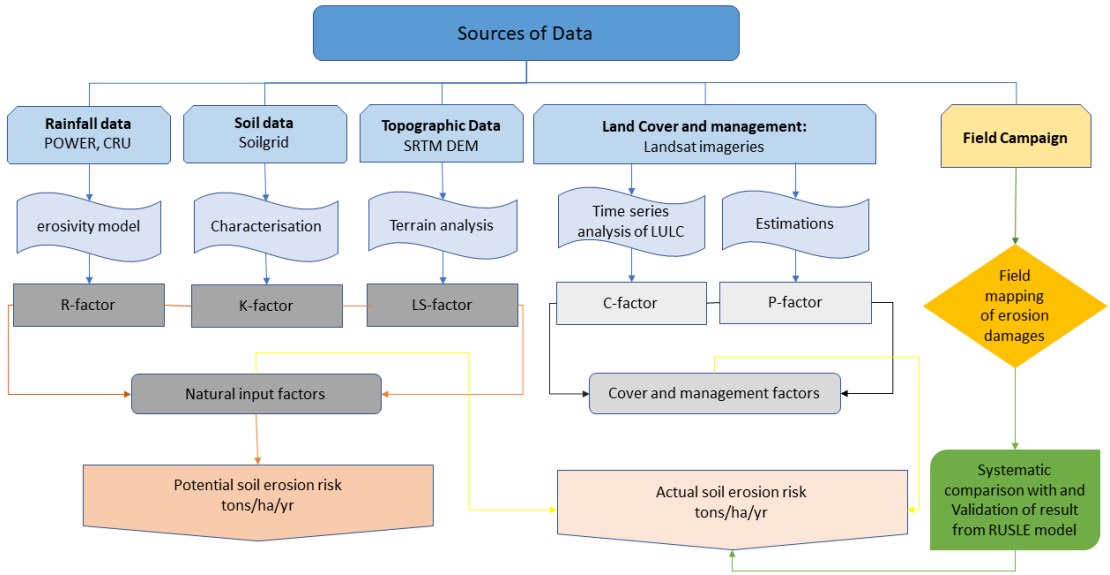

Figure 4.2. Methodological Flow of RUSLE Model Input Parameters for Soil Erosion Risk Modelling.

4.4 Statistical Analysis

A binomial logistic regression model was used to explore the explanatory drivers of urban expansion in the Wa municipality, Ghana (equation 4.2). The Selection of the independent variables (Table 4.2) was based on an evaluation of scientific literature that presents the most influencing variables. The equation for the logistic regression model is:

$$P(y=1) = \frac{1}{1+\mathrm{e}-(\beta_0+\beta_1 X_1+\beta_2 X_2 \ldots+\beta_n X_\mathrm{n})} \quad (4.2)$$

where:

$P(y=1)$ is the probability of the event y occurring (success or the positive outcome); e is the base of the natural logarithm; β_0 is the intercept term; β_1, β_2…, β_n are the coefficients associated with the independent variables X_1, X_2…, X_n respectively.

The statistical significance of the model was established with a significance level (p) of less than 0.05. In accordance with this criterion, independent variables incorporated into the model with associated p-values below 0.05 are considered statistically significant predictors of the dependent variable (Y). The model's performance was assessed through the receiver operating characteristic curve (ROC) and its corresponding area under the curve (AUC). These metrics rely on accuracy matrices, which gauge the proportion of accurately classified positive sampling points (true positive rate: TPR) and the proportion of incorrectly classified positive points (false positive rate: FPR) (Anselm et al., 2018).

Table 4.2. Variables for the Binomial Logistic Regression Analysis applied for Objective 1

ID for variables	Description	Unit
Y	Settlement expansion	Km^2
X_1	Distance from existing settlement	M
X_2	Distance to primary road	M
X_3	Distance to tertiary road	M
X_4	Distance to stream	M
X_5	Distance to river	M
X_6	Aspect	[°]
X_7	Slope	[°]
X_8	TWI	-

CHAPTER 5: ASSESSMENT OF LAND COVER DYNAMICS AND DRIVERS OF URBAN EXPANSION USING GEOSPATIAL AND LOGISTIC REGRESSION APPROACH IN WA MUNICIPALITY, GHANA

Asempah, M., Sahwan, W., & Schütt, B. (2021). ***Assessment of land cover dynamics and drivers of urban expansion using geospatial and logistic regression approach in Wa municipality, Ghana****. Land, 10(11). https://doi.org/10.3390/land10111251.*

Abstract

The current trends of land use dynamics have revealed a significant transformation of settlement spaces. In the Wa Municipality of Ghana, the changes in land use and land cover are inspired by a plethora of driving forces. In this study, we assessed the geo-physical drivers of settlement expansion under land use dynamics in the Wa Municipality of Ghana. The study employed geospatial and remote sensing tools to map and analyse the spatio-temporal dynamics of the landscape, using Landsat satellite imageries: thematic mapper (TM), enhanced thematic mapper (ETM) and operational land imager (OLI) from 1990 to 2020. The study employed a binomial logistic regression model to statistically assess the geo-physical drivers of settlement expansion. Random forest (RF)–supervised classification based on spatio-temporal analyses generated relatively higher classification accuracies, with overall accuracy ranging from 89.33% to 93.3%. Urban expansion for the last three decades was prominent, as the period from 1990 to 2001 gained 11.44 km^2 landmass of settlement, while there was 11.30 km^2 gained from 2001 to 2010, and 29.44 km^2 gained from 2010 to 2020. Out of the independent variables assessed, the distance to existing settlements, distance to river, and distance to primary, tertiary and unclassified roads were responsible for urban expansion.

Keywords*:* savannah vegetation; random forest classifier; regression analyses; receiver operating characteristics (ROC); urbanisation

5.1 Introduction

Urban land covers a relatively small proportion of the global terrestrial landscape but inhabits over half of the global population (G. Chen et al., 2020). It is evident that despite its relatively small coverage, its expansion in the past decades has caused significant alteration to the environments globally (G. Chen et al., 2020; Flörke et al., 2018). Trends in urban land expansion and population over the past decades show that the increase in global population lags behind urban land expansion (Seto et al., 2010), although urban land expansion is associated with urbanisation, which is a product of population growth. Urbanisation coupled with urban land expansion exerts a profound impact on the environment, as it causes the destruction of terrestrial ecosystems, leading to the loss of biodiversity and the degradation of resources (W. Wang et al., 2020). About 70% of the global anthropogenic greenhouse gas emissions emanate from urban areas and more than 80% of the global natural habitat loss is attributed to urban expansion (Churkina, 2016).

Chen et al., (2020) projected that global urban land will continue to expand at an increasing rate before the 2040s. They asserted that China and many other Asian countries might face significant pressure from

the urban population after the 2050s. It is supposed that global food security is endangered, as urbanisation and associated land expansion are expected to encroach on about 50–63% of the current cropland, leading to a consequential 1% to 4% decline in global crop production (D'Amour et al., 2017). Similarly, Africa, with a predominantly rural landmass, is one of the fastest urbanising regions in the world. The continent's population is expected to attain 1.34 billion in 2050 from 2010's 395 million estimates, constituting 21% of the global population projection (United Nations Department of Economic and Social Affairs- Population Division (UNDESA-POP), 2018). Among the numerous drivers of changes in LULC changes, urbanisation presents a lasting and irreversible impact on the environment (Elmqvist et al., 2013; McKinney, 2002; Seto et al., 2012). Increasing urbanisation and associated population exert pressure on natural resources and a high demand for the ecosystem services in effect, leading to critical environmental consequences, such as water crises, microclimatic alteration and natural resources degradation (McKinney, 2002; Seto et al., 2012; Solecki et al., 2013). Temporal changes in landscapes are driven by urban development, as urban expansion coupled with population growth destroys the ecosystem, consequently impacting the provision of ecosystem services (Hails & Ormerod, 2013). The lack of management plans to counteract the repercussions of the urban expansion imposes dire environmental consequences for ecological integrity and the provision of essential ecosystem services, such as water and raw materials. Ferreira et al. (2019) established significant destruction in the ecosystem as a result of urbanisation, among which the reduction of vegetation was prominent.

Exemplarily, we want to focus on Ghana, the second most populated state in Western Africa, which is in transition from an agrarian country to an industrial country. Ampim et al. (2021) assessed land use and land cover (LULC) changes in Ghana from 1995 to 2019 to highlight significant changes and opportunities for sustainable development. They found the built-up area regionally to increase by 131.7% over the entire 1995 to 2019 period. On the other hand, areas of bare land shrank by an average of 92.8%, areas covered by grassland shrank by 51.1%, and areas covered by diverse vegetation shrank by 41%, respectively, over the same period. Ghana experienced significant population growth with associated LULC changes over the past six decades with a doubling of their population since 1990. In Ghana already in 2018, 56% of the country's population dwelled in urban areas, which corresponds to the global trend, as, globally, 55% of people live in urban areas (UNDESA-POP, 2018). Both urban land expansion and population pose serious threats to the integrity of ecosystems and biodiversity (G¨uneralp et al., 2017), especially in drought-sensitive landscapes, such as those occurring in the Wa Municipality that is located within the semi-arid region of Ghana. Based on the above background, this study assessed the drivers of urban expansion in the Wa Municipality of Ghana in the past three decades to provide a basis for future landscape management and town planning to combat the municipality's transformational crisis and ensure ecosystem sustainability.

5.2. Study Area

The Wa Municipality is located in the Upper West region of Ghana (Lat. 10°14′46.32″ N 09°42′5.04″ N and Lon. 02°33′14.04″ W 02°0′57.96″ W). The area covers a total land of 579 km^2 with a population of 102,214 inhabitants in 2010 (Ghana Statistical Service (GSS), 2014) with a projected 132,646 inhabitants in 2020 (Statistics, Research and Information Directorate (SRID), 2011). It shares its administrative boundary with the Wa West District to the West and the Nadowli District to the East. The Wa Municipality (Figure 5.1) is located within the Guinea Savannah agrecological zone and is

dominated by drought adaptation vegetation covers. The landscape is generally undulating with a height ranging from 248 m to 368 m above sea level (Figure 5.2). Low-lying areas constitute two main drainage system in the capital and also retain water for a long period during the long rainy season (Ghana Statistical Service (GSS), 2014) .

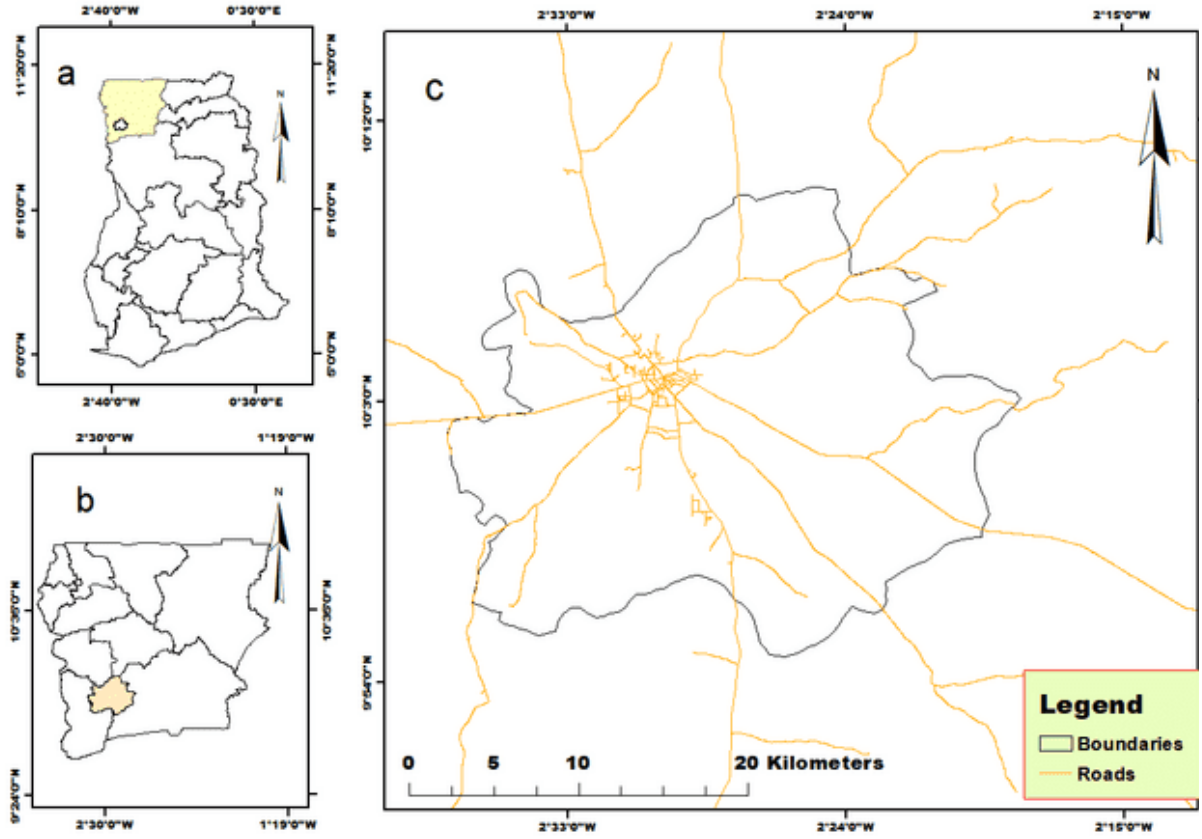

Figure 5.1. Map of the Wa Municipality Located in the Upper West Region of Ghana. (**a**) Map of Ghana showing its sixteen regions separated by administrative boundaries; the Upper West region is marked by shading. (**b**) Upper West region shows its eleven districts separated by administrative boundaries; Wa Municipality is marked by shading. (c) The study area location (Wa Municipality) with road network.

Economic trees, such as baobab (*Adansonia digitata*), shea tree (*Butylosternum paradoxum*), teak (*Tectona grandis*) and dawa dawa (*Parkia biglolosa*) spread across the area where inhabitants leverage their potential for livelihood diversification and development (Ham, 2017; Kent, 2018). Seasonal bushfires coupled with climate variability and increasing built-up areas impose a threat to the benefits derived from the economic trees, thus affecting livelihood (Kpienbaareh, 2016). The climate of the district is characterised by two seasons, at a time controlled by the southwest monsoon winds and the northeast trade winds. The southwest monsoon wind is associated with the rainy season that lasts from May to September.

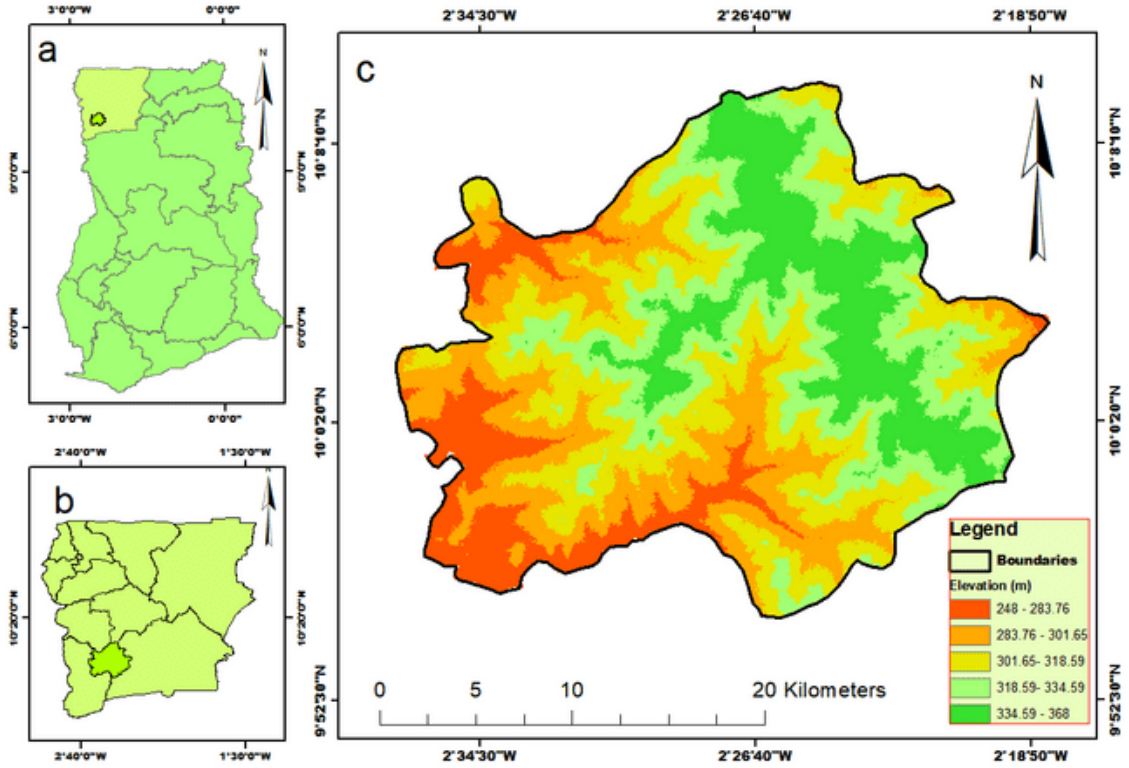

Figure 5.2. Land elevation Map of Wa Municipality located in the Upper West Region of Ghana. (a) Map of Ghana showing its sixteen regions separated by administrative boundaries; the Upper West region is marked by shading. (b) Upper West region shows its eleven districts separated by administrative boundaries; Wa Municipality is marked by shading. (c) Digital elevation model (DEM) of the Wa Municipality; the black line marks the administrative boundary of Wa Municipality. (Data source: Shuttle Radar Topography Mission (SRTM) DEM from the United States Geological Survey's Earth Explorer website, onhttps://earthexplorer.usgs.gov/accessed on 14 September 2020).

The Wa Municipality is located within the semi-arid savannah high plains with characteristic mixed woody vegetation and an open savannah ecosystem with predominating widely spaced trees. Agricultural production and activities related to the agricultural value chain are the major economic activities in the area, employing over 29.3% of the labour force, with a significant proportion (18.5 %) engaged in crafts and related trades (GSS, 2014). The major staple foods cultivated in the district include millet (*Panicum miliaceum*), cowpea (*Vigna unguiculata*), maize (Zea mays), yam (*Dioscorea spp*.), sorghum (*Sorghum bicolor*) and groundnut (*Arachis hypogaea*) (GSS, 2014). Despite the dominant contribution of the agricultural sector to employment and livelihoods in the region, the services sector, in most recent times, has gained importance, employing up to about 25.7% of the labour force in 2010 (GSS, 2014; Kpienbaareh & Oduro Appiah, 2019).

5.3 Data and Methods

5.3.1 Data Acquisition and Processing

This study explores the landscape dynamics of Wa Municipality, Ghana, of the past three decades (from 1990 to 2020), focusing on the time slices 1990, 2001, 2010 and 2020. The study acquired Landsat thematic mapper (TM), enhanced thematic mapper (ETM) and operational land imager (OLI) images of 30 m × 30 m spatial resolution from the United States Geological Survey's (USGS) Earth Explorer

website (https://earthexplorer.usgs.gov/ accessed on 15 March 2021). To achieve the spatio-temporal analysis, Landsat TM5 data were acquired for the year 1990 and ETM data for the years 2001 and 2010, while OLI data were acquired for the year 2020 (Tables 5.1 and S 5.1). All imageries selected are completely free from cloud cover and were acquired for the same season (October to November) to minimise the effects of seasonal variation in the vegetation pattern and distribution.

The selected satellite images were of good quality, except the ETM imageries, which were characterised with defects due to the failed scan line corrector (SLC). The failed SLC resulted in the missing of about 22% of the normal scene area of the ETM data (Storey et al., 2005). This anomaly was corrected, using Landsat Toolbox integrated into ArcGIS 10.5 software to reduce the consequential effects on the image classification accuracy. The imageries were corrected for radiometric distortion to present the inhibition of the spectral characteristics of the land features (Paolini et al., 2006). The semi-automatic classification plugin (SCP) of QGIS 3.4 software was used for dark object subtraction, which, in effect, enabled the correction of the atmospheric distortion and conversion of digital numbers (DNs) to spectral reflectance (Song et al., 2001; Woodcock et al., 2001). Subsequently, the Landsat imageries for all the considered years were subjected to further pre-processing, including stacking and clipping with a projected study area vector map to enable high-precision classification of the image and its associated computations. The spectral bands stacked for all the sensors include blue, green, red, NIR and SWIR; the thermal bands which could impact the quality of the images and affect the classification accuracy were excluded (Sinha et al., 2015; Weng et al., 2004).

Table 5.1. Characteristics of Data Used for Image Classification and their Date of Acquisition.

Satellite Name	Sensor	Number of Bands	Path/Rows	Spatial Resolution	Date of Acquisition
Landsat 5	TM	7	195/053	30 m	12 October 1990
Landsat 7	ETM	9	195/053	30 m	3 November 2001
Landsat 7	ETM	9	195/053	30 m	12 November 2010
Landsat 8	OLI	11	195/053	30 m	15 November 2020

5.3.2 Use of Spectral Indices for Extracting Landscape Features

Spectral indices combine spectral reflectance from wavelengths used in highlighting and enhancing the interpretability of landscape features (Table 5.2; (Robinson et al., 2017)) and, thus, are widely adopted in modelling and monitoring land surface phenomena. The spectral indices used in the LULC classification to extract spectral information for the categorisation of urban areas, vegetation-covered areas and water features include the normalised difference vegetation index (NDVI), normal difference built-up index (NDBI) (Rouse et al., 1973), soil-adjusted vegetation index (SAVI), normalised burn ratio 2 (NBR2) and modified normalised difference water index (MNDW) (K. V. Singh et al., 2015; H. Xu, 2006). These were additionally applied for LULC classification to cope with the regional landscape's high intra-heterogeneity. The identification and classification of built-up areas was supported by NDBI computation (Table 5.2, Equation (5,1)) that utilises shortwave-infrared (SWIR) and near-infrared (NIR) multispectral bands (Zha et al., 2003). These extract built-up areas and barren land and seclude areas covered by water and vegetation. NDBI is applicable with a multispectral sensor with a SWIR band between 1.55 µm and 1.75 µm and a NIR band between 0.76 µm and 0.9 µm.

Table 5.2. Summary of Spectral Indices Used for LULC Classification.

ID	Index	Formula	Equation
1	NDBI	$\frac{\text{SWIR} - \text{NIR}}{\text{SWIR} + \text{NIR}}$	(1)
2	NDVI	$\frac{\text{NIR} - \text{Red}}{\text{NIR} + \text{Red}}$	(2)
3	SAVI	$\frac{\text{NIR} - \text{Red}}{\text{NIR} + \text{Red} + \text{L}} \times (1 + \text{L})$	(3)
4	NBR2	$\frac{\text{SWIR1} - \text{SWIR2}}{\text{SWIR1} + \text{SWIR2}}$	(4)
5	MNDWI	$\frac{\text{Green} - \text{SWIR}}{\text{Green} + \text{SWIR}}$	(5)

Through a normalised computation procedure and mathematical expression, NDVI utilises red and NIR Landsat bands to significantly enhance green vegetation (Table 5.2, Equation (5.2)) (Xue & Su, 2017; Rouse et al., 1973). Since its introduction by Rouse et al. (1973), NDVI has become the most widely used vegetation index in interpreting vegetation characteristics of complex landscapes (Xue & Su, 2017). Due to the complex landscape of the Wa Municipality, the NDVI was corroborated with SAVI and NBR2 (Table 5.2, Equations (5.3) and (5.4)). The SAVI accounted for the deficiencies in NDVI in terms of the stability of vegetation and soil characteristics as a result of the loss of spectral differential red and infrared by vegetation canopy. SAVI incorporates a soil brightness correction factor (L) in the range of 0 (for dense vegetation cover) to 1 (for low vegetation cover). The NBR2, on the other hand, assists in identifying areas recovering from bushfires, which otherwise would be interpreted as built-up areas.

The MNDWI enhances the extraction of open water features from landscapes (Table 5.2, Equation (5). It is an improved form of the normalised difference water index (NDWI) by McFeeters, (1996) that utilises green and NIR bands in extracting water features. McFeeters' NDWI computation shows higher spectral reflectance in green light than NIR light for both built-up areas and areas covered by water, in effect, producing positive values for both. The computation of MNDWI substitutes SWIR for NIR as proposed by Xu, (2006). This procedure yields a better result in extracting water features from the landscape because of water's ability to absorb SWIR better than NIR, leading to an increased positive value for MNDWI (Xu, 2006).

5.3.3 LULC Classification and Change Detection

Pixel-based supervised LULC classification (Phiri & Morgenroth, 2017) was carried out on each pre-processed Landsat images for the years 1990, 2001, 2010 and 2020. Six LULC classes (closed savannah vegetation, closed savannah vegetation, other, settlement, vegetated wetland and water), adapted from Ghana's LULC classification scheme for visual characterisation of remote sensing data (Basommi et al., 2015), were identified through ground truthing for the spatio-temporal classification (Table 5.3). A non-

parametric–based RF classifier was used to generate the thematic maps through a supervised classification approach for each respective year from their stacked spectral bands and the relevant spectral indices. The integration of spectral indices enhances the identification of landscape features for built-up, greenness, brightness and wetness. Built-up areas within the Wa Municipality were classified into settlement areas as identified by diverse spectral features of the Landsat satellite images corroborated by the NDBI spectral index. The characterisation of vegetation cover was supported by enhancement with the SAVI and NDVI spectral indices; integration of the NBR2 index helped to identify vegetation covers that regenerated after bushfire. The vegetation cover was categorised into closed savannah, open savannah and vegetated wetland. The distinction between closed and open savannah vegetation was influenced by the dominance of woody biomass within a hectare space. A threshold of less than 150 trees per hectare is categorised into open savannah, and a hectare of land with more than 150 trees, which is characteristic of forests and reserves, is considered closed savannah. The vegetated wetland class predominantly corresponds to water channels previously inundated with water that are overgrown with dense grasses and shrubs. This class has the highest spectral values in the vegetation indices. The application of MNDWI to the Landsat images supported the identification and classification of water bodies. Ground truthing of the six LULC classes was conducted in a field campaign in 2020 (Table 5.3).

Table 5.3. Description of LULC Classes of the Study.

ID	LULC Class	Description
1	Closed savannah	This is characterised by dense vegetation, predominantly woody cover, such as natural forest, and reserved and protected areas with a population density of more than 150 trees per hectare.
2	Open savannah	These are areas with less dense vegetation cover with a tree population density of fewer than 150 trees per hectare. The vegetation cover is predominantly sacred groves and thick shrubs and grasses.
3	Other	Areas without vegetation cover, bare lands, rocky surfaces, sand, gravel and unregulated open mining pits.
4	Settlement	Built-up areas, towns, and emerging residential areas with low to medium density.
5	Vegetated wetland	Dried-up rivers and stream channels and areas previously inundated with water that are overgrown with grasses and shrubs.
6	Water	Natural and artificial water bodies, including streams, rivers, dams and reservoirs.

On-site random points were collected for each LULC class, using Garmin 60Cx GPS, serving as the reference for the classification and validation of the stacked Landsat image for 2020 with an 80% and 20% split for training and test data, respectively. Training samples were created by digitising polygons and selecting sample pixels from each of the pre-processed Landsat images for the established LULC classes. Each of the ground truth LULC classes was verified by visual interpretation of the Landsat satellite images (Table 5.1) supported by topographic maps (scale 1:50,000 published in 1999 by the Survey of Ghana) and Google Earth and Bing high-resolution imagery (acquired via Web Map Service, WMS) (Borrelli et al., 2015; Schubert et al., 2018). An accuracy matrix was created for the respective years (1990, 2001, 2010 and 2020) to assess the performance of the random forest classification

algorithm by assessing the error matrices and overall accuracy of agreement. Frequency statistics were conducted to establish the quantities of spatial changes in each class for the periods of 1990–2001, 2000–2010, 2010–2020, and the overall period from 1990 to 2020.

5.3.4 **Locational Factors**

Data on locational characters were obtained from broad categories of factors, including topographic factors and location factors. The topographic factors were derived from a shuttle radar topography mission (SRTM) digital elevation model of 30 m ground resolution, acquired from the United States Geological Survey database (https://earthexplorer.usgs.gov/ accessed on 14 September 2020). Topographic factors were calculated as derivatives from this digital elevation model (DEM), including slope, aspect, and topographic wetness index (TWI). The location factors were processed with the Euclidean distance tool in ArcGIS 10.5 version to obtain the raster layers that served as location-independent variables (distance from existing settlement, distance to primary roads, distance to tertiary roads, distance to stream, and distance to rivers). The existing settlements were extracted from the LULC maps for 1990, 2001 and 2020; these data were used to establish the proximity relationship for the changes that occurred from 1990 to 2001, 2001 to 2010 and 2010 to 2020. Additional locations, such as open water, streams, primary roads, and tertiary roads, were acquired from OpenStreetMap and Geofabrik.

5.3.5 Binomial Logistic Regression

Selection of Variables (Factors Contributing to Urban Expansion)

A binomial logistic regression model was used to explore the explanatory drivers of settlement expansion over the study period. The independent variables were selected from previous studies that assessed the drivers of urban expansion in a context similar to our study. According to Xu et al. (2018) and Dubovyk et al. (2011), there are diverse driving factors of settlement expansion. In the modelling of urban expansion, the geographical location and its prevailing conditions are important in selecting the independent variable. In the context of emerging compacted cities, such as the Wa Municipality, topographical and location factors are relevant and could influence urban expansion. Consistent with previous locational studies in developing contexts that have similar attributes to the Wa Municipality (X. Li et al., 2013; Marondedze & Schütt, 2019), topographical and location factors were selected as potential independent variables from various sources (Section 3.4) with the highest likelihood of influencing urban expansion in the studied municipality.

In a study of the linkage between drivers and the axis of urban expansion in Zimbabwe, Marondedze & Schütt, (2019) identified slope and distance proximity characters as statistically significant predictors of urban growth. Similarly, Li et al. (2013) found slope and location factors, such as distance to major roads, distance to highways and distance to city centre, as drivers of urban expansion. This agrees with other studies which established the same characteristics as determinants of urban expansion (Cheng & Masser, 2002; Dubovyk et al., 2011; Luo & Wei, 2009). The proximity to water networks was studied extensively in both developed and developing contexts and was proven to be an important driver of urban expansion (Batisani & Yarnal, 2009; Luo & Wei, 2009). Based on the established relevance of the topography and location characters in urban expansion, our study explores slope, aspect, TWI, distance to settlements, distance to primary roads, distance to tertiary roads, distance to unclassified

road, distance to river, and distance to stream) as the independent variables for modelling urban expansion in the Wa Municipality.

Model Development

The raster layers for areas expanded from the time steps (1990–2001, 2001–2010, 2010–2020 and the entire period of 1990–2020) serve as dependent variables to explore the drivers of change (Figure SM 5.1). The cells from the raster layers were transformed to dichotomous variables, where any area newly transformed to settlement land use is considered settlement expansion and denoted with ”1“, while already existing urban areas and other areas occupied by landscape features that did not transform into settlement areas in the subsequent time slice are considered non-expansion areas and denoted with a dichotomy value of ”0”.

A total of 6000 stratified random sample points were created from all classification maps to extract values for the regression analysis. We set up the binomial logistic model after all the dependent and independent variables were processed. The model was taken to be statistically significant at $p < 0.05$. Given this, all independent variables that were specified and fitted into the model and produced p-values less than 0.05 are taken as statistically significant predictors of urban expansion in the study municipality. The model performance was evaluated to assess the discriminatory of the result using the receiver operating characteristic curve (ROC) and its area under the curve (AUC). The ROC and AUC rely on accuracy matrices, which is a measure of the proportion of correctly classified positive sampling points (true positive rate: TPR), and the proposition of incorrectly classified positive (false positive rate: FPR) (Anselm et al., 2018).

5.4 Results

5.4.1 The Extent of Land Use and Land Cover Change

The spatio-temporal analysis reveals varying extents of change of the LULC features for the three-decade periods that span from 1990 to 2020 (Figures 5.3 and 5.4). In general, the Wa Municipality is characterised by savannah vegetation, with open savannah covering the largest extent of the area. In 1990, the total extent of open savannah was 407.22 km^2 (70.30% of the total spatial extent of the Wa Municipality). The LULC analysis revealed dynamics in the open savannah coverage in subsequent time steps, as there were some gains in the open savannah coverage in the year 2001 with a total spatial extent of 417.06 km^2 (72.0%). Overall, the open savannah reduced to 392.25 km^2 (67.72%) in 2020. As vegetation cover reduced within the three-decade time frame, closed savannah vegetation covered 128.69 km^2 (22.22%) of the total area in 1990 and reduced to 91.34 km^2 (15.77%) in the year 2020 (Table 5.4). The reduction of areas covered by closed savannah vegetation more or less stagnated between the year 2001 (119.32 km^2; 20.60%) and 2010 (107.21 km^2; 18.51%). Similarly, areas covered by vegetated wetland decreased from 13.3 km^2 (2.30%) in 1990 to 12.73 km^2 (2.16%) in 2020; for the year 2010, the highest coverage of 14.59 km^2 (2.52%) was observed.

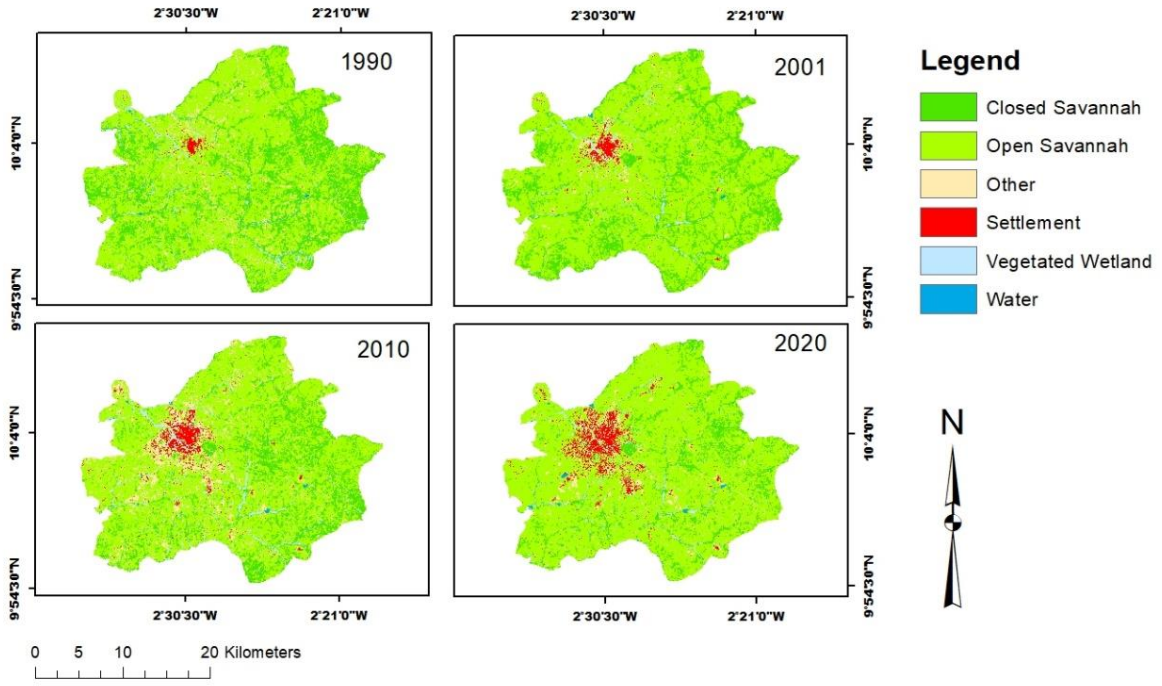

Figure 5.3. Land Use and Land Cover Map for Wa Municipality for the years 1990, 2001, 2010 and 2020.

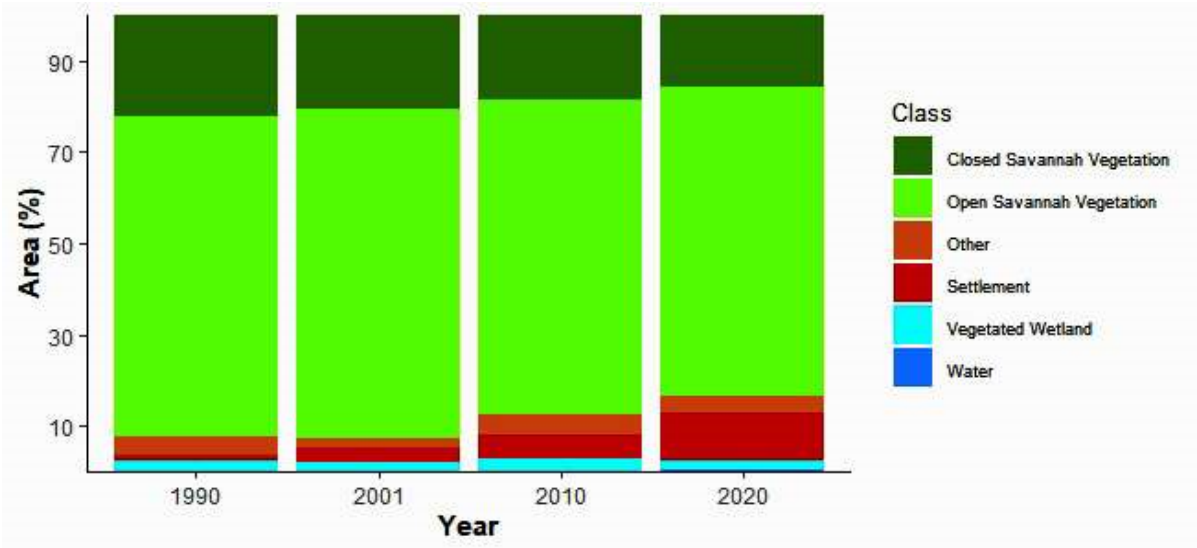

Figure 5.4. The Proportion of LULC Change in Wa Municipality for the Respective Time Slices.

Beyond, the analysis showed a continued increase in settlement expansion with an expansion of eight times the area covered by settlements between 1990 (7.44 km^2, 1.28%) and 2020 (59.86 km^2, 10.33%).

The settlement expansion predominantly took place in the southern direction. Most of these spatial expansions between 1990 and 2020 predominantly occurred within areas previously characterised by open savannah vegetation and areas without vegetation. The class "other" primarily corresponds to areas other than vegetation and water and shows a relatively stable spatial extent over the observation period; the total spatial extent of 22.18 km^2 (3.83%) in the base year 1990 only reduced by 0.01%, as the total area covered in 2020 was 22.11 km^2 (3.82%). Areas covered by water during the entire observation period are relatively low but increased from 0.39 km^2 (0.07%) in 1990 to 0.93 km^2 (0.2%) in 2020.

Table 5.4**.** Spatial Changes of Land Area for the Land Use and Land Cover Classes in Wa Municipality for the 1990, 2001 2010 And 2020 Time Series.

LULC Class	1990		2001		2010		2020	
	Km^2	%	Km^2	%	Km^2	%	Km^2	%
Closed savannah	128.69	22.22	119.32	20.60	107.21	18.51	91.34	15.77
Open savannah	407.22	70.30	417.06	72.00	400.61	69.16	392.25	67.72
Other	22.18	3.83	12.98	2.24	25.62	4.42	22.11	3.82
Settlement	7.44	1.28	19.12	3.30	30.42	5.25	59.86	10.33
Vegetated wetland	13.30	2.30	10.33	1.78	14.59	2.52	12.73	2.16
Water	0.39	0.07	0.41	0.07	0.77	0.13	0.93	0.20

5.4.2 Accuracy Assessment for Land use and land cover Classification

Relatively high overall accuracy (OA) was recorded for each time slice, ranging from 89.33% (2001) to 93.3% (2020) (Table 5.5). The user accuracy (UA) reflects the reliability of the classification, while producer accuracy (PA) reveals how well the reference pixels of land cover types are classified. The class water had the highest producer's accuracy for all the time slices (Table 5.5). Generally, a relatively high degree of classification accuracy runs through all the time slices for all LULC classes.

Table 5.5. User's Accuracy (UA), Producer Accuracy (PA) and Overall Accuracy (OA) For Land Use Land Cover Classification Accuracy Assessment for the Time Slices.

Class	Closed Savannah		Open Savannah		Other		Settlement		Vegetated Wetland		Water		OA
	UA	PA	UA	PA	UA	PA	UA	PA	UA	PA	UA	PA	
1990	92	97.87	94	82.46	80	93.02	96	92.31	98	94.23	96	97.96	92.67
2001	88	93.62	96	78.69	82	78.85	84	93.33	92	97.87	94	97.92	89.33
2010	88	93.6	96	75	88	93.6	92	93.9	82	89.1	92	97.9	89.7
2020	92	92	94	87.0	94	95.9	90	93.8	94	94	96	98	93.3

5.4.3 Binomial Logistic Regression and Model Validation

A receiver operating characteristic (ROC) curve (Figure 5.5) is a graphical plot of the true positive rate (sensitivity) against the false positive rate (1-specificity) and illustrates the diagnostic ability of a binary classifier (Sedano et al., 2016). This produces an area under the curve (AUC) that measures the discriminating power of a model. The area under the curve (AUC) is an effective and combined measure of sensitivity and specificity for assessing the inherent validity of a test (Anselm et al., 2018; Sedano et al., 2016). The larger the area under the ROC curve, the stronger the predictive power of the model (Sedano et al., 2016).

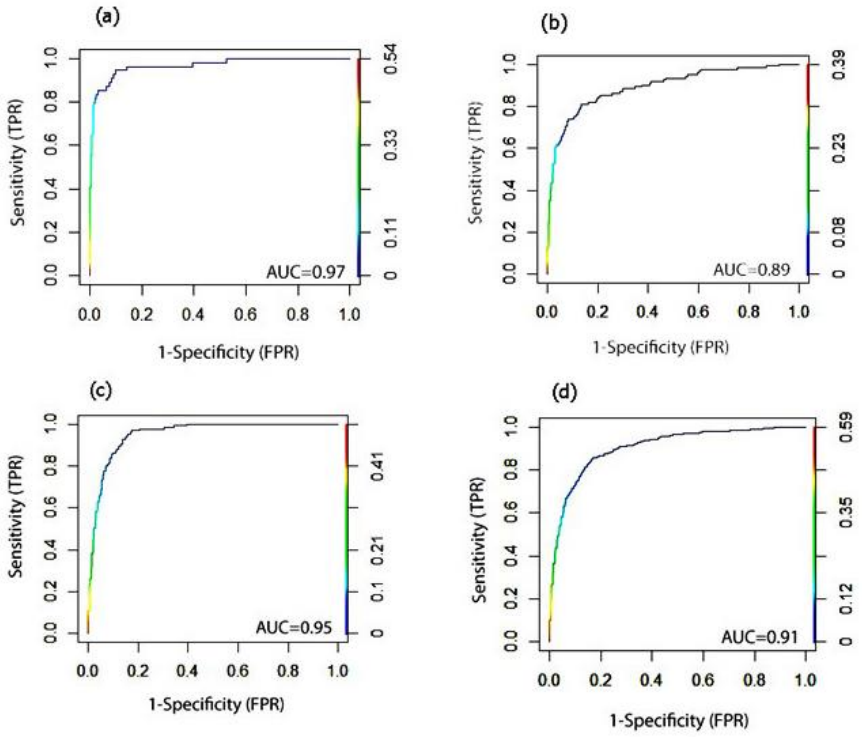

Figure 5.5. Receiver Operating Characteristic (ROC) Curves Depicting Validity and Performance of Binomial Logistic Regression Analyses Results for Urban Expansion in Wa Municipality for the following years: (**a**) 1990, (**b**) 2001, (**c**) 2010 and (**d**) 2020. (FPR: false positive rates; TPR: true positive rates; AUC: area under the curve).

As a broader acceptable standard, a model with maximum AUC (1.0) has a perfect descriptive power, with 0.9 being considered excellent. A perfect descriptive power of the model is an indication of having all the true positive rates (sensitivity) and true negative rates (specificity) as one and both errors (false positive and false negative) as zero. In a complete random relationship, the model produces an AUC of 0.5 with a diagonal line from the left bottom to the upper right corner. For a model to be considered efficient, it must possess at least 0.6 power. A power of 0.7 is considered good, while 0.8 is regarded as very good (Anselm et al., 2018).Through the binomial logistic regression modelling, it was evident that topographic factors (slope, aspect, topographic wetness index) were not statistically significant to urban expansion. In contrast, the location factors were, for all the time steps, statistically significant. The distance to the existing settlement was significant at $p < 0.001$ for all time steps. Similarly, the distances to primary roads, tertiary roads, and unclassified roads were significant at $p < 0.001$ for all time steps, except for the time step of 2001 to 2010, where the distance to tertiary roads and distance to unclassified roads were of less powerful statistical significance ($p < 0.05$). The distance to rivers was also significant at $p < 0.01$ for time step 1990–2001 and $p < 0.001$ for time step 2001–2010. The receiving operating characteristic (ROC) curve was used to validate the model performance. The discriminatory power of the model was very high for all time steps (Figure 5.5). The ROC for 1990 produced the best performing descriptive and predictive model, with an AUC of 0.97. The least was observed in the model for 2001–2010 (AUC = 0.89). Summarising, all the models for the four-time steps selected are valid and satisfactory for describing and predicting the urban expansions in the Wa Municipality.

5.5 Discussion

The transformation of the natural vegetation and the functioning of the terrestrial ecosystems are influenced by the ongoing urban sprawl and its associated environmental changes. The Wa Municipality, and the Upper West Region of Ghana as a whole, has seen significant changes regarding demography and ecological landscapes over the past decades and most likely will be impacted in the years to come (Attua & Fisher, 2011). The spatio-temporal LULC classification of the Wa Municipality reveals the dynamics of urban expansion and associated changes in the landscape between 1990 and 2020. The classification was accomplished with high overall accuracies. The relatively high accuracy was achieved by the non-parametric RF machine learning classifier, which was identified to produce better LULC classification accuracy than non-parametric and traditional parametric classifiers (Carranza-García et al., 2019). In a review of LULC classification using the machine learning classifier for satellite imageries, Talukdar et al. (2020) concluded that in a high dynamic landscape with intra-heterogeneity, as is also typical for the Wa Municipality, the RF classifier provides better classification accuracy than other machine learning classifiers when modelling LULC changes, especially when imageries have the same sensor characteristics, such as spatial and temporal resolution (Ma et al., 2017; Mountrakis et al., 2011).

The random forest (RF) classification algorithm provides a great opportunity to generate higher classification accuracy outputs than parametric classifiers (Talukdar et al., 2020). The success of high classification accuracies was achieved by the corroboration of the RF classifier with the application of spectral indices. The spectral indices in the LULC assessment of this study in turn enhanced the delineation of the landscape features, making the clear distinction between the different LULC classes more prominent and, thus, increased the accurate selection of training samples and, subsequently, the LULC classification accuracy. The high accuracies generated by incorporating spectral indices agree with (Hegazy & Kaloop, 2015), who established increased separability between LULC classes in the quest to analyse land use and land cover changes, using spectral indices. Owing to the vegetation cover complexity of the Wa Municipality, intra-vegetation separability was enhanced by the vegetation indices that enabled the distinction between closed and open savannah vegetation. Misclassifications observed between land-use classes were a result of small-scale intra-heterogeneity of the landscape, which caused a high number of mixed pixels and thus, negatively affected the classification accuracies. In principle, mixed pixels emanating from subpixel objects of various classes exhibit high intra-heterogeneity within a defined landscape unit (Phiri & Morgenroth, 2017). Mixed pixels can affect the classification results, even as they are located along the borders between discrete and easily separable classes, though the occurrence of mixed pixels is not limited to the transition zones of landscape classes and does not underly a continuous gradient, which, in effect, leads to classification errors (Phiri & Morgenroth, 2017). The use of multi-spectral Landsat imageries and the extracting of heterogeneous training data helped to overcome this challenge.

The results obtained from the geospatial analysis reveal that increasing urbanisation was prevalent during all the time slices analysed, predominantly indicating significant urban expansions from the previous time steps at the expense of vegetation cover. This agrees with previous studies (Hegazy & Kaloop, 2015; Marondedze & Schütt, 2019) that show an inverse relationship between the expansion of built-up areas and especially areas covered by vegetation. In consequence, it can be stated that urban expansion reduces the vegetated area. Beyond, the analysis shows that the urban expansion in the Wa

Municipality is in a form of concentration and expansion that is identical to the typical urban development pattern observed in Ghana (Kuusaana et al., 2021). The concentration can be observed by increasing spatial densities of built-up areas, particularly in the Wa township, the capital of the municipality. Simultaneously, there was a massive expansion of built-up areas toward the peripheries of the major towns during all the time steps analysed (Figure 5.3). This also includes the engulfment of already existing peri-urban settlements in the Wa Municipality by urban sprawl. This is in line with the findings of Cobbinah & Amoako, (2012) and Kombe, (2005), who describe characteristic unconsolidated lateral physical urban expansion and urban sprawl with the engulfment of existing built-up areas by new settlements within the peripheral areas of most cities in developing countries.

Urban expansion in the Wa Municipality between 1990 and 2020 strongly correlates to population growth. According to Ghana Statistical Service, (2005), the population of the Wa Municipality increased from 98,675 inhabitants in the year 2000 to 107,214 inhabitants in 2010. This corresponds to an annual growth rate of about 0.77% in the decade of 2000–2010, while, simultaneously, settlement expansion totalled 3.71%. For 2020, the projected population amounted to 132,646 (GSS, 2012), which puts the annual growth rate between 2010 and 2020 at 1.92%, while, in parallel, the observed annual rate of settlement expansion averaged 4.1%. This observation underlines the critical role that population pressure has on urban expansion and agrees with observations on land cover change in West Africa by Herrmann et al., (2020), who revealed that changing intensities of settlement areas were significantly influenced by population pressure. Spatial patterns of the human footprint within the area of the Wa Municipality suggest that population pressure coupled with the socioeconomic statuses of the people and policies geared toward infrastructure development affect the complexity of land cover outcomes. The infrastructure expansion in the Wa Municipality manifests in the LULC changes in the area: the Wa airport, for example, is a prominent infrastructure measure visible in the satellite imageries. It influenced the expansion of the settlement space, especially between 1990 and 2001. Evidence from previous research suggests that other infrastructure measures, such as roads, schools and hospitals, were part of the development phase from 1990 to 2020 as a response to the population's demand (Osumanu et al., 2019; Ziem Bonye et al., 2021), thus controlling large parts of the dynamics in LULC changes within this period.

It was evident that areas previously covered by savannah vegetation changed to settlement areas, as proven for all the time slices selected. This also became explicit in the LULC classification that shows significant spatial settlement expansion in all the time slices. While in the Wa Municipality settlement expansion was prominent, woody biomass, on the other hand, shrank over the past decades; this was confirmed by the LULC analysis based on the satellite images that revealed a depletion of closed savannah vegetation for all the time steps analysed. Between 1990 and 2001, there was a gain in the settlement area in the Wa Municipality of 11.68 km^2 corresponding to a relative increase of 61.09%, while in parallel, there was a reduction of areas covered with closed savannah vegetation by 9.37 km^2 corresponding to a relative decrease of 7.85%. This inverse relationship can be observed for all time steps analysed, with the overall gain in settlement area between 1990 and 2020 of 52.42 km^2 (+87.57%) and the corresponding loss in areas covered by closed savannah vegetation of 37.35 km^2 (−40.89%). This reflects the effects of the characteristic urban agglomeration–population nexus typical of contemporary times, where landscape degradation associated with urban expansion is driven by the need for shelter for the increasing population who engages in livelihood development activities in their respective settlements (Acheampong & Anokye, 2013; Appiah et al., 2014). The current trends of urban

expansion and vegetation dynamics in the Wa Municipality are in line with Bologna & Aquino, (2020) who emphasise a population–urban expansion–deforestation nexus, maintaining that the essential services derived in support of human life are the main driving force behind encroachment on forest spaces. This is supported by Myers et al., (2013) who stated that changes in terrestrial ecosystems are influenced by increasing pressure emanating from population growth, which in effect degrades the landscape and its associated resources.

In Ghana, north-to-south migration is typical for the exploration of livelihood development options. Beyond, people also move within their districts and municipalities, due to the push factors to access resources such as fertile land and water to secure their livelihood (Antabe et al., 2017). Next to LULC change as an effect of migration and population growth, there has been, in recent times, an increase in the proliferation of unregulated small-scale gold mining within the Wa Municipality and its neighbouring Wa East district (Antabe et al., 2017). These economic opportunities are a strong pull factor for intra- and inter-district migration and affect the LULC pattern. While agriculture is the major livelihood and economic

development activity in the Wa Municipality, some inhabitants are shifting to unregulated small-scale mining, which seems to be more lucrative and yields the promise of quick income, despite the environmental consequences it poses. Basommi et al. (2015) observed that settlements expanded within the Wa East district, which has neighboured the Wa Municipality in gold mining activities in the area over the past years. Currently, unregulated small-scale mining operations cause destruction of the ecosystem (Basommi et al., 2015; Mucova et al., 2018).

In the Wa Municipality, the cutting of trees for fuelwood and charcoal production is the major cause of woody biomass depletion (Chiteculo et al., 2018; Sedano et al., 2016), affecting the decline in closed savannah vegetation. In addition, seasonal bushfires occurring predominantly during harmattan seasons (November to March) also contribute to the depletion of woody vegetation (Kusakari et al., 2014). Despite the devastating effects of bushfires on livelihood, there is a lack of understanding of its causes and a clear policy direction to address it (Yahaya & Amoah, 2013). Rainfall in northern Ghana is unimodal with high spatial and temporal variability in the rainy season between May and September (Yengoh et al., 2010). Due to the seasonal occurrence of rainfall, runoff regimes of the major rivers are periodical, causing a water shortage during the dry season. As surface water is an important water source for agricultural activities, the study area is significantly impacted by the competing demand for water between domestic and agricultural uses (Benebere et al., 2017). The increased availability of water, deviated from the extent of open water areas, as seen in the satellite images from 2010 and 2020, is in line with government efforts to construct dams and dugouts to ensure water availability to sustain agriculture and guarantee livelihoods (Diko et al., 2021). Expanding vegetation in the vicinity of the wetlands suggests that in periods of increased water availability, the vegetated wetland expands.

Among the topographical characteristics, slope, aspect and TWI are key determinants in choosing land for settlement (Ye et al., 2013; Z. Zhang et al., 2014). Location factors, such as distance to existing settlements, distance to water sources, and distance to tertiary and primary roads also play a major role in urban expansion. Additionally, the proximity to physical infrastructure and water resources is a driving factor of urban growth, as people are pulled toward areas that are endowed with physical infrastructure and water resources for economic and livelihood activities (Luo & Wei, 2009; Poelmans & Van Rompaey, 2009). However, by applying binary logistic regression to determine the drivers of

urban expansion, it is evident that the topographic factors of slope, aspect and TWI did not obtain statistically significant coefficients to predict the odd logs of their probabilities of influence on urban expansion within the Wa Municipality for all the time steps analysed. This might be due to the nature of the entire landscape, which is almost homogenous and has almost equal suitability of selection for settlement. On the other hand, drivers such as distance to settlement, distance to road networks, and distance to water were statistically significant for all the time steps analysed, strongly indicating their influence on urban expansion. These physical location drivers' influence on urban expansion was reinforced by the direction of the expansion which was predominantly towards the southwestern part of the Wa Municipality, where major primary, tertiary and unclassified road networks are densely formed.

This finding is in line with studies conducted in national and regional contexts, all establishing a significant relation between physical location factors and urban expansion (Das Chatterjee et al., 2016; Poku-Boansi & Adarkwa, 2016). Pravitasari et al., (2018) underlined in their study on the Jakarta–Bandung mega-urban region asserted that among the major drivers of urban expansion is the distance to road, which directly affects the extent and spatial expansion of the area. Similarly, Marondedze & Schütt, (2019) identified roads as a major determinant of urban expansion for the Epworth district, Harare, Zimbabwe. In the Wa Municipality, urban expansion is being driven by the government's commitment to the provision of infrastructure, such as roads, and schools as part of the development agenda. Considering the trend of urban expansion in the Wa Municipality, it is evident that people choose to live close to roads to have easy access to the workplace, school and market. Distance to primary, tertiary and unclassified roads were statistically significant with a negative coefficient, indicating an increased probability of an area being transformed into an urban space controlled by the proximity of the area to roads; thus, the shorter the distance of an area to a road, the higher the possibility of the area being expanded into an urban space.

Beyond, the development of the Wa Municipality and the expansion of built-up areas since the year 2000 was also affected by the establishment of the Wa Campus of the University for Development Studies (now called S.D. Dombo University of Business and Integrated Development Studies), Wa Polytechnic (now called Wa Technical University) and a nursing training college, all distributed across the municipality and acting as pull factors (Korah et al., 2018).

Distance to already existing settlements was also established as a key driver for urban expansion. For all the time steps analysed (1990–2001, 2001–2010 and 2010–2020), the binomial logistic regression shows statistically significant negative coefficients describing the relation between new built-up areas and distance to existing settlements. The result agrees with findings from previous studies, which also observed urban expansion to be influenced by distance to existing settlements and other locations (Dubovyk et al., 2011; Luo & Wei, 2009). The negative coefficient of distance to existing settlement observed for all the time slices in the logistic regression analysis underscores the increasing likelihood of newly developed settlements near already existing settlements, and thus settlement expansion. This observation can be attributed to the higher affinity for easy access to socioeconomic resources and better development opportunities in existing settlements, especially closer to the administrative centre of the municipality (Boamah, 2013).

According to Li et al. (2018), the presence of water bodies in an area could either hinder or promote urban expansion corresponding to the waterborne advantages as well as the opportunities that water resources present for urban development. Correspondingly, proximity to rivers is established as a key

driver of urban expansion, proven to be statistically significant with new built-up areas for the time steps 1990–2001 and 2001–2010; considering the data for the entire observation period (1990–2020), also a statistically significant relation between the development of new built-up areas and their distance to rivers can be observed. The result suggests an increasing probability of urban expansion at a location the closer the distance to open water is. This finding is consistent with findings by (Cheng & Masser, 2002; G. Li et al., 2018; Luo & Wei, 2009) for studies conducted in Asia. During the Colonial era, the people of the Wa Municipality largely relied on hand-dug wells, streams and rivers to cover their daily water needs. In the 1950s, the Hydraulic Division of Public Works Department was mandated to plan and develop water supply systems for the provision of potable water in the Wa Municipality. During the 1950s, the water allocation capacity was as low as 150 m^3 per day and increased to about 1320 m^3 daily water allocation in the 1980s as the ever-increasing population necessitated increasing water availability (Amoah, 2013). Currently, Ghana Water Company Limited is responsible for the operation of the water supply system in the Wa Municipality, with a daily demand of more than 12,000 m^3. As developments and associated infrastructure are still in progress, in particular, the rural population still relies on open water from rivers for domestic and agricultural purposes (GSS, 2014).

5.6 Conclusions

Over the past decades, landscapes have been influenced significantly by climate variability and anthropogenic impacts. The proliferation of rural settlements and urban expansion has further led to landscape modification, as vegetation cover and environmental resources deplete. Owing to the environmental conditions and development potential of Wa Municipality of Ghana, an assessment of the dynamics of land cover and drivers of settlement expansion is a great step to inform developmental policies. This study provides insight into landscape dynamics and the drivers of urban expansion in the Wa Municipality, Ghana, by employing geospatial and remote sensing tools coupled with a binomial logistic regression model. By employing supervised LULC classification using the random forest classifier, we obtained satisfactory overall accuracies. Similarly, we obtained great performance of the binomial logistic model, as the model validation yielded excellent output. The study reveals that the landscape of the Wa Municipality over the past three decades has been influenced by urban expansion, while in parallel, woody biomass has reduced as observed in the reduction of areas covered by closed savannah vegetation. We note that during the 1990–2020 observation period, settlement expansion for all the time steps analysed was consistent with the trend of regional population growth. The urban expansion is relatively compact within the capital city of the Wa Municipality as a result of the infilling of open spaces within the city complex. However, the peripheral areas of the capital city expanded predominantly toward the southwest part of the Wa Municipality. This behaviour was observed for all 10 years' time steps analysed. In parallel, for all 10 years' time steps analysed, a decrease in areas covered by savannah vegetation can be observed. Even when the urban spread predominantly captures areas with bare land, population pressure, and grazing activities as well as fuel wood consumption as a concomitant phenomenon of the urban spread triggers the decline in savannah vegetation.

In consonance with other studies, the LULC change dynamics observed for the Wa Municipality reflect the resultant effects of the influx of population growth and the associated demand for environmental resources for sustainable livelihood and economic development. The drivers identified to influence settlement expansion include distance to existing settlements, distance to rivers and distance road networks. The development of settlements near an already existing settlement is imperative, due to the

potential economic development opportunities they present. Beyond, accessibility and connectivity seem eminent, as distance to roads was also proven to be a driver for settlement expansion. In line with the new spatial planning framework of Ghana, our findings provide relevant information for the Town and Country Planning Department for future development plans of the Wa Municipality. Beyond, our findings provide valuable knowledge to support integrated landscape management decisions and their impacts on the ecosystem and environmental resources. It is expected that future research will expand the scope of the study beyond the Wa Municipality and explore the landscape dynamics and drivers of urban expansion at the macro level. Additionally, beyond the geophysical factors, future research should explore the socioeconomic drivers of urban expansion at the municipal level and beyond. This, together with our findings, informs a holistic framework in sustainable urban planning and development.

5.7 Acknowledgments

We express our appreciation to colleagues from the Freie Universität for their valuable insights and expertise that greatly assisted this study. We also thank the staff of the Water Resources Commission of Ghana, especially those in the Wa Municipality, for their assistance during the field campaign. Finally, we are grateful to the National Aeronautics and Space Administration (NASA) and the United States Geological Survey (USGS), who kindly provided the Landsat imagery and the one Arc-Second Global data from the Shuttle Radar Topography Mission (SRTM) for the study.

Conflicts of Interest: The authors declare no conflict of interest. The roles in the design of the study; in the collection, analysis, or interpretation of data; in the writing of the manuscript; and in the decision to publish the results are solely by the authors.

5.8 The Link of this Chapter to Other Chapters

The chapter is a case study of the Wa municipality in the Black Volta River Basin that addresses the first objective of the study which sought to evaluate and determine the LULC dynamic and drivers of urban expansion in the Wa municipality between 1990 and 2020. The findings informed the understanding of the LULC dynamics and the drivers of the urbanisation in the municipality. The 1990 and 2020 LULC thematic maps from this chapter served as the cover factor input parameter in the next chapter that estimated soil erosion risk in a typical savannah landscape of Wa municipality of Ghana between 1990 and 2020.

CHAPTER 6: MODElLING OF SOIL EROSION RISK IN A TYPICAL TROPICAL SAVANNAH LANDSCAPE

Asempah, M., Shisanya, C. A., & Schütt, B. (2024). ***Modelling of soil erosion risk in a typical tropical savannah landscape****. Scientific African, 23(July 2023), e02042.*

https://doi.org/10.1016/j.sciaf.2023.e02042

Abstract

Tropical savannah landscapes are faced with high soil degradation due to climate change and variability coupled with anthropogenic factors. However, the spatiotemporal dynamics of this is not sufficiently understood particularly, in the tropical savannah contexts. Using the Wa municipality of Ghana as a case, we applied the Revised Universal Soil Loss Equation (RUSLE) model to predict the potential and actual soil erosion risk for 1990 and 2020. Rainfall, soil, topography and land cover data were used as the input parameters. The rate of predicted potential erosion was in the range of 0-111 t ha^{-1} y^{-1} and 0–83 t ha^{-1} y^{-1} for the years 1990 and 2020, respectively. The prediction for the rate of potential soil erosion risk was generally higher than the actual estimated soil erosion risk which ranges from 0 to 59 t ha^{-1} y^{-1} in 1990 and 0 to 58 t ha^{-1} y^{-1}in 2020. The open savannah areas accounted for 75.8 % and 73.2 % of the total soil loss in 1990 and 2020, respectively. The validity of the result was tested using in situ data from 2 km^2 each of closed savannah, open savannah and settlement area. By statistical correlation, the predicted soil erosion risk by the model corresponds to the spatial extent of erosion damages measured in the selected area for the validation. Primarily, areas with steep slopes, particularly within settlements, were identified to have the highest erosion risk. These findings underscore the importance of vegetation cover and effective management practices in preventing soil erosion. The results are useful for inferences towards the development and implementation of sustainable soil conservation practices in landscapes with similar attributes.

Keywords: Erosion risk prediction Potential erosion risk RUSLE model Soil degradation Soil erosion damage.

6.1 Introduction

Soil erosion is influenced by natural factors such as rainfall, topography as well as soil physical and chemical characteristic coupled with anthropogenic activities (Butt et al., 2010; Mutua et al., 2006). The anthropogenic influence of soil erosion includes land modification through agriculture, deforestation, construction and general land use (Flores et al., 2019). Soil erosion results in on-site losses of fines and dense particles, such as clay and humus, that are essential soil nutrient carriers and also function as soil stabilising agents (Wantzen & Mol, 2013). Soil erosion potentials are high within subhumid and dry-subhumid tropics given the high rainfall intensities and amount prevalent in such regions (Arneth et al., 2019; Guerra et al., 2020). Besides rainfall, soil erosion within tropical regions is generally concentrated in space over time (e.g. during changes in cropping systems such as crop rotation) (Labrière et al., 2015). The consequential effects are multi-faceted and include decreasing crop yields and water resource degradation, which are observed in high turbidity and particle-induced

pollutants. The water-holding capacity of reservoirs is reduced through sedimentation thereby altering the hydrological regimes, and further compounding flood risk as a result of riverbed filling and stream plugging(Chomitz et al., 1999; Locatelli et al., 2011; Millennium Ecosystem Assessment, 2005).

Globally, soil erosion disrupts the sustainable functioning of ecosystems (Borrelli et al., 2021). The impacts of soil erosion jeopardise the potential of a variety of ecosystem services, which could be derived from healthy soil. The Millennium Ecosystem Assessment (2005) points out that ecosystem services for soil erosion control are on the decline globally. Globally, the range of soil erosion is highly substantial (Borrelli et al., 2017) and threatens ecological integrity, biodiversity and future agriculture productivity (Arneth et al., 2019). According to Wantzen & Mol, (2013), about 1094×106 hectares - corresponding to c. 8.4 % of global land surface - is affected by soil erosion by water, with 751×106 hectares (5.8 %) even severely affected by water erosion. In contrast, wind-induced soil erosion affected about 549×106 hectares (4.2 %) of the world's land mass, with about 296×106 hectares (2.3 %) being severe (Lal, 2003). Economically, the impact of the deterioration of arable land amounts to billions of dollars (Pimentel et al., 1995). According to. Dregne (2002), Africa faces irreversible soil productivity losses due to water erosion at national scales; in some parts of sub-Saharan Africa already about 20 % of crop yield has been permanently reduced due to soil erosion processes. Obalum et al. (2012) postulate for sub-Saharan Africa about 50 % of productivity losses are attributable to soil erosion processes. In the East Africa region, Fenta et al. (2020) modelled land susceptibility to water and wind erosion risks and established 10 % moderate or elevated water erosion risks (>10 t $ha^{-1}yr^{-1}$) while prediction for wind erosion was 25 % moderate or elevated erosion. Similarly, Okou et al. (2016) predicted 19.5 % of high to very high erosion risk in West Africa following a regional erosion risk mapping. In Ghana, the impact of soil erosion has been felt since the early 1930s (Dregne, 2002). Research has shown that since that time about 29.5 % of the country's erosion impact could be classified as slight-to-moderate sheet erosion, with 23 % being severe sheet and gully erosion, and 43.3 % being classified as high sheet and gully erosion (Baatuuwie et al., 2011). However, it is anticipated that actual Figures may be significantly higher owing to the enormous strain on land due to a mix of physical and socioeconomic reasons, including population pressure, poor farming methods, and the effects of global climate change (Moomen & Dewan, 2017).

The trend of soil erosion poses a great threat to food security, poverty reduction and biodiversity conservation which are core components of the United Nations Sustainable Development Goals (SDGs). While SDG 15 is aimed at protecting, restoring and promoting sustainable use of terrestrial ecosystems as well as halting and reversing land degradation and biodiversity loss, SDGs 1 and 2 seek to end poverty and hunger, respectively (Yin et al., 2022). Aside the destruction of the ecosystem and loss of biodiversity, Soil erosion reduces the fertility and productivity of the soil leading to low agricultural productivity. Soil erosion risk modelling is part of efforts to promote sustainable agriculture, water and biodiversity conservation which are vital to achieving the SDGs (Yin et al., 2022). Assessing soil erosion risk is therefore a step towards planning sustainable conservation practices in the face of climate variability and land use intensification for the realisation of the aforementioned global goals (Foucher et al., 2014). Several empirical, statistical, and physical models are applicable in estimating soil erosion risk (Abdullah et al., 2017; Foucher et al., 2014; Igwe et al., 2017; Meusburger et al., 2010). Generally, the selection of a model is highly dependent on the availability of a data, its applicability to the study area's attributes, intended use, processes and

calibration needs (Merritt et al., 2003; Ranzi et al., 2012). In practice, the Universal Soil Loss Equation (USLE) is one of the widely used empirical models (Wischmeier & Smith, 1978). Also, its derivatives, the Revised Universal Soil Loss Equation (RUSLE) (Renard et al., 1997), the Water Evaluation and Planning (WEAP), the Soil and Water Assessment Tool (SWAT) (Arnold et al., 1998) and the Water Erosion Prediction Project (WEPP) (Laflen et al., 1991) have been extensively explored to model erosion risk under various contexts, including different climatic and soil conditions as well as land use practices.

In this study, Wa municipality, an area typical for the tropical savannah agroecological zone, remote sensing techniques and data processing with Geographic Information Systems (GIS) build the basis for soil erosion risk modelling applying the RUSLE. GIS was applied in extracting, delineating and manipulating land characteristics that serve as input parameters for the estimation of soil erosion risk by the RUSLE model (Chalise et al., 2018; Shamshad et al., 2008; G. Wang et al., 2003). The RUSLE model which was initially developed for plot-based experiments has been applied for modelling at macro-scales and is useful for identifying areas which are vulnerable to soil erosion (Benavidez et al., 2018; Constantine & Ogbu, 2015). However, the means of validating the RUSLE model's result is lacking. This study provides a three-stage approach to better estimate the soil erosion risk by predicting the potential soil erosion risk and the actual soil erosion risk as well as testing the validity of the results using soil erosion damage data that was measured in the field. In order to understand within the vulnerable savannah agroecological zone, the relevant dynamics of soil erosion across time, this case study on Wa municipality models the spatial pattern of soil erosion risk as well as potential erosion for the years 1990. and 2020 owing to changes in climate patterns and land use and land cover over these periods. Thus, the study evaluates how changes in land use and land cover (LULC) influence soil erosion risk in Wa municipality through the analysis of temporal soil erosion estimates. First, we modelled potential erosion for the Wa municipality, and predicted the actual soil erosion risk for the years 1990 and 2020 using the RUSLE model. We then validated the modelled soil erosion risk using field measurements. This approach, especially the validation option, is useful, applicable and provides the basis for making inferences in future studies, especially in the tropical context.

6.2 Materials and Methods

6.2.1 Study Area

Wa municipality is situated in Ghana's Upper West Region, (between 10◦ 14′ 46.32″ N and 09◦ 42′ 5.04″ N and 02◦ 33′ 14.04 W and 02◦ 0′ 57.96″ W). According to the 2010 census, 102,214 people reside in the municipality's 579 km^2 of land (Ghana Statistical Service (GSS), 2005). According to the Ghana population and housing census for the 2021 census, the municipality's population has grown to 200,672 people, of which 143,358 people (71.4 %) live in urban areas while 57,314 people (28.6 %) are residing in rural areas (GSS, 2021).To the western border of the studied municipality lies the Wa West administrative District of Ghana, with the Nadowli administrative district lying to the east. In the Guinea Savannah agroecological zone, the Wa Municipal District (Figure 6.1.) is characterised by flora that has adapted to drought.

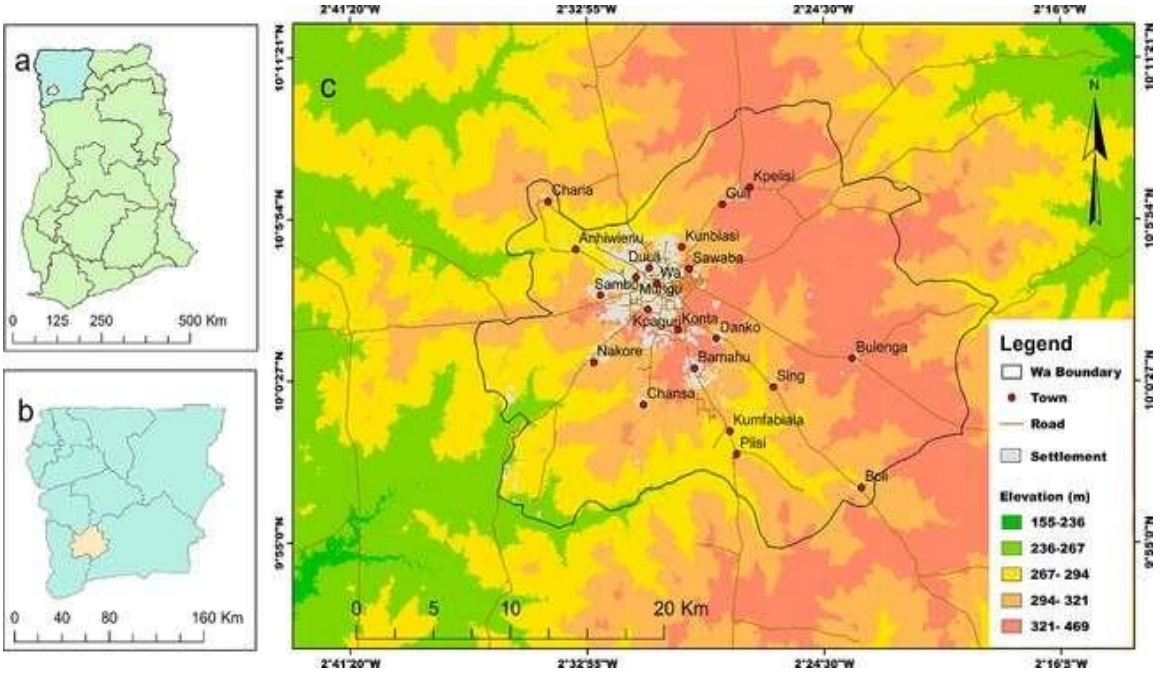

Figure 6.1. Map of Wa Municipality's Land Elevation Within the Context of the Upper West Region of Ghana. (a) A map of Ghana displaying its sixteen administrative regions, with Upper West shaded. (b) Map of the Upper West region displaying the eleven administrative districts and their borders; Wa municipality is shown by shade. (c) Digital elevation model (DEM); the black line designates the Wa municipality's administrative boundary. Data source: See Shuttle Radar Topography Mission (SRTM) DEM, obtained from the United States Geological Survey's (USGS) Earth Explorer database. Retrieved from https://earthexplorer.usgs.gov/ on 18 September 2020).

A savannah landscape characterises the Wa municipality. Its relief is slightly undulating in the savannah high plains, which are located between 160 and 300 m a.s.l. The southern and the northern areas are low-lying and constitute two drainage systems within the municipality with the main drainage system in the north. The main soil types are laterites, which can be found across the entire municipality, but in its western part shallow savannah ochrosols predominate. Locally clayey and sandy textures predominate; especially Nakore township and its environ in the western part of the municipality has abundant occurrence of sandy materials, while the community of Charia township and its environ is well known for a predominance of clay. Rivers in the low-lying areas are peri- odical and provide discharge during the rainy season. The valleys also form the two principal drainage systems in the Wa municipality. The Billi and its tributaries drain the northern part of the Wa municipality, and the Sing-Bakpong and its tributaries drain the southern part (GSS, 2014), both are tributary to the Black Volta River.

The climate of Wa municipality is tropical and characterised by two distinct seasons as controlled by the dry Northeast trade winds (which originate from the sub-tropical high-pressure region) and the South-west monsoon winds (which originate from the Indian sub-continent in a south-westerly direction). The wet season, which runs from May to September, is linked to the southwest monsoon winds (Barry et al., 2005; GSS, 2014). The dry Harmattan season usually commences in November and lasts till around March and is caused by the northeast trade winds. The mean annual temperature ranges from 20.5 to 37.2 ◦C, seldom drops below 15.5 ◦C and occasionally might exceed 40 ◦C.

The relative humidity ranges from 68 to 72 %, with the mean annual rainfall varying between 840 and 1400 mm within the 1990–2020 period (GSS, 2014; Kpienbaareh & Oduro Appiah, 2019). Under the

influence of Harmattan winds, relative humidity can drop below 20 % during extended drought periods. The central part of Wa municipality is highly urbanised with a cluster of towns which significantly expanded since 1990 (Asempah et al., 2021). The northern part of the municipality is an expansion of rural settlements such as the Charia, Guuli and Anhiwienu, with these areas lying in the lowlands close to the major rivers in the region. Piisi, Boli and Sing villages are located in the slightly undulating lowlands south of Wa; also, their location is close to the major rivers. In contrast, the Nakore and Bulenga villages are located in the headwater areas. All these smaller villages correspond to nucleated villages and are directly connected by roads to Wa; between the villages along the roads, dispersed settlements occur. The remaining area is predominantly rural and characterised by savannah vegetation. Agriculture and further processing of agricultural products characterise the economic structure of Wa municipality (GSS, 2021). Major crops cultivated are millet, sorghum, yam, soya beans and groundnuts. Beyond, trees of economic value such as the baobab, the shea tree, and the teak tree among others are widespread in the area, and serve to diversify agricultural products and thus sustain livelihood and development (Ham, 2017; Kent, 2018). Seasonal bushfires, climate change, and expanding built-up regions strain economic trees' advantages and livelihoods. Based on the general characteristics of the municipality coupled with rapid settlement expansion and exposure of the landscape due to anthropogenic activities, the tendency for soil erosion risk in the area is high.

6.2.2 RUSLE Model

We applied the RUSLE model in estimating the average annual rate of soil loss based on the sheet and rill erosion forms, and to show the distribution of potential and predicted soil erosion risks across space in the Wa municipality. The RUSLE model's comparative advantage in modelling data-scarce landscapes owing to its flexible data requirements makes it applicable to the Wa municipality other than physically distributed models with extensive data requirements (Benavidez et al., 2018). We applied ArcGIS in conjunction with QGIS and the machine learning programme R to process the raster-based input data required to implement the RUSLE model. Estimation of soil erosion risk was conducted by applying the formula by Renard et al., (1997):

$$A_{SE}\ [t\ ha^{-1}\ yr^{-1}] = R \times K \times L\ S \times C \times P \tag{6.1}$$

where:

A_{SE} connotes the average soil erosion rate per annum (t ha^{-1} yr^{-1}); R connotes rainfall erosivity factor (R-factor) (MJ mm ha-1 h^{-1} yr^{-1}); K connotes soil erodibility factor (K-factor) (t h MJ^{-1} mm^{-1}); LS represents the slope length and steepness factor (LS-factor); C represents the cover management factor (C-factor), and P connoted the conservation support practice factor (P-factor). Weighted values 0 and 1 are the respective lower and upper limits of C and P values, and this is influenced by the level of vegetation and conservation management practices available on the landscape.

To better explain the effects of land use change on morphodynamics, we applied Eq. (6.1) and set the C-factor and P-factor values to 1 as the identity number for multiplication operations. We define the resulting average potential soil erosion rate per annum Apot (t ha^{-1} yr^{-1}) as the soil loss of a land surface without conservation and management practice. Data from diverse sources were used for the computation of the input variables for the model (Table SM 6.1). The K-factor was generated using

soil grid data from the International Soil Reference Information Centre (ISRIC) database (See https://soilgrids.org). A trapezoidal rule approach was complemented with machine learning for an onward computation to generate the K-factor input parameter. The LS-factor is obtained from the SRTM DEM with a horizontal resolution of 30 × 30 m. C-factors were deduced on the terrain cover characteristic presented in the Wa municipality's LULC classification for the years 1990 and 2020 (Asempah et al., 2021). All the input raster data were of 30 × 30 m horizontal resolution except for the K-factor raster data that was available in 250 × 250 m resolution. By employing nearest neighbour techniques, the K-factor raster was resampled to the same resolution and projection to ensure model accuracy.

Soil Erodibility factor (K). The K-factor defines the proneness of soil to erosion as a result of the soil's inherent properties that influence the resistance to detachment. Soil physical properties (including porosity, structure and texture) play significant roles in soil erosion as they influence the degree of resistance or susceptibility to rainfall impacts in the form of splash or overland flow (Beguería et al., 2015). In computing the soil erodibility factor, we obtained data from the ISRIC database. The soil information applied in estimating the K-factor with the equation proposed by Sharpley & Williams in 1990, which includes contents of silt, clay, sand and organic matter. While these data are at the "SoilGrids" and available for soil layers from 0 cm to 200 cm depth (with other sub-divisions), we used weighted averages of these characters for the soil layers within 0-30 cm depth. By employing numerical integration through a Trapezoidal equation, the average values for each layer of overall depth intervals for 0–30 cm were estimated using a weighted mean of the predictions in the interval (Hengl et al., 2017):

$$\frac{1}{b-a}\int_a^b f(x)dx \approx \frac{1}{(b-a)}\frac{1}{2}\sum_{K=1}^{N-1}(X_K+1-X_K)(f(X_K)+f(X_K+1)) \quad (6.2)$$

where:
N connotes the number of depths; xk represents the kth depth; f(xk) is the estimated value of the target variable (i.e., soil property) at depth xk.

Machine learning was employed in the processing and generating of the weighted averages of the respective raster layers for the various soil properties as inferred from Eq. (2). The output raster layers were used subsequently as the input parameters for the computation of the K-factor using the proposed Eq. (3) (Sharpley & Williams, 1990; Y. Yang et al., 2018).

$$k = 0.1317(0.2+0.3*e^{\{-0.0256SAN\left(1-\frac{SIL}{100}\right)\}*}(\frac{SIL}{CLA+SIL})^{0.3})*\{1-\frac{0.25*TOC}{TOC+e^{(3.72-2.95*TOC)}}\}*\{1-\frac{0.7*SN1}{SN1+e^{(22.9*SN1-5.51)}}\} \quad (6.3)$$

where:
SAN represents sand, SIL connotes silt, CLA is clay, TOC represents the Total organic carbon contents of the soil (mass-%) and SN1=1- SAN/100.

Slope Length and Steepness Factor (LS). LS-factor is an important parameter that influences soil erosion, and it represents the cumulated effects of slope steepness (S) and slope length (L) on soil erosion (S. Schmidt et al., 2019). The distance between an upslope starting point and to downslope point where soil deposition starts is referred to as the slope length (L) (Farhan & Nawaiseh, 2015). The exposure to soil loss is increased by increasing the length of the slope and the steepness per unit area,

which increases the values of runoff and associated flow velocity (Defersha et al., 2010). A steeper slope has a higher tendency to influence erosion because it produces a higher flow velocity of runoff, thereby increasing the shear stress on the surface and in consequence mobilising more material (D. M. Fox & Bryan, 2000). The combined effects of the slope length and the steepness measure the topographic impact on erosion (Defersha et al., 2010; D. M. Fox & Bryan, 2000; Shrestha & Jetten, 2018). The LS-factor utilised in the RUSLE model was derived from a 30 × 30 m resolution SRTM DEM by computation using the Hydrology module (Farhan & Nawaiseh, 2015) of the SAGA GIS software. The fill sink algorithm was used for data pre-processing, utilising the spill-elevation method (L. Wang & Liu, 2006). The DEM was further processed by applying the multiple flow direction tool (MFD) (S. Wu et al., 2008) in SAGA GIS for the attribution of flow directions and accumulation (Tarboton, 1997). The computation of LS-factor considers the unit contributing area that is factored distribution of LS-factor over the entire landscape (X. Yang, 2015).

Rainfall erosivity factor (R). The R-factor is the capacity of rain to trigger soil erosion (Farhan & Nawaiseh, 2015; Stocking & Elwell, 1976). The Rainfall variables that determine the total erosivity include the drop size and drop distribution, amount and intensity coupled with terminal velocity (Meshesha et al., 2014; Thomas et al., 2018). The raindrop impact partly determines the rate of runoff usually associated with rain and, in effect, reflects in the numerical value of rainfall erosivity (Wischmeier & Smith, 1978). Based on high-resolution data, a product of long-term average rainfall energy (E) together with a maximum of 30 min rainfall intensity (I30) for storm events is desirable for the computation of Rainfall erosivity. However, in the absence of high-resolution and sufficient data, several context-specific simplified approaches have been proposed to estimate an R-factor (J. H. Lee & Heo, 2011; Renard et al., 1997). In this study, we explored tropical landscape-specific equations applicable to the context of Wa municipality in computing R-factor (in MJ mm ha^{-1} h^{-1} yr^{-1}). The equation for estimating R (Tilahun et al., 2018) is given as follows:

$$R = 0.562(Ar) - 8.1 \quad (6.4)$$

Where: R denotes the rainfall erosivity factor, and (Ar) denotes average annual rainfall.

Time series erosivity was computed from the long-term rainfall data from 1980 to 1990 and 2010–2020 for the examined years 1990 and 2020, respectively. The inverse distance weighted (IDW) technique was used to interpolate the long-term rainfall data. The output raster of the interpolation was extracted to the extent of the study area and subsequently applied in Eq. (6.4) to compute the erosivity factor.

Land Cover and Management Factor (C). The C-factor is explained as the influence of vegetation cover on erosion (S. Lee, 2004). Barelands are more prone to erosion than vegetated lands as – among others - they are protected from raindrop impact by leave coverage, as soil cohesion is supported by plant roots and as vegetation increases surface roughness and, thus, decelerates flow velocity (Mengistu et al., 2015; Wischmeier & Smith, 1978; Wynants et al., 2018). Therefore, depletion in vegetation cover may cause the C-factor to increase significantly, and in effect increase in soil loss rate. The C-factor corresponds to an assigned numeric value (0–1), which is based on the land cover types and their resistance capability to erosivity capabilities as presented as vegetative protection (Table 6.1). Completely bare land has a C-factor of 1, while densely vegetated land that tends to protect the soil from detachment has a C-factor of 0. Hence, the lower the C-factor value the better erosion prevention

capability and vice versa (Mengistu et al., 2015). Several approaches are proposed for the computation of the C-factor. The approach of Benkobi et al. (1994); and Renard et al. (1997) is based on a field experiment that considers the C-factor as the product of soil loss ratio and the total storm energy of a rainfall event with 30 min intensity (EIn) divided by the total storm erosivity EI.

The soil loss ratio is computed as the product before land use, surface cover, canopy cover, soil moisture and surface roughness (Renard et al., 1997; J. Wu et al., 2021). Though this approach seems preferable, some limitations hinder its adoption. The approach involves a laborious field experiment to obtain the surface cover, canopy cover, soil moisture and surface roughness on the assumption of their uniform distribution throughout the entire landscape (Tanyaş et al., 2015). The samples obtained may not reflect the exact prevailing conditions of the entire landscape and may differ from season to season (Renard et al., 1997; J. Wu et al., 2021). Based on this we employed the option of satellite images which give a better impression of the landscape characteristics in terms of the type and extent of vegetation coverage.

The C-factor was deduced from a supervised LULC classification to establish the type as well as the stretch of land cover and by this to achieve a reliable C-factor as an input parameter for the RUSLE model (Table 6.1). We used LULC maps for the years 1990 and 2020 generated from satellite images adapted from Asempah et al., (2021) (Figure. 6.3). The categorisation and definition of LULC classes (Table SM 6.2) were adapted after Ghana's LULC classification scheme to visualise remote sensing data (Basommi et al., 2015). Based on the land use and land cover classes, we estimated the C-factor by assigning a weighted C-factor value to each land use and land cover types

Table 6.1. Classes of Land Cover and their Spatial Extent (%) in the Wa Municipality. For the C-Factor Values Assigned to their Respective Land Cover Classes, References are Provided**.**

Land cover classes	Area Covered (%)		Weighted C-factor value	Source of Weighted C-factor value
	1990	2020		
Closed savannah	22.22	15.77	0.001	(Kusimi et al., 2015; Watene et al., 2021)
Open savannah	70.30	67.72	0.002	(Kusimi et al., 2015)
Other (bare land)	3.83	3.82	1	(Asiedu, 2018; Girma & Gebre, 2020)
Settlement	1.28	10.33	0.8	(Asiedu, 2018)
Vegetated wetland	2.30	2.16	0.21	(Asiedu, 2018)
Water	0.07	0.20	0	(Asiedu, 2018; Girma & Gebre, 2020)

The weighted values of each land use and land cover type were carefully selected by evaluating literature in the context of tropical savannah landscape (Basommi et al., 2015; Benkobi et al., 1994; Tanyaş et al., 2015; J. Wu et al., 2021; Wynants et al., 2018). The C-factor raster images that served as an input parameter for the RUSLE model were obtained by multiplying the established weighted value for each LULC class by their corresponding weighted C-factor value (Table 6.1).

Conservation Support Practice factor (P). P-factor values range from 0 to 1 and indicate the effectiveness of conservation practices in the landscape as a measure against soil erosion (Karthick et al., 2017; Panagos, Borrelli, Meusburger, et al., 2015). A lower P-factor value implies better management and conservation practices and higher effectiveness in reducing soil erosion. In

comparison, a high P-factor value represents less effective conservation practices and less effective erosion control ability (Tian et al., 2021). Thus, a P-factor value of 0 indicates the highest erosion control ability, while a P-factor value of 1 means no soil conservation or erosion control measure is implemented (Karthick et al., 2017; Panagos, Borrelli, & Meusburger, 2015). The type of conservation and management option highly depends on the topography of the landscape; hence computation of the P-factor considers the slope of the landscape to adopt conservation activities such as contour ploughing, strip cropping and terrace risers and bunds to control surface runoff and force infiltration (Jia Chen et al., 2019; Tian et al., 2021).

6.2.3 Field Survey of On-site Erosion Damages

To validate the results of the RUSLE model, we conducted in January/February 2022 a field survey to measure the spatial extents of on-site soil erosion damages, specifically, rills and inter-rills in the Wa municipality. Specifically, a survey was implemented on 2 km^2 plots each in the Wa municipality's closed savannah, open savannah, and settlement LULC areas. On-site damages that qualify as rills and inter-rill in the context of the RUSLE model specification for soil erosion risk assessment were identified, mapped and measured (Bewket & Sterk, 2003). A portable GPS (Garmin 60Cx) was used in mapping and geocoding the individual damage spots that comprise linear channels whose dimensions are within rill and inter-rills categories other than ephemeral gullies and gullies (Poesen et al., 2003). Rills as linear erosion channels had a cross-sectional area of less than 929 cm^2 and a maximum depth of 0.5 m (Marondedze & Schütt, 2020; Poesen et al., 2003). The spatial extent of damages from various survey plots was categorised into five classes of damages in a digitised damage map depicting the extent of disturbance within each LULC area (Figure 6.5) and systematically and statistically compared to the corresponding soil erosion risk predicted by the RUSLE model. Prior to the systematic and statistical comparison, the data was standardised by logistic transformation.

6.3 Results

6.3.1 RUSLE Model Input Parameters

Soil Erodibility factor (K). Within this model, the K-factor values estimated for the whole landscape of Wa municipality range from 0.024 to 0.034 t h MJ^{-1} mm^{-1}, with the mean value corresponding to 0.029 t h MJ-^{1} mm^{-1} (std.=0.001) (Figure 6.2A). The values spread heterogeneously across the studied municipality with relatively low values (0.024-0.028 t h MJ^{-1} mm^{-1}) in the western and southwestern part of the municipality where coarse-textured soils predominate. In the most western part of Wa municipality K-factor values of 0.029- 0.030 t h MJ^{-1} mm^{-1} can be observed. Isolated patches of the highest K-factor values occur across the entire study area. The field survey showed a distribution of diverse soil characteristics, corresponding to the diversity in the k-factor for the area. Slope Length and Steepness Factor (LS). In the study municipality, the LS-factor values range from 0 to 7.12, with a mean value of 2.96 (std = 0.06) (Figure 6.2B). Due to the overall slightly undulating terrain in the Wa municipality, LS values remain < 2.2. Correspondingly, the variability of the LS-factor is low. Steep slopes and coinciding increased LS factors predominantly occur around the central and northeastern areas of the municipality. Locally slopy areas also occur in the urbanised of Kpelisi, Mungu, Duuli and the Wa township.

Rainfall erosivity factor (R). The decadal rainfall for the entire Wa municipality from 1980 to 1990 averaged 948 mm (std.=0.74) with a corresponding average R-factor of 524.83 MJ mm ha-^{1} h^{-1} yr^{-1} (std.=0.53). In the year 2020 rainfall averaged 723 mm, also with a corresponding R- R-factor of 398.63 MJ mm ha^{-1} h^{-1} yr$^{-1.}$ This data is consistent with the Ghana Meteorological Agency and Ghana Statistical Service's annual rainfall statistics for the Wa municipality (GSS, 2014).

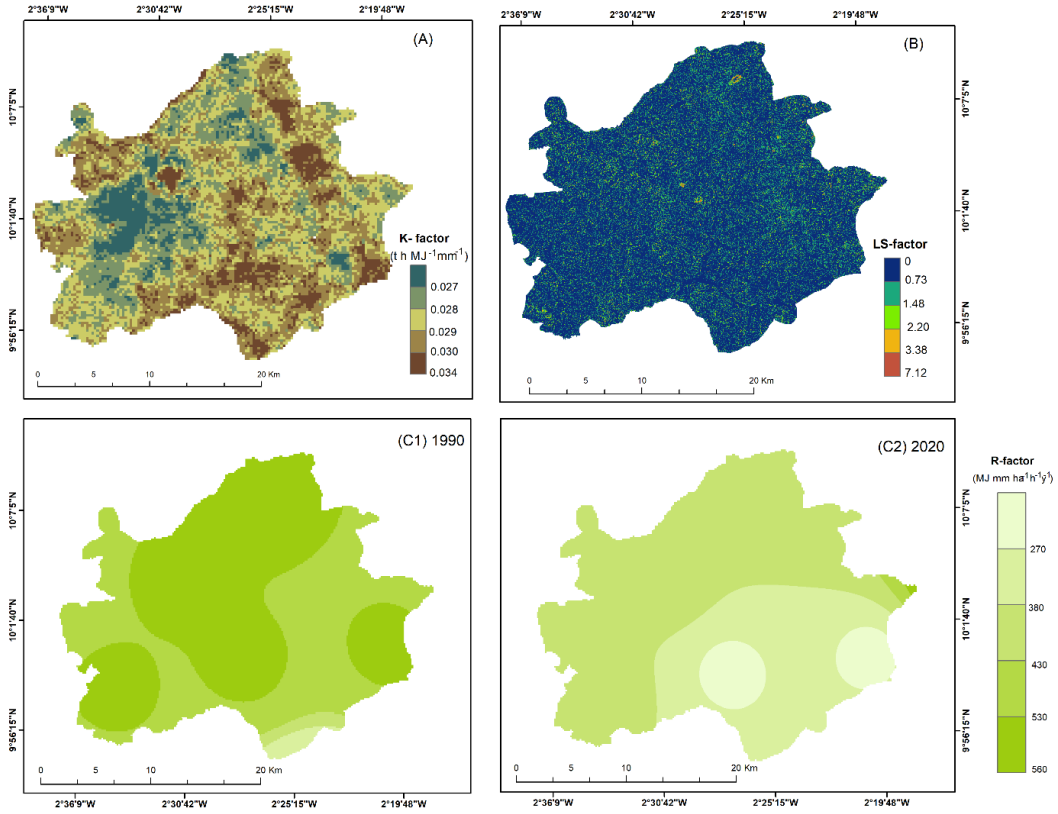

Figure 6.2. Map of K, LS and R-factor. (A) Soil Erodibility Map for the Wa municipality (Data source: ISRIC- World Soil Information "SoilGrids" provides a raster (TIF format) global soil map and associated information (See https://soilgrids.org; accessed on 20 September 2021). (B) LS factor map for the Wa municipality. Source of Data: SRTM DEM from USGS' Earth Explorer website (See https:// earthexplorer.usgs.gov/ 15th September 2020). (C1) The R-factor for 1990 (C2) the R- R-factor for 2020 (See database at: https://power.larc.nasa.gov/ accessed on 15 April 2021).

Generally, rainfall erosivity factors (R) differ in spatial variability across the Wa municipality for the observation years 1990 and 2020. In 1990, the highest R-factors ranging between 530 and 560 MJ mm ha^{-1} h^{-1} yr^{-1} occurred along a N-S corridor across Wa municipality, while in the neighboring areas R-factors varied between 480 and 530 MJ mm ha^{-1} h^{-1} yr^{-1} (Figure 6.2 C1). In contrast, during the study year 2020 the R-factor is evenly distributed across the study area with values predominantly < 480 MJ mm ha^{-1} h^{-1} yr^{-1}. (Figure 6.2 C2).

Estimated Cover factor (C) and Support Practice factor (P). The area of Wa municipality is predominantly covered with the savannah open vegetation that constitutes the arable land for various agricultural activities. Settlement and bare lands areas show the highest C- factor values (0.8 and 1, respectively) (Figure 6.3). The smallest C-factor values are assigned to areas with dense vegetation cover (example the closed savannah vegetation and the vegetated wetland areas). While the closed savannah areas are characterised by a dense cover of trees and bushes and a dense ground vegetation layer, the vegetated wetlands areas are characterised by a dense grass and shrub cover that get

inundated regularly. Due to the expansion of settlement areas and corresponding decline of savannah areas between 1990 and 2020, the area characterised by low C-factor values is distinctly larger in the year 1990 than in the year 2020, as it is also evident in the LULC classification (Table 6.1). Previous scientific works extensively established P-factor values in the context of typical tropical regions. However, our field survey shows that support or erosion control practices is lacking in the Wa municipality; thus, our model considered 1 as the value for the P-factor.

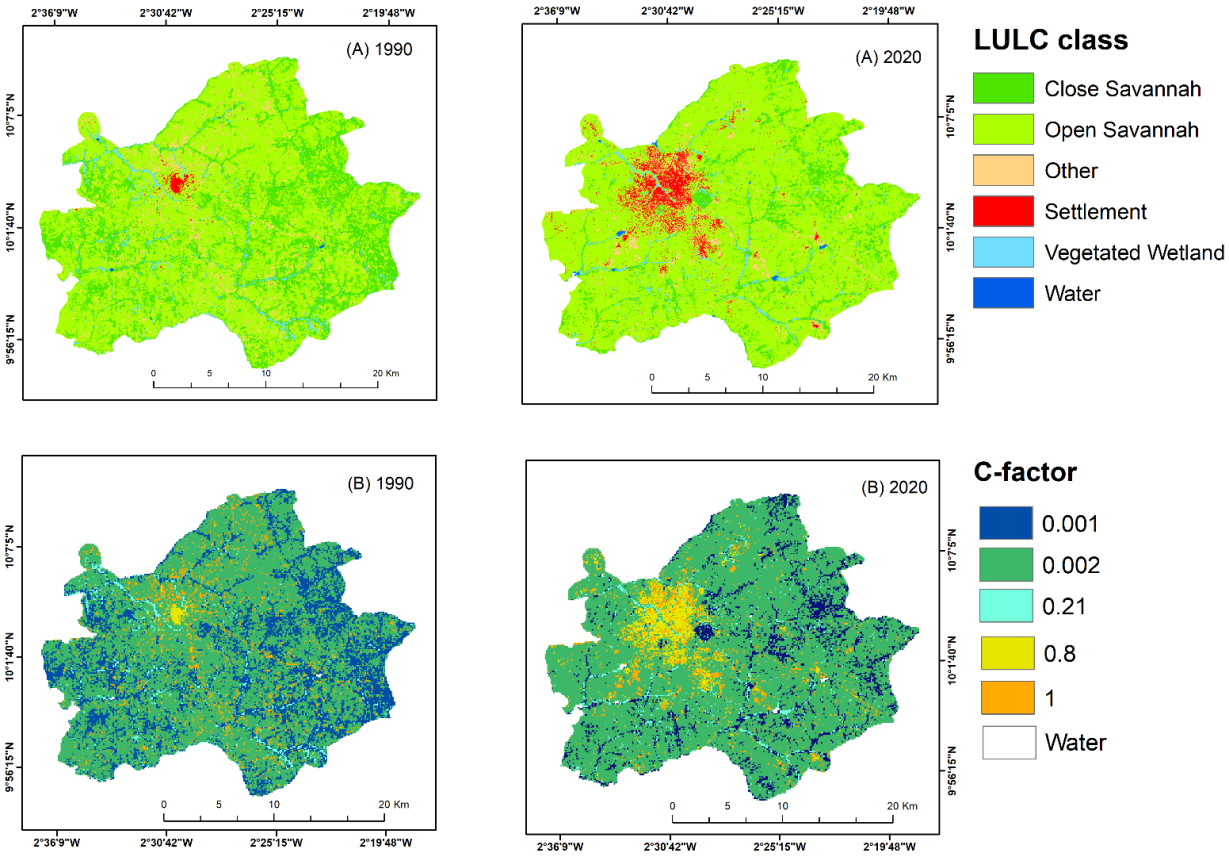

Figure 6.3. LULC Map for the Wa Municipality and Corresponding C-factor Input Parameter for Modelling Soil Erosion Risk for the years 1990 and 2020. (A) 1990 and (A) 2020 are LULC maps for 1990 and 2020, respectively, while (B) 1990 and (B) 2020 are corresponding C-factor input parameters for the years 1990 and 2020, respectively (LULC classification adapted from (Asempah et al., 2021)

6.3.2 Estimated Potential Erosion Risk A_{pot}

The modelled potential erosion risk for the years 1990 and 2020 is expressed as soil loss by potential erosion Apot. and focusses on the physical factors controlling erosion, thus, exclusively the R, LS and K-factors are taken as input for the RUSLE model. The resulting maps of potential erosion risk (Figure SM 6.1) are complemented by the corresponding statistical values (Table 6.2) for the respective years.

Altogether, for 1990 the estimated rate of potential erosion range between 0 and 111 t $ha^{-1}y^{-1}$ corresponding to a total potential soil loss in Wa municipality of c. 395,959 tons. For the year 2020, the rate of potential erosion is estimated to lie within 0- 83 t $ha^{-1}y^{-1}$, with a corresponding total potential soil loss in Wa municipality of c. 376,266 tons. For both observation years, more than 50 % of the landscape was prone to high-to-extreme grades of potential erosion risk. For 1990 36.5 % of the Wa

municipality was exposed to a high potential erosion risk; within the error margins, this equals the area being exposed to high potential erosion in 2020 (38.1 %; Table 6.2). Areas with “low” and “moderate” potential erosion risk predominantly occurred in flat areas. In contrast, areas exposed to the "very high" and "extreme" potential erosion risk corresponded to areas with high LS-factors or occurred in urbanised areas with extensive road networks.

Table 6.2. Estimated soil Loss by Potential Erosion Apot. at Wa Municipality by Different Severity Classes.

		1990: Soil loss by potential erosion $A_{pot.}$				**2020: Soil loss by potential erosion $A_{pot.}$**			
Potential Erosion Risk	Soil Erosion (t $ha^{-1}y^{-1}$)	Total area (ha)	Total area (%)	Total soil loss (t y^{-1})	Total soil loss (%)	Total area (ha)	Total area (%)	Total soil loss (t y^{-1})	Total soil loss (%)
Low	<3	16,933.8	29.3	34,352.6	8.7	15,933.9	27.6	28,840.3	7.7
Moderate	3-5	8,101.2	14.0	42,541.4	10.7	7,050.2	12.2	27,495.6	7.3
High	6-10	21,119.0	36.5	145,261.1	36.7	22,019.0	38.1	147,747.8	39.3
Very High	11-15	8,223.4	14.2	105,664.4	26.7	8,519.3	14.7	104,957.9	27.9
Extreme	>15	3,506.6	6.1	68,139.9	17.2	4,306.5	7.5	67,224.5	17.9
		57,884	100.0	395,959.4	100.0	57,828.9	100.0	376,266.1	100.0

6.3.3 Estimated Soil Erosion Risk A_{SE}

In 1990, about 83.9 % of the Wa municipality was exposed to low to moderate soil erosion risk while in 2020 spatial extent of areas exposed to low to moderate soil erosion risk decreased to 76.0 % (Table 6.3). These areas of low to moderate soil erosion risk contributed in 1990 to 44.8 % of the total erosion in Wa municipality while in 2020 it amounted to 39.3 %. In contrast, areas that were exposed to "high" and "very high" soil erosion risk covered in 1990 15.35 % of the area of Wa municipality, and increased in spatial extent to 23.4 % in 2020; it is estimated that these areas exposed to “high” and “very high” soil erosion risk contributed about half of the municipality’s total soil loss in the respective year. The statistics document the contribution of the different soil erosion risk grades to the estimated annual soil loss: For 1990 total soil loss in Wa municipality was estimated at 150,401 tons but increased to an estimated total erosion of 200,464 tons in 2020. The soil erosion risk in Wa municipality averaged in 1990 2.6 t ha^{-1} y^{-1} (range of spatial distribution: 0-59 t ha^{-1} y^{-1}) and in 2020 3.5 t ha^{-1} y^{-1} (range of spatial distribution:0-68 t ha^{-1} y^{-1}) (Figure 6.4). Exposure to high soil erosion risk especially occurred around the central part of the Wa municipality, with isolated patches of very high and severe soil erosion risk. Very high to extreme soil erosion risk predominantly can be observed at hillside locations within settlement areas; this observation applies for both observation years. Spatial variations in soil erosion risk for Wa municipality closely correlates to land use. In general, the areas covered by open savannah vegetation contributed about three-quarters of the total soil loss in 1990 and 2020 with a spatial extend of open savannah vegetation of 70.4 % in 1990 and 67.8 % in 2020.

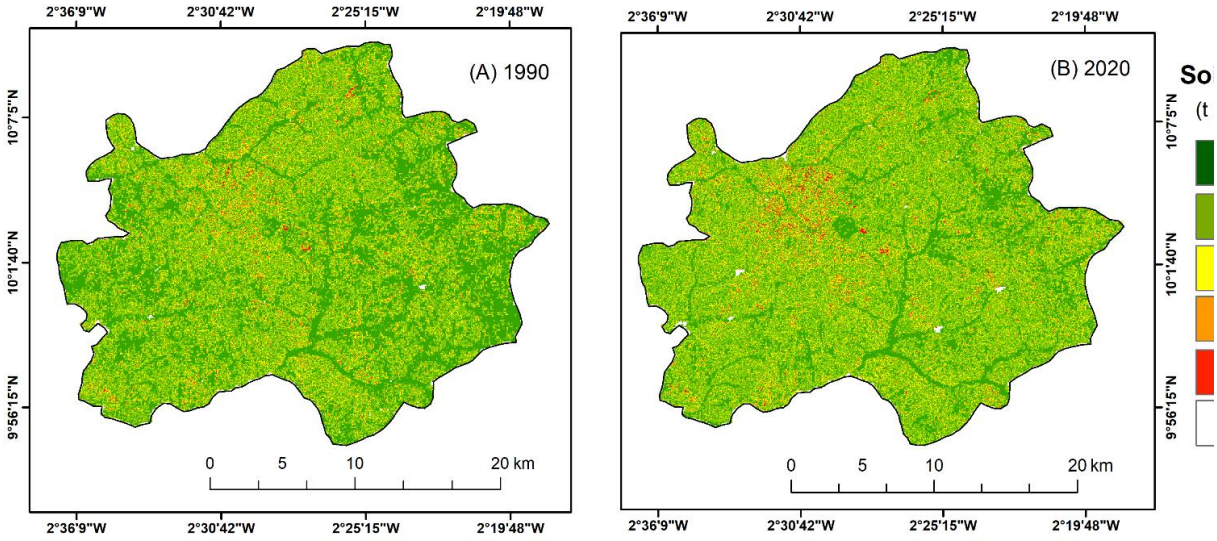

Figure 6.4. Spatial Distribution Map of the Estimated Soil Erosion Risk for Wa Municipality for the years (A) 1990 and (B) 2020.

Table 6.3. Estimated Soil Loss by Soil Erosion A_{SE} at Wa Municipality by Different Severity Classes.

		1990: Soil erosion A_{SE} risk by grade				**2020: Soil erosion risk A_{SE} by grade**			
Soil Erosion Risk	Soil Erosion (t $ha^{-1}y^{-1}$)	Total area (ha)	Total area (%)	Total soil loss (t y^{-1})	Total soil loss (%)	Total area (ha)	Total area (%)	Total soil loss (t y^{-1})	Total soil loss (%)
Low	<3	38,166.1	65.9	23,302	15.5	30,002.5	51.9	26,732	13.3
Moderate	3-5	10,421.2	18.0	44,027	29.3	13,960.1	24.10	52,145	26.0
High	6-10	7,592.7	13.1	58,751	39.1	10,957.0	18.9	73729	36.8
Very High	11-15	1,288.6	2.2	16,934	11.3	2,547.5	4.4	29,811	14.9
Extreme	>15	415.3	0.7	7,387	4.9	361.8	0.6	18,047	9.0
		57,883.9	100.0	150,401	100.0	57,828.9	100.0	200,464	100.0

The areas covered by open savannah vegetation are to a great extent cultivated and grazed, resulting in a high exposure to soil erosion. This is exacerbated by seasonal bushfires that usually occur during the Harmattan season that disturb vegetation cover and, thus, expose the area to erosion at the beginning of the rainy season (which advances the Harmattan season). Closed savannah vegetation covered in 1990 22.2 % (12,869 ha) of Wa municipality and had shrunk until 2020 to 15.8 % coverage (9134 ha) (Table 6.4). Due to the relatively low soil erosion risk under closed savannah vegetation, the decrease in the area covered by the closed savannah vegetation between 1990 and 2020 caused an increased exposure to soil loss in areas covered in 1990 still by the closed savannah. Areas covered by settlements and barelands in general have a high exposure to soil erosion risk (Mariye et al., 2022; Melese et al., 2021). The spatial extent of settlement areas in Wa municipality quadruplicated from 5.1 % in 1990 to 22.2 % in 2020. The contribution of areas covered by settlements or barelands to the total soil loss in Wa municipality amounted 13.4 % in 1990 and increased to 20.4 % in 2020 (Table 6.4).

Table 6.4. Estimates of Soil Loss Under Different LULC Across Wa Municipality.

	1990: Estimated soil loss by land use class				**2020: Estimated soil loss by land use class**			
Land use	Total area (ha)	Total area (%)	Total soil loss (t y^{-1})	Total soil loss (%)	Total (ha)	Total area (%)	Total soil loss (t y^{-1})	Total soil loss (%)
Closed Savannah	12,869.0	22.2	14,584	9.7	9,133.7	15.8	9,627	4.8
Open Savannah	40,722.5	70.4	113,987	75.8	39,224.9	67.8	146,689	73.2
Other	2,218.1	3.8	18,549	12.3	2,211.4	3.8	27,167	13.6
Settlement	744.4	1.3	1,637	1.1	5,985.9	10.4	13,794	6.9
Vegetated Wetland	1,329.9	2.3	1,644	1.1	1,273.1	2.2	3,187	1.6
	57,884.0	100	150,401	100	57,828.9	100.0	200,464	100

6.3.4 Validation of Modelled Soil Erosion Risk Applying RUSLE Model

During 2022 field survey in each of the land use classes, closed savannah (Figure 6.5A), open savannah (Figure 6.5B), and settlement (Figure 6.5C), a 2 km^2 test plot was systematically mapped for soil erosion damages. Mapping results were then applied to validate the RUSLE modelling results for soil erosion risk for the year 2020. For each plot area erosion damage maps (Fig.6. 5 A2, B2, B3) were systematically compared to the 2020 RUSLE modelling results of the soil erosion risk (Figure 6.5 A1, B1, C1). Altogether in all three survey plots, 79 linear erosion forms corresponding to rills were mapped and measured. Eighteen (18) of the rills (coverage: 15.1 m^2) were mapped in the closed Savannah vegetation areas, while 26 of the rills (coverage: 69.8 m^2) were mapped in areas covered by open savannah vegetation. In settlement areas degree of on-site damages was highest with a total number of 35 rills mapped (coverage: 109.9 m^2). In total, an area damaged by soil erosion of 194.8 m^2 was mapped within the 6 Km^2 of the three test plot areas.

The extent of on-site damages measured on each of the test plots is consistent with the modelled soil erosion risk for the respective sites. The soil erosion risk for settlement plot (C1) is classified as "high," "very high," and "severe," with a soil loss estimate of 6- 54 t ha^{-1} y^{-1}. The areas of high to extreme soil erosion risk correspond to the large spatial extent of soil erosion damages mapped and measured in the settlement test plot (C2). In comparison, in the open savannah vegetation test plot (B1) soil erosion risk is "moderate"to "high" (3-10 t ha^{-1} y^{-1}); the corresponding damage map of the open savannah test plot (B2) shows in comparison to the settlement test plot (C2) comparatively small spatial extent of areas with on-site erosion damages (mostly in the range of 2-5 m^2). Overall, the closed savannah test plot (A1) had the lowest soil erosion risk (< 3 t ha^{-1} y^{-1}). This corresponds to the least spatial extent of all the individual eroded area of less than 3 m^2 in the closed savannah damage map (A2). In a nutshell, for the test plots A1, B1 and C2 estimated soil erosion risk corresponds to the area of on-site damages in the respective test plots A2, B2 and C2.

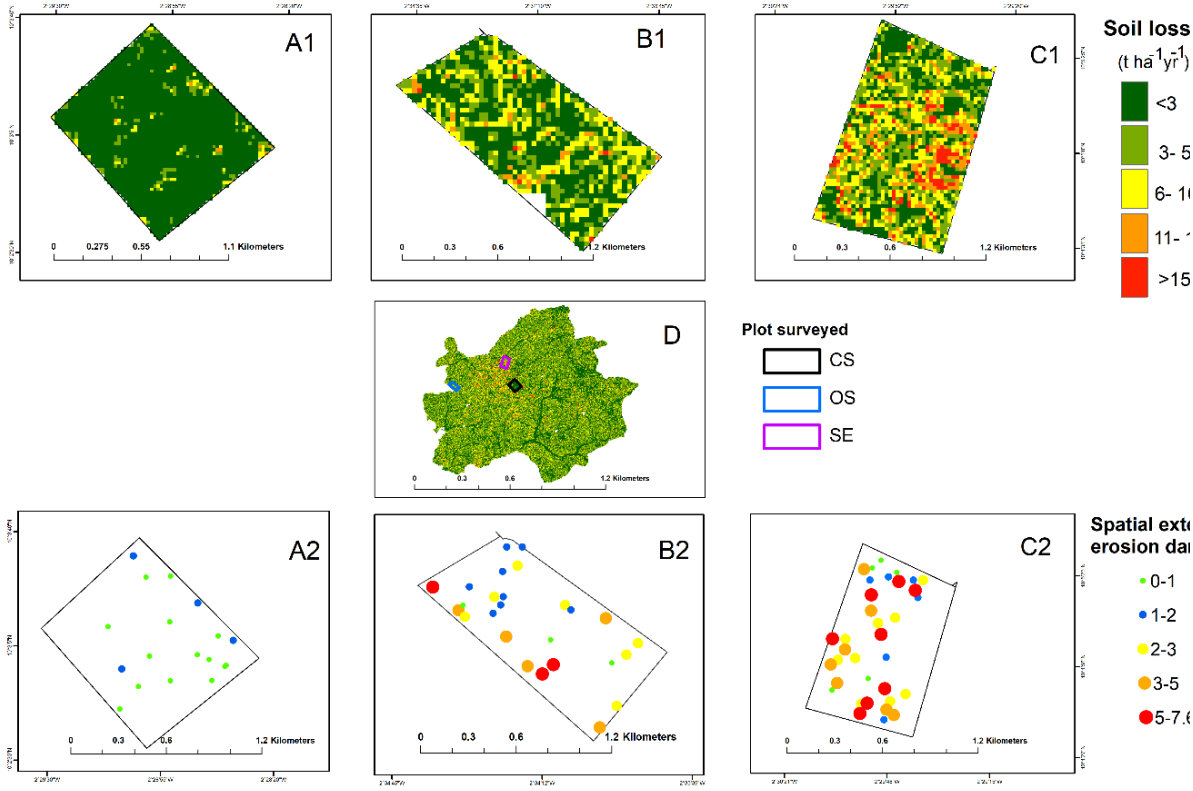

Figure 6.5. Validation Maps for Model Result and Corresponding Maps of Field Plots Surveyed from January to February 2022. (A1) The 2 km^2 model output for closed savannah area with various levels of soil erosion risks for the year 2020; (B1) the 2 km^2 model output for open savannah area with various levels of soil erosion risks for the year 2020; (C1) the 2 km^2 model output for settlement area with various levels of soil erosion risks for the year 2020. (A2) the corresponding plot of A1 with 18 measured spatial extents of soil erosion damages; (B2) the corresponding plot of B1 with 26 measured spatial extents of soil erosion damages;(C2) the corresponding plot of C1 with 35 measured spatial extents of soil erosion damages. (D) The soil erosion risk map for the Wa municipality for the year 2020 from which A1, B1 and C1 were extracted.

The moderate to high exposure to soil erosion risk in the open savannah LULC class indicates the high vulnerability of this area. The spatial pattern of the corresponding damage measurements (Figure 6.4 B2) is in line with the model results (Figure 6.4 B1). The highest exposure to soil erosion was observed in the settlement area plot. The spatial extent of erosion damages (Figure 6.5 C2) and the corresponding soil erosion risk map (Figure 6.5 C1) underline high exposure to soil erosion. However, spatial accordance of soil erosion damages mapped and soil erosion risk modelled is less solid for the settlement areas than for the areas covered by open and closed savannah (Figure 6.6). Overall, the configuration of soil erosion damages observed in the three different study plots largely conforms with the modelling result of soil erosion risk in the respective areas (Figure 6.6).

Figure 6.6. Soil Erosion Damages in the Wa Municipality Observed During the Field Survey. (CS) Damage observed within the closed savannah vegetation area; (OP) damages observed within the open savannah vegetation area; (SE) damage observed within the settlement area.

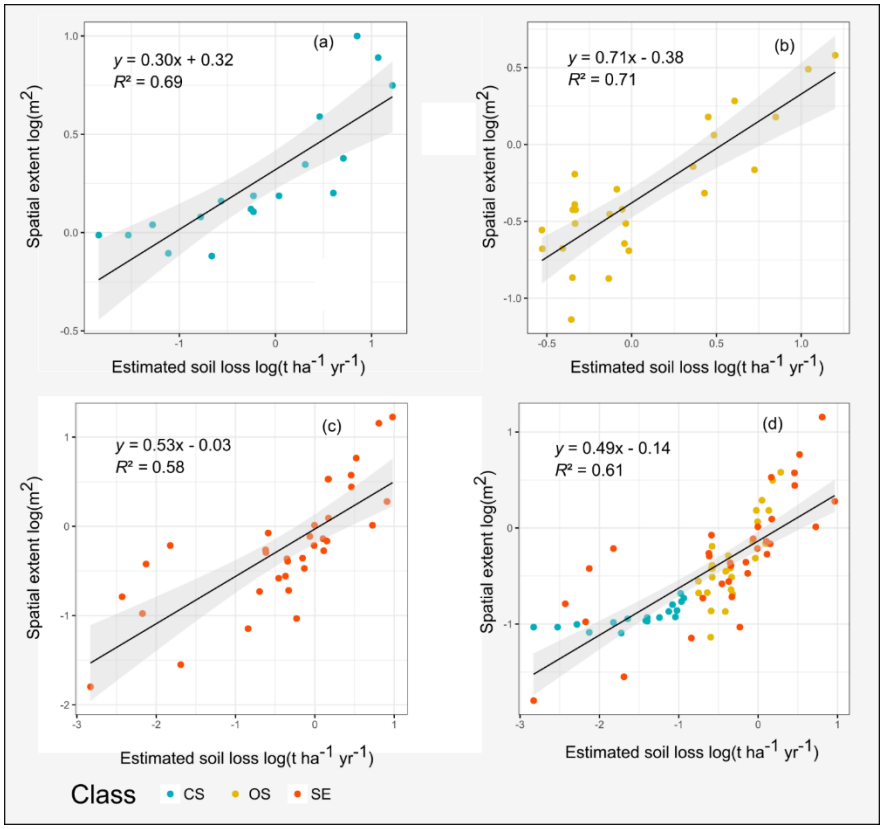

Figure 6.7. Evaluation of the Model's Results and Field Measurement. (a) evaluation for closed savannah LULC class; (b) evaluation for open savannah LULC class (c) evaluation for settlement LULC class; (d) the combined evaluation of a, b and c.

As a means of model validation, a systematic comparison of the RUSLE modelling result for soil erosion risk with the on-site field measurements of soil erosion damages, a satisfactory performance of the modelling results can be pointed out (Figure 6.6). Soil erosion risk modelling results for closed savannah test plot A1 and the corresponding on-site damages A2 show a strong spatial overlap and are significantly positively correlated ($R2 = 0.69$, $n = 18$, $\alpha < 0.05$). This also applies to the mapping results for the open savannah ($R2 = 0.71$, $n = 26$, $\alpha < 0.05$; Figure 6.6b) and the settlement test plot ($R2 = 0.58$, $n = 35$, $\alpha < 0.05$; Figure 6.6c). On the whole, the model output of soil erosion risk for the entire 6 km^2 of plot areas and the on-site mapped 79 linear damage form shows a positive correlation with $R2 = 0.61$ ($n = 79$). The analyses establish a statistical significance at $p < 0.05$ for the individual validations.

6.4 Discussion

The c. 30 % higher erosion risk predicted for the year 2020 than 1990 emphasises the RUSLE model results based on the prevailing driving factors in each year. These results are strongly linked to regional land use dynamics and changes in vegetation cover. The vegetation cover is essential in soil erosion risk reduction as its canopy intercepts rainfall, improves infiltration, and lowers the rainfall energy thereby reducing its impacts on soil erosion (Uddin et al., 2018). The spatial distribution of soil erosion risks presented in the soil erosion risk map (Figure. 6.4) shows that areas with very high and extreme soil erosion risk correspond to areas with relatively low vegetation cover and slopes with steep gradients, a finding that corresponds to those among others of (Pimentel & Burgess, 2013; Tian et al., 2021). This especially applies to urbanised areas which occur in slopy terrain such as Bamahu, Kpelisisi Guli Kpelisi, Mungu, Duuli and the Wa township, which can be characterised as very high to severe rate of exposure to soil erosion risk. During the 30 years between 1990 and 2020 the areas with very high to severe exposure to soil erosion risk expanded, and this was triggered by urban spread and its associated alteration of vegetation cover. These findings correspond to those from other African strongly urbanising areas such as Harare (Marondedze & Schütt, 2020). The observed significance of topographic characteristics (LS-factor) and cover factors as the main drivers for soil erosion risk within the Wa municipality is consistent with (Uddin et al., 2018). Beyond this, Karamage et al. (2017) highlight the relevance of the slope length for controlling soil erosion risk.

The decrease in vegetation cover and the associated increase in soil erosion risk can be explained by the Wa municipality's increasing population and associated developmental activities (Myers et al., 2013). Ghana's population and housing census has estimated growth of the Wa municipality's population by 10 % between 2000 and 2010, counting 98,675 inhabitants in 2000 and 107,214 in 2010 (GSS, 2012). A subsequent population and housing census conducted in 2021 attests to population growth of 200,672 inhabitants in Wa municipality (GSS, 2021), indicating a 6.0 % annual population growth since 2010. Population growth and associated settlement expansion drive infrastructure development, alteration of vegetation cover and environmental degradation as a whole (Acheampong & Anokye, 2013; Appiah et al., 2014). Between 1990 and 2020 settlement spaces expanded spatially from 7.44 km^2 to 59.86 7.44 km^2 (Asempah et al., 2021). In parallel, the estimated soil loss for Wa municipality amounted to 1637 tons in 1990 and octuplicates until 2020 to 13,794 tons in settlement areas. The settlement expansion-based soil erosion risk can be especially attributed to the infrastructure developments that need to be synchronised with the demands of population growth (Acheampong & Anokye, 2013; Osumanu et al., 2019). As the expansion of settlement areas is pronounced within the central part of Wa municipality where most settlements are clustered, construction of roads and other infrastructure developments are in

progress. This leads to the destruction of the ecosystem and exposes surface material due to earth movements. In consequence, urbanisation processes in Wa municipality led to the shrinking of areas covered by woody vegetation, a process especially due to the exploration of savannah-vegetated areas for agriculture and other livelihood diversification options such as unregulated small-scale gold mining (Antabe et al., 2017; Basommi et al., 2015). In total, an increase in settlement areas by 87.57 % between 1990 and 2020 in the Wa municipality parallel to a 40.89 % decrease in areas covered by woody vegetation (Asempah et al., 2021) occurred. These changes in vegetation and land use are reflected in an estimated 25 % rise in the total rate of soil loss between 1990 and 2020.

The strong control of soil erosion risk by LULC is also observed in areas under different savannah vegetation cover. In the years 1990 and 2020 areas under open savannah vegetation in particular contributed to a significant amount of soil loss due to proliferations of human activities within these areas, especially cultivation and grazing. Vulnerability to soil erosion corresponds to high soil erosion risk within the open savannah area with an escalating soil loss wherever canopy cover diminishes, ranging from 2- 4 t ha^{-1} y^{-1} in areas covered by trees and bushes and 16-34 t ha^{-1} y^{-1} for farmlands (Diwediga et al., 2018). These data affirm the consequential effects of exploiting vegetated savannah areas within the Wa municipality for agriculture, which renders this area to high soil erosion risk.

Within the Wa municipality, seasonal bushfires (Plate 6.1), which generally occur during the Harmattan season (Yahaya & Amoah, 2013), could be an exacerbating factor to increase soil erosion risk. Several studies pronounce the significant influence of bushfires on the rate of soil erosion (Agbeshie et al., 2022; O'Brien et al., 2018). According to Agbeshie et al. (2022), the severity level of bushfires is proportional to the rate of soil erosion. The interception functions of the tree canopy are lost after bushfire, thus, increasing generation of surface run-off results and associated with soil detachment and sediment transport (Bento-Gonçalves & Vieira, 2020). Estimated pre-fire soil erosion rates of 69 t $ha^{-1}yr^{-1}$ are distinctly lower than the estimated post-fire soil erosion rates (94 t ha^{-1} y^{-1}) documenting that the soil erosion rate shortly after the fire event increased by 36.2 % (Depountis et al., 2020). However, it has to be considered that bush fires not only affect canopy cover but also soil characters as it is well known that a rise in soil water repellency is a frequent after-effect of bush and forest fires (Kusakari et al., 2014). However, the long-term impact of fire on soil erosion could be higher than the immediate impact: An assessment of soil erosion after a decade of fire events shows a third reduced impact of fire on soil erosion compared to the impact observed immediately after bush fire event (Depountis et al., 2020).

The Wa municipality soils' physical characteristics and resulting erodibility potentials cause their low propensity to resist erosion (Beguería et al., 2015). The dominance of sandy soil texture across Wa municipality and herein formed shallow savannah ochrosols and laterites are reflected in the distribution of soil erosion risk (GSS, 2014). Coarse-textured soils dominate within the southwestern part of the studied municipality, resulting in moderate to severe soil erosion risks. Coarse-textured soils are in general characterised by high infiltration rates and corresponding low surface run-off generation; however, due to poor cohesion effects of sandy material erodibility is high (Duiker et al., 2001; P. M. Fox et al., 2017). Also, the settlement areas of Nakore and Chansa township and the adjourning central part of the Wa municipality are characterised by widely spread soils with sandy texture and were estimated to have high-to-severe soil erosion risk. In contrast, soils with high clay content are characterised by relatively poor infiltration rates and consequently affect strong surface run-off generation, but due to the strong cohesion of clayey soils resistance capabilities are high and erodibility

is low (Zhang et al., 2019). Beyond, soils with high aggregate stability resist the impact of raindrops and have a propensity to affect erosion (Fox et al., 2006; Fox et al., 2017). In the North-western part of Wa municipality, soils with clayey texture are widely spread and frequently covered by savannah vegetation. These areas show low to moderate exposure to soil erosion risk owing to the combined detachment resistance properties of soil characters and soil coverage (GSS, 2021).

The RUSLE model's prediction of a higher risk of potential erosion, compared to the actual risk of soil erosion is attributed to a lack of vegetation cover and underlines the influence of the municipal's climate, soil and topographic characteristics on erosion. The climatic influence on potential erosion risk for 1990 and 2020 is reflected in the R-factor maps (Figure. 6.2 C1 a and C2) and the corresponding potential erosion risk maps (Figure SM 6.1 A and B). Thus, the spatial distribution of potential erosion risk is higher in the year 1990 than in 2020 owing to the higher amount and distribution of rainfall in the year 1990 than in 2020. Increasing rainfall intensity and amount potentially increases soil detachment and soil erosion (Mohamadi & Kavian, 2015). Besides the climatic influence on the potential erosion risk, the topographic characteristics of the study area control erosion as areas with steep slopes show the highest severity of potential erosion risk (Pimentel & Burgess, 2013).

The actual soil erosion risk map (Figure 6.4) shows low soil erosion risk in areas with significant vegetation cover, while the corresponding areas on the potential risk of erosion map (Figure SM1) show "high" to "severe" risk. Most of the high to severe soil erosion risks were estimated for settlement and bareland areas while savannah vegetated areas underlie relatively low to moderate soil erosion risk. According to Ullah et al. (2018), human-induced modification of vegetation cover causes a high exposure to erosion risk in tropical landscapes. Unfortunately, the cover factor's function of erosion control is lacking in the settlement and bareland areas, consequently resulting in severe soil erosion risk (Marondedze & Schütt, 2020) and showing comparable exposure as the potential erosion risk.

The RUSLE model's predictions of soil erosion risk operate on the assumption of detachment of soil on the field (Seutloali et al., 2017). The assessment of the model outputs is improved when data from field surveys (point-like plot-based data) are used for the validation (Pistocchi et al., 2002; Seutloali et al., 20517). The data on spatial damages, estimated from the test plots under different land use represent the effective amount of soil removed. These mapped damages correspond spatially with soil loss estimates generated using the RUSLE model. Settlement areas showed the highest spatial extent of effective soil erosion damage while closed and open savannah areas featured less spatial extent of eroded areas. The spatial extent of eroded areas in each of the test plots agreed widely with the estimated soil erosion risk area applying the RUSLE model. Thus, the validation of the predicted soil erosion risk as provided by applying the RUSLE model by alignment with the spatial extent of measured effective damages has been proven to be a suitable tool to affirm the reliability of a model application to a new environment. Statistical analyses established positive correlations between data resulting from the utilisation of the RUSLE model and on-site measured data. Overall, the statistics for the 79 point-based data from the field survey and the corresponding modelling are positively correlated and highly significant ($\alpha < 0.05$). Though field damage estimation could not account for damages based on sheet erosion, the spatial extent of damages from field measurements reflected the predicted output and enhanced model evaluation and validation. Despite the essence of long-term field measurement as an ideal means for empirical model validation in soil erosion estimation, plot-based point data are suitable for effective validation and the general comprehension of the model performance (Lazzari et al., 2015; Seutloali et al., 2017).

6.5 Conclusions

In the Savanna agroecological zones of Ghana, soil erosion threatens environmental sustainability and agricultural productivity. Although predicting soil erosion risk is critical for developing land management plans sustainably in a vulnerable landscape, research in the Savannah agroecological zones has paid little consideration. This study assesses soil erosion risks within the context of land use dynamics in Wa municipality since 1990, a fast-developing area with rapid population growth. Assessment of soil erosion risk and estimation of average soil erosion rates per annum is based on change detection of LULC in Wa municipality between 1990 and 2020 (Asempah et al., 2021). The application of the RUSLE model emphasises in particular settlement areas and bareland in slopy terrain as highly vulnerable to soil erosion. The predicted rates of potential erosion for the years 1990 and 2020 were distinctly higher than the actual predicted rates of soil erosion of the respective years. The comparative lower actual soil erosion risk rate is due to vegetation cover influence that is reflected in the actual erosion risk model prediction for vegetated areas. Given the high risk associated with altered vegetated areas caused by human disturbances, the importance of a cover factor in soil conservation is emphasised. Aside the alteration of vegetation covers due to settlement activities, it is highlighting that areas with a high soil erosion risk spatially predominantly occur in areas with steep and long slopes.

Urbanisation processes and settlement activities that cause changes and loss of vegetation cover can be attributed to the estimated c. 30 % increase in soil loss between 1990 and 2020. Though the modelling data as well as the field survey identify the settlement areas as a high-risk zone, it can also be pointed out that the open savannah area contributes distinctly to the total rate of soil loss. In consequence, since open savannah is the most widespread land cover class its contribution to the total rate of soil loss is significant. In general, in Wa municipality, the vegetation cover is largely altered through the exploration of the area for agriculture. These coupled with bushfires render the area to high erosion risk. Due to the increasing population in Wa municipality, infrastructural development and agricultural production must synchronise with the populace's demands.

Unfortunately, in the quest to achieve that, the conversion of vegetated areas into settlement areas and agricultural areas has led to significant soil erosion and in consequence land degradation in the Wa municipality. Especially settlement areas and bareland have been identified as areas being highly exposed to soil erosion risk. Overall, the soil erosion risk within the Wa municipality is strongly linked to human-induced activities through land use intensification that renders the municipality vulnerable to erosion. Soil and water conservation strategies are important in such a situation; however, the field survey established that Wa municipality has no such interventions. It is therefore recommended to establish an integrated landscape management inclusive of soil and water conservation strategies to curtail the impending erosion-related menace. The findings from this study are relevant for designing and implementing mitigation strategies for the Wa municipality and tropical savannah landscapes at large. Outcomes of modelling soil erosion risk by applying the RUSLE in Wa municipality for the year 2020 were validated on a plot-based field survey conducted in January 2021. Statistical evaluations document an acceptable performance of the model output data. The statistics from the corroborative validation increase confidence in using the model.

6.6 Acknowledgements

We wish to express our profound gratitude to the colleagues with the Physical Geography unit at the Department of Earth Sciences, Freie Universität for their valuable expert contributions that greatly contributed to the successful implementation of this study. We wish to further appreciate our colleagues at the Ghana Water Resources Commission of Ghana, especially those within the Wa Municipality, for their support that made the field survey a success. Finally, we are thankful to NASA, as well as the USGS where relevant data; specifically, SRTM DEM and Landsat satellite imageries were acquired for the study.

We are thankful to the German Academic Exchange Service (DAAD) for the award of the fellowship through which this study was conducted. Also, we further acknowledge and appreciate the Freie Universität Berlin who provided funds to publish this article.

6.7 The Link of this Chapter to Other Chapters

This chapter is the second objective that estimated soil erosion risk in a typical savannah landscape of Wa municipality of Ghana between 1990 and 2020. As a case study in the Black Volta River Basin, it estimated and evaluated the spatial distribution of soil erosion risk in relation to the physical attributes of the municipality. The results of the RUSLE model estimations were compared with the land cover dynamic and settlement expansion from the previous chapter (5) to understand the impact of changes in land cover and settlement expansion on the severity of soil erosion risk in the municipality. The results of the RUSLE model were validated with field data of measured spatial extent of soil erosion damages in settlement, open savannah and closed savannah areas. Overall, the chapter set the base for the third objective (chapter 6) that sought to estimate and evaluate soil erosion risk across various characterised landscape units of the Black Volta River Basin for the years 1992, 2006 and 2020.

CHAPTER 7: MAJOR LANDSCAPE UNITS OF THE BLACK VOLTA BASIN AND THEIR EXPOSURE TO SOIL EROSION RISK

Asempah, M., Becker, F., Shisanya, C.A., Schütt, B. (Manuscript) ***Major Landscape Units of the Black Volta Basin and their Exposure to Soil Erosion Risk.***

Abstract

Soil erosion within river basins spatio-temporally varies depending on the prevailing environmental conditions and anthropogenic impacts. Analogously, different landscape units exhibit different degrees of susceptibility based on their physical and biological characteristics and the level of human activities. By employing the RUSLE empirical model, soil erosion risk of the Black Volta River basin (138,063 km² area) is modelled for the years 1992, 2006 and 2020 considering varying land use land cover and precipitation in the three-time slices. The Black Volta River basin covers several landscape units reaching from the Sahel zone to the Guinian-Savannah zone. In our study, we compare the varying susceptibility of the different landscape units to soil erosion risk. The results show an increased soil erosion risk in areas with strong relief and rare vegetation cover. The comparison between the time slices shows that in 2020 less than 10% of the basin area was exposed to "high" to "extreme" erosion risk and is in the range of variations of the other years. The highest soil erosion risk was predicted for the landscapes in the wet savannah zone.

Keywords: Black Volta basin, RUSLE model, soil degradation, soil erosion damage

7.1 Background

Tropical regions derive essential societal benefits from their landscapes, including agriculture, water for irrigation, hydropower, and transportation (Labrière et al., 2015; Strasser et al., 2016), all promoting livelihood development by supporting food production and trade. Despite the potential of tropical landscapes, there have been concerns about their degradation by soil erosion and its associated declining agricultural productivity (Amisigo et al., 2008; Pimentel, 2006). Associated sediment fluxes alter water quality and flow dynamics (Dutta, 2016; Morehead et al., 2003). Within river basins, soil erosion accelerates siltation of reservoirs, streams, and channels, thereby reducing their water-holding capacity and disrupting ecosystem functions, with long-term impacts on the availability of a landscape's natural resources (Dutta, 2016; Locatelli et al., 2011; Spalevic et al., 2020).

Soil erosion is controlled by a complex interplay of natural and human factors (Butt et al., 2010; Mutua et al., 2006). The natural causes include climate and weather characteristics, topography, and soil physical and chemical characteristics (Tully et al., 2015; Zhao & Hou, 2019). Beyond, soil erosion is attributed to land use and land management (Boakye et al., 2018). Especially the Sahel Savannah zone of West Africa is due to annual rainfall of 500-1000 mm (Asare-Nuamah & Botchway, 2019) and strong population growth with associated environmental activities and competition for land usage (Zhao & Hou, 2019) highly exposed to soil erosion. Major regional land use activities triggering soil erosion include forest lumbering, bushfires (Amoako & Gambiza, 2019), urbanisation, overgrazing and crop production (Boakye et al., 2018).

Soil erosion varies widely across the tropics, as evident in studies examining land cover and rainfall intensity (Meledje et al., 2021; Taye et al., 2023). De Silva et al. (2023) estimated a mean annual soil

loss rate of 2.99 t ha^{-1} yr^{-1} in a tropical region of Sri Lanka, where rainfall was found to be the major driving factor of soil erosion. Similarly, in Ethiopia's Rift Valley, expanding cropland and bareland coming along with reduced vegetation cover led to high soil erosion rates (Taye et al., 2023). The Black Volta River basin, shared by Ghana, Côte d'Ivoire, Mali, and Burkina Faso, is a critical region for agriculture and hydropower generation (Akpoti et al., 2016). Its vulnerability stems from climate conditions with a distinct rainy season, rapid population growth, and land-use demands. In the adjoining Mo River Basin, Togo, soil loss increased from 23 t ha^{-1} yr^{-1} in 1972 to 44 t ha^{-1} yr^{-1} in 2014, especially in steep, cropland-dominated areas (Diwediga et al., 2018). In the Bia Watershed, Côte d'Ivoire, soil erosion rates locally peak at 1,600 t ha^{-1} yr^{-1}, though around 85% of the area show moderate to low sensitivity (Meledje et al., 2021). Beyond, human activities in the drainage basin areas such as bushfires and sand winning from the riverbed increased river sediment yield (Amoako & Gambiza, 2019). For the Pra Basin, a sub-basin of the Black Volta River basin, an annual soil loss of 1.28 million tons was estimated, with urban and gold-mining areas facing the highest erosion risk (Boakye et al., 2020). In the fast-growing Wa municipality of Ghana, urbanisation at the edges of settlements further heightens soil erosion threats (Asempah et al., 2021).

Modelling soil erosion risk at the landscape offers great potential for the identification of soil erosion hotspots, allowing for tailored interventions such as terracing and buffer strips, which are effective soil conservation measures (Prasuhn et al., 2013). Advances in GIS technology coupled with erosion risk models have enhanced landscape-scale erosion risk predictions, making them valuable for addressing diverse erosion mechanisms, including sheet and rill erosion (Benavidez et al., 2018; Gharari et al., 2011). Applying a soil erosion risk model at the landscape level for the Black Volta River basin allows identification of erosion risk hotspots and provides a planning basis for effective conservation practices planning. Among the numerous soil erosion risk models available, the Revised Universal Soil Loss Equation (RUSLE) is the most superior in data-scarce regions such as the Black Volta River basin, owing to its flexibility in assessing soil erosion risk across landscapes with varying levels of data availability (Benavidez et al., 2018). By applying the RUSLE soil erosion risk model, the study seeks to answer the following research questions: (1) has soil erosion risk changed across the major landscape units of the Black Volta River basin between the years 1992 to 2020? (2) What are the main factors influencing soil erosion risk in the Black Volta River basin?

7.2 Study Area

7.2.1 Study Location and Physical Characteristics

The Black Volta River basin is located between 7.0°N and 14.3°N, and between 5.5°W and 1.5°W. The Black Volta is the major headwater stream of the Volta river system with its source in southern Mali. It flows through Burkina Faso, Côte d'Ivoire and northwestern Ghana covering a drainage system of approximately 138,000 km^2 (Akpoti et al., 2016). The relief of the basin is slightly undulating with an elevation between 84 to 784 meters m a.s.l. The southern part of the basin is low-lying with characteristic 84-300 meters m a.s.l while the northern part lies in general above 280 m a.s.l (Kwakye & Bárdossy, 2020). Rainfall varies across the basin due to the different climatic zones it passes: In the North, the annual precipitation distribution is unimodal with the rainy season between May and September and peak in September and an annual rainfall amount of less than 500 mm. The southern part of the basin is characterised by bimodal annual rainfall distribution with the onset of the major season in April or May and a peak in June or July; the minor rainfall season spans from September to October; this southern

part of the basin receives mean annual rainfall between 1,000 to 1,300 mm (Piacentini et al., 2018). Overall, the basin passes the climatic zones of the Sahelian Zone, the Sudano-Sahelian Zone, the Sudan Zone and the Guinean Zone (Figure 7.1), characterised by an increasing rainfall amount from north to south (Mul et al., 2015).

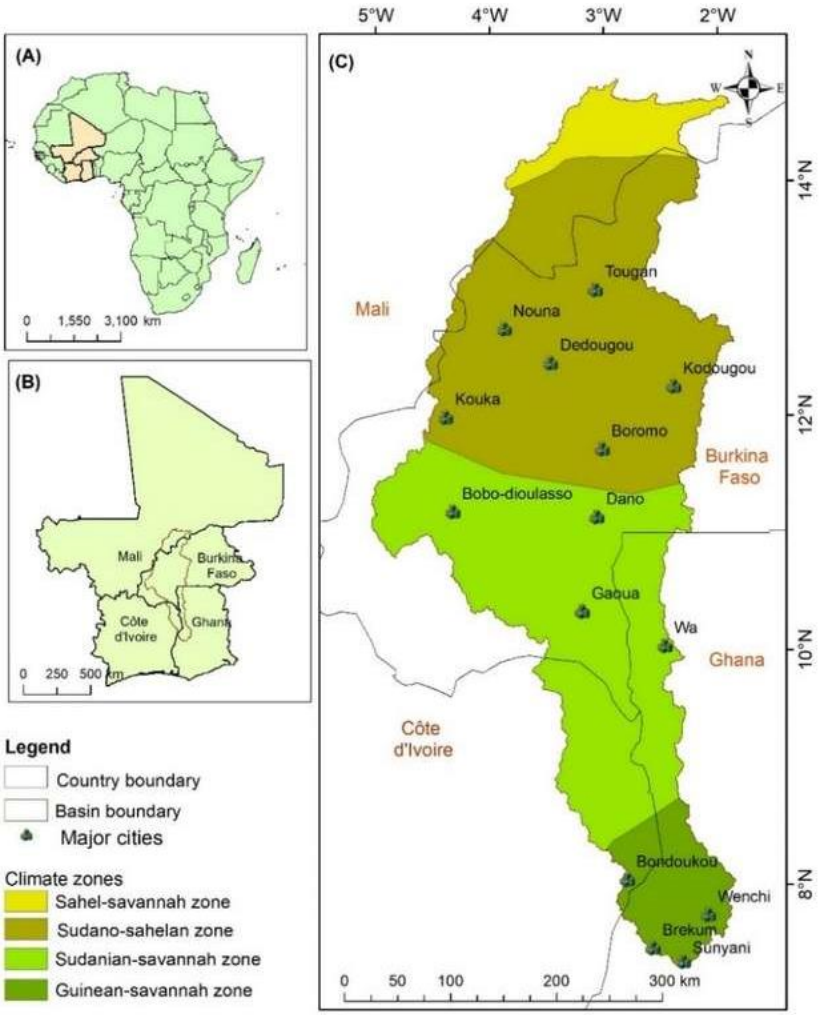

Figure 7.1. Map of climate zones of the Black Volta River basin (A) map of Africa displaying in shade, the four transboundary counties (B) Map of the four transboundary river basin countries and the boundary of the Block Volta River basin. (C) Map of the Black Volta River basin with the major climate zones (source: Lemoalle & Condappa, 2009; Mul et al., 2015).

Daily maximum temperatures within the basin can reach 44 °C and can decrease to about 15 °C at night. In the Sahel Zone, the mean annual temperature rarely falls below 29 °C while the Sudano-Sahelian Zone experiences a mean annual temperature of about 28 to 29 °C (Bagayoko, 2016; Barry et al., 2005). The basin's relative humidity shows significant seasonal variation. In the southern part of the basin, located in Ghana's Guinean zone, relative humidity ranges from 95–100% in the morning, decreasing to approximately 75% in the afternoon. In the northern part of the basin, relative humidity drops to 20–30% during the harmattan season but rises to 70–80% during the rainy season (Barry et al., 2005).

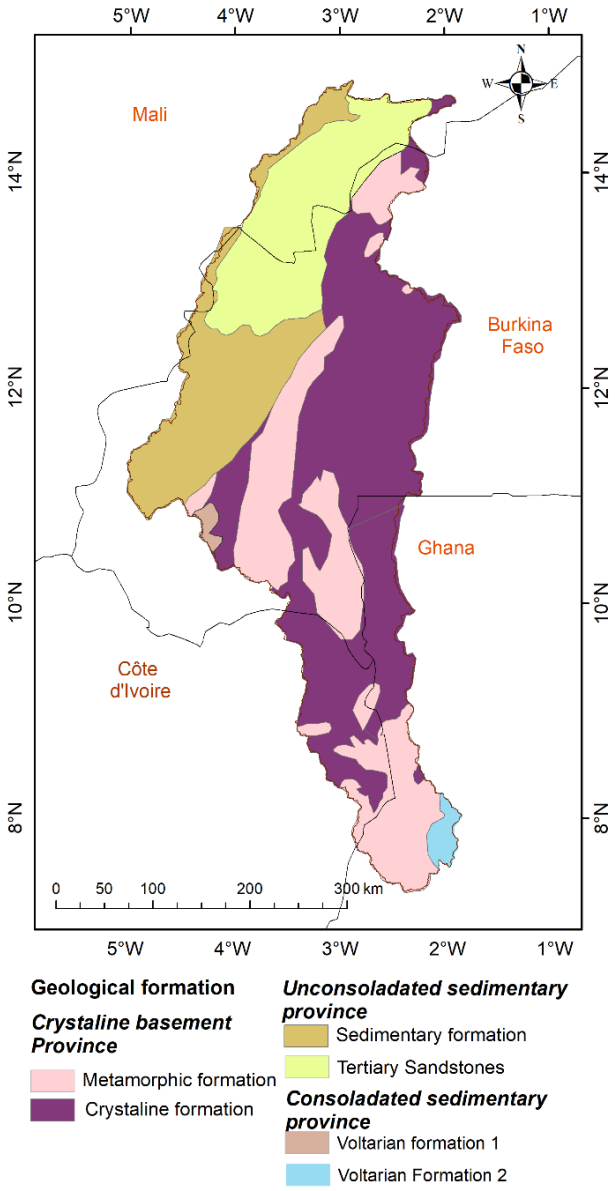

Figure 7.2. Geological Map of the Black Volta River Basin Showing the Various Geological Formations (Data from Lemoalle and de Condappa 2009 and (Source: Mul et al. 2015).

Bedrock in the Black Volta basin is mainly characterised by metamorphic and crystalline rock formations of the Crystalline Basement Province (Mul et al., 2015) Locally, especially in the drainage basin parts located in Mali and Burkina Faso, bedrock is characterised by Tertiary sandstone and sedimentary formations (Figure 7.2).

7.2.2 Landscape Units

The Black Volta River basin exhibits a considerable diversity of topographic, climatic, geologic, and pedologic characteristics. The spatial variations in these attributes allow to subdivide the Black Volta River basin into six major landscape units. To characterise the landscape units, spatial data on topography (slope, aspect, elevation, curvature and TWI), climate, land cover, geology and soil types were evaluated. The six major landscape units of the Black Volta River basin delineated are the Low Sahelian Plains, the Sahelian Upland, the Sahelian Highlands, the Savannah Transition, the Mixed Terrain Plateau and the Savannah Escarpment (Figure 7.3).

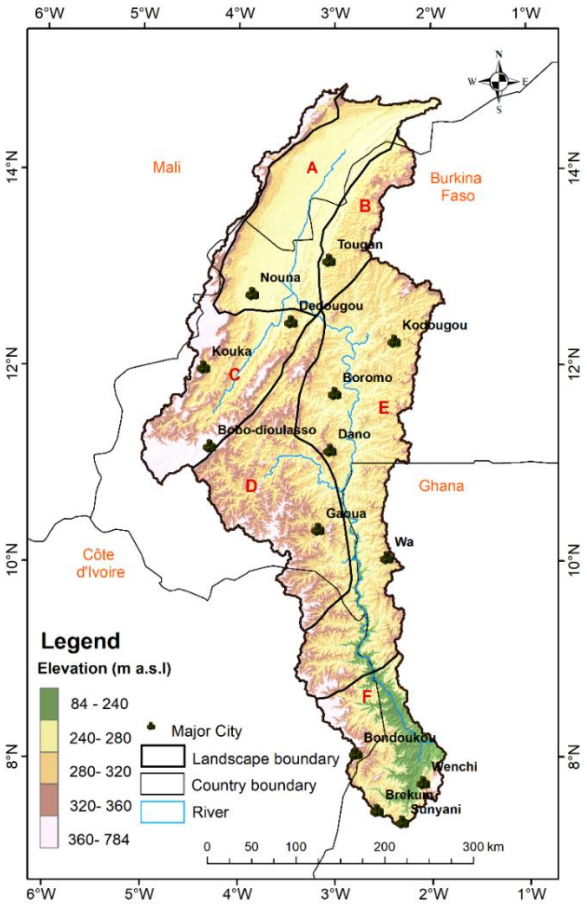

Figure 7.3. Land Elevation Map of the Black Volta River Basin Displayed in Digital Elevation Model (DEM); emphasising Cities, the Black Volta River and Landscape units. (A) Low Sahelian Plains landscape Unit (B) Sahelian Uplands landscape Unit (C) Sahelian Highlands Landscape Unit (D) Savannah Transition landscape Unit (E) Mixed Terrain Plateau landscape Unit (F) Savannah Escarpment landscape Unit. Data source: See Shuttle Radar Topography Mission (SRTM) DEM, obtained from the United States Geological Survey's (USGS) Earth Explorer database. Retrieved from https://earthexplorer.usgs.gov/ on 18 April 2023).

The Low Sahelian Plain landscape unit experiences rainfall in a single rainy season that starts from May to September, followed by a prolonged dry season from November to March. The mean annual rainfall remains below 600 mm, the annual temperature averages around 36 °C (Agyekum et al., 2022; Oguntunde & Abiodun, 2013). The altitudes of the Low Sahelian Plains landscape unit is characterised by average elevations around 2734 m.a.s.l. The landscape unit is mainly flat with about 73% of the area characterised by slopes of 0.3 – 1.1° altogether characterised by gentle slopes with an average slope of 0.64°. The average aspect of 170.89° highlights the eastern to southeastern direction of the slope orientation (Figure SL 7.2). The TWI of the Low Sahelian Plains unit averages (-0.30). Bedrock in the Low Sahelian Plains corresponds to Tertiary sandstones and conglomerates (Barry et al., 2005); soils developed in there are predominantly Ferric Luvisols and Gleyic Luvisols (FAO, 2008).

The Sahelian Uplands have a mean elevation value of 302 m a.s.l., ranging between 256 m a.s.l and 486 m a.s.l (Figure 7.4). Its relief is slightly undulating with about 73% of its area characterized by slopes of 1.1-3.0° (μ=0.71°). Aspect of the slopes is highly variable. Low values of planform and profile curvature (Figure SL 7.1) and average TWI values (-1.01) indicate low water retention capacity. The major geological formations underlying the Sahelian Uplands are crystalline formations (granite). Eutric Regosols, Ferric Luvisols and Gleyic Luvisols' are the predominant soil types. The vegetation cover is mainly open savannah characterised by grasses and short trees spread across the landscape.

The Sahelian Highlands are characterised by a mean elevation of 356 m a.s.l., ranging between 251 m a.s.l. and 772 m a.s.l. The landscape unit exhibits high topographical variability with slopes averaging 1.3° (σ =1.89°) and locally maximum inclinations up to 52°. Mean curvature values of 0 plan curvature and 0 profile curvature reflect the general ruggedness of the terrain; maximum profile curvature reaches 1.18. The mean TWI value (-1.46) is distinctly lower than that of the Low Sahelian Plains (-0.30) and the Shelian Uplands (-1.01), implying a low water retaining capacity of the Sahelian Highlands. The Sahelian Bedrock underlying the Sahelian Highlands are Tertiary sandstones, shales, and conglomerates (Barry et al., 2005). The dominant soil types developed within the Sahelian Highlands are Eutric Regosols Ferric Luvisols and Gleyic Luvisols. Though the natural potential vegetation of the landscape unit is primarily classified as open savannah vegetation the area is actually widely used as cropland.

The Savannah Transition landscape unit is characterised by two major rainy seasons with the primary season starting in April or May, reaching its peak in June or July, while the minor rainy season starts in September or October, with a peak occurring around the same time (Piacentini et al., 2018); mean annual precipitation totals 700 mm. The mean annual temperature in the Savannah Transition landscape unit is 27 °C. The terrain characteristics vary highly between the flat lowlands and the rugged highlands. The mean elevation in the Savannah Transition landscape unit amounts to 320 m a.s.l., and maximum altitudes reach 568 m a.s.l. Slopes average 1.39° and locally reach maximum inclinations of 30°. The curvature in the Savannah Transition landscape unit averages 0 with low variability (σ=0.03), but locally reaching profile curvature values up to 0.56. TWI values average -1.71 (σ=2.10), ranging between minimum values of -6.45 and maximum values of 14.08. The Savannah Transition landscape unit is underlain by metamorphic bedrock including gneisses and migmatites rich in hornblende and biotite (GEF-UNEP, 2002). Soil types in the Savannah Transition landscape unit are dominated by Ferric Luvisols and Gleyic Luvisols soil types with about a quarter of the area covered by Pilnthic Luvisols. Potential natural vegetation corresponds to savannah vegetation, today competing with extensive agricultural activities.

The Mixed Terrain Plateau landscape unit is characterised by an average elevation of 291 m a.s.l., ranging between 191 m a.s.l. and 580 m a.s.l. The topography is characterised by a mean slope of 1.13° (σ=0.90), reaching maximum inclinations of 31°. Planform curvature values (mean=0, σ= 0.03, range=1.16) and profile curvature values (mean=0, σ=0.03, range=1.12) show high stability. The mean TWI of -1.53 (σ=2.13, minimum TWI= -6.34, maximum TWI= 15.21) indicates moderate water retention capacity of the landscape unit. Underlying bedrock corresponds to crystalline formations such as granulites. Ferric Luvisols and Gleyic Luvisols are the predominant soil types in the Mixed Terrain Plaeau landscape unit, however, about a fifth of its area is covered by Eutric Regosols (FAO, 2008).

The Savannah Escarpment landscape unit is characterized by rugged terrain. Though it has the lowest mean elevation (268 m a.s.l.) in the Black Volta River basin, its elevations range between 84 m a.s.l. and 729 m.a.l. This extreme range of elevation range underscores the steep relief of the escarpment. Average slope amouts 2.04° (σ= 1.98), along the escarpment locally reaching vertical walls. The mean TWI value of -2.12 (σ=2.07), suggests a low water retention capacity, corresponding to the steep slopes that promote runoff rather than infiltration and water storage. Metamorphic bedrock such as gneisses and migmatites rich in hornblende and biotite, granulites, and schists crop out in this landscape unit (GEF-UNEP, 2002). The vegetation cover within the Savannah Escarpment landscape unit is dense with a mosaic of trees, grasses and shrubs.

Overall, the major landscape units of the Black Volta basin differ significantly in terms of elevation, slope, aspect, curvature, and topographic wetness index. The Low Sahelian Plains is identified as the flattest unit, while the Sahelian Highlands and Savannah Escarpment are characterized by more rugged terrain. The Savannah Transition and Mixed Terrain Plateau landscape units are considered transitional areas with moderate slopes and varying extent of topographical attributes. Ferric Luvisols and Gleyic Luvisols are the predominating soil types developed across all six major landscape units of the Black Volta River basin. All over the Black Volta River basin open savannah vegetation in competition with cropland characterizes vegetation cover.

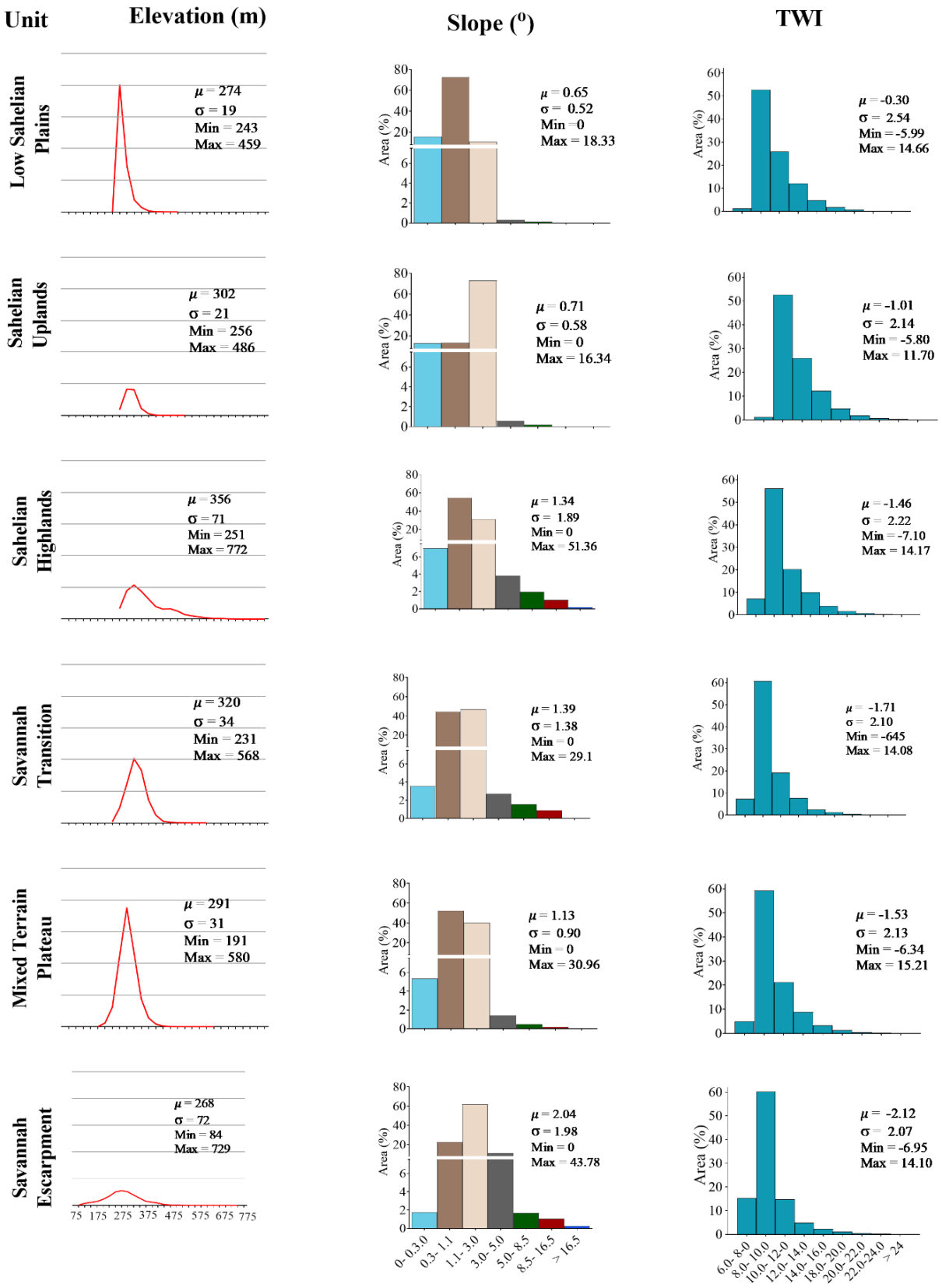

Figure 7.4. Graphs of the Distributions of Topographic Features in the Black Volta River basin's major landscape units.

7.3 Materials and Methods

7.3.1 RUSLE Model Parametrisation

The RUSLE is a flexible computerised model widely used in GIS applications to estimate soil erosion risk (Almouctar et al., 2021; Thakuriah, 2023). Its global acceptance and utilisation for soil erosion risk estimation are given due to its adaptability, efficiency in terms of time and cost and practicality in regions where data is limited (Gelagay & Minale, 2016; Zerihun et al., 2018). The model's input parameters include rainfall erosivity factor (R), soil erodibility factor (K), slope length and steepness factor (LS), land cover and management factor (C) and the support practice factor (P) (Mhiret et al., 2019; Renard et al., 1997). These input parameters (Figure 7.5) are linked in the RUSLE equation (Renard et al., 1997):

$$A_{SE}\ [\text{t ha}^{-1}\ \text{yr}^{-1}] = R \times K \times LS \times C \times P \tag{7.1}$$

where:
the average soil erosion rate per year (t ha^{-1} yr^{-1}) is denoted by A_{SE}; rainfall erosivity factor also known as the R-factor is represented as R and measures in MJ mm ha^{-1} h^{-1} yr^{-1}; soil erodibility factor (K-factor) *is* connoted with K and measured in t h MJ^{-1} mm^{-1}; LS represents the dimensionless slope length and steepness factor (LS-factor); C and P are cover management factor (C-factor) and conservation support practice factor (P-factor). The cover factor is represented by weighted values in the range of 0 to 1.

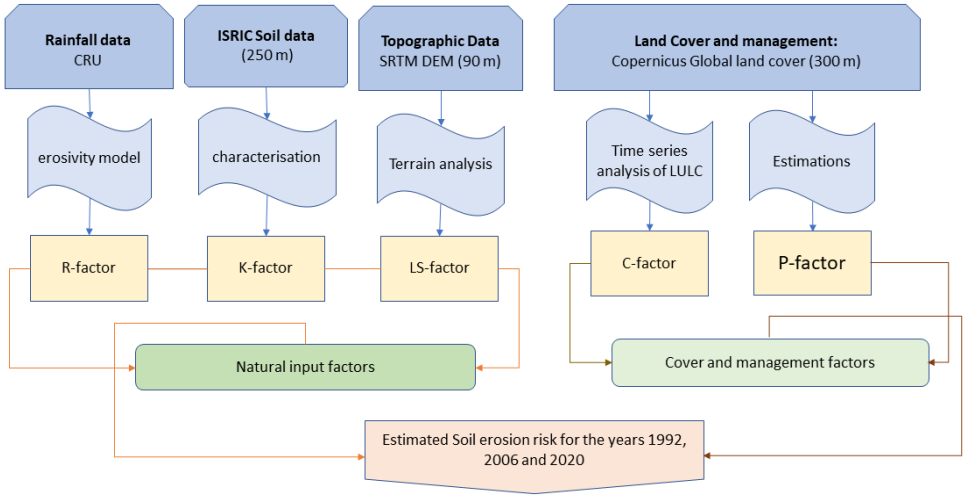

Figure 7.5. Flow Chart Diagram of the Input Requirement for the Soil Erosion Risk Modelling Using RUSLE Model.

We assessed and processed data from various sources to generate each of the model's input parameters. The rainfall data was acquired from the database of the Climatic Research Uni (CRU) of the University of East Anglia (https://crudata.uea.ac.uk/cru/data/hrg/). The CRU gridded data time series that spans from the year 1901 to 2022 (0.5°x 0.5° spatial resolution; monthly temporal resolution). The 250 x 250 m resolution soil grid data from the International Soil Reference Information Centre (ISRIC) database (https://soilgrids.org) was used in generating the *K*-factor. The *LS factor* was generated from the SRTM DEM; due to the large area of the Black Volta basin, it was feasible and applicable to work with a 90m x 90m SRTM DEM. The C-factor input map for the years 1992, 2006 and 2020 was generated from the annual 300 x 300 m resolution historical global land cover data obtained from the Copernicus database (https://cds.climate.copernicus.eu/) (Buchhorn et al., 2020); these land cover datasets provide global

maps with defined land use classes based on the Land Cover Classification System (LCCS) designed by the United Nations Food and Agriculture Organisation (UN FAO). Each of the input parameters was generated separately in raster data format for the onward estimation of soil erosion risk. By employing the nearest neighbour techniques, the raster input parameter of all the factors was resampled to a common resolution of 90 × 90 m resolution and the same projection to ensure model accuracy. Mathematical linking of the input parameters took place using ArcGIS in association with QGIS (Atoma et al., 2020; Ganasri & Ramesh, 2016).

The ***Soil Erodibility factor (K)*** is a quantitative measure of soil's susceptibility to erosion owing to its inherent properties of the soil (Beguería et al., 2015). The computation of the *K*-factor was carried out using raster-based silt, clay, sand and organic carbon contents obtained from the ISRIC database (https://soilgrids.org). We used a trapezoidal rule approach (equation 7.2) to compute the weighted averages of each of the soil physical properties that were accessed in different depths (0, 5, 15 and 30 cm b.g.l.) (Hengl et al., 2017):

$$\frac{1}{b-a}\int_a^b f(x)dx \approx \frac{1}{(b-a)}\frac{1}{2}\sum_{K=1}^{N-1}(X_K+1-X_K)(f(X_K)+f(X_K+1)) \quad (7.2)$$

where:
N connotes the number of depths soil properties; Xk represents the kth depth; f(Xk) is the estimated value of the target variable (i.e., soil property) at depth X_k.

The outputs of the weighted averages of the soil's physical properties complemented the onward computation of the K-factor using equation (7.3) following (Sharpley & Williams, 1990):

$$k = 0.1317(0.2 + 0.3 * e^{\left\{-0.0256SAN\left(1-\frac{SIL}{100}\right)\right\}*}(\frac{SIL}{CLA+SIL})^{0.3})*\{1-\frac{0.25*TOC}{TOC+e^{(3.72-2.95*TOC)}}\}*\{1-\frac{0.7*SN1}{SN1+e^{(22.9*SN1-5.51)}}\} \quad (7.3)$$

where:
SAN connotes the amount of sand components in mass-%, SIL connotes silt components in mass-%, CLA connotes clay components in mass-% and TOC connotes the total organic carbon contents of the soil (mass-%). The variable S N1 connotes the sand-index and is calculates as S N1=1-SAN/100.

The ***Rainfall erosivity factor (R)*** presents the propensity of rainfall to initiate soil erosion (Farhan & Nawaiseh, 2015; Stocking & Elwell, 1976). The rain drops size and distribution, amount and intensity of rainfall coupled with terminal velocity are determining factors of total erosivity (Meshesha et al., 2014; Thomas et al., 2018). In this study, we applied equation 7.4 (Adongo et al., 2019; Endalamaw et al., 2021) to derive the rainfall erosivity factor from annual rainfall in tropical regions:

$$R = 0.562\ (Ar) - 8.12 \quad (7.4)$$

where:
R denotes the rainfall erosivity factor (MJ mm ha^{-1} h^{-1} yr^{-1}) and (Ar) denotes long-term mean annual rainfall (in MJ mm ha^{-1} h^{-1} yr^{-1}).

The long-term mean annual rainfall data is required for the approximation of the rainfall erosivity factor (equation 7.4) and was generated from the spatially differentiated CRU rainfall data. Monthly rainfall data that was available in the NETCDF file format were processed in ArcGIS. Data for each year comprise twelve bands of monthly rainfall; these bands were stacked using the composite tool in ArcGIS

and summed to obtain an annual rainfall raster for each year. The long-term averages were obtained using the raster statistics function of ArcGIS. The raster images of 5° x 5° tiles resolution were converted into points and the inverse distance weighted (IDW) technique was employed to generate a raster of 90 x 90 m spatial resolution in harmony with the other input parameters. The output raster of the interpolation was extracted to the extent of the study area and subsequently applied in equation (7.4) to compute the erosivity factor for each of the time slices. The decadal mean annual rainfall data of the three periods 1983-1992, 1997-2006 and 2011-2020 were used for the computation of rainfall erosivity factor for the years 1992, 2006 and 2020.

Slope Length and Steepness Factor (LS). LS factor is the representation of the effect of slope length (L) and steepness (S) on soil erosion in the RUSLE model. It presents the influence of topography on soil erosion based on the combined impact of slope steepness (*S*) and length of slope (*L*) (S. Schmidt et al., 2019). As established by Wischmeier & Smith, (1978) the *L* factor is the ratio of erosion from horizontal slope length to the corresponding loss from the slope length of a unit plot (22.13 m). The LS factor was generated from the 90 x 90 m resolution SRTM DEM based on the equation proposed by Moore & Burch (1986) (equation 7.5). The 90m x 90m SRTM DEM was obtained from the database of the Consortium of International Agricultural Research Centers' Consortium for spatial-information (CGIAR-CSI) (https://bigdata.cgiar.org/srtm-90m-digital-elevation-database/) in mosaiced 5° x 5° tiles. The *LS* factor incorporates parameters related to slope length (*A* and *m*) and slope steepness (θ and *n*). Equation 7.5 allows the quantification of the combined effect of these factors on soil erosion, considering both the length and steepness of slopes in the landscape.

$$LS = \left(\frac{A}{22.13}\right)^{m} * \left(\frac{\sin\theta}{0.0896}\right)^{n} \tag{7.5}$$

where:
A =Accumulated up-slope contribution catchment region for a specific cell (m^2/m); θ is slope steepness angle (°); m is a variable slope length exponent; n is a slope steepness exponent.

The ***Land Cover and Management Factor (C)*** is a significant factor in erosion risk modelling as the landscape's susceptibility to soil erosion is greatly dependent on the level of vegetation cover. The presence of vegetation cover enhances surface roughness thereby lowering the flow velocity of rainwater (Mengistu et al., 2015; Wischmeier & Smith, 1978; Wynants et al., 2018). The C-factor corresponds to a numerical value in a range of 0 to 1. Areas fully protected by vegetative cover are designated with a value of 0, while a complete bare land is designated with a value of 1. This implies that the lower the C-factor value the better erosion prevention capability and vice versa (Mengistu et al., 2015). The time series of global land cover data for the years 1992, 2006 and 2020 were obtained from the Copernicus database (Buchhorn et al., 2020) and were used to compute the C-factor for the Black Volta River basin. The land cover classes appearing in the study area include cropland, closed savannah, open savannah, grassland, bareland, urban area, vegetated wetland and water bodies. The C-factor values for these different land cover classes are based on a weighted average of soil loss ratio calculated from a reference plot where the C-factor for a bareland is set at 1 (Renard et al., 1997). The weighted values for the C-factors for the land cover classes were evaluated from literature (Girma & Gebre, 2020; Kusimi et al., 2015; Watene et al., 2021). The C-factor was generated by assigning the established respective weighted values (Table 7.1) designed for each of the defined land cover classes. A C-factor value of 0.2 is assigned to the cropland land cover class; open savannah land cover offers better erosion resistance than grassland, thus, a better C-factor value for open savannah is set at 0.002 and the C-factor value for

grassland is set at 0.05. Close savannah land cover has a relatively high protective cover and thus C-factor value was set at 0.001. For settlement areas, the C-factor value was set at 0.8 while completely bare land has a C-factor value of 1. The vegetated wetland area was assigned a C-factor value of 0.21.

The ***Support practice factor (P)*** expresses the influence of land surface management on runoff and soil erosion (Kebede et al., 2021). The determination of the P-factor is based on prevailing land management techniques encompassing terracing, strip cropping and contour ploughing (Renard et al., 1997). The P-factor values are in the range of 0 to 1, with 0 representing the most effectively implemented conservation practices, while 1 signifies the absence of any support practices. Owing to the widespread lack of support management practices in the Black Volta basin a P-factor of 1 was uniformly applied.

7.3.2 Soil Erosion Estimation Based on Different Land Cover and Rainfall Erosivity Factors

By employing the RUSLE model soil erosion risk for the years 1992, 2006 and 2020 was estimated. To evaluate the influences of the R-factor and the C-factor on soil erosion risk four scenarios were set up by replacing land cover and rainfall erosivity data of the initial models for the years 1992, 2006 and 2020 while all other input parameters remained constant:
In scenario 1 all the input parameters for the 1992 RUSLE model application were held constant except for the R-factor values which were substituted by the 2006 R-factor values to assess the effect of the R-factor on the results of the initial model that used the 1992 R-factor values. In scenario 2 the C-factor input parameter for the year 1992 RUSLE model application was substituted by the 2006 C-factor. Correspondingly, in scenario 3 the R-factor values of the 2006 RUSLE model application were substituted by the 2020 R-factor values. In scenario 4 the C-factor 2006 RUSLE model application was substituted by the 2020 C-factor values. For each scenario, total soil loss (t $ha^{-1}y^{-1}$) was calculated and subsequently, changes in soil loss were estimated between the initial models and their respective models when the C and R factors were substituted.

7.4 Results

7.4.1 RUSLE Model Input Parameters

Soil Erodibility factor (K). The estimated K-factor values for the Black Volta River basin range from less than 0.015 to 0.047 t ha MJ^{-1} mm^{-1} (mean = 0.030; σ.=0.005) (Figure SL 7.3A). Low mean values were estimated for the Low Sahelian Plains landscape unit; 0.024 t h MJ^{-1} mm^{-1} (σ=0.003) and Sahelian Uplands landscape unit; 0.025 t h MJ^{-1} $mm^{-1,}$ (σ=0.003) which are located in the northern part of the basin. The Sahelian Highlands landscape unit has a mean K-factor value of 0.031 t ha MJ^{-1} mm^{-1}, (σ=0.004) with patches of values estimated with a range of 0.026 t ha MJ^{-1} mm^{-1} (Table 7.1). Similarly, the estimated mean values of 0.031 t ha MJ^{-1} mm^{-1}, (σ=0.004) for the Mixed Terrain Plateau landscape unit and 0.032 t ha MJ^{-1} mm^{-1} (σ=0.004) for the Savannah Escarpment landscape unit characterised the central part within Burkina Faso toward the south where the Ghana part is located (Figure 7. SL 3A).

Slope Length and Steepness Factor (LS)*.* The *LS*-factor value for the Black Volta River Basin reflects the slightly undulating topographic characteristics of the basin. The estimated LS-factor for the basin ranges from 0-26. Over 90% of the basin has a low *LS* factor value of less than 3 (Figure SL 7.3 B). Conspicuously, Steep slopes and corresponding *LS*-factor values above 7 are predominantly in the Sahelian Highlands, Low Sahelian Plains and Savannah Escarpment landscape units.

Rainfall erosivity factor (R). For each of the time slices (1992, 2006, 2002), the *R*-factor values show a north-south gradient with the highest values in the southernmost part of the basin and lowest values in the northmost part (Figure 7.6; SL 7.4). The spatial distribution of the *R*-factor for the year 1992 spans from less than 250 MJ mm ha^{-1} h^{-1} yr^{-1} in the northern part of the basin to 650 MJ mm ha^{-1} h^{-1} yr^{-1} in the southern part of the basin with a mean value of 338.0 MJ mm ha^{-1} h^{-1} yr^{-1} (σ=95.6). The landscape units located in the north, particularly, the Low Sahelian Plains and the Sahelian Uplands show lower mean R-factor values than other landscape units. The change across all landscape units shows an increase in mean R-factor value from the year 1992 to 2006, followed by a decrease in the year 2020 (Figure SL 7.4). The Savannah Escarpment landscape unit shows a mean R-factor value of 485.06 MJ mm ha^{-1} $h^{-1}yr^{-1}$ (σ=113.5) in 1992 that increases to 617.1 MJ mm ha^{-1} $h^{-1}yr^{-1}$ (σ=11.3) in the year 2006 and in the year 2020 again declines to 454.30 MJ mm ha^{-1} $h^{-1}yr^{-1}$ (σ= 55.3). Parallel variations were observed for the other landscape units.

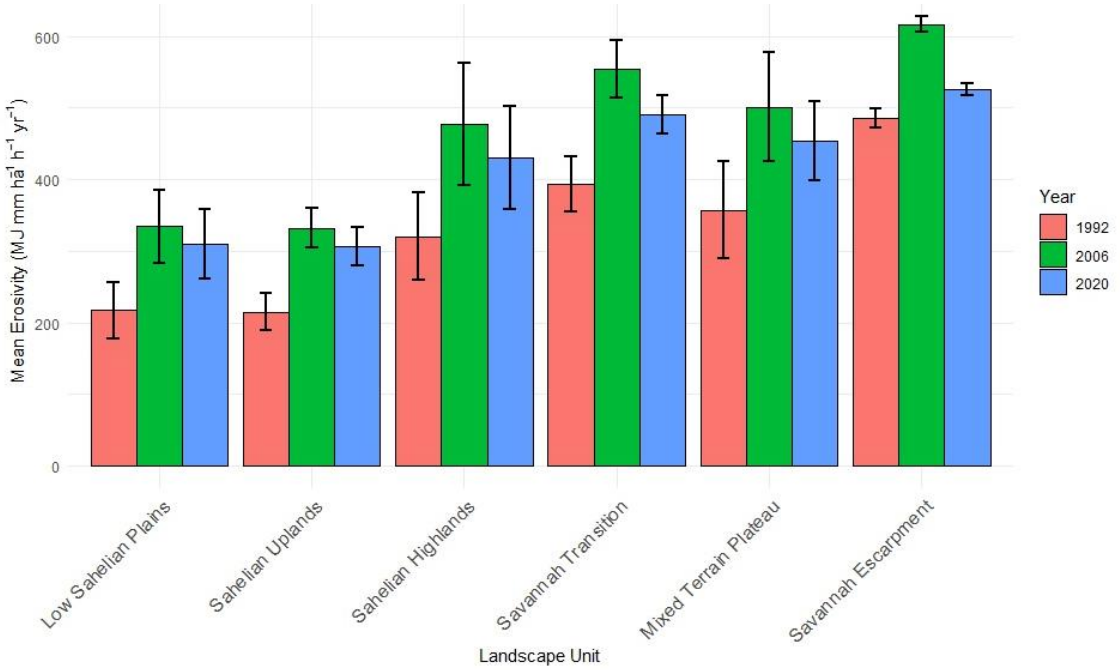

Figure 7.6. The Mean Rainfall Erosivity in the Six Major Landscape Units of the Black Volta River Basin in the Years 1992, 2006 And 2020.

The Savannah Transition and the Escarpment unit landscape units that stretch from the central to the southern part of the basin show a comparatively higher mean rainfall erosivity in all its three-time slices while the highest was in the year 2006 (Table 7.1). The inter-annual difference of the *R*-factor is in consonant with the long-term annual rainfall for the three-time step.

Land Cover Factor (C). The basin experienced a significant change in land cover and due to this, C-factor values underlie strong changes (Table SL 7.1, 7.2 and 7.3). The land cover maps and graphs of the Black Volta River basin for the years 1992, 2006 and 2020 (Figure SL 7.5 and 7.6) show that cropland is concentrated in the northern part of the basin within the Sahelian Highlands, Low Sahelian Plains and Sahelian Uplands landscape unit. Dominant land cover types in the basin are grassland and open savannah vegetation. In the year 1992 about 29.8% of the drainage basin area was covered by grassland and since then slightly decreased to a coverage of 24.1% in 2006 and 22.6% in 2020. Open savannah vegetation covered about 23.8% of the drainage basin area in the year 1992 and until 2006

spread to an extent of 25.7%, since then remaining widely stable (2020: 25.9%) (Table 7.2 and Figure 7.7).

Table 7.1. Summarizing Statistics of RUSLE Input Parameters Across the Six Major Landscape Units of the Back Volta River Basin.

Erodibility K-factor [t ha MJ^{-1} mm^{-1}]	**Mean**	**Standard Deviation**	**Range**
Low Sahelian Plains	0.02	0.003	0.02
Sahelian Uplands	0.02	0.003	0.02
Sahelian Highlands	0.03	0.004	0.03
Savannah Transition	0.03	0.003	0.02
Mixed Terrain Plateau	0.03	0.004	0.02
Escarpment unit	0.03	0.004	0.02
LS-factor			
Low Sahelian Plains	0.6	3.04	34.1
Sahelian Uplands	0.4	1.02	60.7
Sahelian Highlands	1.2	5.10	84.5
Savannah Transition	1.0	2.70	42.3
Mixed Terrain Plateau	1.0	6.90	109.6
Escarpment unit	2.2	12.28	216.8
Erosivity factor (1992)- [MJ mm ha^{-1} $h^{-1}yr^{-1}$]			
Low Sahelian Plains	217.5	39.41	156.2
Sahelian Uplands	214.8	25.66	119.7
Sahelian Highlands	320.5	61.54	281.7
Savannah Transition	393.3	38.36	182.2
Mixed Terrain Plateau	357.2	68.05	234.1
Escarpment unit	485.1	13.52	59.9
Erosivity factor (2006) [MJ mm ha^{-1} $h^{-1}yr^{-1}$]			
Low Sahelian Plains	334.4	50.89	205.0
Sahelian Uplands	332.4	27.34	131.3
Sahelian Highlands	477.7	85.88	377.1
Savannah Transition	554.3	40.51	211.2
Mixed Terrain Plateau	501.6	76.57	259.2
Escarpment unit	617.1	11.30	47.6
Erosivity factor (2020) [MJ mm ha^{-1} $h^{-1}yr^{-1}$]			
Low Sahelian Plains	310.0	49.00	194.1
Sahelian Uplands	306.6	26.61	140.0
Sahelian Highlands	431.0	72.18	329.0
Savannah Transition	491.0	26.84	152.6
Mixed Terrain Plateau	454.3	55.30	211.0
Svannah Escarpment	526.4	8.43	51.3

The land cover classification indicates an expansion of settlement areas of less than 0.05% in 1992 to 0.01% in 2006 and spread abruptly up to 0.2% in 2020. These data correspond to a relative increase of settled area +91% from 1992 to 2006 and of +146% from 2006 to 2020. Bareland areas spread slightly by +10% from 1992 to 2006 and abruptly +83% between 2006 to 2020. Cropland areas spread all over the Black Volta basin between 1992 to 2006 by 8%. In the Mixed Terrain Plateau landscape unit during the same period, between 1992 and 2006, cropland expanded by +61%; in contrast, simultaneously in the Low Sahelian Plains landscape unit cropland areas halved (-50%). In contrast, the Low Sahelian Plains landscape unit doubled between 2006 to 2020 (+99%), Stron spread of cropland areas was also observed for the Savannah Transition landscape unit (+75%). The area covered by water bodies remained stable between 1992 to 2006 but doubled between 2006 and 2020 (+100%). This tendency is extremely pronounced in the Savannah

Escarpment landscape unit where between 2006 to 2020 the areas covered by water bodies spread by +1342% due to the construction of the Bui power dam that was commissioned in 2013.

Table 7.2. Spatial Extent of LULC Classes and their Corresponding C-Factor Values (database: https://cds.climate.copernicus.eu/).

Area Cover							
	1992		2006		2020		
LULC Classes	Area (km^2)	%	Area (km^2)	%	Area (km^2)	%	Weighted C-factor value
Cropland	63,397.6	45.9	68,376.4	49.5	68,216.5	49.4	0.2
Grassland	41,086.7	29.8	33,319.1	24.1	31,259.0	22.6	0.05
Open Savannah	32,804.6	23.8	35,459.6	25.7	35,775.2	25.9	0.002
Closed Savannah	280.2	0.2	396.2	0.3	1,844.0	1.3	0.001
Vegetated Wetland	135.5	0.1	121.4	0.1	63.7	<0.05	0.21
Urban areas	62.0	<0.05	118.6	0.1	291.4	0.2	0.8
Bareland	12.4	<0.05	13.6	<0.05	24.9	<0.05	1.0
Water bodies	283.9	0.2	258.0	0.2	588.3	0.4	0.00
	138,062.9	100.0	138,062.9	100.0	138,062.9	100.0	

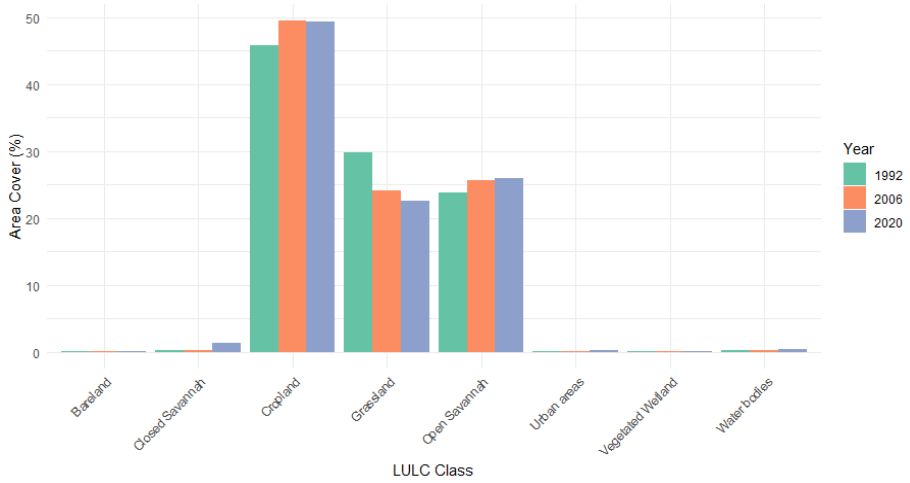

Figure 7.7. Frequencies Distribution of Land Cover Across the Black Volta Basin for the years 1992, 2006 and 2020 (database: https://cds.climate.copernicus.eu/).

7.4.2 Estimated Soil Erosion Risk

For the three steps examined soil erosion risk in more than three-fourth of the Black Volta basin was exposed to a low soil erosion risk (Table 7.3). The drainage basin area exposed to moderate soil erosion risk in the basin fluctuated between 11.3% and 13.1% (Table 7.3). The spatial distribution of the soil erosion risk classes (Figure 7.8) estimated as "high", "very high" and "extreme" exposure amounted at large around 10% of the Black Volta basin, being subject to slight temporal variations. The six landscape units differ in exposure to soil erosion risks and show different temporal variations considering the selected time slices of 1992, 2006 and 2020. In the Low Sahelian Plains and Sahelian Uplands landscape units consistently more than 90% of the area is exposed to the low soil erosion risk (Table 7.4).

In contrast, the Savannah Transition landscape unit area exposed to low erosion risk remained during all three-time slices below 70%. In the Savannah Escarpment landscape unit areas exposed to high to

extreme soil erosion risk amounted to 15.3% in 1992 and until 2020 slightly declined to 12.2%. Also, the Savannah Transition landscape unit showed relatively widely spread areas of high to extreme soil erosion risk varying between 11-13.5% for the three-time steps.

Table 7.3. Estimated soil loss by soil erosion A_{SE} and Soil Erosion Risk by Different Severity Classes.

		1992: Soil erosion A_{SE} risk by grade		**2006: Soil erosion A_{SE} risk by grade**		**2020: Soil erosion A_{SE} risk by grade**	
Soil erosion risk	**Soil Erosion (t $ha^{-1}y^{-1}$)**	**Area (km^2)**	**Area (%)**	**Area (km^2)**	**Area (%)**	**Area (km^2)**	**Area (%)**
Low Erosion	0-2	111,019.7	80.4	104,373.5	75.6	107,950.2	78.2
Moderate erosion	3-5	15,650.2	11.3	18,113.0	13.1	16,917.3	12.3
High erosion	6-10	6,331.0	4.6	8,558.9	6.2	7,275.3	5.3
Very high erosion	11-15	2,559.3	1.9	3,360.8	2.4	2,868.0	2.1
Extreme erosion	>15	2,502.6	1.8	3,656.6	2.6	3,052.1	2.2
		138,062.9	100.0	138,062.9	100.0	138,062.9	100.0

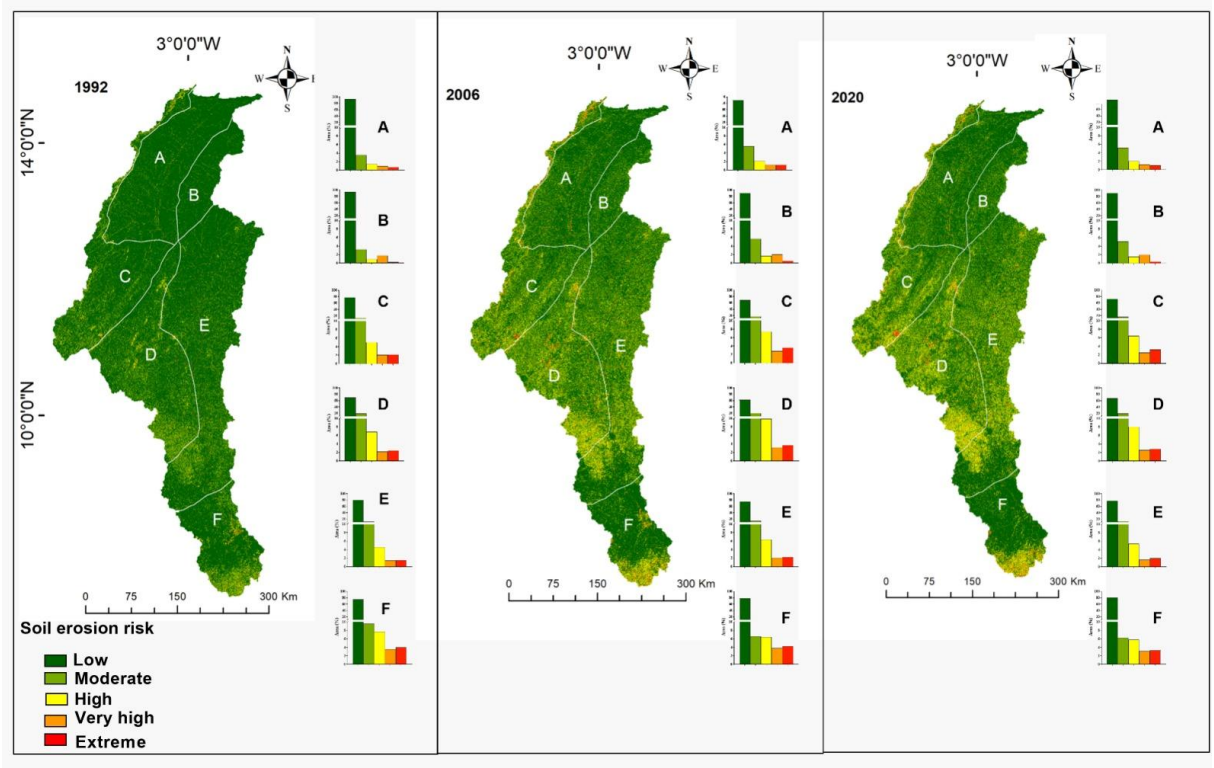

Figure 7.8. Spatial Distribution of Soil Erosion Risk in the Black Volta River Basin for the years 1992, 2006 and 2020 for major landscape units. A: Low Sahelian Plains, B: Sahelian Uplands, C: Sahelian Highlands, D: Savannah Transition, E: Mixed Terrain Plateau and F: Savannah Escarpment).

Table 7.4. Estimated Soil Erosion Risk by Different Severity Classes for the six major landscape units of the Black Volta River basin for the years 1992, 2006 and 2020

		Low Sahelian Plains		Sahelian Uplands		Sahelian Highlands		Savannah Transition		Mixed Terrain Plateau		Savannah Escarpment	
Soil erosion risk	**Soil Erosion ($t\ ha^{-1}y^{-1}$)**	**Area (km^2)**	**%**	**Area (km^2)**	**%**	**Area (km^2)**	**%**	**Area (km^2)**	**%**	**Area (km^2)**	**%**	**Area (km^2)**	**%**
1992													
Low Erosion	0-2	22,846	93.3	8,034	93.9	17,243	77.2	18,517	69.8	33,619	80.3	10,761	75.1
Moderate erosion	2-5	890	3.6	270	3.2	3,040	13.6	4,979	18.8	5,091	12.2	1,381	9.6
High erosion	5-10	338	1.4	81	0.9	1,108	5.0	1,799	6.8	1,909	4.6	1,097	7.7
Very high erosion	10-15	24	1.0	150	1.8	460	2.1	593	2.2	598	1.4	518	3.6
Extreme erosion	>15	165	0.7	18	0.2	492	2.2	633	2.4	626	1.5	568	4.0
		24,481	100.0	8,552	100.0	22,341	100.0	26,523	100.0	41,843	100.0	14,324	100.0
2006													
Low Erosion	0-2	21,985	89.8	7,711	90.2	15,454	69.2	16,521	62.3	31,397	75.0	11,306	78.9
Moderate erosion	2-5	1,381	5.6	488	5.7	3,808	17.0	5,546	20.9	5,949	14.2	942	6.6
High erosion	5-10	521	2.1	142	1.7	1,644	7.4	2,637	9.9	2,696	6.4	918	6.4
Very high erosion	10-15	306	1.2	169	2.0	631	2.8	846	3.2	865	2.1	544	3.8
Extreme erosion	>15	289.	1.2	41	0.5	805	3.6	971	3.7	937	2.2	614	4.3
		24,481	100.0	8,552	100.0	22,342	100.0	26,522	100.0	41,843	100.0	14,324	100.0
2020													
Low Erosion	0-2	22,166	90.5	7,776	90.9	16,100	72.1	17,794	67.1	32,456	77.6	11,659	81.4
Moderate erosion	2-5	1,276	5.2	440	5.1	3,551	15.9	5,161	19.5	5,581	13.3	909	6.3
High erosion	5-10	482	2.0	132	1.5	1,428	6.4	2,133	8.0	2,272	5.4	828	5.8
Very high erosion	10-15	293	1.2	167	2.0	559	2.5	682	2.6	717	1.7	451	3.1
Extreme erosion	>15	264	1.1	38	0.4	704	3.2	752.	2.8	817	2.0	477	3.3
		24,481	100.0	8,552	100.0	22,342	100.0	26,522	100.0	41,843	100.0	14,324	100.0

7.4.3 Estimated Soil Losses Based on Different Land Cover and Rainfall Erosivity Factors

Considering the overall Black Volta basin estimated soil loss in 2006 amounted to c. 21,538,580 tons was distinctly higher than in 2020 (c. 19,191,212 tons) (Table 6) and 1992 (c. 15,746,453 tons) (Table 7.5). Across all six major landscape units in the Black Volta basin between the years 1992 and 2006 the soil loss increased; relative increase in the three northern landscape units, the Sahelian Highlands, the Low Sahelian Plains and the Sahelian Uplands, varied between 45-55% (Table 7.5), while in the landscape units located in the southern part of the Black Volta basin, the Savannah Escarpment, the Savannah Transition and the Mixed Terrain Plateau, during the same period estimated soil loss increased by landscape unit it only increased by c. 25-36% (Table 7.5). In contrast, in 2020 the estimated soil loss across the Black Volta basin had decreased compared to 2006, reaching a maximum decrease in the Savannah Transition landscape unit by -17.5% and a minimum decrease of -5.4% in the Savannah Escarpment landscape unit.

Assessing the effect of differing land cover and rainfall on soil erosion risk, scenarios 1-4 were set up. In scenario 1 soil erosion risk of the Black Volta basin applying 1992 land cover data and 2006 rainfall erosivity data for the RUSLE model. Differences of resulting soil loss estimates to those of the data achieved by applying 1992 land cover and rainfall erosivity data are all over the Black Volta basin positive, documenting the controlling effect of rainfall erosivity on soil loss (Table 7.5). This observation is confirmed by soil loss data generated by applying scenario 3 where 2006 land cover data and 2020 rainfall erosivity data were applied. Corresponding to the comparatively low rainfall erosivity data (Figure 7.6 and SL 7.4) resulting soil loss estimates to those of the data achieved by applying 2006 land cover and rainfall erosivity data are negative for all the landscape units of the Black Volta basin (Table 7.6). Likewise, the controlling effect of land cover changes was assessed by applying 1992 rainfall erosivity data and 2006 land cover data for the RUSLE model (scenario 2); additionally, the same procedure was conducted by applying 2006 rainfall erosivity data and 2020 land cover data. The resulting soil loss data were widely stable (Table 7.5), indicating a general minor effect of land use change on soil erosion processes.

Table 7.5. Estimates of soil Loss for the years 1992 and 2006 and the relative changes under different scenarios

		Base Model				Scenario1 (1992 model varying R-factor)			Scenario 2 (1992 model varying C-factor)		
		1992	2006	Δ (2006-1992)	Δ	1992_R06	Δ (1992_R061992)	Δ	1992_C06	Δ (1992_C06-1992)	Δ
Landscape Unit	Area(ha)	Soil loss (tons)	Soil loss (tons)	Soil loss change (tons)	%	Soil loss (tons)	Soil loss change (tons)	%	Soil loss (tons)	Soil loss change (tons)	%
Low Sahelian Plains	2,448,090	1,082,795	1,673,357	590,562	54.5	1,653,981	571,186	52.8	1,095,622	12,827	1.2
Sahelian Uplands	855,210	270,147	413,458	143,312	53.0	417,186	147,039	54.4	267,705	-2,442	-0.9
Sahelian Highlands	2,234,170	4,615,605	6,715,717	2,100,112	45.5	6,910,352	2,294,747	49.7	4,483,497	-132,108	-2.9
Savannah Transition	2,652,150	3,322,218	4,504,345	1,182,127	35.6	4,668,699	1,346,481	40.5	3,206,906	-115,312	-3.5
Mixed Terrain Plateau	4,184,300	3,897,381	5,046,151	1,148,770	29.5	5,449,576	1,552,195	39.8	3,798,521	-98,860	-2.5
Savannah Escarpment	1,432,380	2,558,307	3,185,552	627,245	24.5	3,879,971	1,321,664	51.7	2,505,718	-52,589	-2.1
Total	13,806,300	15,746,453	21,538,580	5,792,128	26.9	22,979,765	7,233,312	45.9	15,357,969	-388,484	-2.5

Table 7.6. Estimates of soil loss for the years 2006 and 2020 and the relative changes under different scenarios

		Base Model				Scenario 3 (2006 model varying R-factor)			Scenario 4 (2006 model varying C-factor)		
		2006	2020	Δ (2020-2006)	Δ	2006_R20	Δ (2006_R20-2006)	Δ	2006_C20	Δ (2006_C20_2006)	Δ
Landscape Unit	Area(ha)	Soil loss (tons)	Soil loss (tons)	Soil loss change (ton)	%	Soil loss (tons)	Soil loss change (tons)	%	Soil loss (tons)	Soil loss change (tons)	%
Low Sahelian Plains	2,448,090	1,673,357	1,558,002	-115,355	-6.9	1,553,480	-119,877	-7.2	1,678,191	4,834	0.3
Sahelian Uplands	855,210	413,458	389,950	-23,508	-5.7	381,425	-32,033	-7.7	422,713	9,255	2.2
Sahelian Highlands	2,234,170	6,715,717	6,018,182	-697,535	-10.4	6,055,114	-660,603	-10	6,679,497	-36,220	-0.5
Savannah Transition	2,652,150	4,504,345	3,717,792	-786,553	-17.5	3,982,143	-522,202	-11.6	4,405,758	-98,587	-2.2
Mixed Terrain Plateau	4,184,300	5,046,151	4,494,970	-551,181	-10.9	4,557,854	-488,297	-9.7	4,973,011	-73,140	-1.4
Savannah Escarpment	1,432,380	3,185,552	3,012,316	-173,236	-5.4	3,416,075	230,523	7.2	3,143,817	-41,735	-1.3
Total	13,806,300	21,538,580	19,191,212	-2,347,368	-10.9	19,946,091	-1,592,489	-7.4	21,302,987	-235,593	-1.1

7.5 Discussion

Soil erosion risk across the major landscape units of the Black Volta River basin is primarily controlled by topographical characters and rainfall erosivity. One of the important landscape attributes that influences soil erosion risk is slope. Across the northern part of the Black Volta basin, the Sahelian Highlands landscape unit is characterised by a high average elevation of 356 m a.s.l. and is particularly characterised by relatively steep terrain and is exposed to high annual rainfall. These conditions promote substantial runoff generation and high flow velocities (Ao et al., 2024), leading to severe soil erosion risk. Similarly, the Savannah Escarpment landscape unit, with long and steep slopes in the southern part of the Black Volta River basin shows extended areas exposed to severe soil erosion risks corresponding to the long steep slopes. This relationship is in consonant with Ayele et al. (2021) who estimated increased soil erosion risk in hilly to mountainous landscapes with steep slopes, particularly in areas with fragmented landscapes such as typical for Sahelian Highlands and Savannah Escarpment landscape units.

Conversely, soil erosion risk in the Low Sahelian Plains and Sahelian Uplands landscape units, characterised by flat terrains and gentle slopes, is consistently predicted as low for the three time slices considered (the years 1992, 2006 and 2020). Faint relief makes them less prone to runoff generation and high flow velocities and, consequently, only few areas are exposed to severe soil erosion risk. As emphasised by Montgomery, (2007), steep slopes exacerbate erosion, leading to reduced soil fertility and posing significant threats to agricultural productivity. In effect, the Low Sahelian Plains and Sahelian Uplands are well-suited for agriculture due to their favourable terrain conditions that promote enhanced infiltration and reduced soil erosion. The findings are supported by Ziadat & Taimeh (2013) who affirm the significance of steep slopes to high erosion risk due to the increased flow velocity of runoff. Additionally, the Savannah Transition landscape unit, with a considerable and moderate slope shows that erosion risk can be exacerbated under extensive land use and low vegetation cover conditions. The aspect of slope across the landscape units suggests minor differences in the exposure to sunlight. The variation spans from 171° in the Low Sahelian Plains to 185° in the Sahelian Uplands. The south-facing slopes of the Sahelian Uplands are exposed to faster desiccation than especially the north and east-facing slopes and, thus, are generally drier, leading due to the phenomenon of water repellency to reduced infiltration (Ribolzi et al., 2006) and in consequence enhanced soil erosion risk. This is particularly evident in areas where vegetation is sparse, as the lack of vegetation cover makes the soil more susceptible to soil erosion due to its protecting and stabilizing functions (Akpoti et al., 2016).

Though plan and profile curvature across all landscape units exhibit low average values corresponding to the extended arching of the landforms, the Savannah Escarpment and Sahelian Highlands are, corresponding to their relatively strong relief, characterised by areas with locally strong convex and concave curvature. Stron convex plan and profile curvature of slopes such as on ridges is associated with downslope increasing runoff velocities exposing especially ridges to increased erosion (Noroozpour et al., 2014). In contrast, areas with concave plan and profile curvature are prone to accumulation processes. This is consistent with Stefano et al. (2000) who emphasise that concave areas are more prone to cumulation of runoff; in consequence, these areas are often characterised as hotspots for soil erosion. The high erosion risk in the Savannah Escarpment landscape unit is predominantly controlled by the steep slopes occurring widespread in this area. This coincides with relatively low TWI values indicating poor water retention capacity (Meles et al., 2020). The Low Sahelian Plains landscape unit, on the other

hand, showing relatively high TWI values can be characterized by a good water retention capacity and resulting lower erosion risk (Winzeler et al., 2022). This finding is supported by Seutloali et al. (2017), who pronounced the nexus between high erosion risk and areas with low TWI values, particularly in terrains that are characterised by steep slopes and dry conditions.

The influence of rainfall erosivity is especially evident in the Savannah Transition and Savannah Escarpment landscape units where the high erosivity factor results in high soil erosion risk compared to the other landscape units where the rainfall erosivity factor is lower. These findings are consistent with Mohamadi & Kavian (2015) which point out a strong relationship between high soil erosion risk and high erosivity factors. Further analysis of various scenarios for soil loss underscores the influence of rainfall erosivity on soil erosion risk. A +55% relative change in R-factor between 1992 and 2006 resulted in a relative increase of soil loss of 53% in the Sahelian Uplands landscape unit (Table 7.5). In contrast, the negative change in the R-factor between the years 2006 to 2020 led to a decrease of soil loss across all landscape units (Table 7.6). This reflects the strong influence of rainfall erosivity on soil erosion and is consistent with studies by Panagos et al. (2017), which emphasise rainfall erosivity as a primary driver of soil erosion, particularly in regions with low vegetation cover. Also, the findings by Oliveira et al. (2013) reported that decreases in rainfall erosivity coincide with reduced rainfall intensity and often result in reduced soil loss.

Previous studies (Asempah et al., 2024; Boakye et al., 2020; Obiahu & Elias, 2020) highlight a strong relationship between vegetation cover and soil loss. However, the findings of this study underscore a low influence of land use factor C on soil loss; however, assessing this statement the altogether low variability of the C-factor values across the landscape units has to be considered. The major land cover types - cropland, grassland, and open savannah vegetation - exhibited moderate stability across all time slices. The major change in the land use and land cover occurred in all the six landscape units in and around the settlements. Settlement expanded significantly across all the landscape units with an estimated increase by 148% between 1992 and 2006 and an estimated increase by 119% between 2006 to 2020. The overall land use land cover dynamics and the associated spatial distribution of soil erosion risk particularly in and around settlement areas can be linked to increasing population growth and coinciding urbanisation processes in the Black Volta River basin (Asempah et al., 2021). Especially major towns across the Mixed Terrain Plateau and Savannah Escarpment landscape units established rapid population growth and associated vegetation depletion (Acheampong & Anokye, 2013; Appiah et al., 2014). The Wa municipality located in the Mixed Terrain Plateau landscape unit showed an estimated population growth by 10% between the years 2000 and 2010 (Ghana Statistical Service (GSS), 2012). A subsequent population and housing census conducted in 2021 attests to population growth to 200,672 inhabitants from 107, 214 in 2010 in Wa municipality. (GSS, 2021). The spatial expansion of settlement areas in the Wa municipality from 7.44 km^2 to 59.86 km^2 between the years 1990 and 2020 is paralleled by a 41% reduction of areas in Wa municipality covered by woody vegetation (Asempah et al., 2021).

Other human influences of high soil erosion risk in the Black Volta River basin, especially in the Savannah Escarpment landscape unit, include lumbering of trees for timber and fuelwood, bushfire, infrastructural expansion and overgrazing and unsustainable agricultural practices such as improper crop rotation practices, excessive tillage methods and lack of soil and water conservation measures (Amoako & Gambiza, 2019; Reynolds et al., 2007). Due to low economic status and limited access to resources,

inhabitants prioritise short-term economic livelihood gain options such as unregulated small-scale gold mining activities that predispose the land to degradation (Bagah et al., 2016; GEF-UNEP, 2013).

In many parts of the West African sub-region, many households still rely on fuelwood and charcoal as a primary source of energy (GEF-UNEP, 2013). Extraction of trees for fuelwood and charcoal production is an unsustainable venture that depletes forest cover thereby triggering erosion and environmental degradation (GEF-UNEP, 2013; Obahoundje et al., 2018), both getting aggravated by overgrazing and seasonal bushfires (GEF-UNEP, 2002). According to Fielmua et al. (2014), besides the direct environmental destruction through overgrazing, pastoralism also contributes to bushfires as herdsmen deliberately burn vegetation covers for the germination of tender grasses for grazing animals. These activities are notable across all six major landscape units, especially in the Low Sahelian Plains Sahelian Uplands and Sahelian Highlands landscape units where pastoralism is prominent. Agbeshie et al. (2022) emphasise that the intensity of bushfire is proportional to the rate of soil erosion as higher intensity fires cause enormous vegetation cover loss, thus, triggering increased surface runoff with an associated soil detachment, sediment transport and deposition (Bento-Gonçalves & Vieira, 2020).

There has been major infrastructure development over the past few decades across the Black Volta River basin, driven by the need to support a growing population and meet increasing demands for transportation, energy, and water. The key infrastructure projects such as the construction of dams, road networks, and other essential facilities greatly contributed to the socio-economic development and the same time affected earth movement across the whole area (Gocking, 2021). In the Savannah Escarpment landscape unit, the construction of the 400-megawatt hydroelectric power dam with an active storage capacity of 7,720,000,000 m^3 completed in 2013 was one of these projects (Gocking, 2021). In addition, the road networks were expanded to improve accessibility and facilitate economic activities. These developments have accelerated environmental challenges, including soil erosion and land degradation (Gocking, 2021).

7.6 Conclusions

A major environmental concern in the tropics is soil erosion risk owing to changing rainfall characteristics coupled with land use and land cover changes. Modelling soil erosion risk in the Black Volta River basin improved the understanding of the spatio-temporal varying soil erosion risk and its relation to overall landscape characteristics. By applying the RUSLE model the soil erosion risk was predicted based on the basin's characteristics in terms of topography, land use and land cover, soil characteristics and rainfall distribution. Soil erosion risk was estimated for the three-time steps 1992, 2006 and 2020 for the Black Volta River basin. The severity of soil erosion risk across the landscape units of the Black Volta River basin is ranked in descending order as follows: Savannah Escarpment, Savannah Transition, Sahelian Highlands, Mixed Terrain Plateau, Low Sahelian Plains, and Sahelian Uplands. The lower erosion risk in the Low Sahelian Plains and Sahelian Uplands is primarily attributed to their low relief and their low rainfall erosivity values. In contrast, the Savannah Escarpment, Sahelian Highlands, and Savannah Transition are characterised by long, steep slopes and high rainfall erosivity, making them more prone to soil erosion. These observations emphasise the dominant influence of topographical features and rainfall erosivity on soil erosion risk within the basin.

The spatial distribution of soil erosion risk across the three-time slices analysed shows an expansion of areas of high risk in and around settlement units as well between the years 1992 and 2006 as between

the years 2006 and 2020, underscoring the influence of settlement expansion and human activities on high-erosion risk. The spatial patterns of soil erosion risk and their linkages to landscape attributes, rainfall erosivity, and human activities provide critical insights for targeted interventions. Effective soil and water conservation strategies tailored to the specific needs of each landscape unit are essential to mitigate soil erosion and to sustain agricultural productivity. Such strategies should focus on reducing human-induced pressures, enhancing vegetative cover, and implementing erosion control measures. Addressing these challenges is imperative to safeguarding the ecological and economic sustainability of the Black Volta River basin. Given the continuous pressure of environmental changes and human activities in the Black Volta basin, it is imperative to incorporate these topographic insights into soil conservation strategies to mitigate erosion and protect the fragile landscape units such as the Savannah Escarpment, Sahelian Highlands, and Savannah Transition landscape units.

7.7 Acknowledgements

We appreciate the support of colleagues at the Department of Earth Sciences, Freie Universität throughout this study. We are thankful to NASA and the Consortium of International Agricultural Research Centers' Consortium for Spatial-Information (CGIAR-CSI) for the SRTM DEM. We also acknowledge the International Soil Reference Information Centre (ISRIC) for the soil grid data. Finally, we thank Copernicus for the global land cover data and the Climatic Research Unit (CRU)of the University of East Anglia for the rainfall data. Thank you to the German Academic Exchange Service (DAAD) for awarding a doctoral fellowship through which the research was conducted. *We acknowledge support by the Open Access Publication Fund of the Freie Universität Berlin.*

CHAPTER 8: ANALYSES AND MODELLING OF SOIL EROSION RISK IN THE BLACK VOLTA TRANSBOUNDARY RIVER BASIN OF WEST AFRICA – SYNTHESIS AND CONCLUSIONS

The vulnerability of the West Africa sub-region to land degradation is to a large extent controlled by soil erosion and stems from the regional climatic conditions and unadapted land use land cover changes as evident in the Black Volta riparian countries including Mali, Burkina Faso, Côte d'Ivoire and Ghana. The degradation resulting from the regional climatic conditions is exacerbated by the continued exploration of natural resources that put pressure on water, arable land and forest resources, leading to a loss of biodiversity, soil fertility, low agricultural productivity and food insecurity (Gomiero, 2016; Sinshaw et al., 2021; Xie et al., 2019). For the Black Volta River basin, it is typical that especially in rural settlements there occur rapid expansions of settlement areas including road networks, dams, schools, hospitals and other infrastructure and social amenities. This is shown exemplarily for the Wa municipality, a fast-developing settlement area within the Ghana part of the Black Volta basin. The Wa municipality has experienced a doubling of its population since 2010 (2021: 200,672 population) which led to rapid settlement expansion (Ghana Statistical Service (GSS), 2021). Exemplarily, for Wa municipality at a regional level, a case study was conducted to model land cover dynamics, drivers of urban expansion and the effects of resulting land use land cover change soil erosion risk. Based on these in-depth studies necessary for a valid model set-up soil erosion risk assessment for the whole Black Volta basin with a focus on its major landscape units was conducted to understand the dynamics of the landscapes' susceptibility to soil erosion risk.

8.1 Land Use and Land Cover Dynamics and the Drivers of Urban Expansion in Wa Municipality, Ghana - Synthesis

The assessment of the land use land cover changes on a decadal between 1990 and 2020 the informed understanding of the dynamics of land use land cover changes in the Wa municipality to aspire conservation practices to halt and avert further degradation and biodiversity loss in line with the UN SDG number 15. The land use land cover classification conducted by applying Landsat satellite images shows a continued reduction in close savannah vegetation since 1990. From 1990 to 2001, there was a reduction of close savannah vegetation by c. 7% which came along with an increase in open savannah vegetation, water areas and settlement areas. Similarly, a decrease in areas covered by closed savannah vegetation from 2001-2010 went along with a spread of settlement areas covered by water bodies and bareland. Overall, since 1990 the decrease of areas covered by closed savannah coincides with increased settlement areas and bare land. These findings emphasise the nexus between settlement expansion and the reduction in woody biomass within the Wa Municipality over the past three decades as expansion of settlement areas led to a decrease in woody biomass, particularly in areas previously covered by woody savannah vegetation.

The increasing settlement expansion and its associated shrinking areas covered by closed savannah in the Wa municipality can be attributed to the doubling of population over the past decades. In the fast-growing Wa municipality, there is competing demand for environmental resources especially arable land for crop production and land for settlement. This coupled with seasonal bushfires leads to the depletion of woody biomass (Kuunibe et al., 2013).

The settlement expansion observed corresponds to infilling, edge/urban fringe and leapfrogging types of expansion (Asempah et al., 2021). Over the past decades, settlement areas have undergone significant expansion within the cities and towns and have become more clustered and compacted as characterised by infilling settlement expansion. However, there is significant expansion toward the peripheries of the existing settlement as an indication of fringe/edge expansion (Asempah et al., 2021; Fletcher, 2019). With leapfrogging attributes, the classification shows new settlement patches without spatial connection to existing settlement areas with sprawling rural settlements strategically toward resources such as streams and rivers as an indication of the drive for livelihood and economic development opportunities (Asempah et al., 2021). By statistical analysis of the driver of urban expansion in the municipality, it was established that accessibility and connectivity factors such as distance to water resources, road networks and already existing settlements were major drivers of settlement expansion in the Wa municipality.

The Wa municipality can be taken as a settlement located in a typical Savannah landscape characterised by a semi-arid to dry-subhumid climate with distinct periods of drought. Landscapes with similar attributes undergo tremendous transformation due to degradation and desertification, leading to a reduction in the provision of ecosystem services (Schneibel et al., 2017; Symeonakis et al., 2018). Owing to the delicate and vulnerable nature of the savannah districts, the United Nations consider the assessment of degradation in the savannah a high priority as trends of decreasing productivity of dryland savannahs are quantified, pointing to major social and political implications (Maestre et al., 2016; Symeonakis et al., 2018). Therefore, the assessment of the land cover dynamics in the fast-growing savannah landscape such as the Wa municipality is a significant step to understanding the direction of land cover changes as a basis for sustainable land management strategies and policies.

8.2 Spatial Dynamics of Soil Erosion Risk in the Wa Municipality, Ghana -Synthesis

The spatial distribution of soil erosion risk is dependent on the natural characteristics of a landscape, especially soil, rainfall and relief attributes. To understand the effects of land use and land cover change on soil erosion, the potential erosion risk is exclusively controlled by natural characteristics and the soil erosion risk was assessed for Wa municipality for the years 1990 and 2020 by applying the RUSLE model. The estimation of the potential erosion risk showed higher values, thus a higher exposure, for the year 1990 than for 2020. This change was exclusively controlled by the temporally varying rainfall characteristics, which had a higher erosivity in 1990 than in 2020. Beyond, areas with steep slopes were predicted as areas of severe erosion risk.

Inclusion of the land use land cover characters into the RUSLE model allowed the prediction of soil erosion risk. The estimated mean annual soil erosion risk was lower in 1990 and was distinctly lower than in 2020 – even despite the lower rainfall erosivity in 2020. This clearly shows the strong control of soil erosion by land use. Especially settlement areas, bareland and areas in slopy terrain were estimated as areas of extreme soil erosion risk. In particular, the loss of natural vegetation, thus of open and closed savannah, went along with an expansion of settlement areas. In consequence, this led to a multiplication (factor 7) of expected soil loss in the settlement areas between 1990 to 2020. These findings underscore the importance of vegetation cover as a buffer against the erosive power of rainfall. On the other hand, low-lying landscapes with short slope lengths coupled with high vegetation cover that provides high

surface roughness and soil stability have the highest propensity to lower runoff and its inherent erosive power (Esa et al., 2018).

The dynamics of soil erosion risk in the Wa municipality for the years 1990 and 2020 amplifies the impact of land use land cover change, settlement expansion and the overall depletion of vegetation cover. This enhances understanding of the changes in the municipality's land cover and its impacts on erosion risk. The changes in land use patterns from 1990 to 2020 explain the comparatively lower soil erosion risk in 1990 than in 2020 due to more effective vegetation cover in 1990. Though the RUSLE model is limited to detachment and unable to model deposition and gully erosion its application stimulates the general understanding of soil erosion risk in the Wa municipality to inform integrated landscape and environmental resource management practices. Summarising, the findings provide a valuable background for soil and water conservation management practices, particularly in the highly urbanising areas that are identified as highly susceptible to erosion risk.

8.3 Exposure of Major Landscape Units to Soil Erosion Risk in the Black Volta basin – Synthesis

Different landscape units respond differently to adverse environmental conditions due to their Different landscape units respond differently to adverse environmental conditions due to their biophysical characteristics which are key determinants of the degree of degradation in a landscape (Yousefi et al., 2021) Also, land cover characteristics in each landscape may lead to distinct hydrological functions, different runoff and erosion and sediment transport (Ciampalini et al., 2012; Ouyang et al., 2010). This informed the characterisation of the black Volta River basin into different landscape units and the onward assessment of soil erosion risk and total soil loss in the units for 1992, 2006 and 2020 time slices. The characterised landscape units are unique in terms of biophysical characteristics and show different degrees of vulnerability to erosion risk.

The variations of soil erosion risks across the Black Volta River basin are influenced primarily by topographical attributes and rainfall erosivity. The topographical characters slope, and curvature significantly control soil erosion susceptibility across all major landscape units of the basin, highlighting the Sahelian Highlands with its long and steep slopes being exposed to severe soil erosion risk. In contrast, the landscape unit characterised by gentle slopes such as the Low Sahelian Plains are mostly exposed to low erosion risks. The Savannah Escarpment landscape unit with the steep slopes along its long escarpment is exposed to extreme and exacerbated soil erosion risk. The slopes planform and profile curvatures as well as the topographic wetness index (TWI) next to the slope inclination significantly control runoff generation and, thus, exposure to soil erosion risk.

In comparing the influence of rainfall erosivity and land cover on soil erosion risk across the six major landscape units of the Black Volta River basin, it got evident that the erosivity factor domninates. The total soil loss for all the landscape units was higher in the base year 2006 than in the year 1992 corresponding to the mean erosivity factor being higher in 2006 than in 1992. Between the years 1992 and 2006, the Sahelian Uplands landscape experienced a 55% increase in the mean erosivity factor, which was associated with an estimated 53% increase in soil loss. Similarly, in the Savannah Escarpment landscape unit a 27% increase in the mean erosivity factor during the same period corresponded to a 24.5% increase in soil loss. In 2020 the overall rainfall erosivity was lower than in the base year 2006: correspondingly soil loss decreased inn all landscape units of the Black Volta River basin. The effects

of land use and land cover on soil loss across the Black Volta River basin were difficult to assess due to its low fluctuations between the landscape units. Summarising, topographic characters and rainfall erosivity were identified as the major factors controlling soil erosion risk and soil loss in the Black Volta River basin.

8.4 General Implications of Soil Erosion Risk and Soil Loss- Synthesis

This section highlights the implications of soil erosion risk in the Black Volta River basin. The implications are multi-faceted and of ecological, agricultural, hydrological, climatic and economic dimensions.

8.4.1 Ecological Destruction and Biodiversity Loss

Unsustainable land use frequently results in degradation at both regional and landscape scales with ecological implications (Qu et al., 2023). The findings of the study emphasise that land use change led to the depletion of vegetation cover in the Black Volta basin especially in highly urbanising areas. A typical case study is the Wa municipality which underwent increasing urban expansion and associated depletion of woody biomass on decadal time steps at least during the past 30 years. Additionally, soil erosion damages are evident in the Wa municipality due to unregulated land use and practices such as bush burning and small-scale gold mining (Barry et al., 2005; Kusakari et al., 2014). Soil erosion damages have numerous interconnected ecological implications that can significantly threaten the natural ecosystems as well as infrastructure. The spatial and temporal dynamics of land use land cover and hereby triggered soil erosion and soil loss alludes to significant ecological disruption. These ecological consequences may include changes in species composition as well as disruption of food webs and altering of nutrient cycles (Laine & Tylianakis, 2024). Also, natural habitats may be destroyed as erosion alters the landscape and causes fragmentation, thereby negatively impacting the survival, especially of species that are dependent on specific habitat types (Heinken & Weber, 2013). On the whole, ecosystem resilience and ecological health are compromised under unsustainable land use and severe soil erosion leading to loss of biodiversity (Khattak et al., 2025)**.** In consequence, conversation practices and integrated landscape management are imperative in line with United Nations SDG 15 of the 2030 Agenda for Sustainable Development which seeks to "protect, restore and promote sustainable use of terrestrial ecosystems, sustainably manage forests, combat desertification and halt and reverse land degradation and halt biodiversity loss."

8.4.2 Agricultural Production and Productivity

Soil erosion reduces the fertility and productivity of the soil leading to low agricultural productivity (Sartori et al., 2024). Soil erosion risk modelling is part of efforts to promote sustainable agriculture and food security which are vital to the SDGs (Yin et al., 2022). The RUSLE estimates as applied in this study focus on processes of rill and sheet erosion. Hereby triggered top-soil removal affects depletion of major plant nutrients such as nitrogen, phosphorus and potassium. Self-enforcing, the loss of organic matter by wash out results in a destabilisation of soil structure. Owing to the rapid population growth and associated settlement expansions there is a high likelihood of an expansion of arable land and an increased competition for productive land in the surroundings of the settlements which in turn leads to

a loss of savannah areas. With unadapted land use land degradation gets triggered and as a result, efforts to achieve food security may be jeopardised.

8.4.3 Economic Cost and Impacts

There is growing evidence of the economic impacts of soil erosion in West African river basins and landscapes. According to the World Bank, (2019) in 2017 the costs for environmental degradation emanating from erosion, floods and pollution in the coastal zones of West Africa amounted to about US $ 3.8 billion. Exclusively focusing on the costs resulting from soil erosion this amount accounted for 2017 about US $ 964 million in the same area, thus a quarter of the total costs (World Bank, 2019). Wherever soil erosion damages appear, costs for repair or reconstruction of damaged infrastructure, cost of land reclamation and restoration of land and increased costs of input for farming come along (Huang et al., 2022). The budget for agriculture could increase due to the investment needed in crop production inputs such as fertilizers, pesticides and irrigation to compensate for the soil erosion damages that lead to nutrient loss and soil fertility depletion (Pandian et al., 2024). Also, soil erosion and its associated off-site damages such as deposition may lead to a consequential cost for investments in more advanced water treatment for rural communities in the basin that rely on reservoirs and surface water (Huang et al., 2022). The assessment of soil erosion risk provides information about areas with high exposure to soil erosion, and, thus, supports the implementation of soil conservation measures before the damages take place (Buraka et al., 2024).

8.4.4 Hydrological Impacts

Surface water is the major source of water supply in the Black Volta riparian countries (Kwakye & Bárdossy, 2020). The spatial dynamics of land use and related soil erosion processes in the basin imply earth movements and accelerated deposition of sediments. These processes may affect channel dynamics as well as the siltation of dams (Mosaid et al., 2024). Owing to the application of agro-chemicals and POPs in crop production and mining within the river basin, sediments may also contain chemical pollutants, such as pesticides and heavy metals (Adnan et al., 2024) Overall, the distribution and availability of water may be altered, leading to changes in the timing and volume of river flow (Döll et al., 2009).

8.4 Conclusions

The Black Volta River basin is a major transboundary river basin in West Africa that provides notably arable land for agriculture production, water resources for domestic consumption, irrigation and hydropower generation and mineral resources. Settlement expansion as a result of population growth influences space demand and competes with other uses, frequently causing unadapted land use or over-exploitation and thereby depletion of vegetative cover and soil degradation. A large part of the basin particularly the areas located within the semi-arid to dry-subhumid zones of the Sahel and savannah are highly susceptible to degradation due to climatic conditions and sparse vegetation cover. This vulnerability is exacerbated by human activities triggered by the rapid population growth in the basin as displayed by the Wa municipality.

The case study of Wa municipality reveals information on the spatio-temporal transformation of the land cover in its administrative area. The expansion of settlement areas in the municipality consistently causes

a decrease in areas covered by closed savannah vegetation which coincides with a loss of woody biomass. The degradation of vegetation cover through human-induced activities such as bushfires and unregulated small-scale gold mining by the inhabitants of the municipality could be pointed out. Geostatistical analysis of location factors in particular such as distance to existing settlements, distance to rivers and distance to road networks were identified as the major drivers of settlement expansion. Accessibility and connectivity driving factors of settlement expansion emphasise the quest by the inhabitants for economic and livelihood development.

Comparing the potential and actual soil erosion risk in the Wa municipality for the years 1990 and 2020 the higher potential erosion risk estimated for the year 1990 than 2020 affirms the strong control of potential erosion by rainfall erosivity. The assessment of the soil erosion risk by including land use as a factor in the modelling approach shows that even despite the higher rainfall erosivity in 1990 land use changes affected a higher soil erosion risk in 2020 than in 1990. The high erosion in the year 2020 is mainly influenced by the depletion of vegetation cover as a result of urban expansion. Settlement and bareland areas were identified as areas of highest exposure to soil erosion risk. Additionally, the relief especially in areas with steep and long slopes was identified triggering high soil erosion risk.

Overall, the study provides insights into the relationships between topographic attributes, settlement expansion, land use changes and soil erosion risk. Also, the major landscape units including the Savannah Escarpment, the Sahelian Highlands and the Savannah Transition were identified as the most vulnerable owing to the biophysical attribute that exposes them to high soil erosion risk. The findings are imperative and could serve as a guide in planning conservation management practices in line with goals to protect, restore and promote sustainable use of terrestrial ecosystems and halt degradation and biodiversity loss as proposed by the United Nations SDGs. Finally, in promoting integrated watershed management and sustainable development as mandated by the Volta Basin Authority, the understanding of the land use land cover dynamics and associated soil erosion risk will be a valuable basis for future decision-making and conservation planning.

References

Abbaspour, K. C., Yang, J., Maximov, I., Siber, R., Bogner, K., Mieleitner, J., Zobrist, J., & Srinivasan, R. (2007). Modelling hydrology and water quality in the pre-alpine/alpine Thur watershed using SWAT. *Journal of Hydrology*, *333*(2–4), 413–430. https://doi.org/10.1016/j.jhydrol.2006.09.014

Abdalrahman, Y., Spence, K., & Rotherham, I. D. (2010). The main causes of direct human-induced land degradation in the Libyan Al Jabal Alakhdar region. *Landscape Archaeology and Ecology-End of Tradition*, *8*(September), 7–21.

AbdelRahman, M. A. E. (2023). An overview of land degradation, desertification and sustainable land management using GIS and remote sensing applications. In *Rendiconti Lincei* (Vol. 34, Issue 3). Springer International Publishing. https://doi.org/10.1007/s12210-023-01155-3

Abdullah, M., Feagin, R., & Musawi, L. (2017). The use of spatial empirical models to estimate soil erosion in arid ecosystems. *Environmental Monitoring and Assessment*, *189*(2). https://doi.org/10.1007/s10661-017-5784-y

Abungba, J. A., Adjei, K. A., Gyamfi, C., Odai, S. N., Pingale, S. M., & Khare, D. (2022). Implications of Land Use/Land Cover Changes and Climate Change on Black Volta Basin Future Water Resources in Ghana. *Sustainability (Switzerland)*, *14*(19). https://doi.org/10.3390/su141912383

Acheampong, R., & Anokye, P. (2013). Understanding Households' Residential Location Choice in Kumasi's Peri-Urban Settlements and the Implications for Sustainable Urban Growth. *Research on Humanities and Social Sciences*, *3*(9), 60–70.

Adams, H. D., Park Williams, A., Xu, C., Rauscher, S. A., Jiang, X., & McDowell, N. G. (2013). Empirical and process-based approaches to climate-induced forest mortality models. *Frontiers in Plant Science*, *4*(NOV), 1–5. https://doi.org/10.3389/fpls.2013.00438

Adnan, M., Xiao, B., Ali, M. U., Xiao, P., Zhao, P., Wang, H., & Bibi, S. (2024). Heavy metals pollution from smelting activities: A threat to soil and groundwater. *Ecotoxicology and Environmental Safety*, *274*(December 2023). https://doi.org/10.1016/j.ecoenv.2024.116189

Adongo, T. A., Agyare, W. A., Abagalec, F. K., & Kyei-Baffour, N. (2019). Spatial soil loss estimation using an integrated GIS-based revised universal soil loss equation (RUSLE) in selected watersheds in northern Ghana. *International Journal of Engineering, Science and Technology*, *11*(4), 58–74. https://doi.org/10.4314/ijest.v11i4.6

Agbeshie, A. A., Abugre, S., Atta-Darkwa, T., & Awuah, R. (2022). A review of the effects of forest fire on soil properties. *Journal of Forestry Research*. https://doi.org/10.1007/s11676-022-01475-4

Aghsaei, H., Mobarghaee Dinan, N., Moridi, A., Asadolahi, Z., Delavar, M., Fohrer, N., & Wagner, P. D. (2020). Effects of dynamic land use/land cover change on water resources and sediment yield in the Anzali wetland catchment, Gilan, Iran. *Science of the Total Environment*, *712*, 136449. https://doi.org/10.1016/j.scitotenv.2019.136449

Agyekum, J., Annor, T., Quansah, E., Lamptey, B., & Okafor, G. (2022). Extreme precipitation indices over the Volta Basin: CMIP6 model evaluation. *Scientific African*, *16*, e01181. https://doi.org/10.1016/j.sciaf.2022.e01181

Ahmad, N. N. S. B., Mustafa, F. B., & Muhammad Yusoff, S. Y. (2023). Spatial prediction of soil erosion risk using knowledge-driven method in Malaysia's Steepland Agriculture Forested Valley. *Environment, Development and Sustainability*, *0123456789*. https://doi.org/10.1007/s10668-023-03251-8

Ahnert, F. (1996). *Introduction to geomorphology*.utb GmbH, Berlin.

Akinsete, E., Apostolaki, S., Chatzistamoulou, N., Koundouri, P., & Tsani, S. (2019). The link between ecosystem services and human wellbeing in the implementation of the European water framework directive: Assessing Four River basins in Europe. *Water (Switzerland)*, *11*(3), 1–20. https://doi.org/10.3390/w11030508

Akinsete, E., Koundouri, P., Kartala, X., Englezos, N., Lautze, J., Yihdego, Z., Gibson, J., Scholz, G., van Bers, C., & Sodoge, J. (2022). Sustainable WEF Nexus Management: A Conceptual Framework to Integrate Models of Social, Economic, Policy, and Institutional Developments. *Frontiers in Water*, *4*(June), 1–13. https://doi.org/10.3389/frwa.2022.727772

Akpoti, K., Antwi, E. O., & Kabo-bah, A. T. (2016). Impacts of rainfall variability, land use and land cover change on stream flow of the Black Volta basin, West Africa. *Hydrology*, *3*(3), 1–24. https://doi.org/10.3390/hydrology3030026

Al-Kindi, K. M., & Alabri, Z. (2024). Investigating the Role of the Key Conditioning Factors in Flood Susceptibility Mapping Through Machine Learning Approaches. *Earth Systems and Environment*, *8*(1), 63–81. https://doi.org/10.1007/s41748-023-00369-7

Alewell, C., Borrelli, P., Meusburger, K., & Panagos, P. (2019). Using the USLE: Chances, challenges and limitations of soil erosion modelling. *International Soil and Water Conservation Research*, *7*(3), 203–225. https://doi.org/10.1016/j.iswcr.2019.05.004

Alivio, M. B., Bezak, N., & Mikoš, M. (2023). The size distribution metrics and kinetic energy of raindrops above and below an isolated tree canopy in urban environment. *Urban Forestry and Urban Greening*, *85*. https://doi.org/10.1016/j.ufug.2023.127971

Allwaters Consult. (2012). *Diagnostic Study of The Black Volta Basin in Ghana; Final Report; ALLWATERS Consult Limited: Kumasi, Ghana*.

Almouctar, M. A. S., Wu, Y., Zhao, F., & Dossou, J. F. (2021). Soil erosion assessment using the RUSLE model and geospatial techniques (Remote sensing and GIS) in south-central Niger (Maradi region). *Water (Switzerland)*, *13*(24). https://doi.org/10.3390/w13243511

Altrock, U. (2022). New (sub)urbanism? - How German cities try to create "urban" neighborhoods in their outskirts as a contribution to solving their recent housing crises. *Urban Governance*, *2*(1), 130–143. https://doi.org/10.1016/j.ugj.2022.04.001

Amisigo, B. A., van de Giesen, N., Rogers, C., Andah, W. E. I., & Friesen, J. (2008). Monthly streamflow prediction in the Volta Basin of West Africa: A SISO NARMAX polynomial modelling. *Physics and Chemistry of the Earth*, *33*(1–2), 141–150. https://doi.org/10.1016/j.pce.2007.04.019

Amoah, T. S. (2013). *Evolution of Water Systems and Its Challenges in the Wa Municipal of Ghana*. *3*(7).

Amoako, E. E., & Gambiza, J. (2019). Effects of anthropogenic fires on soil properties and the implications of fire frequency for the Guinea savanna ecological zone, Ghana. *Scientific African*, *6*. https://doi.org/10.1016/j.sciaf.2019.e00201

Ampim, P. A. Y., Ogbe, M., Obeng, E., Akley, E. K., & Maccarthy, D. S. (2021). Land cover changes in Ghana over the past 24 years. *Sustainability (Switzerland)*, *13*(9). https://doi.org/10.3390/su13094951

Andah, W. E. I., van de Giesen, N., & Biney, C. A. (2003). *Water , Climate , Food , and Environment in the Volta Basin Adaptation strategies to changing environments: Vol. Vol.4* (Issue No.16). http://www.weap21.org/downloads/ADAPTVolta.pdf

Anees, M. M., Mann, D., Sharma, M., Banzhaf, E., & Joshi, P. K. (2020). Assessment of urban dynamics to understand spatiotemporal differentiation at various scales using remote sensing and geospatial tools. *Remote Sensing*, *12*(8). https://doi.org/10.3390/RS12081306

Anselm, N., Brokamp, G., & Schütt, B. (2018). Assessment of land cover change in peri-urban high Andean environments south of Bogotá, Colombia. *Land*, *7*(2), 1–28. https://doi.org/10.3390/land7020075

Antabe, R., Atuoye, K. N., Kuuire, V. Z., Sano, Y., Arku, G., & Luginaah, I. (2017). Community health impacts of surface mining in the Upper West Region of Ghana: The roles of mining odors and dust. *Human and Ecological Risk Assessment*, *23*(4), 798–813. https://doi.org/10.1080/10807039.2017.1285691

Antrop, M. (2005). Why landscapes of the past are important for the future. *Landscape and Urban Planning*, *70*(1–2), 21–34. https://doi.org/10.1016/j.landurbplan.2003.10.002

Ao, L., Wu, Y., Xu, Q., Huang, G., Zheng, J., Dai, J., Fu, Z., & Chen, H. (2024). Subsurface flow aggravates the soil erosion on steep slopes in karst post-mining areas. *Journal of Hydrology: Regional Studies*, *51*(12), 1–12. https://doi.org/10.1016/j.ejrh.2024.101667

Appiah, D. O., Bugri, J. T., Forkuo, E. K., & Boateng, P. K. (2014). Determinants of peri-urbanization and land use change patterns in peri-urban Ghana. *Journal of Sustainable Development*, *7*(6), 95–109. https://doi.org/10.5539/jsd.v7n6p95

Arabameri, A., Rezaei, K., Pourghasemi, H. R., Lee, S., & Yamani, M. (2018). GIS-based gully erosion susceptibility mapping: a comparison among three data-driven models and AHP knowledge-based technique. *Environmental Earth Sciences*, *77*(17), 1–22. https://doi.org/10.1007/s12665-018-7808-5

Arega, E., Deribew, K. T., Moisa, M. B., & Gemeda, D. O. (2024). Assessment of soil erosion and prioritization of conservation and restoration measures using RUSLE and Geospatial techniques: the case of upper Bilate watershed. *Geomatics, Natural Hazards and Risk*, *15*(1). https://doi.org/10.1080/19475705.2024.2336016

Arneth, A., Denton, F., Agus, F., Elbehri, A., Erb, K., Elasha, B. O., Rahimi, M., Rounsevell, M., Spence, A., & Valentini, R. (2019). Chapter 1: Framing and context. *Climate Change and Land: An IPCC Special Report on Climate Change, Desertification, Land Degradation, Sustainable Land Management, Food Security, and Greenhouse Gas Fluxes in Terrestrial Ecosystems [P.R. Shukla, J. Skea, E. Calvo Buendia, V. Masson-Delmot*, 77–129.

Arnold, J. G., Moriasi, D. N., Gassman, P. W., Abbaspour, K. C., White, M. J., R. Srinivasan, Santhi, C., Harmel, R. D., Griensven, A. van, Liew, M. W. Van, Kannan, N., & Jha, M. K. (2012). SWAT: Model Use, Calibration, and Validation. *American Society of Agricultural and Biological Engineers*, *55*(4), 1491–1508.

Arnold, J. G., Srinivasan, R., Muttiah, R. S., & Williams, J. R. (1998). Large Area Hydrologic Modeling and Assessment Part I: Model Development. *Journal of the American Water Resources Association*, *34*(1), 73–89.

Asare-Nuamah, P., & Botchway, E. (2019). Understanding climate variability and change: analysis of temperature and rainfall across agroecological zones in Ghana. *Heliyon*, *5*(10), e02654. https://doi.org/10.1016/j.heliyon.2019.e02654.

Asempah, M., Sahwan, W., & Schütt, B. (2021). Assessment of land cover dynamics and drivers of urban expansion using geospatial and logistic regression approach in Wa municipality, Ghana. *Land*, *10*(11). https://doi.org/10.3390/land10111251

Asempah, M., Shisanya, C. A., & Schütt, B. (2024). Modeling of soil erosion risk in a typical tropical savannah landscape. *Scientific African*, *23*(December 2023), e02042. https://doi.org/10.1016/j.sciaf.2023.e02042

Asiedu, J. K. (2018). Assessing the threat of erosion to nature-based interventions for stormwater management and flood control in the Greater Accra Metropolitan Area, Ghana. *Journal of Ecological Engineering*, *19*(1), 1–13. https://doi.org/10.12911/22998993/79418

Atoma, H., Suryabhagavan, K. V., & Balakrishnan, M. (2020). Soil erosion assessment using RUSLE model and GIS in Huluka watershed, Central Ethiopia. *Sustainable Water Resources Management*, *6*(1), 1–17. https://doi.org/10.1007/s40899-020-00365-z

Attua, E. M., & Fisher, J. B. (2011). Historical and future land-cover change in a municipality of Ghana. *Earth Interactions*, *15*(9), 1–26. https://doi.org/10.1175/2010EI304.1

Ayele, G. T., Kuriqi, A., Jemberrie, M. A., Saia, S. M., Seka, A. M., Teshale, E. Z., Daba, M. H., Ahmad Bhat, S., Demissie, S. S., Jeong, J., & Melesse, A. M. (2021). Sediment yield and reservoir sedimentation in highly dynamic watersheds: The case of koga reservoir, ethiopia. *Water (Switzerland)*, *13*(23), 1–20. https://doi.org/10.3390/w13233374

Baatuuwie, B. N., Ochire-Boadu, K., Abdul-Ganiyu, S., & Asante, W. J. (2011). Assessment of soil and water conservation measures practiced by farmers: A case study in the Tolon-Kumbungu District of Northern Ghana. *Journal of Soil Science and Environmental Management*, *2*(4), 103–109. https://academicjournals.org/journal/JSSEM/article-abstract/1100C1F1732%0Ahttp://www.academicjournals.org/JSSEM

Badorreck, A., Gerke, H. H., & Hüttl, R. F. (2013). Morphology of physical soil crusts and infiltration patterns in an artificial catchment. *Soil and Tillage Research*, *129*, 1–8. https://doi.org/10.1016/j.still.2013.01.001

Bagah, D. A., Angko, W., & Tanyeh, J. P. (2016). Environmental Degradation and Small Scale Mining Nexus : Emerging Trends and Challenges in Northern Ghana. *Developing Country Studies*, *6*(2), 38–45. www.iiste.org

Bagayoko, F. (2016). Impact of land-use intensity on evaporation and surface runoff: Processes and parameters for eastern Burkina Faso, West Africa. In *Ecology and Development Series No. 40, 2006* (Issue March).

Barry, B., Obuobie, E., Andreini, M., Andah, W., & Pluquet, M. (2005). The Volta River basin, Assessment, Comprehensive Management, Water. In *Water*.

Basommi, P. L., Guan, Q., & Cheng, D. (2015). Exploring Land use and Land cover change in the mining areas of Wa East District, Ghana using Satellite Imagery. *Open Geosciences*, *7*(1), 618–626. https://doi.org/10.1515/geo-2015-0058

Batisani, N., & Yarnal, B. (2009). Urban expansion in Centre County, Pennsylvania: Spatial dynamics and landscape transformations. *Applied Geography*, *29*(2), 235–249. https://doi.org/10.1016/j.apgeog.2008.08.007

Beguería, S., Angulo-Martínez, M., Gaspar, L., & Navas, A. (2015). Detachment of soil organic carbon by rainfall splash: Experimental assessment on three agricultural soils of Spain. *Geoderma*, *245–246*, 21–30. https://doi.org/10.1016/j.geoderma.2015.01.010

Benavidez, R., Jackson, B., Maxwell, D., & Norton, K. (2018). A review of the (Revised) Universal Soil Loss Equation (R)USLE): With a view to increasing its global applicability and improving soil loss estimates. *Hydrology and Earth System Sciences*, *22*(11), 6059–6086. https://doi.org/10.5194/hess-22-6059-2018

Benebere, P., Asante, F., & Odame Appiah, D. (2017). Hindrances to adaptation to water insecurity under climate variability in peri-urban Ghana. *Cogent Social Sciences*, *3*(1), 1–17. https://doi.org/10.1080/23311886.2017.1394786

Benkobi, L., Trlica, M. J., & Smith, J. L. (1994). Evaluation of a refined surface cover subfactor for use in RUSLE. *Journal of Range Management*, *47*(1), 74–78. https://doi.org/10.2307/4002845

Bento-Gonçalves, A., & Vieira, A. (2020). Wildfires in the wildland-urban interface: Key concepts and evaluation methodologies. *Science of the Total Environment*, *707*(xxxx), 135592. https://doi.org/10.1016/j.scitotenv.2019.135592

Berberoglu, S., Donmez, C., & Cilek, A. (2021). Modelling climate change impacts on regional net primary productivity in Turkey. *Environmental Monitoring and Assessment*, *193*(5), 1–16. https://doi.org/10.1007/s10661-021-09031-z

Berihun, M. L., Tsunekawa, A., Haregeweyn, N., Meshesha, D. T., Adgo, E., Tsubo, M., Masunaga, T., Fenta, A. A., Sultan, D., & Yibeltal, M. (2019). Exploring land use/land cover changes, drivers and their implications in contrasting agro-ecological environments of Ethiopia. *Land Use Policy*, *87*(March), 104052. https://doi.org/10.1016/j.landusepol.2019.104052

Bernik, B. M., Pardue, J. H., & Blum, M. J. (2018). Soil erodibility differs according to heritable trait variation and nutrient-induced plasticity in the salt marsh engineer Spartina alterniflora. *Marine Ecology Progress Series*, *601*, 1–14. https://doi.org/10.3354/meps12689

Bettencourt, L. M. A. (2013). The origins of scaling in cities. *Science*, *340*(6139), 1438–1441. https://doi.org/10.1126/science.1235823

Bettoni, M., Maerker, M., Bosino, A., Conedera, M., Simoncelli, L., & Vogel, S. (2023). Land use effects on surface runoff and soil erosion in a southern Alpine valley. *Geoderma*, *435*(October 2022), 116505. https://doi.org/10.1016/j.geoderma.2023.116505

Bewket, W., & Sterk, G. (2003). Assessment of soil erosion in cultivated fields using a survey methodology for rills in the Chemoga watershed, Ethiopia. *Agriculture, Ecosystems and Environment*, *97*(1–3), 81–93. https://doi.org/10.1016/S0167-8809(03)00127-0

Boakye, E., Anyemedu, F. O. K., Donkor, E. A., & Quaye-Ballard, J. A. (2020). Spatial distribution of soil erosion and sediment yield in the Pra River Basin. *SN Applied Sciences*, *2*(3), 1–12. https://doi.org/10.1007/s42452-020-2129-1

Boakye, E., Geophery, K. A., Jonathan, A. Q.-B., & Emmanuel, A. D. (2018). Land use change and sediment yield studies in Ghana: Review. *Journal of Geography and Regional Planning*, *11*(9), 122–133. https://doi.org/10.5897/jgrp2018.0707

Boamah, N. A. (2013). Urban Land Market in Ghana: A Study of the Wa Municipality. *Urban Forum*, *24*(1), 105–118. https://doi.org/10.1007/s12132-013-9187-z

Bologna, M., & Aquino, G. (2020). Deforestation and world population sustainability: a quantitative analysis. *Scientific Reports*, *10*(1), 1–9. https://doi.org/10.1038/s41598-020-63657-6

Bongaarts, J. (2009). Human population growth and the demographic transition. *Philosophical Transactions of the Royal Society B: Biological Sciences*, *364*(1532), 2985–2990. https://doi.org/10.1098/rstb.2009.0137

Bonilla, C. A., & Johnson, O. I. (2012). Soil erodibility mapping and its correlation with soil properties in Central Chile. *Geoderma*, *189–190*, 116–123. https://doi.org/10.1016/j.geoderma.2012.05.005

Boretti, A., & Rosa, L. (2019). Reassessing the projections of the World Water Development Report. *Npj Clean Water*, *2*(1). https://doi.org/10.1038/s41545-019-0039-9

Borrelli, P., Alewell, C., Alvarez, P., Anache, J. A. A., Baartman, J., Ballabio, C., Bezak, N., Biddoccu, M., Cerdà, A., Chalise, D., Chen, S., Chen, W., De Girolamo, A. M., Gessesse, G. D., Deumlich, D., Diodato, N., Efthimiou, N., Erpul, G., Fiener, P., … Panagos, P. (2021). Soil erosion modelling: A global review and statistical analysis. *Science of the Total Environment*, *780*. https://doi.org/10.1016/j.scitotenv.2021.146494

Borrelli, P., Armenteras, D., Panagos, P., Modugno, S., & Schütt, B. (2015). The implications of fire management in the andean paramo: A preliminary assessment using satellite remote sensing. *Remote Sensing*, *7*(9), 11061–11082. https://doi.org/10.3390/rs70911061

Borrelli, P., Robinson, D. A., Fleischer, L. R., Lugato, E., Ballabio, C., Alewell, C., Meusburger, K., Modugno, S., Schütt, B., Ferro, V., Bagarello, V., Oost, K. Van, Montanarella, L., & Panagos, P. (2017). An assessment of the global impact of 21st century land use change on soil erosion. *Nature Communications*, *8*(1). https://doi.org/10.1038/s41467-017-02142-7

Borrelli, P., Robinson, D. A., Panagos, P., Lugato, E., Yang, J. E., Alewell, C., Wuepper, D., Montanarella, L., & Ballabio, C. (2020). Land use and climate change impacts on global soil erosion by water (2015-2070). *Proceedings of the National Academy of Sciences of the United States of America*, *117*(36), 21994–22001. https://doi.org/10.1073/pnas.2001403117

Buchhorn, M., Lesiv, M., Tsendbazar, N. E., Herold, M., Bertels, L., & Smets, B. (2020). Copernicus global land cover layers-collection 2. *Remote Sensing*, *12*(6), 1–14. https://doi.org/10.3390/rs12061044

Buhai, R. D., Halpern, Y., Kim, Y., Risteski, A., & Sontag, D. (2020). Empirical study of the benefits of overparameterization in learning latent variable models. *37th International Conference on Machine Learning, ICML 2020*, *PartF16814*, 1188–1196.

Buraka, T., Elias, E., Suryabhagavan, K. V., & Lelago, A. (2024). Assessment of soil erosion risks in response to land-use and land-cover changes in Coka watershed, Southern Ethiopia. *Geology, Ecology, and Landscapes*, *8*(2), 140–153. https://doi.org/10.1080/24749508.2022.2109825

Butt, M. J., Waqas, A., & Mahmood, R. (2010). The Combined Effect of Vegetation and Soil Erosion in the Water Resource Management. *Water Resources Management*, *24*(13), 3701–3714. https://doi.org/10.1007/s11269-010-9627-7

Carranza-García, M., García-Gutiérrez, J., & Riquelme, J. C. (2019). A framework for evaluating land use and land cover classification using convolutional neural networks. *Remote Sensing*, *11*(3). https://doi.org/10.3390/rs11030274

Carrier, M. A., Lefebvre, R., Racicot, J., & Asare, E. B. (2008). Northern Ghana hydrogeological assessment project. *Access to Sanitation and Safe Water: Global Partnerships and Local Actions - Proceedings of the 33rd WEDC International Conference*, *May*, 353–361.

Cavender-Bares, J., Gamon, J. A., & Townsend, P. A. (2020). Remote sensing of plant biodiversity. In *Remote Sensing of Plant Biodiversity*. https://doi.org/10.1007/978-3-030-33157-3

Cen, Y., Zhang, B., Luo, J., Deng, Q., Liu, H., & Wang, L. (2022). Influence of Topographic Factors on the Characteristics of Gully Systems in Mountainous Areas of Ningnan Dry-Hot Valley, SW China. *International Journal of Environmental Research and Public Health*, *19*(14). https://doi.org/10.3390/ijerph19148784

Cerdan, O., Souchère, V., Lecomte, V., Couturier, A., & Le Bissonnais, Y. (2002). Incorporating soil surface crusting processes in an expert-based runoff model: Sealing and transfer by runoff and erosion related to agricultural management. *Catena*, *46*(2–3), 189–205. https://doi.org/10.1016/S0341-8162(01)00166-7

Chalise, D., Kumar, L., Shriwastav, C. P., & Lamichhane, S. (2018). Spatial assessment of soil erosion in a hilly watershed of Western Nepal. *Environmental Earth Sciences*, *77*(19), 0. https://doi.org/10.1007/s12665-018-7842-3

Chen, G., Li, X., Liu, X., Chen, Y., Liang, X., Leng, J., Xu, X., Liao, W., Qiu, Y., Wu, Q., & Huang, K. (2020). Global projections of future urban land expansion under shared socioeconomic pathways. *Nature Communications*, *11*(1), 1–12. https://doi.org/10.1038/s41467-020-14386-x

Chen, Jia, Xiao, H., Li, Z., Liu, C., Wang, D., Wang, L., & Tang, C. (2019). Threshold effects of vegetation coverage on soil erosion control in small watersheds of the red soil hilly region in China. *Ecological Engineering*, *132* (November 2018), 109–114. https://doi.org/10.1016/j.ecoleng.2019.04.010

Chen, Jinyue, Chen, S., Fu, R., Li, D., Jiang, H., Wang, C., Peng, Y., Jia, K., & Hicks, B. J. (2022). Remote Sensing Big Data for Water Environment Monitoring: Current Status, Challenges, and Future Prospects. *Earth's Future*, *10*(2), 1–33. https://doi.org/10.1029/2021EF002289

Chen, L., Wang, J., Wang, H., Xu, F., Song, P., Yang, C., & Li, J. (2022). Variation in soil detachment capacity of structural and sedimentary crusts induced by simulated rainfall formed on ridge and furrow. *Catena*, *211*(December 2021), 105971. https://doi.org/10.1016/j.catena.2021.105971

Cheng, J., & Masser, I. (2002). Urban growth pattern modelling : a case study of Wuhan city , PR China Urban growth pattern modeling : a case study of Wuhan city , PR China. *Landscape and Urban Planning*, *62*(August), 199–217.

Chiteculo, V., Lojka, B., Surový, P., Verner, V., Panagiotidis, D., & Woitsch, J. (2018). Value chain of charcoal production and implications for forest degradation: Case study of Bié Province, Angola. *Environments - MDPI*, *5*(11), 1–13. https://doi.org/10.3390/environments5110113

Chomitz, K. M., Brenes, E., & Constantino, L. (1999). Financing environmental services: The Costa Rican experience and its implications. *Science of the Total Environment*, *240*(1–3), 157–169. https://doi.org/10.1016/S0048-9697(99)00310-1

Churkina, G. (2016). The role of urbanization in the global carbon cycle. *Frontiers in Ecology and Evolution*, *3*(JAN), 1–9. https://doi.org/10.3389/fevo.2015.00144

Ciampalini, R., Billi, P., Ferrari, G., Borselli, L., & Follain, S. (2012). Soil erosion induced by land use changes as determined by plough marks and field evidence in the Aksum area (Ethiopia). *Agriculture, Ecosystems and Environment*, *146*(1), 197–208. https://doi.org/10.1016/j.agee.2011.11.006

Cobbinah, P. B., & Amoako, C. (2012). Urban sprawl and the loss of peri-urban land in Kumasi, Ghana. *International Journal of Social and Human Sciences*, *6*(1), 388–397. http://www.researchgate.net/publication/232957200_Urban_Sprawl_and_the_Loss_of_Peri_Urban_Land_in_Kumasi_Ghana/file/d912f509af6f7c7ef5.pdf

Conoscenti, C., Angileri, S., Cappadonia, C., Rotigliano, E., Agnesi, V., & Märker, M. (2014). Gully erosion susceptibility assessment by means of GIS-based logistic regression: A case of Sicily (Italy). *Geomorphology*, *204*, 399–411. https://doi.org/10.1016/j.geomorph.2013.08.021

Constantine, M., & Ogbu, K. N. (2015). Assessment of Soil Erosion using RUSLE2 Model and GIS in Upper Ebonyi River Watershed, Enugu State, Nigeria. *International Journal of Remote Sensing & Geoscience*, *4*(4), 7–17.

Cullum, C., Rogers, K. H., Brierley, G., & Witkowski, E. T. F. (2016). Ecological classification and mapping for landscape management and science: Foundations for the description of patterns and processes. *Progress in Physical Geography*, *40*(1), 38–65. https://doi.org/10.1177/0309133315611573

D'Amour, C. B., Reitsma, F., Baiocchi, G., Barthel, S., Güneralp, B., Erb, K. H., Haberl, H., Creutzig, F., & Seto, K. C. (2017). Future urban land expansion and implications for global croplands. *Proceedings of the National Academy of Sciences of the United States of America*, *114*(34), 8939–8944. https://doi.org/10.1073/pnas.1606036114

d'Andrimont, R., Yordanov, M., Martinez-Sanchez, L., Eiselt, B., Palmieri, A., Dominici, P., Gallego, J., Reuter, H. I., Joebges, C., Lemoine, G., & van der Velde, M. (2020). Harmonised LUCAS in-situ land cover and use database for field surveys from 2006 to 2018 in the European Union. *Scientific Data*, *7*(1), 1–15. https://doi.org/10.1038/s41597-020-00675-z

Dalzell, B. J., Fissore, C., & Nater, E. A. (2022). Topography and land use impact erosion and soil organic carbon burial over decadal timescales. *Catena*, *218*(August), 106578. https://doi.org/10.1016/j.catena.2022.106578

Dambeebo, D., & Jalloh, C. A. (2018). Sustainable Urban Development and Land Use Management: Wa Municipality in Perspective, Ghana. *Journal of Sustainable Development*, *11*(5), 235. https://doi.org/10.5539/jsd.v11n5p235

Dangol, S., Zhang, X., Liang, X. Z., Anderson, M., Crow, W., Lee, S., Moglen, G. E., & McCarty, G. W. (2023). Multivariate Calibration of the SWAT Model Using Remotely Sensed Datasets. *Remote Sensing*, *15*(9), 1–22. https://doi.org/10.3390/rs15092417

Dapaah-Siakwan, S., & Gyau-Boakye, P. (2000). Hydrogeologic framework and borehole yields in Ghana. *Hydrogeology Journal*, *8*(4), 405–416. https://doi.org/10.1007/PL00010976

Das Chatterjee, N., Chatterjee, S., & Khan, A. (2016). Spatial modeling of urban sprawl around Greater Bhubaneswar city, India. *Modeling Earth Systems and Environment*, *2*(1), 1–21. https://doi.org/10.1007/s40808-015-0065-7

de Andrade Bonetti, J., Anghinoni, I., de Moraes, M. T., & Fink, J. R. (2017). Resilience of soils with different texture, mineralogy and organic matter under long-term conservation systems. *Soil and Tillage Research*, *174*(October 2016), 104–112. https://doi.org/10.1016/j.still.2017.06.008

De Jong, S. M., Paracchini, M. L., Bertolo, F., Folving, S., Megier, J., & De Roo, A. P. J. (1999). Regional assessment of soil erosion using the distributed model SEMMED and remotely sensed data. *Catena*, *37*(3–4), 291–308. https://doi.org/10.1016/S0341-8162(99)00038-7

De Roo, A. P. J., Offermans, R. J. E., & Cremers, N. H. D. T. (1996). Lisem: A single-event, physically based hydrological and soil erosion model for drainage basins. II: Sensitivity analysis, validation and application. *Hydrological Processes*, *10*(8), 1119–1126. https://doi.org/10.1002/(sici)1099-1085(199608)10:8<1119::aid-hyp416>3.0.co;2-v

de Silva, S. S., Abeysingha, N. S., Nirmanee, K. G. S., Sandamali Pathirage, P. D. S., & Mallawatantri, A. (2023). Effect of land use–land cover and projected rainfall on soil erosion intensities of a tropical catchment in Sri Lanka. *International Journal of Environmental Science and Technology*, *20*(8), 9173–9188. https://doi.org/10.1007/s13762-022-04606-w

Defersha, M. B., Quraishi, S., & Melesse, A. (2010). Interrill erosion, runoff and sediment size distribution as affected by slope steepness and antecedent moisture content. *Hydrology and Earth System Sciences Discussions*, *7*(4), 6447–6489. https://doi.org/10.5194/hessd-7-6447-2010

DeFries, R., & Rosenzweig, C. (2010). Toward a whole-landscape approach for sustainable land use in the tropics. *Proceedings of the National Academy of Sciences of the United States of America*, *107*(46), 19627–19632. https://doi.org/10.1073/pnas.1011163107

Demetrius, L., Gundlach, V. M., & Ochs, G. (2004). Complexity and demographic stability in population models. *Theoretical Population Biology*, *65*(3), 211–225. https://doi.org/10.1016/j.tpb.2003.12.002

Deng, C., Zhang, G., Liu, Y., Nie, X., Li, Z., Liu, J., & Zhu, D. (2021). Advantages and disadvantages of terracing: A comprehensive review. *International Soil and Water Conservation Research*, *9*(3), 344–359. https://doi.org/10.1016/j.iswcr.2021.03.002

Depountis, N., Michalopoulou, M., Kavoura, K., Nikolakopoulos, K., & Sabatakakis, N. (2020). Estimating soil erosion rate changes in areas affected by wildfires. *ISPRS International Journal of Geo-Information*, *9*(10). https://doi.org/10.3390/ijgi9100562

Dewandel, B., Lachassagne, P., Wyns, R., Maréchal, J. C., & Krishnamurthy, N. S. (2006). A generalized 3-D geological and hydrogeological conceptual model of granite aquifers controlled by single or multiphase weathering. *Journal of Hydrology*, *330*(1–2), 260–284. https://doi.org/10.1016/j.jhydrol.2006.03.026

Dialynas, Y. G., Bastola, S., Bras, L. R., Billings, S. A., Markewitz, D., & Richter, D. (2016). Global Biogeochemical Cycles of soil erosion on the carbon cycle. *Global Biogeochemical Cycles*, 644–660. https://doi.org/10.1002/2015GB005302

Diko, S. K., Okyere, S. A., Opoku Mensah, S., Ahmed, A., Yamoah, O., & Kita, M. (2021). Are local development plans mainstreaming climate-smart agriculture? A mixed-content analysis of medium-term development plans in semi-arid Ghana. *Socio-Ecological Practice Research*, *3*(2), 185–206. https://doi.org/10.1007/s42532-021-00079-2

Diwediga, B., Le, Q. B., Agodzo, S. K., Tamene, L. D., & Wala, K. (2018). Modelling soil erosion response to sustainable landscape management scenarios in the Mo River Basin (Togo, West Africa). *Science of the Total Environment*, *625*, 1309–1320. https://doi.org/10.1016/j.scitotenv.2017.12.228

Döll, P., Fiedler, K., & Zhang, J. (2009). Global-scale analysis of river flow alterations due to water withdrawals and reservoirs. *Hydrology and Earth System Sciences*, *13*(12), 2413–2432. https://doi.org/10.5194/hess-13-2413-2009

Dominati, E., Patterson, M., & Mackay, A. (2010). A framework for classifying and quantifying the natural capital and ecosystem services of soils. *Ecological Economics*, *69*(9), 1858–1868. https://doi.org/10.1016/j.ecolecon.2010.05.002

Dornik, A., Cheţan, M. A., Drăguţ, L., Iliuţă, A., & Dicu, D. D. (2022). Importance of the mapping unit on the land suitability assessment for agriculture. *Computers and Electronics in Agriculture*, *201*(April). https://doi.org/10.1016/j.compag.2022.107305

Dregne, H. E. (2002). Land degradation in the drylands, Arid Land Research and Management. In *Arid Land Research and Management* (Vol. 16, Issue 2). https://doi.org/10.1080/153249802317304422

Dubovyk, O., Sliuzas, R., & Flacke, J. (2011). Spatio-temporal modelling of informal settlement development in Sancaktepe district, Istanbul, Turkey. *ISPRS Journal of Photogrammetry and Remote Sensing*, *66*(2), 235–246. https://doi.org/10.1016/j.isprsjprs.2010.10.002

Dudley, N., Eufemia, L., Fleckenstein, M., Periago, M. E., Petersen, I., & Timmers, J. F. (2020). Grasslands and savannahs in the UN Decade on Ecosystem Restoration. *Restoration Ecology*, *28*(6), 1313–1317. https://doi.org/10.1111/rec.13272

Duiker, S. W., Flanagan, D. C., & Lal, R. (2001). Erodibility and infiltration characteristics of five major soils of southwest Spain. *Catena*, *45*(2), 103–121. https://doi.org/10.1016/S0341-8162(01)00145-X

Dutta, S. (2016). Soil erosion, sediment yield and sedimentation of reservoir: a review. *Modeling Earth Systems and Environment*, *2*(3), 1–18. https://doi.org/10.1007/s40808-016-0182-y

Eekhout, J. P. C., & de Vente, J. (2022). Global impact of climate change on soil erosion and potential for adaptation through soil conservation. *Earth-Science Reviews*, *226*, 103921. https://doi.org/10.1016/j.earscirev.2022.103921

Ehrlich, A. H. (1985). The human population: Size and dynamics. *Integrative and Comparative Biology*, *25*(2), 395–406. https://doi.org/10.1093/icb/25.2.395

Ehrlich, P. R., & Ehrlich, A. H. (1991). The Population Explosion. *Ecology Law Quarterly*, *18*(1), 259–263.

Elmqvist, T., Fragkias, M., Goodness, J., Güneralp, B., J., M. P., McDonald, R. I., & Wilkinson, …. (2013). Regional assessment of Africa. In *Urbanization, Biodiversity and Ecosystem Services: Challenges and Opportunities: A Global Assessment* (Elmqvist,). Springer Dordrecht Heidelberg New York London. https://doi.org/10.1007/978-94-007-7088-1_23

Endalamaw, N. T., Moges, M. A., Kebede, Y. S., Alehegn, B. M., & Sinshaw, B. G. (2021). Potential soil loss estimation for conservation planning, upper Blue Nile Basin, Ethiopia. *Environmental Challenges*, *5*(August), 100224. https://doi.org/10.1016/j.envc.2021.100224

Esa, E., Assen, M., & Legass, A. (2018). Implications of land use/cover dynamics on soil erosion potential of agricultural watershed, northwestern highlands of Ethiopia. *Environmental Systems Research*, *7*(1). https://doi.org/10.1186/s40068-018-0122-0

Estoque, R. C., & Murayama, Y. (2015). Intensity and spatial pattern of urban land changes in the megacities of Southeast Asia. *Land Use Policy*, *48*, 213–222. https://doi.org/10.1016/j.landusepol.2015.05.017

Fang, H., Sun, L., & Tang, Z. (2015). Effects of rainfall and slope on runoff, soil erosion and rill development: An experimental study using two loess soils. *Hydrological Processes*, *29*(11), 2649–2658. https://doi.org/10.1002/hyp.10392

Fang, S., Gertner, G. Z., Sun, Z., & Anderson, A. A. (2005). The impact of interactions in spatial simulation of the dynamics of urban sprawl. *Landscape and Urban Planning*, *73*(4), 294–306. https://doi.org/10.1016/j.landurbplan.2004.08.006

Farhan, Y., & Nawaiseh, S. (2015). Spatial assessment of soil erosion risk using RUSLE and GIS techniques. *Environmental Earth Sciences*, *74*(6), 4649–4669. https://doi.org/10.1007/s12665-015-4430-7

Fell, R., Hanson, G., Herrier, G., Marot, D., Wahl, T., Fell, R., Hanson, G., Herrier, G., Marot, D., & Wahl, T. (2017). *Relationship between the erosion properties of soils and other parameters To cite this version : HAL Id : hal-01007538 Relationship between the Erosion Properties of Soils and Other Parameters*.

Fenta, A. A., Tsunekawa, A., Haregeweyn, N., Poesen, J., Tsubo, M., Borrelli, P., Panagos, P., Vanmaercke, M., Broeckx, J., Yasuda, H., Kawai, T., & Kurosaki, Y. (2020). Land susceptibility to water and wind erosion risks in the East Africa region. *Science of the Total Environment*, *703*. https://doi.org/10.1016/j.scitotenv.2019.135016

Ferreira, C. S. S., Seifollahi-Aghmiuni, S., Destouni, G., Ghajarnia, N., & Kalantari, Z. (2022). Soil degradation in the European Mediterranean region: Processes, status and consequences. *Science of the Total Environment*, *805*, 150106. https://doi.org/10.1016/j.scitotenv.2021.150106

Ferreira, L. M. R., Esteves, L. S., de Souza, E. P., & dos Santos, C. A. C. (2019). Impact of the Urbanisation Process in the Availability of Ecosystem Services in a Tropical Ecotone Area. *Ecosystems*, *22*(2), 266–282. https://doi.org/10.1007/s10021-018-0270-0

Ferro, V., & Porto, P. (2000). Sediment Delivery Distributed (SEDD) Model. *J. Hydrol. Eng*, *5*(4), 411–422.

Fielmua, N., Bandie, R. D. B., & Ziemah, M. K. (2014). Managing pastoralism and water rights in the upper west region of ghana: A blame game among actors. *Journal of Sustainable Development*, *7*(1), 72–84. https://doi.org/10.5539/jsd.v7n1p72

Fischer, G., Nachtergaele, F. O., Prieler, S., Teixeira, E., Tóth, G., Velthuizen, H. van, Verelst, L., & Wiberg, D. (2008). Global Agro-ecological Zones (GAEZ v3.0). *IIASA and FAO*, 196.

Flato, G. J., Marotzke, B., Abiodun, P., BraconnotS.C., Chou, W., Collins, P., Cox, F., Driouech, S., Emori, V., Eyring, C., Forest, P., Gleckler, E., Guilyardi, C., Jakob, V., Kattsov, C., M., R. and, & Rummukainen. (2013). Evaluation of climate models. In T. F. Stocker, D. Qin, G.-K. Plattner, M. Tignor, S. K. Allen, J. Boschung, A. Nauels, Y. Xia, V. Bex, & P. M. Midgley (Eds.), *Climate Change 2023:The Physical Science Basis. Contribution of Working Group I to the Fifth Assessment Report of the Intergovernmental Panel on Climate Change*. Cambridge University Press.

Fletcher, R. (2019). Trajectories to Low-Density Settlements Past and Present: Paradox and Outcomes. *Frontiers in Digital Humanities*, *6*(August), 1–21. https://doi.org/10.3389/fdigh.2019.00014

Flores, B. M., Staal, A., Jakovac, C. C., Hirota, M., Holmgren, M., & Oliveira, R. S. (2019). Soil erosion as a resilience drain in disturbed tropical forests. *Plant and Soil*, 11–25. https://doi.org/10.1007/s11104-019-04097-8

Flörke, M., Schneider, C., & McDonald, R. I. (2018). Water competition between cities and agriculture driven by climate change and urban growth. *Nature Sustainability*, *1*(1), 51–58. https://doi.org/10.1038/s41893-017-0006-8

Foley, J. A., DeFries, R., Asner, G. P., Barford, C., Bonan, G., Carpenter, S. R., Chapin, F. S., Coe, M. T., Daily, G. C., Gibbs, H. K., Helkowski, J. H., Holloway, T., Howard, E. A., Kucharik, C. J., Monfreda, C., Patz, J. A., Prentice, I. C., Ramankutty, N., & Snyder, P. K. (2005). Global consequences of land use. *Science*, *309*(5734), 570–574. https://doi.org/10.1126/science.1111772

Food and Agriculture Organization of the United Nations (FAO). (2008). *No Title*. Harmonized World Soil Database (Version 2.1). hhttps://www.fao.org/soils-portal/data-hub/soil-maps-and-databases/harmonized-world-soil-database-v20/en/

Foster, G. R., Yoder, D. C., Weesies, G. A., & Toy, T. J. (2013). The Design Philosophy Behind RUSLE2: Evolution of an Empirical Model. *Soil Erosion Research for the 21st Century*, *January*, 95–98. https://doi.org/10.13031/2013.3211

Foucher, A., Salvador-Blanes, S., Evrard, O., Simonneau, A., Chapron, E., Courp, T., Cerdan, O., Lefèvre, I., Adriaensen, H., Lecompte, F., & Desmet, M. (2014). Increase in soil erosion after agricultural intensification: Evidence from a lowland basin in France. *Anthropocene*, *7*(2014), 30–41. https://doi.org/10.1016/j.ancene.2015.02.001

Fox, D. M., & Bryan, R. B. (2000). The relationship of soil loss by interrill erosion to slope gradient. *Catena*, *38*(3), 211–222. https://doi.org/10.1016/S0341-8162(99)00072-7

Fox, O., Vetter, S., Ekschmitt, K., & Wolters, V. (2006). Soil fauna modifies the recalcitrance-persistence relationship of soil carbon pools. *Soil Biology and Biochemistry*, *38*(6), 1353–1363. https://doi.org/10.1016/j.soilbio.2005.10.014

Fox, P. M., Nico, P. S., Tfaily, M. M., Heckman, K., & Davis, J. A. (2017). Characterization of natural organic matter in low-carbon sediments: Extraction and analytical approaches. *Organic Geochemistry*, *114*, 12–22. https://doi.org/10.1016/j.orggeochem.2017.08.009

Frejka, T. (2016). The demographic transition revisited: a cohort perspective. In *MPIDR Working Papers* (Vol. 49, Issue 0).

G¨uneralp, B., Seto, K. C., Lwasar, S., Masundire, H., & Parnell, S. (2017). Urbanization in Africa : challenges and opportunities for conservation OPEN ACCESS Urbanization in Africa : challenges and opportunities for conservation. *Environmental Research Letters*, *13*, 1–9.

Ganasri, B. P., & Ramesh, H. (2016). Assessment of soil erosion by RUSLE model using remote sensing and GIS - A case study of Nethravathi Basin. *Geoscience Frontiers*, *7*(6), 953–961. https://doi.org/10.1016/j.gsf.2015.10.007

Gayen, A., Pourghasemi, H. R., Saha, S., Keesstra, S., & Bai, S. (2019). Gully erosion susceptibility assessment and management of hazard-prone areas in India using different machine learning algorithms. *Science of the Total Environment*, *668*, 124–138. https://doi.org/10.1016/j.scitotenv.2019.02.436

Gebrechorkos, S. H., Pan, M., Lin, P., Anghileri, D., Forsythe, N., Pritchard, D. M. W., Fowler, H. J., Obuobie, E., Darko, D., & Sheffield, J. (2022). Variability and changes in hydrological drought in the Volta Basin, West Africa. *Journal of Hydrology: Regional Studies*, *42*(June). https://doi.org/10.1016/j.ejrh.2022.101143

Gelagay, H. S., & Minale, A. S. (2016). Soil loss estimation using GIS and Remote sensing techniques: A case of Koga Watershed, Northwestern Ethiopia. *International Soil and Water Conservation Research*, *4*(2), 126–136. https://doi.org/10.1016/j.iswcr.2016.01.002

Georg, G., Dudhia, J., & Stauffer, D. R. (1994). A description of the Fifth-generation Penn State/NCAR Mesoscale Model (MM5). *NCAR Technical Note NCAR/TN-398+STR*, *December*, 121. https://doi.org/10.5065/D60Z716B

Gerke, J. (2022). The Central Role of Soil Organic Matter in Soil Fertility and Carbon Storage. *Soil Systems*, *6*(2). https://doi.org/10.3390/soilsystems6020033

Ghana Statistical Service (GSS). (2005). Population Data Analysis Reports. *Policy Implications of Population Trends Data*, *2*(August), 1–495.

Ghana Statistical Service (GSS). (2012). 2010 Population and Housing Census, summary of Report final results. In *Ghana Statistical Service*.

Ghana Statistical Service (GSS). (2014). Wa municipality. In *2010 Population and Housing Cenus. District Analytical Report : Wa Municipality*.

Ghana Statistical Service (GSS). (2021). *Ghana 2021 Population abnd Housing Cencus:population of Regions and Disticts*. *3A*, 1–6.

Gharari, S., Hrachowitz, M., Fenicia, F., & Savenije, H. H. G. (2011). Hydrological landscape classification: Investigating the performance of HAND based landscape classifications in a central European meso-scale catchment. *Hydrology and Earth System Sciences*, *15*(11), 3275–3291. https://doi.org/10.5194/hess-15-3275-2011

Giertz, S., Junge, B., & Diekkrüger, B. (2005). Assessing the effects of land use change on soil physical properties and hydrological processes in the sub-humid tropical environment of West Africa. *Physics and Chemistry of the Earth*, *30*(8–10), 485–496. https://doi.org/10.1016/j.pce.2005.07.003

Girma, R., & Gebre, E. (2020). Spatial modeling of erosion hotspots using GIS-RUSLE interface in Omo-Gibe river basin, Southern Ethiopia: implication for soil and water conservation planning. *Environmental Systems Research*, *9*(1). https://doi.org/10.1186/s40068-020-00180-7

Girmay, G., Moges, A., & Muluneh, A. (2021). Assessment of Current and Future Climate Change Impact on Soil Loss Rate of Agewmariam Watershed, Northern Ethiopia. *Air, Soil and Water Research*, *14*. https://doi.org/10.1177/1178622121995847

Global Environment Facility-United Nations Environment Programme (GEF-UNEP). (2002). Volta River Basin Preliminary Transboundary Diagnostic Analysis Final Report. In *Water* (Issue December).

Global Environment Facility-United Nations Environment Programme (GEF-UNEP). (2013a). Volta Basin Transboundary Diagnostic Analysis. In *IWLearn*. www.gefvolta.iwlearn.org

Global Environment Facility-United Nations Environment Programme (GEF-UNEP). (2013b). *Volta Basin Transboundary Diagnostic Analysis - Addressing Transboundary Concerns in the Volta River Basin and its Downstream Coastal Area. UNEP/GEF/Volta/RR 4/2013* (Issue March).

Gocking, R. (2021). Ghana's Bui Dam and the Contestation over Hydro Power in Africa. *African Studies Review*, *64*(2), 339–362. https://doi.org/10.1017/asr.2020.41

Goldewijk, K. K. (2001). Estimating global land use change over the past 300 years: The HYDE database. *Global Biogeochemical Cycles*, *15*(2), 417–433. https://doi.org/10.1029/1999GB001232

Gomiero, T. (2016). Soil degradation, land scarcity and food security: Reviewing a complex challenge. *Sustainability (Switzerland)*, *8*(3), 1–41. https://doi.org/10.3390/su8030281

Gong, W., Wang, H., Wang, X., Fan, W., & Stott, P. (2017). Effect of terrain on landscape patterns and ecological effects by a gradient-based RS and GIS analysis. *Journal of Forestry Research*, *28*(5), 1061–1072. https://doi.org/10.1007/s11676-017-0385-8

Gordon, C., Nukpezah, D., Tweneboah-Lawson, E., Ofori, B. D., Yirenya-Tawiah, D., Pabi, O., Ayivor, J. S., Koranteng, S., Darko, D., & Mensah, A. M. (2013). West Africa - Water Resources Vulnerability Using a Multidimensional Approach: Case Study of Volta Basin. *Climate Vulnerability: Understanding and Addressing Threats to Essential Resources*, *5*(July 2020), 283–309. https://doi.org/10.1016/B978-0-12-384703-4.00518-9

Govers, G., Gobin, A., Cerdan, O., van Rompaey, A., Kirkby, M., Irvine, B., Le Bissonais, Y., Daroussin, J., King, D., & Jones, R. J. A. (2003). Pan-European soil erosion risk assessment for Europe: the PESERA Map. *JRC, Ispra, Italy.Available Online at Http://Eusoils.Jrc.It/ESDB_Archive/Pesera/Pesera_cd/Pdf/ThePeseraMap.Pdf [Verified 25 October 2006]*, *Version 1*(Explanation of Special Publication Ispra 2004 No.73 (S.P.I.04.73). No.16, EUR 21176), 1–9.

Grams, C. (2008). *The Atlantic Inflow: atmosphere-land-ocean interaction at the south-western edge of the Saharan heat low*. Institut f¨ur Meteorologie und Klimaforschung Universit¨at Karlsruhe / Forschungszentrum Karlsruhe.

Gray, E., Henninger, N., Reij, C., Winterbottom, R., & Agostini, P. (2016). Integrated Landscape Approaches for Africa's Drylands. In *Integrated Landscape Approaches for Africa's Drylands*. https://doi.org/10.1596/978-1-4648-0826-5

Gu, Z., Xie, Y., Gao, Y., Ren, X., Cheng, C., & Wang, S. (2018). Quantitative assessment of soil productivity and predicted impacts of water erosion in the black soil region of northeastern China. *Science of the Total Environment*, *637–638*, 706–716. https://doi.org/10.1016/j.scitotenv.2018.05.061

Guerra, C. A., Rosa, I. M. D., Valentini, E., Wolf, F., Filipponi, F., Karger, D. N., Nguyen Xuan, A., Mathieu, J., Lavelle, P., & Eisenhauer, N. (2020). Global vulnerability of soil ecosystems to erosion. *Landscape Ecology*, *35*(4), 823–842. https://doi.org/10.1007/s10980-020-00984-z

Hails, R. S., & Ormerod, S. J. (2013). Ecological science for ecosystem services and the stewardship of Natural Capital. *Journal of Applied Ecology*, *50*(4), 807–810. https://doi.org/10.1111/1365-2664.12127

Hajigholizadeh, M., Melesse, A. M., & Fuentes, H. R. (2018). Erosion and sediment transport modelling in shallowwaters: A review on approaches, models and applications. *International Journal of Environmental Research and Public Health*, *15*(3). https://doi.org/10.3390/ijerph15030518

Ham, J. R. (2017). Cooking to be Modern but Eating to be Healthy: The Role of Dawa-Dawa in Contemporary Ghanaian Foodways. *Food, Culture and Society*, *20*(2), 237–256. https://doi.org/10.1080/15528014.2017.1305827

Hansen, M. C., Potapov, P. V., Moore, R., Moore, R., Turubanova, S. A., Tyukavina, A., Thau, D., Stehman, S. V., Goetz, S. J., Loveland, T. R., Kommareddy, Egorov, A. A., Chini, L., Justice, C. O., Townshend, & Quantification, J. R. G. (2013). *High-Resolution Global Maps of 21st-Century Forest Cover Change* (Vol. 342, Issue November). https://doi.org/10.1126/science.1244693

Hecht, H., & Oguchi, T. (2017). Global evaluation of erosion rates in relation to tectonics. *Progress in Earth and Planetary Science*, *4*(1). https://doi.org/10.1186/s40645-017-0156-3

Hegazy, I. R., & Kaloop, M. R. (2015). Monitoring urban growth and land use change detection with GIS and remote sensing techniques in Daqahlia governorate Egypt. *International Journal of Sustainable Built Environment*, *4*(1), 117–124. https://doi.org/10.1016/j.ijsbe.2015.02.005

Heinken, T., & Weber, E. (2013). Consequences of habitat fragmentation for plant species: Do we know enough? *Perspectives in Plant Ecology, Evolution and Systematics*, *15*(4), 205–216. https://doi.org/10.1016/j.ppees.2013.05.003

Held, I. M., Delworth, T. L., Lu, J., Findell, K. L., & Knutson, T. R. (2005). Simulation of Sahel drought in the 20th and 21st centuries. *Proceedings of the National Academy of Sciences of the United States of America*, *102*(50), 17891–17896. https://doi.org/10.1073/pnas.0509057102

Hengl, T., De Jesus, J. M., Heuvelink, G. B. M., Gonzalez, M. R., Kilibarda, M., Blagotić, A., Shangguan, W., Wright, M. N., Geng, X., Bauer-Marschallinger, B., Guevara, M. A., Vargas, R., MacMillan, R. A., Batjes, N. H., Leenaars, J. G. B., Ribeiro, E., Wheeler, I., Mantel, S., & Kempen, B. (2017). SoilGrids250m: Global gridded soil information based on machine learning. In *PLoS ONE* (Vol. 12, Issue 2). https://doi.org/10.1371/journal.pone.0169748

Hentschel, T., Hruschka, F., & Priester, M. (2003). *Artisanal and small-scale mining: challenges and opportunities*. Russell Press Ltd.

Herrmann, S. M., Brandt, M., Rasmussen, K., & Fensholt, R. (2020). Accelerating land cover change in West Africa over four decades as population pressure increased. *Communications Earth & Environment*, *1*(1), 1–10. https://doi.org/10.1038/s43247-020-00053-y

Holechek, J. L., Cibils, A. F., Bengaly, K., & Kinyamario, J. I. (2017). Human Population Growth, African Pastoralism, and Rangelands: A Perspective. *Rangeland Ecology and Management*, *70*(3), 273–280. https://doi.org/10.1016/j.rama.2016.09.004

Hong, F., He, G., Wang, G., Zhang, Z., & Peng, Y. (2023). Monitoring of Land Cover and Vegetation Changes in Juhugeng Coal Mining Area Based on Multi-Source Remote Sensing Data. *Remote Sensing*, *15*(13). https://doi.org/10.3390/rs15133439

Hrachowitz, M., Stockinger, M., Coenders-Gerrits, M., Van Der Ent, R., Bogena, H., Lücke, A., & Stumpp, C. (2021). Reduction of vegetation-accessible water storage capacity after deforestation affects catchment travel time distributions and increases young water fractions in a headwater catchment. *Hydrology and Earth System Sciences*, *25*(9), 4887–4915. https://doi.org/10.5194/hess-25-4887-2021

Huang, Y., Wu, L., Li, P., Li, N., & He, Y. (2022). What's the cost-effective pattern for rural wastewater treatment? *Journal of Environmental Management*, *303*(December 2021). https://doi.org/10.1016/j.jenvman.2021.114226

Huete, A. R. (1988). *A Soil-Adjusted Vegetation Index (SAVI)*. *25*(3), 295–309. https://doi.org/doi.org/10.1016/0034-4257(88)90106-X

Hunter, L. M. (2000). The Implications of Population Dynamics on the Environmental Issues. In *COVID-19 and Climate Change in BRICS Nations*. RAND. https://doi.org/10.4324/9781032643182-14

Ibrahim, B., Karambiri, H., Polcher, J., Yacouba, H., & Ribstein, P. (2014). Changes in rainfall regime over Burkina Faso under the climate change conditions simulated by 5 regional climate models. *Climate Dynamics*, *42*(5–6), 1363–1381. https://doi.org/10.1007/s00382-013-1837-2

Igwe, P. U., Onuigbo, A. A., Chinedu, O. C., Ezeaku, I. I., & Muoneke, M. M. (2017). Soil Erosion: A Review of Models and Applications. *International Journal of Advanced Engineering Research and Science*, *4*(12), 138–150. https://doi.org/10.22161/ijaers.4.12.22

Iles, C. E., Vautard, R., Strachan, J., Joussaume, S., Eggen, B. R., & Hewitt, C. D. (2020). The benefits of increasing resolution in global and regional climate simulations for European climate extremes. *Geoscientific Model Development*, *13*(11), 5583–5607. https://doi.org/10.5194/gmd-13-5583-2020

Intergovernmental Panel on Climate Change (IPCC). (2021). Technical Summary. Contribution of Working Group I to the Sixth Assessment Report of the Intergovernmental Panel on Climate Change. In *Climate Change 2021: The Physical Science Basis.*

International Monetary Fund (IMF). (2023). *Time for Transformation: The Middle East and North Africa* (G. Bhatt, M. Burke, A. R. Bala, M. Henriquez, J. Kearns, N. Owen, P. Walker, S. Aggarwal, & A. Stanley (eds.); Issue 3). MF Publication Services. https://doi.org/DOI:10.5089/9798400225406.071

Ito, A., & Hajima, T. (2020). Biogeophysical and biogeochemical impacts of land-use change simulated by MIROC-ES2L. *Progress in Earth and Planetary Science*, *7*(1). https://doi.org/10.1186/s40645-020-00372-w

Jafarbiglu, H., & Pourreza, A. (2022). A comprehensive review of remote sensing platforms, sensors, and applications in nut crops. *Computers and Electronics in Agriculture*, *197*(July 2021). https://doi.org/10.1016/j.compag.2022.106844

Jiang, L., & O'Neill, B. C. (2017). Global urbanization projections for the Shared Socioeconomic Pathways. *Global Environmental Change*, *42*, 193–199. https://doi.org/10.1016/j.gloenvcha.2015.03.008

Jin, L., Whitehead, P. G., Appeaning Addo, K., Amisigo, B., Macadam, I., Janes, T., Crossman, J., Nicholls, R. J., McCartney, M., & Rodda, H. J. E. (2018). Modeling future flows of the Volta River system: Impacts of climate change and socio-economic changes. *Science of the Total Environment*, *637–638*, 1069–1080. https://doi.org/10.1016/j.scitotenv.2018.04.350

Jourgholami, M., Karami, S., Tavankar, F., Lo Monaco, A., & Picchio, R. (2021). Effects of slope gradient on runoff and sediment yield on machine-induced compacted soil in temperate forests. *Forests*, *12*(1), 1–19. https://doi.org/10.3390/f12010049

Jung, G., & Kunstmann, H. (2007). High-resolution regional climate modeling for the Volta region of West Africa. *Journal of Geophysical Research Atmospheres*, *112*(23), 1–17. https://doi.org/10.1029/2006JD007951

Kanga, S. (2023). Advancements in remote sensing tools for forestry analysis. *Sustainable Forestry*, *6*(1), 1–24. https://doi.org/10.24294/sf.v6i1.2269

Karamage, F., Zhang, C., Fang, X., Liu, T., Ndayisaba, F., Nahayo, L., Kayiranga, A., & Nsengiyumva, J. B. (2017). Modeling rainfall-runoffresponse to land use and land cover change in Rwanda (1990-2016). *Water (Switzerland)*, *9*(2). https://doi.org/10.3390/w9020147

Karthick, P., Lakshumanan, C., & Ramki, P. (2017). *Estimation of soil erosion vulnerability in Perambalur Taluk , Tamilnadu using revised universal soil loss equation model (RUSLE) and geo information technology*. *5*(8), 8–14.

Kasei, R. A. (2010). *Ecology and Development Series No . 15 , 2004*. *15*, 1960–2010.

Kebede, B., Tsunekawa, A., Haregeweyn, N., Adgo, E., Ebabu, K., Meshesha, D. T., Tsubo, M., Masunaga, T., & Fenta, A. A. (2021). Determining C- and P-factors of RUSLE for different land uses and management practices across agro-ecologies: case studies from the Upper Blue Nile basin, Ethiopia. *Physical Geography*, *42*(2), 160–182. https://doi.org/10.1080/02723646.2020.1762831

Keesstra, S., Pereira, P., Novara, A., Brevik, E. C., Azorin-Molina, C., Parras-Alcántara, L., Jordán, A., & Cerdà, A. (2016). Effects of soil management techniques on soil water erosion in apricot orchards. *Science of the Total Environment*, *551–552*, 357–366. https://doi.org/10.1016/j.scitotenv.2016.01.182

Kent, R. (2018). "Helping" or "Appropriating"? Gender Relations in Shea Nut Production in Northern Ghana. *Society and Natural Resources*, *31*(3), 367–381. https://doi.org/10.1080/08941920.2017.1382626

Key, R. M. (1992). An introduction to the crystalline basement of Africa. *Geological Society Special Publication*, *66*(66), 29–57. https://doi.org/10.1144/GSL.SP.1992.066.01.02

Khanifar, J., & Khademalrasoul, A. (2021). Effects of neighborhood analysis window forms and derivative algorithms on the soil aggregate stability – Landscape modeling. *Catena*, *198*(December 2020). https://doi.org/10.1016/j.catena.2020.105071

Khattak, W. A., Sun, J., Zaman, F., Jalal, A., Shafiq, M., Manan, S., Hameed, R., Khan, I., Khan, I. U., Khan, K. A., & Du, D. (2025). The role of agricultural land management in modulating water-carbon interplay within dryland ecological systems. *Agriculture, Ecosystems and Environment*, *378*(September 2024). https://doi.org/10.1016/j.agee.2024.109315

Kindu, M., Angelova, D., Schneider, T., Döllerer, M., Teketay, D., & Knoke, T. (2020). Monitoring of urban growth patterns in rapidly growing Bahir Dar city of northwest Ethiopia with 30 year landsat imagery record. *ISPRS International Journal of Geo-Information*, *9*(9), 1–19. https://doi.org/10.3390/ijgi9090548

Klik, A., & Eitzinger, J. (2010). Impact of climate change on soil erosion and the efficiency of soil conservation practices in Austria. *Journal of Agricultural Science*, *148*(5), 529–541. https://doi.org/10.1017/S0021859610000158

Kombat, R., Sarfatti, P., & Fatunbi, O. A. (2021). A review of climate-smart agriculture technology adoption by farming households in sub-saharan africa. *Sustainability (Switzerland)*, *13*(21), 1–16. https://doi.org/10.3390/su132112130

Kombe, W. J. (2005). Land use dynamics in peri-urban areas and their implications on the urban growth and form: The case of Dar es Salaam, Tanzania. *Habitat International*, *29*(1), 113–135. https://doi.org/10.1016/S0197-3975(03)00076-6

Korah, P. I., Nunbogu, A. M., & Akanbang, B. A. A. (2018). Spatio-temporal dynamics and livelihoods transformation in Wa, Ghana. *Land Use Policy*, *77*(May), 174–185. https://doi.org/10.1016/j.landusepol.2018.05.039

Kpemoua, T. P. I., Barré, P., Chevallier, T., Houot, S., & Chenu, C. (2022). Drivers of the amount of organic carbon protected inside soil aggregates estimated by crushing: A meta-analysis. *Geoderma*, *427*(August). https://doi.org/10.1016/j.geoderma.2022.116089

Kpienbaareh, D. (2016). Assessing the relationship between climate and patterns of wildfires in Ghana. *Int. J. Humanit. Soc. Sci*, *8*(3), 1–20.

Kpienbaareh, D., & Oduro Appiah, J. (2019). A geospatial approach to assessing land change in the built-up landscape of Wa Municipality of Ghana. *Geografisk Tidsskrift - Danish Journal of Geography* , *119*(2), 121–135. https://doi.org/10.1080/00167223.2019.1587307

Kusakari, Y., Asubonteng, K. O., Jasaw, G. S., Dayour, F., Dzivenu, T., Lolig, V., Donkoh, S. A., Obeng, F. K., Gandaa, B., & Kranjac-Berisavljevic, G. (2014). Farmer-perceived effects of climate change on livelihoods in WA west district, upper west region of Ghana. *Journal of Disaster Research*, *9*(4), 516–528. https://doi.org/10.20965/jdr.2014.p0516

Kusimi, J. M., Yiran, G. A. B., & Attua, E. M. (2015). Soil Erosion and Sediment Yield Modelling in the Pra River Basin of Ghana using the Revised Universal Soil Loss Equation (RUSLE). *Ghana Journal of Geography*, *7*(2), 38–57.

Kuule, D. A., Ssentongo, B., Magaya, P. J., Mwesigwa, G. Y., Okurut, I. T., Nyombi, K., Egeru, A., & Tabuti, J. R. S. (2022). Land Use and Land Cover Change Dynamics and Perceived Drivers in Rangeland Areas in Central Uganda. *Land*, *11*(9). https://doi.org/10.3390/land11091402

Kuunibe, N., Issahaku, H., & Department, P. K. N. (2013). Wood Based Biomass Fuel Consumption in the Upper West Region of Ghana: Implications for Environmental Sustainability. *Journal of Sustainable Development Studies*, *3*(2), 181–198.

Kuusaana, E. D., Kosoe, E. A., Niminga-Beka, R. Y., & Ahmed, A. (2021). Spatial Justice and Inner-City Development in Secondary Cities of Ghana: Implications for New Urban Agenda in the Global South. *Urban Forum*, *32*(3), 373–391. https://doi.org/10.1007/s12132-021-09415-x

Kwakye, S. O., & Bárdossy, A. (2020). Hydrological modelling in data-scarce catchments: Black Volta basin in West Africa. *SN Applied Sciences*, *2*(4), 1–19. https://doi.org/10.1007/s42452-020-2454-4

Labrière, N., Locatelli, B., Laumonier, Y., Freycon, V., & Bernoux, M. (2015). Soil erosion in the humid tropics: A systematic quantitative review. *Agriculture, Ecosystems and Environment*, *203*, 127–139. https://doi.org/10.1016/j.agee.2015.01.027

Laflen, J. M., Elliot, W. J., Simanton, J. R., Holzhey, C. S., & Kohl, K. D. (1991). WEPP: soil erodibility experiments for rangeland and cropland soils. *Journal of Soil & Water Conservation*, *46*(1), 39–44.

Laine, A. L., & Tylianakis, J. M. (2024). The coevolutionary consequences of biodiversity change. *Trends in Ecology and Evolution*, *39*(8), 745–756. https://doi.org/10.1016/j.tree.2024.04.002

Lal, R. (1984). Soil Erosion from Tropical Arable Lands and its Control. *Advances in Agronomy*, *37*, 183–248. https://doi.org/doi.org/10.1016/S0065-2113(08)60455-1

Lal, R. (2003). Soil erosion and the global carbon budget. *Environment International*, *29*(4), 437–450. https://doi.org/10.1016/S0160-4120(02)00192-7

Lal, R. (2012). Climate Change and Soil Degradation Mitigation by Sustainable Management of Soils and Other Natural Resources. *Agricultural Research*, *1*(3), 199–212. https://doi.org/10.1007/s40003-012-0031-9

Lal, R. (2019). Accelerated Soil erosion as a source of atmospheric CO2. *Soil and Tillage Research*, *188*(February 2018), 35–40. https://doi.org/10.1016/j.still.2018.02.001

Lann, T., Bao, H., Lan, H., Zheng, H., Yan, C., & Peng, J. (2024). Hydro-mechanical effects of vegetation on slope stability: A review. *Science of the Total Environment*, *926*(November 2023). https://doi.org/10.1016/j.scitotenv.2024.171691

Larson, W. E., Pierce, F. J., & Dowdy, R. H. (1983). The threat of soil erosion to long-term crop production. *Science*, *219*(4584), 458–465. https://doi.org/10.1126/science.219.4584.458

Lazzari, M., Gioia, D., Piccarreta, M., Danese, M., & Lanorte, A. (2015). Sediment yield and erosion rate estimation in the mountain catchments of the Camastra artificial reservoir (Southern Italy): A comparison between different empirical methods. *Catena*, *127*, 323–339. https://doi.org/10.1016/j.catena.2014.11.021

Le Bissonnais, Y. (2016). Aggregate stability and assessment of soil crustability and erodibility: I. Theory and methodology. *European Journal of Soil Science*, *67*(1), 11–21. https://doi.org/10.1111/ejss.4_12311

Lee, J. H., & Heo, J. H. (2011). Evaluation of estimation methods for rainfall erosivity based on annual precipitation in Korea. *Journal of Hydrology*, *409*(1–2), 30–48. https://doi.org/10.1016/j.jhydrol.2011.07.031

Lee, S. (2004). Soil erosion assessment and its verification using the Universal Soil Loss Equation and Geographic Information System: A case study at Boun, Korea. *Environmental Geology*, *45*(4), 457–465. https://doi.org/10.1007/s00254-003-0897-8

Leh, M., Bajwa, S., & Chaubey, I. (2013). Impact of land use change on erosion risk: AN integrated remote sensing, geographic information system and modeling methodology. *Land Degradation and Development*, *24*(5), 409–421. https://doi.org/10.1002/ldr.1137

Lemoalle, J., & Condappa, D. De. (2009). *Water atlas of the Volta Basin-Atlas de l'eau dans le bas- sin de la Volta*.

Lew, R., Dobre, M., Srivastava, A., Deval, C., Brooks, E. S., Elliot, W. J., & Robichaud, P. R. (2022). WEPPcloud: An online watershed-scale hydrologic modeling tool. Part II. Model performance assessment and applications to forest management and wildfires. *Journal of Hydrology*, *610*(February). https://doi.org/10.1016/j.jhydrol.2022.127776

Li, C., Li, Z., Yang, M., Ma, B., & Wang, B. (2021). Article grid-scale impact of climate change and human influence on soil erosion within east african highlands (Kagera basin). *International Journal of Environmental Research and Public Health*, *18*(5), 1–17. https://doi.org/10.3390/ijerph18052775

Li, G., Sun, S., & Fang, C. (2018). The varying driving forces of urban expansion in China: Insights from a spatial-temporal analysis. *Landscape and Urban Planning*, *174*(November 2016), 63–77. https://doi.org/10.1016/j.landurbplan.2018.03.004

Li, H., Wei, Y. H. D., & Huang, Z. (2014). Urban land expansion and spatial dynamics in Globalizing Shanghai. *Sustainability (Switzerland)*, *6*(12), 8856–8875. https://doi.org/10.3390/su6128856

Li, J., Pei, Y., Zhao, S., Xiao, R., Sang, X., & Zhang, C. (2020). A review of remote sensing for environmental monitoring in China. *Remote Sensing*, *12*(7), 1–25. https://doi.org/10.3390/rs12071130

Li, N., Zhang, Y., Wang, T., Li, J., Yang, J., & Luo, M. (2022). Have anthropogenic factors mitigated or intensified soil erosion over the past three decades in South China? *Journal of Environmental Management*, *302*(PB), 114093. https://doi.org/10.1016/j.jenvman.2021.114093

Li, S., Liu, X., Li, Z., Wu, Z., Yan, Z., Chen, Y., & Gao, F. (2018). Spatial and temporal dynamics of urban expansion along the Guangzhou-Foshan inter-city rail transit corridor, China. *Sustainability (Switzerland)*, *10*(3). https://doi.org/10.3390/su10030593

Li, X., Zhou, W., & Ouyang, Z. (2013). Forty years of urban expansion in Beijing: What is the relative importance of physical, socioeconomic, and neighborhood factors? *Applied Geography*, *38*(1), 1–10. https://doi.org/10.1016/j.apgeog.2012.11.004

Li, Y., Grimaldi, S., Pauwels, V. R. N., & Walker, J. P. (2018). Hydrologic model calibration using remotely sensed soil moisture and discharge measurements: The impact on predictions at gauged and ungauged locations. *Journal of Hydrology*, *557*, 897–909. https://doi.org/10.1016/j.jhydrol.2018.01.013

Li, Z., & Fang, H. (2016). Impacts of climate change on water erosion: A review. *Earth-Science Reviews*, *163*, 94–117. https://doi.org/10.1016/j.earscirev.2016.10.004

Ligonja, P. J., & Shrestha, R. P. (2015). Soil erosion assessment in kondoa eroded area in Tanzania using universal soil loss equation, geographic information systems and socioeconomic approach. *Land Degradation and Development*, *26*(4), 367–379. https://doi.org/10.1002/ldr.2215

Linder, H. L., & Horne, J. K. (2018). Evaluating statistical models to measure environmental change: A tidal turbine case study. *Ecological Indicators*, *84*(March 2017), 765–792. https://doi.org/10.1016/j.ecolind.2017.09.041

Liu, L., Zhang, K., Zhang, Z., & Qiu, Q. (2015). Identifying soil redistribution patterns by magnetic susceptibility on the black soil farmland in Northeast China. *Catena*, *129*, 103–111. https://doi.org/10.1016/j.catena.2015.03.003

Llena, M., Vericat, D., Cavalli, M., Crema, S., & Smith, M. W. (2019). The effects of land use and topographic changes on sediment connectivity in mountain catchments. *Science of the Total Environment*, *660*, 899–912. https://doi.org/10.1016/j.scitotenv.2018.12.479

Locatelli, B., Imbach, P., Vignola, R., Metzger, M. J., & Hidalgo, E. J. L. (2011). Ecosystem services and hydroelectricity in Central America: Modelling service flows with fuzzy logic and expert knowledge. *Regional Environmental Change*, *11*(2), 393–404. https://doi.org/10.1007/s10113-010-0149-x

Lujan, D. L. (2003). Soil Physical Properties Affecting Soil Erosion in Tropical Soils. *Production, March*.

Luo, J., & Wei, Y. H. D. (2009). Modeling spatial variations of urban growth patterns in Chinese cities: The case of Nanjing. *Landscape and Urban Planning*, *91*(2), 51–64. https://doi.org/10.1016/j.landurbplan.2008.11.010

Ma, L., Li, M., Ma, X., Cheng, L., Du, P., & Liu, Y. (2017). A review of supervised object-based land-cover image classification. *ISPRS Journal of Photogrammetry and Remote Sensing*, *130*, 277–293. https://doi.org/10.1016/j.isprsjprs.2017.06.001

Maestre, F. T., Eldridge, D. J., Soliveres, S., Kéfi, S., Delgado-Baquerizo, M., Bowker, M. A., García-Palacios, P., Gaitán, J., Gallardo, A., Lázaro, R., & Berdugo, M. (2016). Structure and Functioning of Dryland Ecosystems in a Changing World. *Annual Review of Ecology, Evolution, and Systematics*, *47*, 215–237. https://doi.org/10.1146/annurev-ecolsys-121415-032311

Maetens, W., Vanmaercke, M., Poesen, J., Jankauskas, B., Jankauskiene, G., & Ionita, I. (2012). Effects of land use on annual runoff and soil loss in Europe and the Mediterranean: A meta-analysis of plot data. *Progress in Physical Geography*, *36*(5), 599–653. https://doi.org/10.1177/0309133312451303

Malhi, Y., Gardner, T. A., Goldsmith, G. R., Silman, M. R., & Zelazowski, P. (2014). Tropical forests in the anthropocene. *Annual Review of Environment and Resources*, *39*, 125–159. https://doi.org/10.1146/annurev-environ-030713-155141

Måren, I. E., Karki, S., Prajapati, C., Yadav, R. K., & Shrestha, B. B. (2015). Facing north or south: Does slope aspect impact forest stand characteristics and soil properties in a semiarid trans-Himalayan valley? *Journal of Arid Environments*, *121*, 112–123. https://doi.org/10.1016/j.jaridenv.2015.06.004

Mariye, M., Mariyo, M., Changming, Y., Teffera, Z. L., & Weldegebrial, B. (2022). Effects of land use and land cover change on soil erosion potential in Berhe district: a case study of Legedadi watershed, Ethiopia. *International Journal of River Basin Management*, *20*(1), 79–91. https://doi.org/10.1080/15715124.2020.1767636

Marondedze, A. K., & Schütt, B. (2019). Dynamics of land use and land cover changes in Harare, Zimbabwe: A case study on the linkage between drivers and the axis of urban expansion. *Land*, *8*(10). https://doi.org/10.3390/land8100155

Marondedze, A. K., & Schütt, B. (2020). Assessment of soil erosion using the rusle model for the Epworth district of the harare metropolitan province, zimbabwe. *Sustainability (Switzerland)*, *12*(20), 1–24. https://doi.org/10.3390/su12208531

Maurya, S. P., Yadav, A. K., & Singh, R. (2023). Modeling and Simulation of Environmental Systems. In S. P. Maurya, A. K. Yadav, & R. Singh (Eds.), *Modeling and Simulation of Environmental Systems* (1st ed., Issue March). CRC Press. https://doi.org/10.1201/9781003203445

McCartney, M. G. ., Sood, A. ., Amisigo, B., Hattermann, F., & Muthuwatta, L. (2012). *The Water Resource Implications of Changing Climate in the Volta River Basin*.

McFeeters, S. K. (1996). The use of the Normalized Difference Water Index (NDWI) in the delineation of open water features. *International Journal of Remote Sensing*, *17*(7), 1425–1432. https://doi.org/10.1080/01431169608948714

McKinney, M. L. (2002). Urbanization, biodiversity, and conservation: the impacts of urbanization on native species are poorly studied, but educating a highly urbanized human population about these impacts can greatly improve species conservation in all ecosystems. *Bioscience*, *52*(10), 883–890. https://doi.org/10.1641/0006-3568(2002)052[0883:UBAC]2.0.CO;2

McVey, I., Michalek, A., Mahoney, T., & Husic, A. (2023). Urbanization as a limiter and catalyst of watershed-scale sediment transport: Insights from probabilistic connectivity modeling. *Science of the Total Environment*, *894*(April), 165093. https://doi.org/10.1016/j.scitotenv.2023.165093

Mechiche-Alami, A., & Abdi, A. M. (2020). Agricultural productivity in relation to climate and cropland management in West Africa. *Scientific Reports*, *10*(1), 3393. https://doi.org/10.1038/s41598-020-59943-y

Meledje, N. E. H., Kouassi, K. L., & N'Go, Y. A. (2021). Quantification of water related soil erosion in the transboundary basin of the Bia (West Africa). *Proceedings of the International Association of Hydrological Sciences*, *384*, 107–112. https://doi.org/10.5194/piahs-384-107-2021

Meles, M. B., Younger, S. E., Jackson, C. R., Du, E., & Drover, D. (2020). Wetness index based on landscape position and topography (WILT): Modifying TWI to reflect landscape position. *Journal of Environmental Management*, *255*(November), 109863. https://doi.org/10.1016/j.jenvman.2019.109863

Melese, T., Senamaw, A., Belay, T., & Bayable, G. (2021). The Spatiotemporal Dynamics of Land Use Land Cover Change, and Its Impact on Soil Erosion in Tagaw Watershed, Blue Nile Basin, Ethiopia. *Global Challenges*, *5*(7), 2000109. https://doi.org/10.1002/gch2.202000109

Mengistu, D., Bewket, W., & Lal, R. (2015). Sustainable Intensification to Advance Food Security and Enhance Climate Resilience in Africa. *Sustainable Intensification to Advance Food Security and Enhance Climate Resilience in Africa*. https://doi.org/10.1007/978-3-319-09360-4

Merritt, W. S., Letcher, R. A., & Jakeman, A. J. (2003). A review of erosion and sediment transport models. *Environmental Modelling and Software*, *18*(8–9), 761–799. https://doi.org/10.1016/S1364-8152(03)00078-1

Meshesha, D. T., Tsunekawa, A., Tsubo, M., Haregeweyn, N., & Adgo, E. (2014). Distribution de la taille de gouttes de pluie et de l'énergie cinétique des précipitations dans les hautes terres de la vallée du Rift Central, Ethiopie. *Hydrological Sciences Journal*, *59*(12), 2203–2215. https://doi.org/10.1080/02626667.2013.865030

Meusburger, K., Konz, N., Schaub, M., & Alewell, C. (2010). Soil erosion modelled with USLE and PESERA using QuickBird derived vegetation parameters in an alpine catchment. *International Journal of Applied Earth Observation and Geoinformation*, *12*(3), 208–215. https://doi.org/10.1016/j.jag.2010.02.004

Mhiret, D. A., Dagnew, D. C., Assefa, T. T., Tilahun, S. A., Zaitchik, B. F., & Steenhuis, T. S. (2019). Erosion hotspot identification in the sub-humid Ethiopian highlands. *Ecohydrology and Hydrobiology*, *19*(1), 146–154. https://doi.org/10.1016/j.ecohyd.2018.08.004

Millennium Ecosystem Assessment, M. (2005). Ecosystems and Human Well-being: Opportunities for Business and Industry. *Millennium Ecosystem Management*, 36. https://www.millenniumassessment.org/documents/document.754.aspx.pdf

Mineo, C., Ridolfi, E., Moccia, B., Russo, F., & Napolitano, F. (2019). Assessment of rainfall kinetic-energy-intensity relationships. *Water (Switzerland)*, *11*(10). https://doi.org/10.3390/w11101994

Mitasova, H., Hofierka, J., Zlocha, M., & Iverson, L. R. (1996). Modelling topographic potential for erosion and deposition using GIS. *International Journal of Geographical Information Systems*, *10*(5), 629–641. https://doi.org/10.1080/02693799608902101

Mohamadi, M. A., & Kavian, A. (2015). Effects of rainfall patterns on runoff and soil erosion in field plots. *International Soil and Water Conservation Research*, *3*(4), 273–281. https://doi.org/10.1016/j.iswcr.2015.10.001

Moisa, M. B., Dejene, I. N., Roba, Z. R., & Gemeda, D. O. (2022). Impact of urban land use and land cover change on urban heat island and urban thermal comfort level: a case study of Addis Ababa City, Ethiopia. *Environmental Monitoring and Assessment*, *194*(10). https://doi.org/10.1007/s10661-022-10414-z

Montgomery, D. R. (2007). Soil erosion and agricultural sustainability. *Proceedings of the National Academy of Sciences of the United States of America*, *104*(33), 13268–13272. https://doi.org/10.1073/pnas.0611508104

Moomen, A. W., & Dewan, A. (2017). Assessing the spatial relationships between mining and land degradation: evidence from Ghana. *International Journal of Mining, Reclamation and Environment*, *31*(7), 505–518. https://doi.org/10.1080/17480930.2016.1188253.

Moore, I. A. N. D., & Burch, G. J. (1986). Physical Basis of the Length Slope Factor in the Universal Soil Loss Equation. *Science Society of America*, *50*(1986), 1294–1298. https://doi.org/10.2136/sssaj1986.03615995005000050042x

Morehead, M. D., Syvitski, J. P., Hutton, E. W. H., & Peckham, S. D. (2003). Modeling the temporal variability in the flux of sediment from ungauged river basins. *Global and Planetary Change*, *39*(1–2), 95–110. https://doi.org/10.1016/S0921-8181(03)00019-5

Morgan, R. P. C., Morgan, D. D. V., & Finney, H. J. (1984). A predictive model for the assessment of soil erosion risk. *Journal of Agricultural Engineering Research*, *30*(C), 245–253. https://doi.org/10.1016/S0021-8634(84)80025-6.

Morgan, R. P. C., Quinton, J. N., Smith, R. E., Govers, G., Poesen, J. W. A., Auerswald, K., Chisci, G., Torri, D., & Styczen, M. E. (1998). The European soil erosion model (EUROSEM): a dynamic approach for predicting sediment transport from fields and small catchments. *Earth Surface Processes and Landforms*, *23*(6), 527–544. https://doi.org/10.1002/(SICI)1096-9837(199806)23:6<527::AID-ESP868>3.0.CO;2-5

Mortey, E. M., Annor, T., Arnault, J., Inoussa, M. M., Madougou, S., Kunstmann, H., & Nyantakyi, E. K. (2023). Interactions between Climate and Land Cover Change over West Africa. *Land*, *12*(2). https://doi.org/10.3390/land12020355

Mosaid, H., Barakat, A., Bouras, E. H., Ismaili, M., El Garnaoui, M., Abdelrahman, K., & Kahal, A. Y. (2024). Dam Siltation in the Mediterranean Region Under Climate Change: A Case Study of Ahmed El Hansali Dam, Morocco. *Water (Switzerland)*, *16*(21). https://doi.org/10.3390/w16213108

Mountrakis, G., Im, J., & Ogole, C. (2011). Support vector machines in remote sensing: A review. *ISPRS Journal of Photogrammetry and Remote Sensing*, *66*(3), 247–259. https://doi.org/10.1016/j.isprsjprs.2010.11.001

Mucova, S. A. R., Filho, W. L., Azeiteiro, U. M., & Pereira, M. J. (2018). Assessment of land use and land cover changes from 1979 to 2017 and biodiversity & land management approach in Quirimbas National Park, Northern Mozambique, Africa. *Global Ecology and Conservation*, *16*. https://doi.org/10.1016/j.gecco.2018.e00447

Mul, M., Obuobie, E., Appoh, R., Kankam-Yeboah, K., Bekoe-Obeng, E., Amisigo, B., Logah, F. Y., Ghansah, B., & McCartney, M. (2015). Water resources assessment of the Volta River Basin. In *IWMI Working Papers* (Vol. 166, Issue January). https://doi.org/10.5337/2015.220

Mustafa, A., Minggang, X., Ali Shah, S. A., Abrar, M. M., Nan, S., Baoren, W., Zejiang, C., Saeed, Q., Naveed, M., Mehmood, K., & Núñez-Delgado, A. (2020). Soil aggregation and soil aggregate stability regulate organic carbon and nitrogen storage in a red soil of southern China. *Journal of Environmental Management*, *270*(June). https://doi.org/10.1016/j.jenvman.2020.110894

Mutua, B. M., Klik, A., & Loiskandl, W. (2006). Modelling soil erosion and sediment yield at a catchment scale: The case of Masinga catchment, Kenya. *Land Degradation and Development*, *17*(5), 557–570. https://doi.org/10.1002/ldr.753

Myers, S. S., Gaffikin, L., Golden, C. D., Ostfeld, R. S., Redford, K. H., Ricketts, T. H., Turner, W. R., & Osofsky, S. A. (2013). Human health impacts of ecosystem alteration. *Proceedings of the National Academy of Sciences of the United States of America*, *110*(47), 18753–18760. https://doi.org/10.1073/pnas.1218656110

Nearing, M. A., Wei, H., Stone, J. J., Pierson, F. B., Spaeth, K. E., Weltz, M. A., Flanagan, D. C., & Hernandez, M. (2011). A Rangeland Hydrology and Erosion Model. *American Society of Agricultural and Biological Engineers ISSN*, *54*(3), 901–908.

Newton, A. C., Hill, R. A., Golicher, D., Rey, J. M., Cayuela, L., Hinsley, S. A., Campus, T., & Bh, P. (2009). *Remote sensing and the future of landscape ecology*. *33*(4), 528–546. https://doi.org/10.1177/0309133309346882

Nguyen, T. T., Grote, U., Neubacher, F., Rahut, D. B., Do, M. H., & Paudel, G. P. (2023). Security risks from climate change and environmental degradation: implications for sustainable land use transformation in the Global South. *Current Opinion in Environmental Sustainability*, *63*(June), 101322. https://doi.org/10.1016/j.cosust.2023.101322

Nicholson, S. E. (2009). A revised picture of the structure of the "monsoon" and land ITCZ over West Africa. *Climate Dynamics*, *32*(7–8), 1155–1171. https://doi.org/10.1007/s00382-008-0514-3

Nkpeebo, A. Y., & Mavimbela, S. S. W. (2023). Analyzing changes in land use practices and livelihoods in the Bhungroo irrigation technology Volta basin piloted sites, West Mamprusi District, Ghana. *Heliyon*, *9*(4), e14907. https://doi.org/10.1016/j.heliyon.2023.e14907

Nkrumah, F., Vischel, T., Panthou, G., Klutse, N. A. B., Adukpo, D. C., & Diedhiou, A. (2019). Recent trends in the daily rainfall regime in Southern West Africa. *Atmosphere*, *10*(12), 1–15. https://doi.org/10.3390/ATMOS10120741

Noroozpour, S., Saghafian, B., Akhondali, A. M., & Radmanesh, F. (2014). Travel time of curved parallel hillslopes. *Hydrology Research*, *45*(2), 190–199. https://doi.org/10.2166/nh.2013.171

Nut, N., Mihara, M., Jeong, J., Ngo, B., Sigua, G., Prasad, P. V. V., & Reyes, M. R. (2021). Land use and land cover changes and its impact on soil erosion in Stung sangkae Catchment of Cambodia. *Sustainability (Switzerland)*, *13*(16). https://doi.org/10.3390/su13169276

Nyamekye, C., Thiel, M., Schönbrodt-Stitt, S., Zoungrana, B. J. B., & Amekudzi, L. K. (2018). Soil and water conservation in Burkina Faso, West Africa. *Sustainability (Switzerland)*, *10*(9), 1–24. https://doi.org/10.3390/su10093182

Nyatuame, M., Amekudzi, L. K., & Agodzo, S. K. (2020). Assessing the land use/land cover and climate change impact on water balance on Tordzie watershed. *Remote Sensing Applications: Society and Environment*, *20*(June), 100381. https://doi.org/10.1016/j.rsase.2020.100381

O'Brien, J. J., Hiers, J. K., Varner, J. M., Hoffman, C. M., Dickinson, M. B., Michaletz, S. T., Loudermilk, E. L., & Butler, B. W. (2018). Advances in Mechanistic Approaches to Quantifying Biophysical Fire Effects. *Current Forestry Reports*, *4*(4), 161–177. https://doi.org/10.1007/s40725-018-0082-7

Obahoundje, S., Diedhiou, A., Ofosu, E. A., Anquetin, S., François, B., Adounkpe, J., Amoussou, E., Kouame, Y. M., Kouassi, K. L., Bi, V. H. N., & Ta, M. Y. (2018). Assessment of spatio-temporal changes of land use and land cover over South-Western African basins and their relations with variations of discharges. *Hydrology*, *5*(4). https://doi.org/10.3390/hydrology5040056

Obalum, S. E., Buri, M. M., Nwite, J. C., Hermansah, Watanabe, Y., Igwe, C. A., & Wakatsuki, T. (2012). Soil degradation-induced decline in productivity of sub-saharan African soils: The prospects of looking downwards the lowlands with the sawah ecotechnology. *Applied and Environmental Soil Science*, *2012*(January). https://doi.org/10.1155/2012/673926

Obiahu, O. H., & Elias, E. (2020). Effect of land use land cover changes on the rate of soil erosion in the Upper Eyiohia river catchment of Afikpo North Area, Nigeria. *Environmental Challenges*, *1*, 100002. https://doi.org/10.1016/j.envc.2020.100002

Ofoezie, E. I., Eludoyin, A. O., Udeh, E. B., Onanuga, M. Y., Salami, O. O., & Adebayo, A. A. (2022). Climate, Urbanization and Environmental Pollution in West Africa. In *Sustainability (Switzerland)* (Vol. 14, Issue 23). https://doi.org/10.3390/su142315602

Oguntunde, P. G., & Abiodun, B. J. (2013). The impact of climate change on the Niger River Basin hydroclimatology, West Africa. *Climate Dynamics*, *40*(1–2), 81–94. https://doi.org/10.1007/s00382-012-1498-6

Okou, F. A. Y., Tente, B., Bachmann, Y., & Sinsin, B. (2016). Regional erosion risk mapping for decision support: A case study from West Africa. *Land Use Policy*, *56*, 27–37. https://doi.org/10.1016/j.landusepol.2016.04.036

Olanipekun, I. O., Olasehinde-Williams, G. O., & Alao, R. O. (2019). Agriculture and environmental degradation in Africa: The role of income. *Science of the Total Environment*, *692*, 60–67. https://doi.org/10.1016/j.scitotenv.2019.07.129

Oliveira, P. T. S., Wendland, E., & Nearing, M. A. (2013). Rainfall erosivity in Brazil: A review. *Catena*, *100*, 139–147. https://doi.org/10.1016/j.catena.2012.08.006

Osawe, A. I., & Ojeifo, M. O. (2019). Unregulated Urbanization and challenge of environmental security in Africa. *World Journal of Innovative Research (WJIR)*, *6*(4), 1–0.

Ostovari, Y., Moosavi, A. A., Mozaffari, H., & Pourghasemi, H. R. (2021). RUSLE model coupled with RS-GIS for soil erosion evaluation compared with T value in Southwest Iran. *Arabian Journal of Geosciences*, *14*(2). https://doi.org/10.1007/s12517-020-06405-4

Osumanu, I. K., Akongbangre, J. N., Tuu, G. N. Y., & Owusu-Sekyere, E. (2019). From Patches of Villages to a Municipality: Time, Space, and Expansion of Wa, Ghana. *Urban Forum*, *30*(1), 57–74. https://doi.org/10.1007/s12132-018-9341-8

Ouyang, W., Hao, F., Skidmore, A. K., & Toxopeus, A. G. (2010). Soil erosion and sediment yield and their relationships with vegetation cover in upper stream of the Yellow River. *Science of the Total Environment*, *409*(2), 396–403. https://doi.org/10.1016/j.scitotenv.2010.10.020

Özdemir, N., Demir, Z., & Bülbül, E. (2022). Relationships between some soil properties and bulk density under different land use. *Soil Studies*, *11*(2), 43–50. https://doi.org/10.21657/soilst.1218353

Panagos, P., Borrelli, P., & Meusburger, K. (2015). A new European slope length and steepness factor (LS-factor) for modeling soil erosion by water. *Geosciences (Switzerland)*, *5*(2), 117–126. https://doi.org/10.3390/geosciences5020117

Panagos, P., Borrelli, P., Meusburger, K., van der Zanden, E. H., Poesen, J., & Alewell, C. (2015). Modelling the effect of support practices (P-factor) on the reduction of soil erosion by water at European scale. *Environmental Science and Policy*, *51*, 23–34. https://doi.org/10.1016/j.envsci.2015.03.012

Panagos, P., Borrelli, P., Meusburger, K., Yu, B., Klik, A., Lim, K. J., Yang, J. E., Ni, J., Miao, C., Chattopadhyay, N., Sadeghi, S. H., Hazbavi, Z., Zabihi, M., Larionov, G. A., Krasnov, S. F., Gorobets, A. V., Levi, Y., Erpul, G., Birkel, C., … Ballabio, C. (2017). Global rainfall erosivity assessment based on high-temporal resolution rainfall records. *Scientific Reports*, *7*(1), 1–12. https://doi.org/10.1038/s41598-017-04282-8

Pandey, A., Bishal, K. C., Kalura, P., Chowdary, V. M., Jha, C. S., & Cerdà, A. (2021). A Soil Water Assessment Tool (SWAT) Modeling Approach to Prioritize Soil Conservation Management in River Basin Critical Areas Coupled With Future Climate Scenario Analysis. *Air, Soil and Water Research*, *14*. https://doi.org/10.1177/11786221211021395

Pandian, K., Mustaffa, M. R. A. F., Mahalingam, G., Paramasivam, A., John Prince, A., Gajendiren, M., Rafiqi Mohammad, A. R., & Varanasi, S. T. (2024). Synergistic conservation approaches for nurturing soil, food security and human health towards sustainable development goals. *Journal of Hazardous Materials Advances*, *16*(September), 100479. https://doi.org/10.1016/j.hazadv.2024.100479

Paolini, L., Grings, F., Sobrino, J., Jiménez Muñoz, J. C., & Karszenbaum, H. (2006). Radiometric correction effects in Landsat multi-date/multi-sensor change detection studies. *International Journal of Remote Sensing*, *27*(4), 685–704. https://doi.org/10.1080/01431160500183057

Peng, X., & Dai, Q. (2022). Drivers of soil erosion and subsurface loss by soil leakage during karst rocky desertification in SW China. *International Soil and Water Conservation Research*, *10*(2), 217–227. https://doi.org/10.1016/j.iswcr.2021.10.001

Phiri, D., & Morgenroth, J. (2017). Developments in Landsat land cover classification methods: A review. *Remote Sensing*, *9*(9). https://doi.org/10.3390/rs9090967

Piacentini, T., Galli, A., Marsala, V., & Miccadei, E. (2018). Analysis of soil erosion induced by heavy rainfall: A case study from the NE Abruzzo Hills Area in Central Italy. *Water (Switzerland)*, *10*(10), 11–13. https://doi.org/10.3390/w10101314

Pielke, R. A., Pitman, A., Niyogi, D., Mahmood, R., McAlpine, C., Hossain, F., Goldewijk, K. K., Nair, U., Betts, R., Fall, S., Reichstein, M., Kabat, P., & de Noblet, N. (2011). Land use/land cover changes and climate: Modeling analysis and observational evidence. *Wiley Interdisciplinary Reviews: Climate Change*, *2*(6), 828–850. https://doi.org/10.1002/wcc.144

Pimentel, D. (2006). Soil erosion: A food and environmental threat. *Environment, Development and Sustainability*, *8*(1), 119–137. https://doi.org/10.1007/s10668-005-1262-8

Pimentel, D., & Burgess, M. (2013). Soil erosion threatens food production. *Agriculture (Switzerland)*, *3*(3), 443–463. https://doi.org/10.3390/agriculture3030443

Pimentel, D., Harvey, C., Resosudarmo, P., Sinclair, K., Kurz, D., McNair, M., Crist, S., Shpritz, L., Fitton, L., Saffouri, R., & Blair, R. (1995). Environmental and economic costs of soil erosion and conservation benefits. *Science*, *267*(5201), 1117–1123. https://doi.org/10.1126/science.267.5201.1117

Pimentel, D., & Kounang, N. (1998). Ecology of soil erosion in ecosystems. *Ecosystems*, *1*(5), 416–426. https://doi.org/10.1007/s100219900035

Pintaldi, E., D'Amico, M. E., Stanchi, S., Catoni, M., Freppaz, M., & Bonifacio, E. (2018). Humus forms affect soil susceptibility to water erosion in the Western Italian Alps. *Applied Soil Ecology*, *123*(December 2016), 478–483. https://doi.org/10.1016/j.apsoil.2017.04.007

Pistocchi, A., Cassani, G., & Zani, O. (2002). Use of the USPED model for mapping soil erosion and managing best land conservation practices. *Proceedings of the First Biennial Meeting of the International Environmental Modelling and Software Society on Integrated Assessment and Decision Support*, *3*, 163–168. http://www.iemss.org/iemss2002/

Poelmans, L., & Van Rompaey, A. (2009). Detecting and modelling spatial patterns of urban sprawl in highly fragmented areas: A case study in the Flanders-Brussels region. *Landscape and Urban Planning*, *93*(1), 10–19. https://doi.org/10.1016/j.landurbplan.2009.05.018

Poesen, J., Nachtergaele, J., Verstraeten, G., & Valentin, C. (2003). Gully erosion and environmental change: Importance and research needs. *Catena*, *50*(2–4), 91–133. https://doi.org/10.1016/S0341-8162(02)00143-1

Pohlert, T., Huisman, J. A., Breuer, L., & Frede, H. G. (2007). Integration of a detailed biogeochemical model into SWAT for improved nitrogen predictions-Model development, sensitivity, and GLUE analysis. *Ecological Modelling*, *203*(3–4), 215–228. https://doi.org/10.1016/j.ecolmodel.2006.11.019

Poku-Boansi, M., & Adarkwa, K. K. (2016). Determinants of residential location in the Adenta Municipality, Ghana. *GeoJournal*, *81*(5), 779–791. https://doi.org/10.1007/s10708-015-9665-z

Pontes, S. F., Silva, Y. J. A. B. da, Martins, V., Boechat, C. L., Araújo, A. S. F., Dantas, J. S., Costa, O. S., & Barbosa, R. S. (2022). Prediction of Soil Erodibility by Diffuse Reflectance Spectroscopy in a Neotropical Dry Forest Biome. *Land*, *11*(12). https://doi.org/10.3390/land11122188

Prasannakumar, V., Vijith, H., Abinod, S., & Geetha, N. (2012). Estimation of soil erosion risk within a small mountainous sub-watershed in Kerala, India, using Revised Universal Soil Loss Equation (RUSLE) and geo-information technology. *Geoscience Frontiers*, *3*(2), 209–215. https://doi.org/10.1016/j.gsf.2011.11.003

Prasuhn, V., Liniger, H., Gisler, S., Herweg, K., Candinas, A., & Clément, J. P. (2013). A high-resolution soil erosion risk map of Switzerland as strategic policy support system. *Land Use Policy*, *32*, 281–291. https://doi.org/10.1016/j.landusepol.2012.11.006

Pravitasari, A. E., Rustiadi, E., Mulya, S. P., Setiawan, Y., Fuadina, L. N., & Murtadho, A. (2018). Identifying the driving forces of urban expansion and its environmental impact in Jakarta-Bandung mega urban region. *IOP Conference Series: Earth and Environmental Science*, *149*(1). https://doi.org/10.1088/1755-1315/149/1/012044

Prosser, R. S., Hoekstra, P. F., Gene, S., Truman, C., White, M., & Hanson, M. L. (2020). A review of the effectiveness of vegetated buffers to mitigate pesticide and nutrient transport into surface waters from agricultural areas. *Journal of Environmental Management*, *261*(July 2019). https://doi.org/10.1016/j.jenvman.2020.110210

Qu, Y., Su, D., Wei, C., Zhang, Q., & Jiang, G. (2023). How to prevent landscape ecological risk with a land use optimal allocation system: An empirical study of the Yellow River Delta in China. *Ecological Indicators*, *154*(19), 110888. https://doi.org/10.1016/j.ecolind.2023.110888

Raduła, M. W., Szymura, T. H., & Szymura, M. (2018). Topographic wetness index explains soil moisture better than bioindication with Ellenberg's indicator values. *Ecological Indicators*, *85*(March 2017), 172–179. https://doi.org/10.1016/j.ecolind.2017.10.011

Ramankutty, N., & Foley, J. A. (1999). Estimating historical changes in global land cover: Croplands from 1700 to 1992. *Global Biogeochemical Cycles*, *13*(4), 997–1027. https://doi.org/10.1029/1999GB900046

Ranzi, R., Le, T. H., & Rulli, M. C. (2012). A RUSLE approach to model suspended sediment load in the Lo river (Vietnam): Effects of reservoirs and land use changes. *Journal of Hydrology*, *422–423*, 17–29. https://doi.org/10.1016/j.jhydrol.2011.12.009

Razavi, S., Jakeman, A., Saltelli, A., Prieur, C., Iooss, B., Borgonovo, E., Plischke, E., Lo Piano, S., Iwanaga, T., Becker, W., Tarantola, S., Guillaume, J. H. A., Jakeman, J., Gupta, H., Melillo, N., Rabitti, G., Chabridon, V., Duan, Q., Sun, X., … Maier, H. R. (2021). The Future of Sensitivity Analysis: An essential discipline for systems modeling and policy support. *Environmental Modelling and Software*, *137*(December 2020). https://doi.org/10.1016/j.envsoft.2020.104954

Reddy, M. T., Pandravada, S. R., Sivaraj, N., Kamala, V., Sunil, N., & Dikshit, N. (2017). Classification and Characterization of Landscapes in the Territory of Adilabad District, Telangana, Deccan Region, India. *OALib*, *04*(07), 1–39. https://doi.org/10.4236/oalib.1103745

Rehfeld, K., Hebert, R., Lora, J. M., Lofverstrom, M., & Brierley, C. M. (2020). Variability of surface climate in simulations of past and future. *Earth System Dynamics*, *11*(2), 447–468. https://doi.org/10.5194/esd-11-447-2020

Renard, K., Foster, G., Weesies, G., McCool, D., & Yoder, D. (1997). Predicting soil erosion by water: a guide to conservation planning with the Revised Universal Soil Loss Equation (RUSLE). In *Agricultural Handbook No. 703*. United States Government Printing. http://www.ars.usda.gov/SP2UserFiles/Place/64080530/RUSLE/AH_703.pdf

Renschler, C. S. (2003). Designing geo-spatial interfaces to scale process models: the GeoWEPP approach. *Hydrological Processes*, *17*(5), 1005–1017. https://doi.org/10.1002/hyp.1177

Reynolds, J. F., Stafford Smith, D. M., Lambin, E. F., Turner, B. L., Mortimore, M., Batterbury, S. P. J., Downing, T. E., Dowlatabadi, H., Fernández, R. J., Herrick, J. E., Huber-Sannwald, E., Jiang, H., Leemans, R., Lynam, T., Maestre, F. T., Ayarza, M., & Walker, B. (2007). Ecology: Global desertification: Building a science for dryland development. *Science*, *316*(5826), 847–851. https://doi.org/10.1126/science.1131634

Ribolzi, O., Hermida, M., Karambiri, H., Delhoume, J. P., & Thiombiano, L. (2006). Effects of aeolian processes on water infiltration in sandy Sahelian rangeland in Burkina Faso. *Catena*, *67*(3), 145–154. https://doi.org/10.1016/j.catena.2006.03.006

Ristić, R., Kostadinov, S., Abolmasov, B., Dragićević, S., Trivan, G., Radić, B., Trifunović, M., & Radosavljević, Z. (2012). Torrential floods and town and country planning in Serbia. *Natural Hazards and Earth System Science*, *12*(1), 23–35. https://doi.org/10.5194/nhess-12-23-2012

Robinson, N. P., Allred, B. W., Jones, M. O., Moreno, A., Kimball, J. S., Naugle, D. E., Erickson, T. A., & Richardson, A. D. (2017). A dynamic landsat derived normalized difference vegetation index (NDVI) product for the conterminous United States. *Remote Sensing*, *9*(8), 1–14. https://doi.org/10.3390/rs9080863

Rodgers, C., Giesen, N., Laube, W., Vlek, P. L. G., & Youkhana, E. (2007). The GLOWA volta project: A framework for water resources decision-making and scientific capacity building in a transnational West African Basin. *Water Resources Management*, *21*(1), 295–313. https://doi.org/10.1007/s11269-006-9054-y

Rouse, J. W., Haas, R. H., Schell, J. A., & Deering, D. W. (1973). Monitoring vegetation systems in the Great Plains with ERTS. *Proceedings of the Third Earth Resources Technology Satellite-1 Symposium, NASA*, 309–317. https://doi.org/10.1021/jf60203a024

Roy, P., Pal, S. C., Arabameri, A., Chakrabortty, R., Pradhan, B., Chowdhuri, I., Lee, S., & Bui, D. T. (2020). Novel ensemble of multivariate adaptive regression spline with spatial logistic regression and boosted regression tree for gully erosion susceptibility. *Remote Sensing*, *12*(20), 1–35. https://doi.org/10.3390/rs12203284

Sartori, M., Ferrari, E., M'Barek, R., Philippidis, G., Boysen-Urban, K., Borrelli, P., Montanarella, L., & Panagos, P. (2024). Remaining Loyal to Our Soil: A Prospective Integrated Assessment of Soil Erosion on Global Food Security. *Ecological Economics*, *219*(December 2022). https://doi.org/10.1016/j.ecolecon.2023.108103

Scherer, U., Zehe, E., Träbing, K., & Gerlinger, K. (2012). Prediction of soil detachment in agricultural loess catchments: Model development and parameterisation. *Catena*, *90*, 63–75. https://doi.org/10.1016/j.catena.2011.11.003

Schmidt, J., Werner, M. V., & Michael, A. (1999). Application of the EROSION 3D model to the CATSOP watershed, the Netherlands. *Catena*, *37*(3–4), 449–456. https://doi.org/10.1016/S0341-8162(99)00032-6

Schmidt, S., Tresch, S., & Meusburger, K. (2019). Modification of the RUSLE slope length and steepness factor (LS-factor) based on rainfall experiments at steep alpine grasslands. *MethodsX*, *6*, 219–229. https://doi.org/10.1016/j.mex.2019.01.004

Schneibel, A., Frantz, D., Röder, A., Stellmes, M., Fischer, K., & Hill, J. (2017). Using annual landsat time series for the detection of dry forest degradation processes in south-central Angola. *Remote Sensing*, *9*(9). https://doi.org/10.3390/rs9090905

Schubert, H., Calvo, A. C., Rauchecker, M., Rojas-Zamora, O., Brokamp, G., & Schütt, B. (2018). Article assessment of land cover changes in the hinterland of Barranquilla (Colombia) using landsat imagery and logistic regression. *Land*, *7*(4), 1–24. https://doi.org/10.3390/land7040152

Schürz, C., Mehdi, B., Kiesel, J., Schulz, K., & Herrnegger, M. (2020). A systematic assessment of uncertainties in large-scale soil loss estimation from different representations of USLE input factors-a case study for Kenya and Uganda. *Hydrology and Earth System Sciences*, *24*(9), 4463–4489. https://doi.org/10.5194/hess-24-4463-2020

Schweizer, S. A., Mueller, C. W., Höschen, C., Ivanov, P., & Kögel-Knabner, I. (2021). The role of clay content and mineral surface area for soil organic carbon storage in an arable toposequence. *Biogeochemistry*, *156*(3), 401–420. https://doi.org/10.1007/s10533-021-00850-3

Scotton, M., & Andreatta, D. (2021). Anti-erosion rehabilitation: Effects of revegetation method and site traits on introduced and native plant cover and richness. *Science of the Total Environment*, *776*. https://doi.org/10.1016/j.scitotenv.2021.145915

Sedano, F., Silva, J. A., Machoco, R., Meque, C. H., Sitoe, A., Ribeiro, N., Anderson, K., Ombe, Z. A., Baule, S. H., & Tucker, C. J. (2016). The impact of charcoal production on forest degradation: A case study in Tete, Mozambique. *Environmental Research Letters*, *11*(9). https://doi.org/10.1088/1748-9326/11/9/094020

Selby, M. J. (1982). Rock mass strength and the form of some inselbergs in the central namib desert. *Earth Surface Processes and Landforms*, *7*(5), 489–497. https://doi.org/10.1002/esp.3290070509

Senf, C. (2022). Seeing the System from Above: The Use and Potential of Remote Sensing for Studying Ecosystem Dynamics. *Ecosystems*, *25*(8), 1719–1737. https://doi.org/10.1007/s10021-022-00777-2

Seto, K. C., Fragkias, M., Guneralp, B., & Reilly, M. K. (2012). A Meta-Analysis of Global Urban Land Expansion. *PloS One*, *7*(4), 1–10. https://doi.org/10.1371/journal.pone.0023777

Seto, K. C., Sánchez-Rodríguez, R., & Fragkias, M. (2010). The new geography of contemporary urbanization and the environment. *Annual Review of Environment and Resources*, *35*, 167–194. https://doi.org/10.1146/annurev-environ-100809-125336

Seutloali, K. E., Dube, T., & Mutanga, O. (2017). Assessing and mapping the severity of soil erosion using the 30-m Landsat multispectral satellite data in the former South African homelands of Transkei. *Physics and Chemistry of the Earth*, *100*, 296–304. https://doi.org/10.1016/j.pce.2016.10.001

Shah, N. W., Baillie, B. R., Bishop, K., Ferraz, S., Högbom, L., & Nettles, J. (2022). The effects of forest management on water quality. *Forest Ecology and Management*, *522*(August). https://doi.org/10.1016/j.foreco.2022.120397

Shamshad, A., Azhari, M. N., Isa, M. H., Hussin, W. M. A. W., & Parida, B. P. (2008). Development of an appropriate procedure for estimation of RUSLE EI30 index and preparation of erosivity maps for Pulau Penang in Peninsular Malaysia. *Catena*, *72*(3), 423–432. https://doi.org/10.1016/j.catena.2007.08.002

Sharpley, A. N., & Williams, J. R. (1990). EPIC: The erosion-productivity impact calculator. *U.S. Department of Agriculture Technical Bulletin*, *1768*, 235. http://agris.fao.org/agris-search/search.do?recordID=US9403696

Shi, D., Wu, Q., Shi, Y., Li, Z., Xia, B., Chen, Y., Zhang, N., Meng, J., & Li, Y. (2022). Multidimensional assessment of soil conservation ecosystem services and multiscale analysis of influencing mechanisms. *Journal of Cleaner Production*, *381*(August). https://doi.org/10.1016/j.jclepro.2022.135162

Shikangalah, R., Paton, E., Jetlsch, F., & Blaum, N. (2017). Quantification of areal extent of soil erosion in dryland urban areas: An example from Windhoek, Namibia. *Cities and the Enviroment(CATE)*, *10*(1), 8. https://digitalcommons.lmu.edu/cate/vol10/iss1/8/

Shongwe, M. E., Van Oldenborgh, G. J., Van Den Hurk, B. J. J. M., De Boer, B., Coelho, C. A. S., & Van Aalst, M. K. (2009). Projected changes in mean and extreme precipitation in Africa under global warming. Part I: Southern Africa. *Journal of Climate*, *22*(13), 3819–3837. https://doi.org/10.1175/2009JCLI2317.1

Shrestha, D. P., & Jetten, V. G. (2018). Modelling erosion on a daily basis, an adaptation of the MMF approach. *International Journal of Applied Earth Observation and Geoinformation*, *64*(August 2017), 117–131. https://doi.org/10.1016/j.jag.2017.09.003

Simensen, T., Halvorsen, R., & Erikstad, L. (2018). Land Use Policy Methods for landscape characterisation and mapping : A systematic review. *Land Use Policy*, *75*(April), 557–569. https://doi.org/10.1016/j.landusepol.2018.04.022

Singh, K. V., Setia, R., Sahoo, S., Prasad, A., & Pateriya, B. (2015). Evaluation of NDWI and MNDWI for assessment of waterlogging by integrating digital elevation model and groundwater level. *Geocarto International*, *30*(6), 650–661. https://doi.org/10.1080/10106049.2014.965757

Singh, S. (2018). Understanding the role of slope aspect in shaping the vegetation attributes and soil properties in Montane ecosystems. *Tropical Ecology* , *59*(3), 417–430. www.tropecol.com

Sinha, S., Sharma, L. K., & Nathawat, M. S. (2015). Improved Land-use/Land-cover classification of semi-arid deciduous forest landscape using thermal remote sensing. *Egyptian Journal of Remote Sensing and Space Science*, *18*(2), 217–233. https://doi.org/10.1016/j.ejrs.2015.09.005

Sinshaw, B. G., Belete, A. M., Mekonen, B. M., Wubetu, T. G., Anley, T. L., Alamneh, W. D., Atinkut, H. B., Gelaye, A. A., Bilkew, T., Tefera, A. K., Dessie, A. B., Fenta, H. M., Beyene, A. M., Bizuneh, B. B., Alem, H. T., Eshete, D. G., Atanaw, S. B., Tebkew, M. A., & Mossie Birhanu, M. (2021). Watershed-based soil erosion and sediment yield modeling in the Rib watershed of the Upper Blue Nile Basin, Ethiopia. *Energy Nexus*, *3*, 100023. https://doi.org/10.1016/j.nexus.2021.100023

Sissoko, K., van Keulen, H., Verhagen, J., Tekken, V., & Battaglini, A. (2011). Agriculture, livelihoods and climate change in the West African Sahel. *Regional Environmental Change*, *11*(SUPPL. 1), 119–125. https://doi.org/10.1007/s10113-010-0164-y

Siswanto, S. Y., & Sule, M. I. S. (2019). The Impact of slope steepness and land use type on soil properties in Cirandu Sub-Sub Catchment, Citarum Watershed. *IOP Conference Series: Earth and Environmental Science*, *393*(1). https://doi.org/10.1088/1755-1315/393/1/012059

Sitch, S., Friedlingstein, P., Gruber, N., Jones, S. D., Murray-Tortarolo, G., Ahlström, A., Doney, S. C., Graven, H., Heinze, C., Huntingford, C., Levis, S., Levy, P. E., Lomas, M., Poulter, B., Viovy, N., Zaehle, S., Zeng, N., Arneth, A., Bonan, G., … Myneni, R. (2015). Recent trends and drivers of regional sources and sinks of carbon dioxide. *Biogeosciences*, *12*(3), 653–679. https://doi.org/10.5194/bg-12-653-2015

Sitch, S., Smith, B., Prentice, I. C., Arneth, A., Bondeau, A., Cramer, W., Kaplan, J. O., Levis, S., Lucht, W., Sykes, M. T., Thonicke, K., & Venevsky, S. (2003). Evaluation of ecosystem dynamics, plant geography and terrestrial carbon cycling in the LPJ dynamic global vegetation model. *Global Change Biology*, *9*(2), 161–185. https://doi.org/10.1046/j.1365-2486.2003.00569.x

Smith, D. A. (1977). Human Population Growth: Stability or Explosion? *Mathematics Magazine*, *50*(4), 186. https://doi.org/10.2307/2690216

Solecki, W., Seto, K. C., & Marcotullio, P. J. (2013). It's time for an urbanization science. *Environment*, *55*(1), 12–17. https://doi.org/10.1080/00139157.2013.748387

Song, C., Woodcock, C. E., Seto, K. C., Lenney, M. P., & Macomber, S. A. (2001). Classification and Change Detection Using Landsat TM Data. *Remote Sensing of Environment*, *75*(2), 230–244. https://doi.org/10.1016/s0034-4257(00)00169-3

Spalevic, V., Barovic, G., Vujacic, D., Curovic, M., Behzadfar, M., Djurovic, N., Dudic, B., & Billi, P. (2020). The impact of land use changes on soil erosion in the river basin of miocki potok, montenegro. *Water (Switzerland)*, *12*(11), 1–28. https://doi.org/10.3390/w12112973

Ssewankambo, G., Kabenge, I., Nakawuka, P., Wanyama, J., Zziwa, A., Bamutaze, Y., Gwapedza, D., Palmer, C. T., Tanner, J., Mantel, S., & Tessema, B. (2023). Assessing soil erosion risk in a peri-urban catchment of the Lake Victoria basin. *Modeling Earth Systems and Environment*, *9*(2), 1633–1649. https://doi.org/10.1007/s40808-022-01565-6

Stanchi, S., Falsone, G., & Bonifacio, E. (2015). Soil aggregation, erodibility, and erosion rates in mountain soils (NW Alps, Italy). *Solid Earth*, *6*(2), 403–414. https://doi.org/10.5194/se-6-403-2015

Stavi, I., & Lal, R. (2011). Variability of soil physical quality and erodibility in a water-eroded cropland. *Catena*, *84*(3), 148–155. https://doi.org/10.1016/j.catena.2010.10.006

Stefanidis, S., & Stathis, D. (2018). Spatial and temporal rainfall variability over the mountainous central Pindus (Greece). *Climate*, *6*(3). https://doi.org/10.3390/cli6030075

Stefano, C. Di, Ferro, V., Porto, P., & Tusa, G. (2000). *Slope curvature influence on soil erosion and deposition processes C. 36*(2), 607–617.

Stenfert Kroese, J., Batista, P. V. G., Jacobs, S. R., Breuer, L., Quinton, J. N., & Rufino, M. C. (2020). Agricultural land is the main source of stream sediments after conversion of an African montane forest. *Scientific Reports*, *10*(1), 1–15. https://doi.org/10.1038/s41598-020-71924-9

Stocking, M. A., & Elwell, H. A. (1976). Rainfall Erosivity over Rhodesia. *Transactions of the Institute of British Geographers*, *1*(2), 231. https://doi.org/10.2307/621986

Storey, J., Engineer, P. S., & Falls, S. (2005). Landsat 7 Scan Line Corrector-Off Gap-Filled Product Gap-Filled Product Development Process. *Pecora 16 "Global Priorities in Land Remote Sensing."*

Strasser, D. L., Lipponen, A., Howells, M., Stec, S., & Bréthaut, C. (2016). A methodology to assess thewater energy food ecosystems nexus in transboundary river basins. *Water (Switzerland)*, *8*(2), 1–28. https://doi.org/10.3390/w8020059.

Stringer, L. C., Dyer, J. C., Reed, M. S., Dougill, A. J., Twyman, C., & Mkwambisi, D. (2009). Adaptations to climate change, drought and desertification: local insights to enhance policy in southern Africa. *Environmental Science and Policy*, *12*(7), 748–765. https://doi.org/10.1016/j.envsci.2009.04.002

Sylla, M. B., Dimobe, K., & Sanfo, S. (2021). *Burkina Faso - land, climate, energy, agriculture and development: A study in the Sudano-Sahel Initiative for regional development, jobs, and food security ZEF* (197 Provided; ZEF Working Paper Series, No. 197 Provided).

Symeonakis, E., Higginbottom, T. P., Petroulaki, K., & Rabe, A. (2018). Optimisation of savannah land cover characterisation with optical and SAR data. *Remote Sensing*, *10*(4), 1–18. https://doi.org/10.3390/rs10040499

Tahat, M. M., Alananbeh, K. M., Othman, Y. A., & Leskovar, D. I. (2020). Soil health and sustainable agriculture. *Sustainability (Switzerland)*, *12*(12), 1–26. https://doi.org/10.3390/SU12124859

Talbot, M. R., & Williams, M. A. J. (1978). Erosion of Fixed Dunes in the Sahel, Central Niger. *Earth Surf Processes*, *3*(2), 107–113. https://doi.org/10.1002/esp.3290030202

Talukdar, S., Singha, P., Mahato, S., Shahfahad, Pal, S., Liou, Y. A., & Rahman, A. (2020). Land-use land-cover classification by machine learning classifiers for satellite observations-A review. *Remote Sensing*, *12*(7). https://doi.org/10.3390/rs12071135

Tanyaş, H., Kolat, Ç., & Süzen, M. L. (2015). A new approach to estimate cover-management factor of RUSLE and validation of RUSLE model in the watershed of Kartalkaya Dam. *Journal of Hydrology*, *528*(September), 584–598. https://doi.org/10.1016/j.jhydrol.2015.06.048

Tarboton, D. G. (1997). A new method for the determination of flow directions and upslope areas in grid digital elevation models. *Water Resources Research*, *33*(2), 309–319.

Tarolli, P., & Sofia, G. (2016). Human topographic signatures and derived geomorphic processes across landscapes. *Geomorphology*, *255*, 140–161. https://doi.org/10.1016/j.geomorph.2015.12.007

Taye, G., Teklesilassie, T., Teka, D., & Kassa, H. (2023). Assessment of soil erosion hazard and its relation to land use land cover changes: Case study from alage watershed, central Rift Valley of Ethiopia. *Heliyon*, *9*(8), e18648. https://doi.org/10.1016/j.heliyon.2023.e18648

Tengapoe, K., Baddianaah, I., & Agyemang, I. (2023). Anthropogenic induced land use land cover dynamics of the Black Volta River Corridor in north-western Ghana, 2011-2021. *Trees, Forests and People*, *14*(September), 100449. https://doi.org/10.1016/j.tfp.2023.100449

Thakuriah, G. (2023). GIS-based revised universal soil loss equation for estimating annual soil erosion: a case of lower Kulsi basin, India. *SN Applied Sciences*, *5*(3). https://doi.org/10.1007/s42452-023-05303-0

Thomas, J., Joseph, S., & Thrivikramji, K. P. (2018). Assessment of soil erosion in a tropical mountain river basin of the southern Western Ghats, India using RUSLE and GIS. *Geoscience Frontiers*, *9*(3), 893–906. https://doi.org/10.1016/j.gsf.2017.05.011

Tian, P., Zhu, Z., Yue, Q., He, Y., Zhang, Z., Hao, F., Guo, W., Chen, L., & Liu, M. (2021). Soil erosion assessment by RUSLE with improved P factor and its validation: Case study on mountainous and hilly areas of Hubei Province, China. *International Soil and Water Conservation Research*, *9*(3), 433–444. https://doi.org/10.1016/j.iswcr.2021.04.007

Tilahun, H., Taddesse, G., Melese, A., & Mebrate, T. (2018). Assessment of spatial soil erosion hazard in Ajema Watershed, North Shewa Zone, Ethiopia. *Advances in Plants & Agriculture Research Research*, *8*(6), 552–558. https://doi.org/10.15406/apar.2018.08.00384

Timpong-Jones, E. C., Samuels, I., Sarkwa, F. O., Oppong-Anane, K., & Majekodumni, A. O. (2023). Transhumance pastoralism in West Africa–its importance, policies and challenges. *African Journal of Range and Forage Science*, *40*(1), 114–128. https://doi.org/10.2989/10220119.2022.2160012

Tola, F. K. (2023). Drivers of Forest cover changes in and around Jorgo Wato Forest, West Wallagga, Oromia, Ethiopia. *Heliyon*, *9*(8), e19053. https://doi.org/10.1016/j.heliyon.2023.e19053

Tonah, S. (2002). Fulani Pastoralists , Indigenous Farmers and the Contest for Land in Northern Ghana Author (s): Steve Tonah farmers and the contest for land in Northern Fulani pastoralists , indigenous Ghana. *Africa Spectrum*, *37*(1), 43–59.

Tosh, J. (1980). The cash-crop revolution in tropical Africa: An agricultural reappraisal. *African Affairs*, *79*(314), 79–94. https://doi.org/10.1093/oxfordjournals.afraf.a097201

Tripathi, H. G., Woollen, E. S., Carvalho, M., Parr, C. L., & Ryan, C. M. (2021). Agricultural expansion in African savannas: effects on diversity and composition of trees and mammals. *Biodiversity and Conservation*, *30*(11), 3279–3297. https://doi.org/10.1007/s10531-021-02249-w

Tully, K., Sullivan, C., Weil, R., & Sanchez, P. (2015). The State of soil degradation in sub-Saharan Africa: Baselines, trajectories, and solutions. *Sustainability (Switzerland)*, *7*(6), 6523–6552. https://doi.org/10.3390/su7066523

Turner, G. M., Rorbert, G. H., & O'Neill, V. R. (2001). LANDSCAPE ECOLOGY IN THEORY AND PRACTICE. In *Patter n an d Proceses* (Issue 1). Springer-Verlag.

Uber, M., Rössler, O., Astor, B., Hoffmann, T., Van Oost, K., & Hillebrand, G. (2022). Climate Change Impacts on Soil Erosion and Sediment Delivery to German Federal Waterways: A Case Study of the Elbe Basin. *Atmosphere*, *13*(11), 1–21. https://doi.org/10.3390/atmos13111752

Uddin, K., Matin, M. A., & Maharjan, S. (2018). Assessment of land cover change and its impact on changes in soil erosion risk in Nepal. *Sustainability (Switzerland)*, *10*(12). https://doi.org/10.3390/su10124715

Ullah, S., Ali, A., Iqbal, M., Javid, M., & Imran, M. (2018). Geospatial assessment of soil erosion intensity and sediment yield: a case study of Potohar Region, Pakistan. *Environmental Earth Sciences*, *77*(19), 1–13. https://doi.org/10.1007/s12665-018-7867-7

United Nations Department of Economic and Social Affairs- Population Division (UNDESA-POP). (2018). *The World 's Cities in 2018*.

United Nations Department of Economic and Social Affairs- Population Division (UNDESA-POP). (2022). Global Population Growth and Sustainable Development. In *(UN DESA/POP/2021/TR/NO.2)*. https://doi.org/10.18356/9789210052467

van der Waal, B., & Rowntree, K. (2018). Landscape Connectivity in the Upper Mzimvubu River Catchment: An Assessment of Anthropogenic Influences on Sediment Connectivity. *Land Degradation and Development*, *29*(3), 713–723. https://doi.org/10.1002/ldr.2766

Van Oost, K., Govers, G., & Desmet, P. (2000). Evaluating the effects of changes in landscape structure on soil erosion by water and tillage. *Landscape Ecology*, *15*(6), 577–589. https://doi.org/10.1023/A:1008198215674

Vereecken, H., Schnepf, A., Hopmans, J. W., Javaux, M., Or, D., Roose, T., Vanderborght, J., Young, M. H., Amelung, W., Aitkenhead, M., Allison, S. D., Assouline, S., Baveye, P., Berli, M., Brüggemann, N., Finke, P., Flury, M., Gaiser, T., Govers, G., … Young, I. M. (2016). Modeling Soil Processes: Review, Key Challenges, and New Perspectives. *Vadose Zone Journal*, *15*(5), 1–57. https://doi.org/10.2136/vzj2015.09.0131

Verheijen, F. G. A., Jones, R. J. A., Rickson, R. J., & Smith, C. J. (2009). Tolerable versus actual soil erosion rates in Europe. *Earth-Science Reviews*, *94*(1–4), 23–38. https://doi.org/10.1016/j.earscirev.2009.02.003

Viana, C. M., Oliveira, S., Oliveira, S. C., & Rocha, J. (2019). Land Use/Land Cover Change Detection and Urban Sprawl Analysis. In *Spatial Modeling in GIS and R for Earth and Environmental Sciences*. https://doi.org/10.1016/b978-0-12-815226-3.00029-6

Visser, S., Keesstra, S., Maas, G., de Cleen, M., & Molenaar, C. (2019). Soil as a basis to create enabling conditions for transitions towards sustainable land management as a key to achieve the SDGs by 2030. *Sustainability (Switzerland)*, *11*(23). https://doi.org/10.3390/su11236792

Wang, B., & Cheng, W. (2023). Geomorphic influences on land use/cover diversity and pattern. *Catena*, *230*(May). https://doi.org/10.1016/j.catena.2023.107245

Wang, B., Cheng, W., Xu, H., Wang, R., Song, K., Bao, A., & Shi, Q. (2024). Vegetation differentiation characteristics and control mechanisms in the Altay region based on topographic gradients. *Ecological Indicators*, *160*(March), 111838. https://doi.org/10.1016/j.ecolind.2024.111838

Wang, C., Shan, L., Liu, X., Yang, Q., Cruse, R. M., Liu, B., Li, R., Zhang, H., & Pang, G. (2020). Impacts of horizontal resolution and downscaling on the USLE LS factor for different terrains. *International Soil and Water Conservation Research*, *8*(4), 363–372. https://doi.org/10.1016/j.iswcr.2020.08.001

Wang, G., Gertner, G., Fang, S., & Anderson, A. B. (2003). Mapping multiple variables for predicting soil loss by geostatistical methods with TM images and a slope map. *Photogrammetric Engineering and Remote Sensing*, *69*(8), 889–898. https://doi.org/10.14358/PERS.69.8.889

Wang, H., Xie, T., Yu, X., & Zhang, C. (2021). Simulation of soil loss under different climatic conditions and agricultural farming economic benefits: The example of Yulin City on Loess Plateau. *Agricultural Water Management*, *244*(June 2020), 106462. https://doi.org/10.1016/j.agwat.2020.106462

Wang, L., & Liu, H. (2006). An efficient method for identifying and filling surface depressions in digital elevation models for hydrologic analysis and modelling. *International Journal of Geographical Information Science*, *20*(2), 193–213. https://doi.org/10.1080/13658810500433453

Wang, S., McGehee, R. P., Guo, T., Flanagan, D. C., & Engel, B. A. (2023). Calibration, validation, and evaluation of the Water Erosion Prediction Project (WEPP) model for hillslopes with natural runoff plot data. *International Soil and Water Conservation Research*, *11*(4), 669–687. https://doi.org/10.1016/j.iswcr.2022.10.004

Wang, W., Wu, T., Li, Y., Xie, S., Han, B., Zheng, H., & Ouyang, Z. (2020). Urbanization impacts on natural habitat and ecosystem services in the Guangdong-Hong Kong-Macao "Megacity." *Sustainability (Switzerland)*, *12*(16). https://doi.org/10.3390/su12166675

Wang, Y., He, Y., Zhan, J., & Li, Z. (2022). Identification of soil particle size distribution in different sedimentary environments at river basin scale by fractal dimension. *Scientific Reports*, *12*(1), 1–12. https://doi.org/10.1038/s41598-022-15141-6

Wantzen, K. M., & Mol, J. H. (2013). Soil erosion from agriculture and mining: A threat to tropical stream ecosystems. *Agriculture (Switzerland)*, *3*(4), 660–683. https://doi.org/10.3390/agriculture3040660

Watene, G., Yu, L., Nie, Y., Zhu, J., Ngigi, T., Nambajimana, J. D. D., & Kenduiywo, B. (2021). Water erosion risk assessment in the kenya great Rift Valley region. *Sustainability (Switzerland)*, *13*(2), 1–31. https://doi.org/10.3390/su13020844

Weng, Q., Lu, D., & Schubring, J. (2004). Estimation of land surface temperature-vegetation abundance relationship for urban heat island studies. *Remote Sensing of Environment*, *89*(4), 467–483. https://doi.org/10.1016/j.rse.2003.11.005.

Williams, J. R., Jones, C. A., & Dyke, and P. T. (1983). The EPIC Model and Its Application. *Proceedings of the International Symposium on Minimum Data Sets for Agrotechnology Transfer, Patancheru, India.*, 111–121.

Winzeler, H. E., Owens, P. R., Read, Q. D., Libohova, Z., Ashworth, A., & Sauer, T. (2022). Topographic Wetness Index as a Proxy for Soil Moisture in a Hillslope Catena: Flow Algorithms and Map Generalization. *Land*, *11*(11). https://doi.org/10.3390/land11112018

Wischmeier, W. H., & Smith, D. D. (1978). *Predicting rainfall erosion losses—a guide to conservation planning.* (No. 537). The USDA Agricultural Handbook No. 537.

Woodcock, C. E., Macomber, S. A., Pax-Lenney, M., & Cohen, W. B. (2001). Monitoring large areas for forest change using Landsat: Generalization across space, time and Landsat sensors. *Remote Sensing of Environment*, *78*(1–2), 194–203. https://doi.org/10.1016/S0034-4257(01)00259-0

World Bank. (2019). *The cost of coastal zone degradation in west Africa: Benin, Côte d'Ivoire, Senegal and Togo* (Issue March).

Wu, J., Kurosaki, Y., Gantsetseg, B., Ishizuka, M., Sekiyama, T. T., Buyantogtokh, B., & Liu, J. (2021). Estimation of dry vegetation cover and mass from MODIS data: Verification by roughness length and sand saltation threshold. *International Journal of Applied Earth Observation and Geoinformation*, *102*, 102417. https://doi.org/10.1016/j.jag.2021.102417

Wu, S., Li, J., & Huang, G. H. (2008). A study on DEM-derived primary topographic attributes for hydrologic applications: Sensitivity to elevation data resolution. *Applied Geography*, *28*(3), 210–223. https://doi.org/10.1016/j.apgeog.2008.02.006

Wuddivira, M. N., Stone, R. J., & Ekwue, E. I. (2013). Influence of cohesive and disruptive forces on strength and erodibility of tropical soils. *Soil and Tillage Research*, *133*(August 2018), 40–48. https://doi.org/10.1016/j.still.2013.05.012

Wulder, M. A., Loveland, T. R., Roy, D. P., Crawford, C. J., Masek, J. G., Woodcock, C. E., Allen, R. G., Anderson, M. C., Belward, A. S., Cohen, W. B., Dwyer, J., Erb, A., Gao, F., Griffiths, P., Helder, D., Hermosilla, T., Hipple, J. D., Hostert, P., Hughes, M. J., … Zhu, Z. (2019). Current status of Landsat program, science, and applications. *Remote Sensing of Environment*, *225*(November 2018), 127–147. https://doi.org/10.1016/j.rse.2019.02.015

Wynants, M., Solomon, H., Ndakidemi, P., & Blake, W. H. (2018). Pinpointing areas of increased soil erosion risk following land cover change in the Lake Manyara catchment, Tanzania. *International Journal of Applied Earth Observation and Geoinformation*, *71*, 1–8.

Xie, Y., Lin, H., Ye, Y., & Ren, X. (2019). Changes in soil erosion in cropland in northeastern China over the past 300 years. *Catena*, *176*(19), 410–418. https://doi.org/10.1016/j.catena.2019.01.026

Xu, H. (2006). Modification of normalised difference water index (NDWI) to enhance open water features in remotely sensed imagery. *International Journal of Remote Sensing*, *27*(14), 3025–3033. https://doi.org/10.1080/01431160600589179

Xu, Q., Zheng, X., & Zhang, C. (2018). Quantitative analysis of the determinants influencing urban expansion: A case study in Beijing, China. *Sustainability (Switzerland)*, *10*(5). https://doi.org/10.3390/su10051630

Xue, J., & Su, B. (2017). Significant remote sensing vegetation indices: A review of developments and applications. *Journal of Sensors*, *2017*. https://doi.org/10.1155/2017/1353691

Yahaya, A. K., & Amoah, S. T. (2013). Bushfires in the Nandom district of the Upper West Region of Ghana: perpetual threat to food crop production. *Journal of Environment and Earth Science*, *3*(7), 10–14. http://citeseerx.ist.psu.edu/viewdoc/download?doi=10.1.1.875.3490&rep=rep1&type=pdf

Yang, D., Kanae, S., Oki, T., Koike, T., & Musiake, K. (2003). Global potential soil erosion with reference to land use and climate changes. *Hydrological Processes*, *17*(14), 2913–2928. https://doi.org/10.1002/hyp.1441

Yang, X. (2015). Digital mapping of RUSLE slope length and steepness factor across New South Wales, Australia. *Soil Research*, *53*(2), 216–225. https://doi.org/10.1071/SR14208

Yang, Y., Zhao, R., Shi, Z., Viscarra Rossel, R. A., Wan, D., & Liang, Z. (2018). Integrating multi-source data to improve water erosion mapping in Tibet, China. *Catena*, *169*(May), 31–45. https://doi.org/10.1016/j.catena.2018.05.021

Yap, C. K., Nulit, R., Syazwan, W. M., Omar, H., Aguol, K. A., Nawi, M., Leow, C. S., Syazwan, W. M., & Omar, H. (2024). *Population Growth and Environmental Resources : A Short Note on their Relationships and Consequences and Impacts*. 46884–46896. https://doi.org/10.26717/BJSTR.2024.55.008685

Ye, Y., Legates, R., & Qin, B. (2013). Coordinated Urban-rural development planning in China. *Journal of the American Planning Association*, *79*(2), 125–137. https://doi.org/10.1080/01944363.2013.882223

Yengoh, G. T., Armah, F. A., Onumah, E. E., & Odoi, J. O. (2010). Trends in Agriculturally-Relevant Rainfall Characteristics for Small-scale Agriculture in Northern Ghana. *Journal of Agricultural Science*, *2*(3), 3–16. https://doi.org/10.5539/jas.v2n3p3

Yin, C., Zhao, W., & Pereira, P. (2022). Soil conservation service underpins sustainable development goals. *Global Ecology and Conservation*, *33*(November 2021), e01974. https://doi.org/10.1016/j.gecco.2021.e01974

Young, P., Parkinson, S., & Lees, M. (1996). Simplicity out of complexity in environmental modelling: Occam's razor revisited. *Journal of Applied Statistics*, *23*(2–3), 165–210. https://doi.org/10.1080/02664769624206

Young, R. A., Onstad, C. A., Bosch, D. D., & Anderson, W. P. (1989). AGNPS: A nonpoint-source pollution model for evaluating agricultural watersheds. *J. Soil Water Conservat.*, *44*(2), 168–173.

Yousefi, M., Darvishi, A., Tello, E., Barghjelveh, S., Dinan, N. M., & Marull, J. (2021). Comparison of two biophysical indicators under different landscape complexity. *Ecological Indicators*, *124*(January), 107439. https://doi.org/10.1016/j.ecolind.2021.107439

Yuan, Z., Chu, Y., & Shen, Y. (2015). Simulation of surface runoff and sediment yield under different land-use in a Taihang Mountains watershed, North China. *Soil and Tillage Research*, *153*, 7–19. https://doi.org/10.1016/j.still.2015.04.006

Zeraatpisheh, M., Ayoubi, S., Mirbagheri, Z., Mosaddeghi, M. R., & Xu, M. (2021). Spatial prediction of soil aggregate stability and soil organic carbon in aggregate fractions using machine learning algorithms and environmental variables. *Geoderma Regional*, *27*(June), e00440. https://doi.org/10.1016/j.geodrs.2021.e00440

Zerihun, M., Mohammedyasin, M. S., Sewnet, D., Adem, A. A., & Lakew, M. (2018). Assessment of soil erosion using RUSLE, GIS and remote sensing in NW Ethiopia. *Geoderma Regional*, *12*(September 2024), 83–90. https://doi.org/10.1016/j.geodrs.2018.01.002

Zha, Y., Gao, J., & Ni, S. (2003). Use of normalized difference built-up index in automatically mapping urban areas from TM imagery. *International Journal of Remote Sensing*, *24*(3), 583–594. https://doi.org/10.1080/01431160304987

Zhang, K., Yu, Y., Dong, J., Yang, Q., & Xu, X. (2019). Agriculture , Ecosystems and Environment Adapting & testing use of USLE K factor for agricultural soils in China. *Agriculture, Ecosystems and Environment*, *269*(June 2018), 148–155. https://doi.org/10.1016/j.agee.2018.09.033

Zhang, Lanlan, Huang, Y., Rong, L., Duan, X., Zhang, R., Li, Y., & Guan, J. (2021). Effect of soil erosion depth on crop yield based on topsoil removal method: a meta-analysis. *Agronomy for Sustainable Development*, *41*(5). https://doi.org/10.1007/s13593-021-00718-8

Zhang, Lei, Yang, L., Zohner, C. M., Crowther, T. W., Li, M., Shen, F., Guo, M., Qin, J., Yao, L., & Zhou, C. (2022). Direct and indirect impacts of urbanizationon vegetation growth across the world's cities. *Science Advances*, *8*(27), 1–11. https://doi.org/10.1126/sciadv.abo0095

Zhang, Z., Xiao, R., Shortridge, A., & Wu, J. (2014). Spatial point pattern analysis of human settlements and geographical associations in eastern coastal China - A case study. *International Journal of Environmental Research and Public Health*, *11*(3), 2818–2833. https://doi.org/10.3390/ijerph110302818

Zhao, L., & Hou, R. (2019). Human causes of soil loss in rural karst environments: a case study of Guizhou, China. *Scientific Reports*, *9*(1), 1–11. https://doi.org/10.1038/s41598-018-35808-3

Zhipeng, L., Ma, D., Hu, W., & Li, X. (2018). Land use dependent variation of soil water infiltration characteristics and their scale-specific controls. *Soil and Tillage Research*, *178*(January), 139–149. https://doi.org/10.1016/j.still.2018.01.001

Zhou, Y. (2016). *Agricultural Mechanization in West Africa*. 1–11.

Zhu, Z., Qiu, S., & Ye, S. (2022). Remote sensing of land change: A multifaceted perspective. *Remote Sensing of Environment*, *282*(September). https://doi.org/10.1016/j.rse.2022.113266

Ziadat, F. M., & Taimeh, A. Y. (2013). Effect of rainfall intensity, slope, land use and antecedent soil moisture on soil erosion in an arid environment. *Land Degradation and Development*, *24*(6), 582–590. https://doi.org/10.1002/ldr.2239

Ziem Bonye, S., Yenglier Yiridomoh, G., & Derbile, E. K. (2021). 'Urban expansion and agricultural land use change in Ghana: Implications for peri-urban farmer household food security in Wa Municipality.' *International Journal of Urban Sustainable Development*, *13*(2), 383–399. https://doi.org/10.1080/19463138.2021.1915790

Zittis, G., Almazroui, M., Alpert, P., Ciais, P., Cramer, W., Dahdal, Y., Fnais, M., Francis, D., Hadjinicolaou, P., Howari, F., Jrrar, A., Kaskaoutis, D. G., Kulmala, M., Lazoglou, G., Mihalopoulos, N., Lin, X., Rudich, Y., Sciare, J., Stenchikov, G., … Lelieveld, J. (2022). Climate Change and Weather Extremes in the Eastern Mediterranean and Middle East. *Reviews of Geophysics*, *60*(3). https://doi.org/10.1029/2021RG000762

Zoderer, B. M., Tasser, E., Carver, S., & Tappeiner, U. (2019). An integrated method for the mapping of landscape preferences at the regional scale. *Ecological Indicators*, *106*(June). https://doi.org/10.1016/j.ecolind.2019.05.061

Zorn, M., & Komac, B. (2009). Response of soil erosion to land use change with particular reference to the last 200 years (Julian Alps, Western Slovenia). *Revista de Geomorfologie*, *11*, 39–47. http://geo.unibuc.ro/revista_geomorfo/volum11/05.zorn.pdf

SUPPLEMENTARY MATERIALS

Chapter 5. Supplementary Figures and Tables

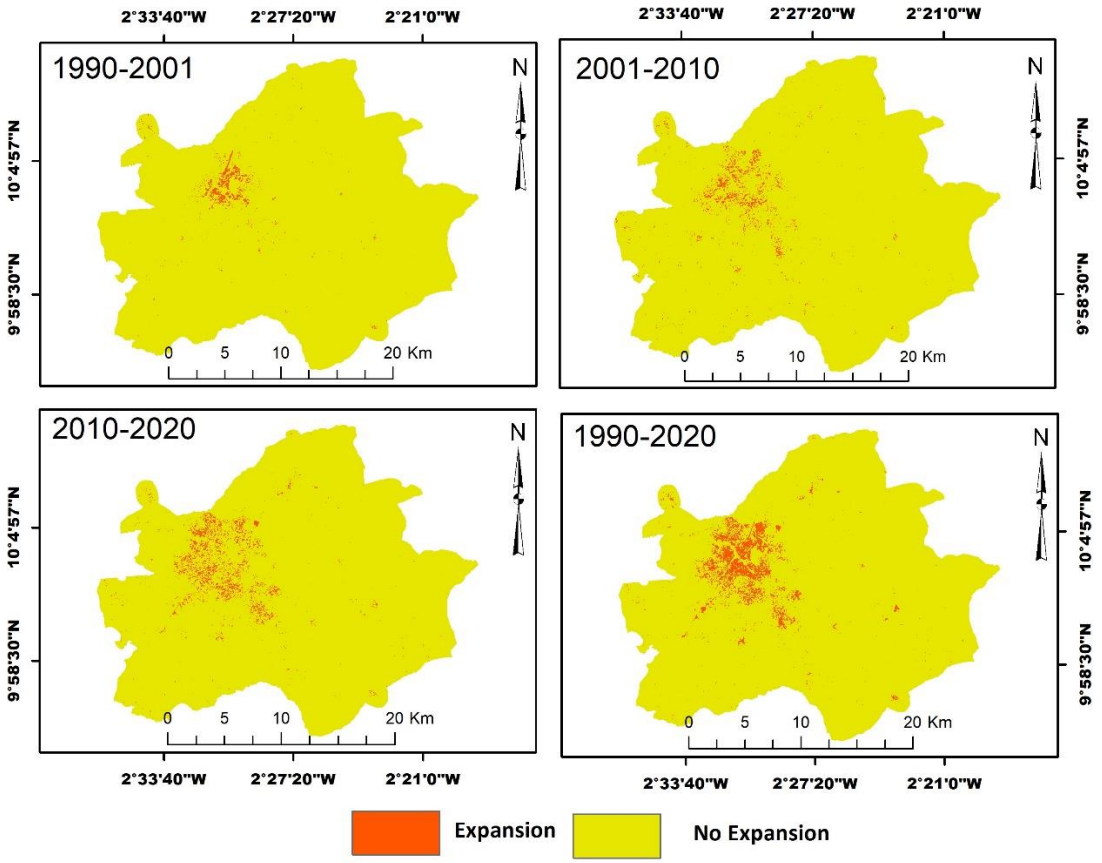

Figure SL 5.1. The Raster layer of urban expansion was obtained from change detection for all the time slices and served as dependent variables in the logistic regression analysis. The dichotomous variables were 1=expansion and 0=no expansion.

Table SL 5.1. Landsat Satellites Used for Classification, their Scene ID Number and the Time of Acquisition

Satellite Name	Scene ID number	Date of Acquisition	Time of Acquisition
Landsat 5	LT51950531990285MPS00	October 12, 1990	09:46:28.2240060Z
Landsat 7	LE71950532001307EDC00	November 03, 2001	10:15:13.1215482Z
Landsat 7	LE71950532010316ASN00	November 12, 2010	10:19:33.0561608Z
Landsat 8	LC81950532020320LGN00	November 15, 2020	10:27:08.9585710Z

Chapter 6. Supplementary Figures and Tables

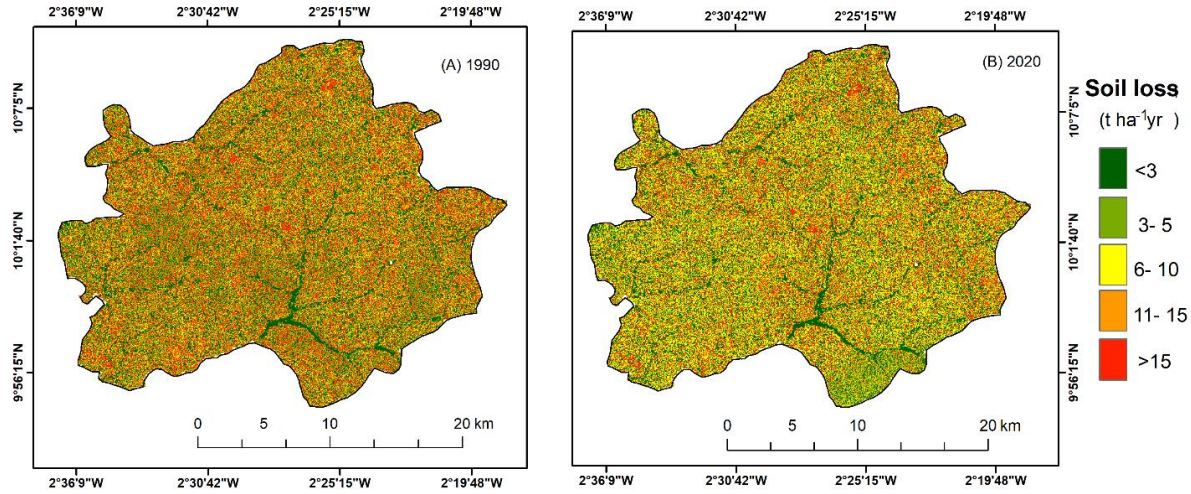

Figure SL.6.1. Potential Erosion Risk. (A)1990 is the Map of Potential Erosion Risk for the year 1990; (B)2020 is the Map of Potential Erosion Risk for the year 2020.

Table SL 6.1. Summary of Data and their Sources used in the Soil Erosion Risk Modelling

Factors	Resolution	Source
R-factor	-	NASA's POWER project (See https://power.larc.nasa.gov access date: 15 April 2022).
K-factor	250x250 m	ISRIC- World Soil Information "SoilGrids" provides a raster (TIF format) global soil map and associated information (https://soilgrids.org; (accessed on 20 September 2021).
LS-factor	30x30 m	SRTM Digital Elevation Model (DEM): (See the USGS database at https://earthexplorer.usgs.gov/, Retrieved on 15 October 2020).
C-factor		Supervised LULC classification maps adopted from (Asempah et al., 2021)and adopted weighted C-factor values in the context of the landscape.
P-factor	30x30 m	A p-factor value, 1, was assigned based on the non-availability of soil erosion conservation and support management practices.

Table SL 6.2. Description of Land Use Land Cover classes

ID	LULC class	Description
1	Closed savannah	Dense cover, usually woody biomass-dominated areas (including natural forests, protected and reserved areas) with over 150 tree/ha density.
2	Open savannah	Dense cover, usually fewer woody biomass than close savannah with less than 150 tree/ha density. Main cover includes shrubs, grasses and gloves.
3	Other	Highly exposed areas without vegetation cover. These are predominantly bare lands, unregulated open small-scale mining pits, sandy and gravel surfaces.
4	Settlement	Areas that are built-up (particularly towns, villages and other emerging residential zones with characteristic low to medium population densities).
5	Vegetated wetland	Characterised by dried up river courses and stream channels. Such areas are often previously swamped and have overgrown grasses and shrubs.
6	Water	Areas covered with water bodies (such as rivers, streams, reservoirs and dams.

Chapter 7. Supplementary Figures and Tables

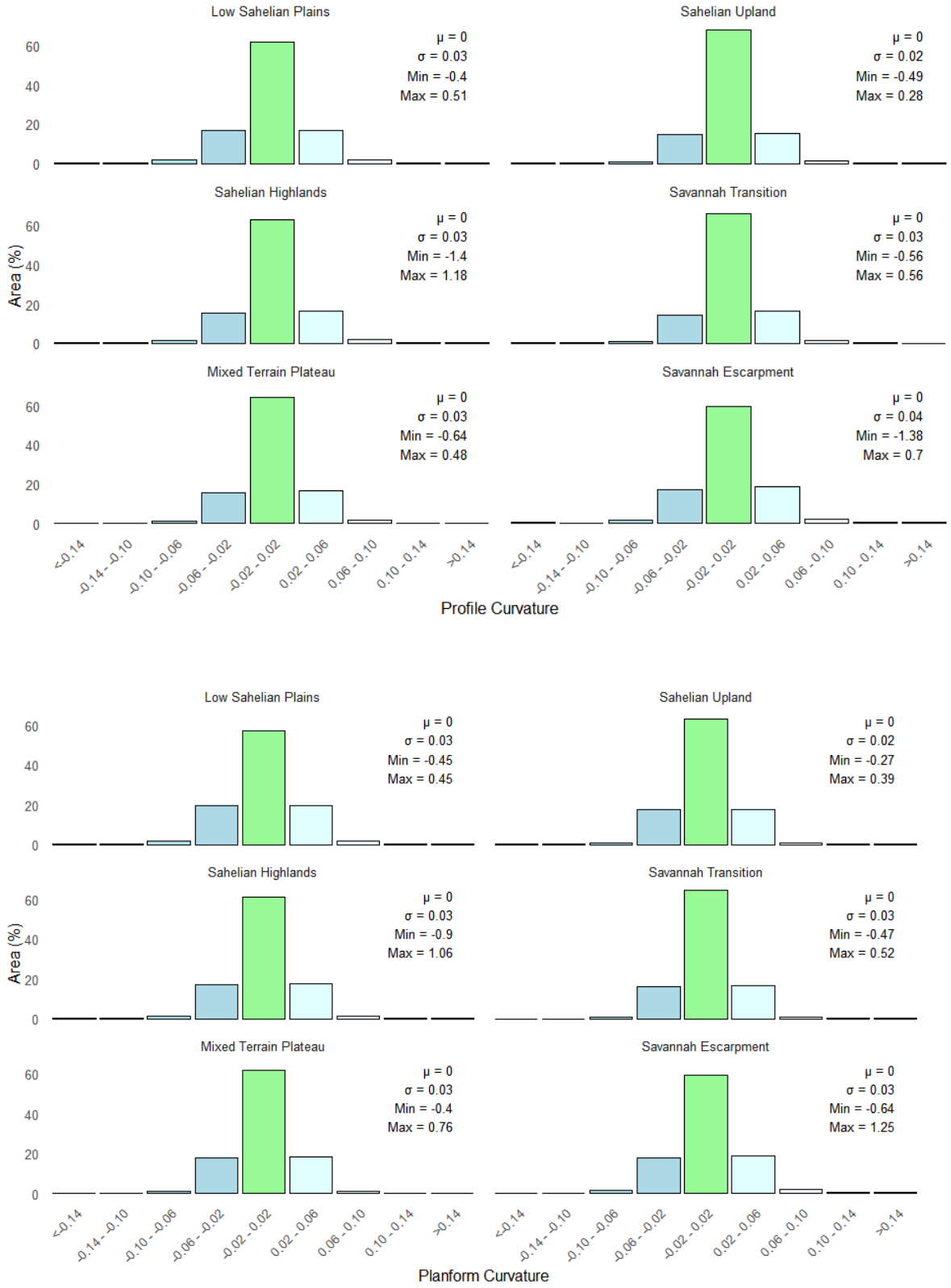

Figure SL 7.1. The Profile and Planform Curvature of the Six Landscape Units

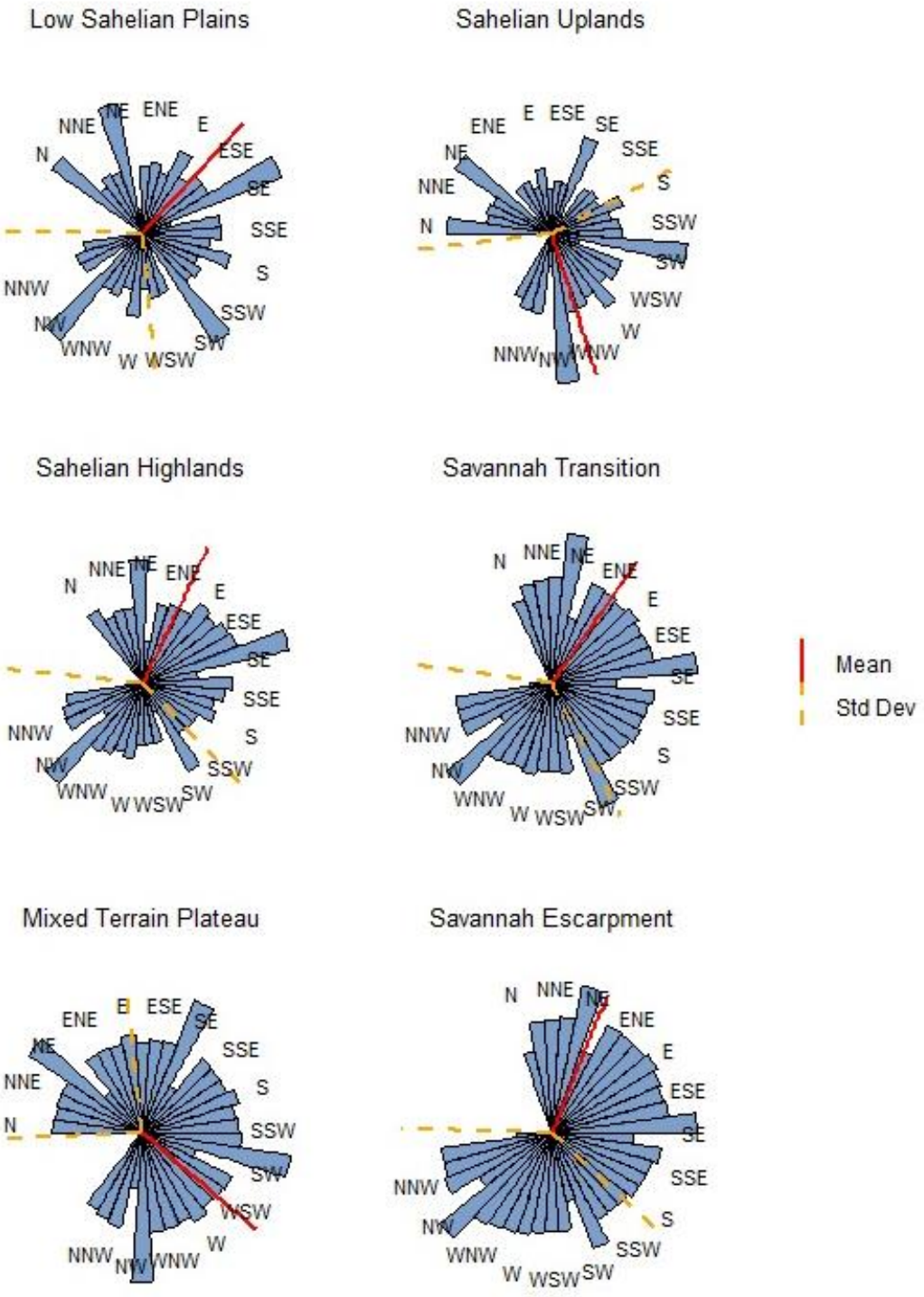

Figure SL 7.2. The Aspect of Slope (°) for the Six Landscape Units

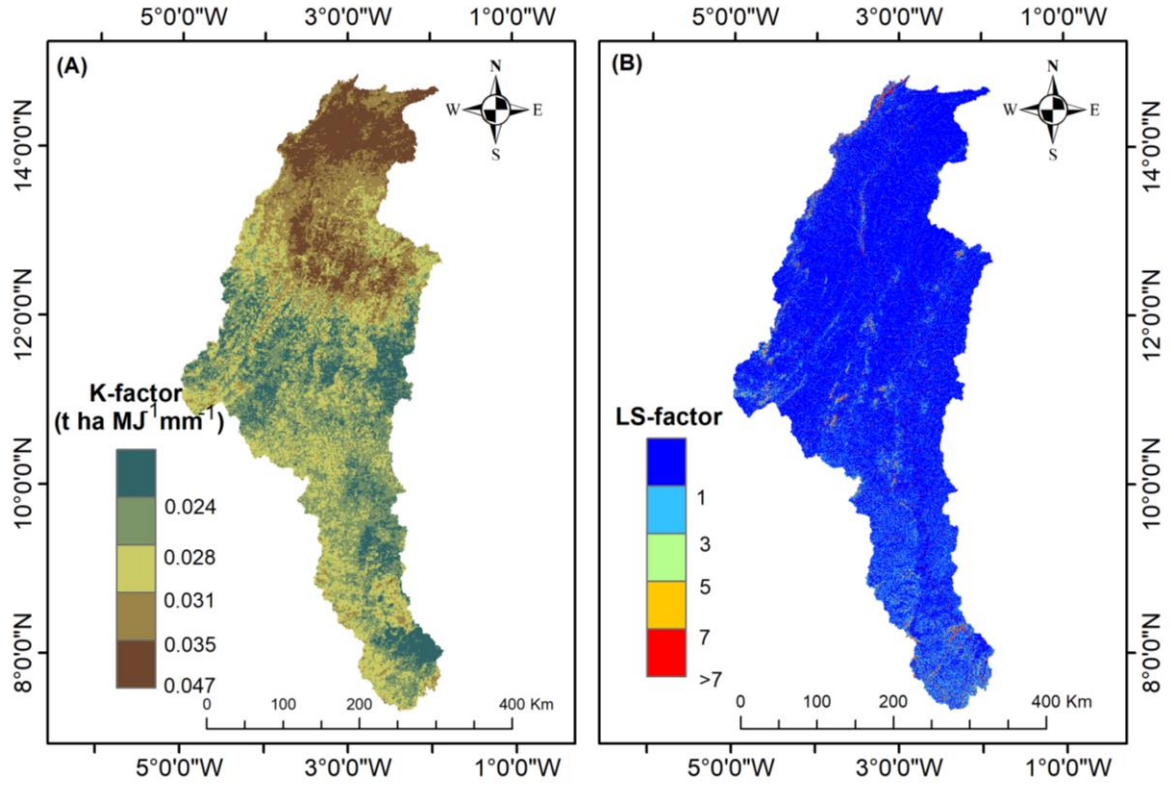

Figure SL 7. 3. Map of K and LS Factors. (A) Soil erodibility map for the basin (Data source: ISRIC-World Soil Information "SoilGrids" provides a raster (TIF format) global soil map and associated information (See https://soilgrids.org; accessed on 20 September 2021). (B) LS factor map for the basin. Source of Data: SRTM DEM from CGIAR-CSI database (https://bigdata.cgiar.org/srtm-90m-digital-elevation-database/). The specific landscape units within the maps are labelled A, B, C, D, E and F. A is Low Sahelian Plains, B is Sahelian Uplands, C is Sahelian highlands, D is Savannah Transition, E is Mixed Terrain Plateau and F is Savannah Escarpment).

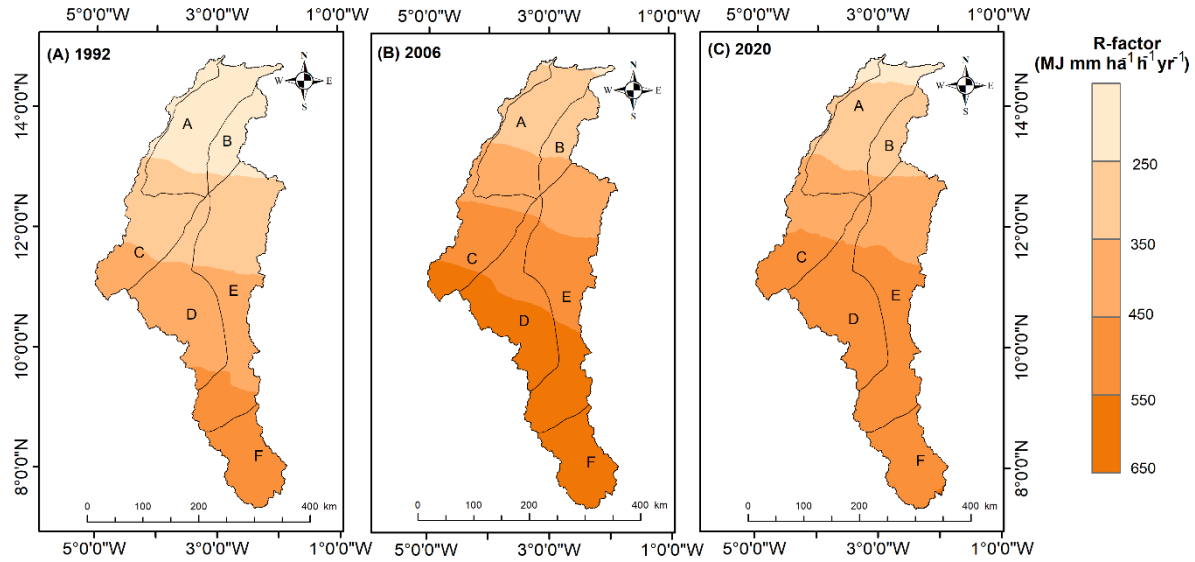

Figure SL 7.4. Map of R-factor for the years 1992, 2006 and 2020 (A) R-factor for the year 1992 (B) R-factor for the year 2006 (C) R-factor for the year 2020. Data for the respective R-factors was obtained from the CRU database https://crudata.uea.ac.uk/cru/data/hrg/). The specific landscape units within the maps are labelled A, B, C, D, E and F. A is Low Sahelian Plains, B is Sahelian Uplands, C is Sahelian Highlands, D is Savannah Transition, E is Mixed Terrain Plateau and F is Savannah Escarpment).

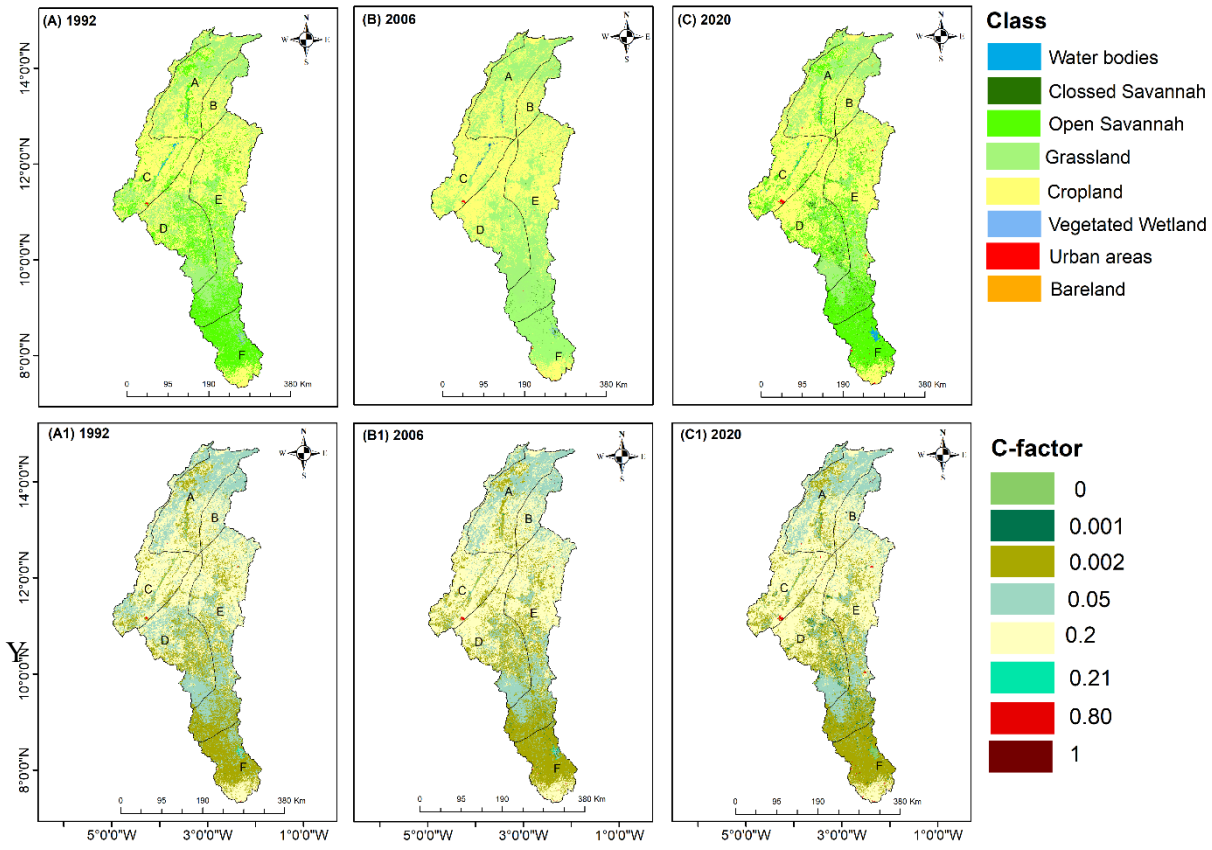

Figure SL 7.5. LULC Maps For The Black Volta River Basin and their Corresponding C-factors for Soil Erosion Risk Modelling for the years 1992, 2006 and 2020. (A) 1992, (B) 2006 and (C) 2020 are LULC maps for 1992, 2006 and 2020, respectively, while (A1) 1992, (B1)2006 and (C1) 2020 are their corresponding C-factor maps for the years 1992, 2006 and 2020, respectively (LULC classification from the Copernicus database) The specific landscape units within the maps are labeled A, B, C, D, E and F. A is Low Sahelian Plains, B is Sahelian Uplands, C is Sahelian highlands, D is Savannah Transition, E is Mixed Terrain Plateau and F is Savannah Escarpment).

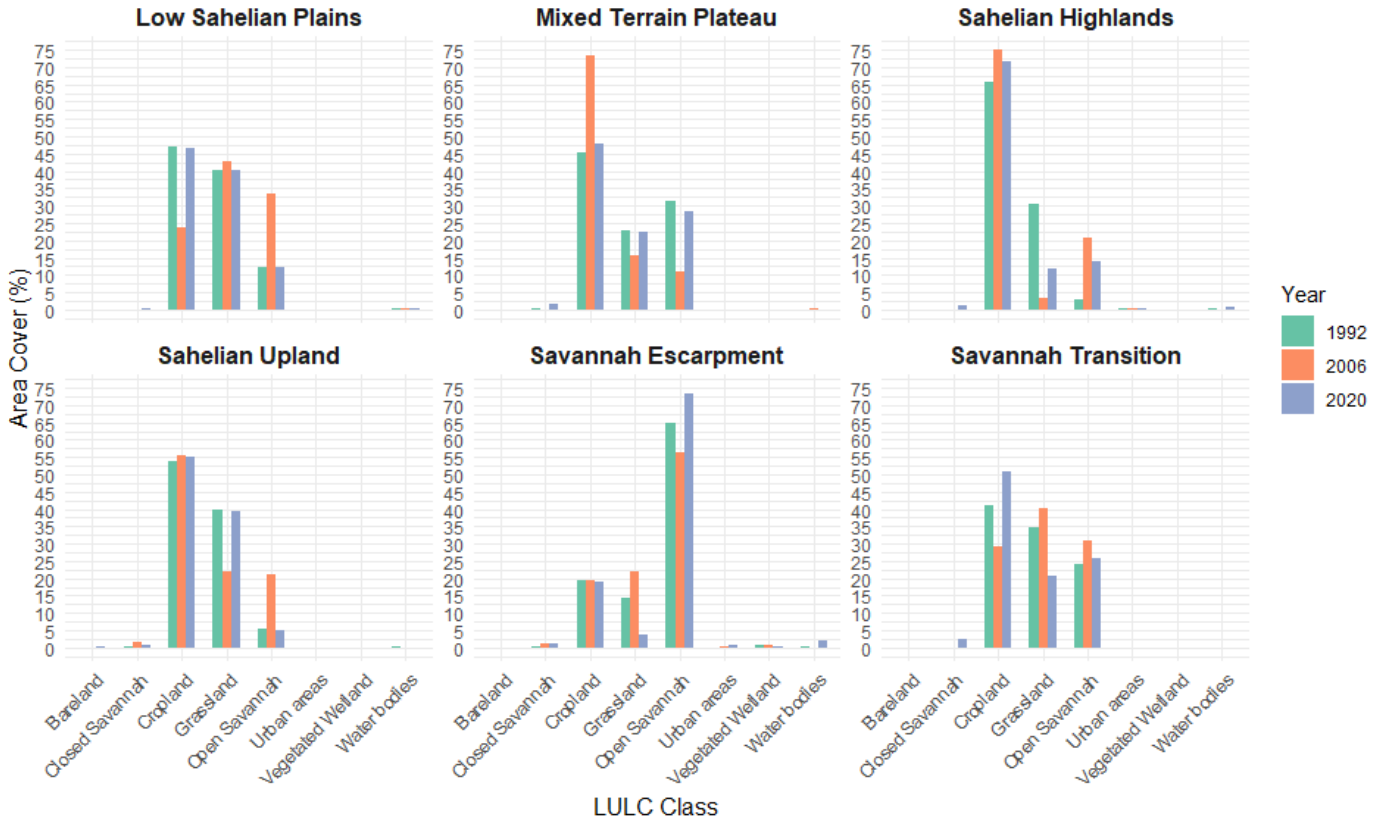

Figure SL 7.6. Frequencies Distribution of Land Cover Across the Six Landscape Units for the years 1992, 2006 and 2020

Table SL 7.1. Land Cover for the year for each Landscape Unit for 1992 Time Slice

	Land cover per landscape unit											
	Low Sahelian Plains		**Sahelian Uplands**		**Sahelian Highlands**		**Savannah Transition**		**Mixed Terrain Plateau**		**Savannah Escarpment**	
LULC Class	**Area (km^2)**	%	**Area (km^2)**	**%**	**Area (km^2)**	**%**	**Area (km^2)**	**%**	**Area (km^2)**	**%**	**Area (km^2)**	**%**
Cropland	11,481.2	46.9	4,594.8	53.7	14,666.9	65.6	10,870.3	41.0	18,999.3	45.4	2,785.1	19.4
Grassland	9,894.2	40.4	3,412.3	39.9	6,850.6	30.7	9,241.0	34.8	9,641.1	23.0	2,047.4	14.3
Open Savannah	2,954.6	12.1	461.0	5.4	687.0	3.1	6,360.7	24.0	13,043.5	31.2	9,297.8	64.9
Closed Savannah	24.8	0.1	40.1	0.5	30.6	0.1	19.0	0.1	112.0	0.3	53.7	0.4
Vegetated Wetland	8.3	<0.05	0.0	0.0	31.9	0.1	0.7	<0.05	0.5	<0.05	94.1	0.7
Urban areas	3.0	0.1	1.1	0.0	35.3	0.2	0.2	<0.05	4.6	<0.05	17.7	0.1
Bareland	1.9	<0.05	8.8	0.1	0.2	<0.05	0.2	<0.05	1.3	<0.05	0.0	0.0
Water bodies	112.9	0.5	34.0	0.4	39.1	0.2	29.2	0.1	40.7	0.1	28.1	0.2

Table SL 7.2. Land cover for the year for each Landscape Unit for the 2006 Time Slice

	Land cover per landscape unit											
	Low Sahelian Plains		**Sahelian Uplands**		**Sahelian Highlands**		**Savannah Transition**		**Mixed Terrain Plateau**		**Savannah Escarpment**	
LULC Class	**Area (km^2)**	%	**Area (km^2)**	**%**	**Area (km^2)**	**%**	**Area (km^2)**	**%**	**Area (km^2)**	**%**	**Area (km^2)**	**%**
Cropland	5,750.7	23.5	4,725.9	55.3	16,806.8	75.2	7,684.5	29.0	30,631.8	73.2	2,776.8	19.4
Grassland	10,427.4	42.6	1,861.2	21.8	770.0	3.4	10,625.5	40.1	6,480.5	15.5	3,154.3	22.0
Open Savannah	8,197.6	33.5	1,817.7	21.3	4,643.9	20.8	8,184.2	30.9	4,543.9	10.9	8,072.2	56.4
Closed Savannah	27.8	0.1	128.7	1.5	31.9	0.1	19.6	0.1	31.9	0.1	156.3	1.1
Vegetated Wetland	8.7	<0.05	0.0	0.0	6.1	<0.05	0.7	<0.05	6.1	<0.05	99.8	0.7
Urban areas	6.9	<0.05	1.4	<0.05	51.0	0.2	0.3	<0.05	15.0	<0.05	43.9	0.3
Bareland	1.4	<0.05	10.9	0.1	0.0	<0.05	1.3	<0.05	0.0	0.0	0.0	0.0
Water bodies	60.4	0.2	6.2	0.1	31.9	0.1	5.4	<0.05	133.6	0.3	20.5	0.1

Table SL 7.3. Land Cover for the year for each Landscape Unit for the 2020 Slice

	Low Sahelian Plains		**Sahelian Uplands**		**Sahelian Highlands**		**Savannah Transition**		**Mixed Terrain Plateau**		**Savannah Escarpment**	
LULC Class	**Area (km^2)**	%	**Area (km^2)**	**%**	**Area (km^2)**	**%**	**Area (km^2)**	**%**	**Area (km^2)**	**%**	**Area (km^2)**	**%**
Cropland	11,441.9	46.7	4,695.8	54.9	16,000.1	71.6	13,467.8	50.8	20,023.8	47.9	2,698.9	18.8
Grassland	9,840.4	40.2	3,366.2	39.4	2,682.5	12.0	5,462.7	20.6	9,316.3	22.3	540.0	3.8
Open Savannah	3,019.8	12.3	406.5	4.8	3,111.5	13.9	6,899.5	26.0	11,797.5	28.2	10,484.9	73.2
Closed Savannah	78.9	0.3	50.3	0.6	246.3	1.1	678.1	2.6	614.9	1.5	172.8	1.2
Vegetated Wetland	20.3	0.1	0.0	0.0	5.4	0.0	0.7	<0.05	2.0	<0.05	35.4	0.2
Urban areas	14.8	0.1	4.2	<0.05	108.9	0.5	6.1	<0.05	58.7	0.1	96.2	0.7
Bareland	1.4	<0.05	22.0	0.3	0.0	0.0	0.2	<0.05	1.2	<0.05	0.0	0.0
Water bodies	63.5	0.3	7.0	0.1	187.1	0.8	6.4	<0.05	28.6	0.1	295.7	2.1
	24,480.9	100.0	8,552.1	100.0	22,341.7	100.0	26,521.5	100.0	41,842.9	100.0	14,323.8	100.0

Eidesstattliche Erklärung

Hiermit erkläre ich, dass ich die Dissertation "*Modelling Soil Erosion Risk in the Black Volta Transboundary River Basin of West Africa* " selbstständig angefertigt und keine anderen als die von mir angegebenen Quellen und Hilfsmittel verwendet habe.

Ich erkläre weiterhin, dass die Dissertation bisher nicht in dieser oder in anderer Form in einem anderen Prüfungsverfahren vorgelegen hat.

……

Mawuli Asempah

Berlin, 12.03.2024